Universitat Autònoma de Barcelona

Identification and characterization of the TRPVs protein-protein interactions, a comprehensive approach to elucidate TRPVs function and regulation

Pablo Doñate Macian

Identification and characterization of the TRPVs protein-protein interactions, a comprehensive approach to elucidate TRPVs function and regulation

Pablo Doñate Macian

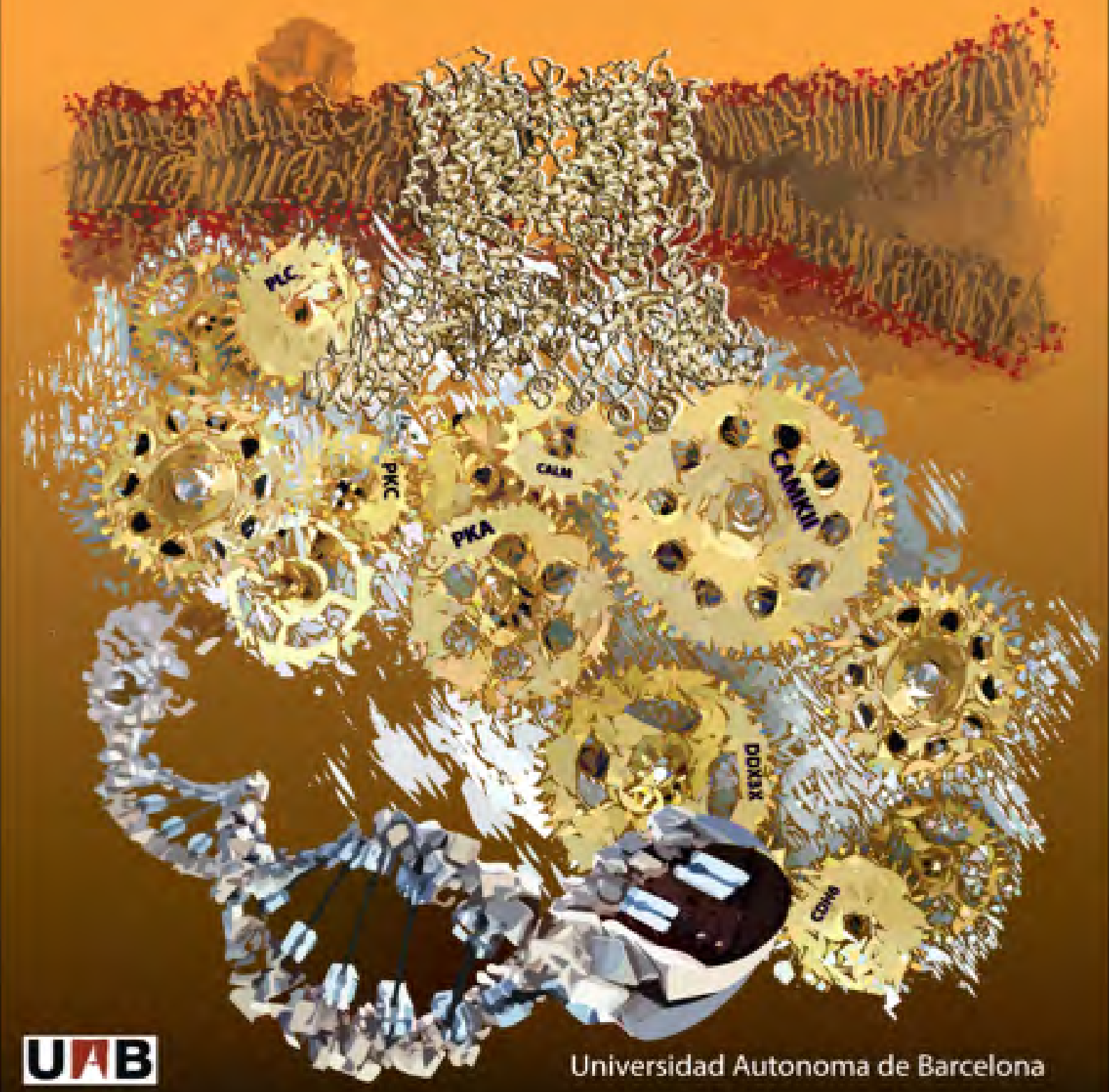

Universidad Autonoma de Barcelona

Universitat Autònoma de Barcelona

Identification and characterization of the TRPVs protein-protein interactions, a comprehensive approach to elucidate TRPVs function and regulation

Pablo Doñate Macian

Ph.D. supervisor: Dr. Alejandro Perálvarez Marín

Unidad de Biofísica, Departamento de Bioquímica y Biología molecular. Fac. Medicina.

Universidad Autónoma de Barcelona, Campus Bellaterra

Pablo Doñate Macian

Ph.D. student

Dr. Alejandro Perálvarez Marín

Ph.D. supervisor

´´Understanding the way we sense at the molecular level is the first wise step in order to comprehend the complexity and hidden nature of our world``

Pablo Doñate Macian

Preface

I) Acknowledgements

Writing this thesis has been a challenge for me, and I am grateful for all the people that support me and encourage me to go on. Although sometimes difficult, during these years I had a great time, and learned a lot, not just scientifically but from life itself.

In the first place, I want to thank my family and friends for all the support received. I would not have been able to go through this stage of my life without your help and I am sorry for being lost in the writing for the last months. Hope now we can retake our hangouts. I am in debt with all of you, specially with Julio. You made me believe in myself when nobody else can and I am so glad I found someone who was there when all my hopes fail and was able to restore my trust and confidence. Also to Kyra, for her unconditional support during the writing, being by my side at all times.

Second, I want to thank to Dr. Alex Perálvarez for the chance of developing this work, for trusting me from the first day to carry out this project and supporting me scientifically. From you I have learned most part of what I know nowadays as Science and I consider myself lucky to choose you as Thesis supervisor. Likewise, not all the times were easy and I want to thank Dr. Miguel Valverde for supporting us in times of need. You not only supervise my thesis as part of the following committee, but made possible much part of this work by offering your lab and treating me as one more of your team. I am thankful for everything I had the chance to learn during this last year by your side. I do not know what will be next step in my scientific carrier but I am sure it will be thanks to everything I learned from you both.

I also wanted to thank to the other members of my following committee. Dr. Patrick Aloy for introducing me to Alex and trusting me for this project, and Dr. Jose Luis Vazquez for all the advise provided during our time together in UAB. I hope you both the best.

It has been 5 years, sharing moments in the lab, and I have met lot of people, either in UAB and PRBB/UPF. I want to thank Elodia Serrano for her kindness, Mateu Company for his efficiency and Neus for her support during the library amplification. For all the students that pass through the lab during the last years and made my life quite much entertained: Carla Das, Danial Afsharzadeh, Guillem Marco, Vidhya Ravi, Yun Ping, Fanli Zeng, Lying Wang, Marc Viader, Albert Suades, Dra. Elena Alvarez, Dr. Roger and Dra. Gloria Palou, David Montpetllo, Dr. Asrar Malik, Marco Martins. I want to highlight the good times with Carla in the lab, when we could not stop laughing; the calçotadas with Guillem at his home and the Wok Sundays with Danial. Finally thanks to all the members of Biophysic Unit, Dr. Esteve Padros, Dr. Josep Cladera, Dr. David Garcia, Dr. Ramon Barnadas, Dra. Tzvetana Lazarova, Dr. Joan Manyosa and so many others that shared these years with me.

From UPF, I want to thank everyone for making me feel home even though my project was not based there. Especially to Dr. Ruben Vicente, for trusting me despite his skepticism in helicases; to Dr. Jose Maria Fernandez and Dr. Francisco Muñoz, for their particular sense of humor. Thanks to all them for their valuable scientific advice and counseling that guide my project. Furthermore this work would not been possible without the endless scientific discussions and help received from Dr. Alejandro Berna,

Dra. Fanny Rubio and Dra. Selma Serra. You were always there willing to help planning experiments, designing next steps on my research, helping with the performance of those experiments, even in the hard times, and I am especially grateful for all the support received. Thanks also for sharing with me your sight of the world during lunch and lab times.

I am also grateful to Cristina Plata, for her technical support, mice killing skills and for introducing myself to the voley. I want also to thank Dra. Carole Jung for her advance knowledge of drugs and concentrations and her sympathy and energy. I want to highlight the good times in the office, with Kerstin Keifer, Carlos Pardo, Roberto García, Vicky Valls and Biuse Guivernau. Thanks for your friendship to all of you, I will never forget the October fest, the calçotadas, panelletadas or pabladas. Finally, thanks to former members of the UPF Physiology lab Dra. Anna Garcia-Elias, Dra. Mònica Bosch and Dra. Isabel Bahamonde for their valuable scientific knowledge and friendliness.

Thanks for being so special and genuine and for everything I received from all of you, because you all made this possible and I will never forget everything you gave to me.

II) Abstract

TRPV channels are cation channels involved in the ion homeostasis with polymodal activation properties. They regulate intracellular calcium levels promoting a fine tune cellular response to several physicochemical stimuli, allowing the cell to adapt to the environmental changes. TRPV subfamily contains 6 members classified in two groups attending to their sequence identity: TRPV1-4 and TRPV5-6. TRPV1-4 are non selective calcium channels mainly involved in thermoception, mechanoception and pain transduction. TRPV1-4 members are of special biomedical interest as they have been associated with a wide spectrum of pathological conditions, from muscular or neuronal dystrophies to cancer.

This thesis aims to expand the knowledge on the regulation of TRPV1-4 subgroup. First, we have compiled the available information in the field by means of a review based on TRPV2, one of the least described and more intriguing members of the TRPV subfamily. Primary sequence data mining and conservation study of TRPV domains revealed that TRPV1-4 channels share common basic working mechanisms as folding and trafficking. Using TRPV2 as benchmark, we have determined the folding properties and topology of this channel and the importance of the distal N-terminal domain for TRPV2 trafficking. Protein protein interactions were given a special attention as TRPV channels act within the cell forming protein complexes. We have mapped the interaction with SNARE proteins within the MPD domain of TRPV1 and TRPV2 and the TRPV1-4 interactome was further expanded by means of a yeast two hybrid specific for membrane proteins (MYTH) based on TRPV1, TRPV2 and TRPV4.

II) Resumen

Los canales TRPV son canales de cationes que participan en la homeostasis de iones con propiedades de activación polimodales. Los TRPVs regulan los niveles de calcio intracelular y promueven una respuesta celular precisa a varios estímulos físico-químicos, lo que permite a la célula adaptarse al entorno cambiante. La subfamilia TRPV contiene 6 miembros, clasificados en dos grupos atendiendo a su identidad de secuencia: TRPV1-4 y TRPV5-6. TRPV1-4 son canales no selectivos de calcio que participan principalmente en termocepción, mecanocepción y la transducción del dolor. Los TRPV1-4 son de un especial interés biomédico, ya que se han asociado con un amplio espectro de estados patológicos, desde distrofias musculares o neuronales a cáncer.

Esta tesis tiene como objetivo ampliar el conocimiento sobre la regulación del subgrupo TRPV1-4. En primer lugar, hemos recopilado la información disponible por medio de una revisión basada en TRPV2, uno de los miembros menos descritos y más interesante de la subfamilia TRPV. El análisis de la secuencia primaria y estudio de conservación de los dominios TRPV revelaron que los canales TRPV1-4 comparten mecanismos básicos de funcionamiento, como el plegado y el transporte a membrana. Usando TRPV2 como punto de referencia, hemos determinado las propiedades de plegado y la topología de este canal y la importancia del dominio N-terminal distal para el tráfico de TRPV2. Se les dio una atención especial a las interacciones proteína proteína, dado que los TRPV actúan dentro de las células formando complejos. Hemos mapeado la interacción con las proteínas SNARE al dominio MPD de TRPV1 y TRPV2 y el interactoma de los TRPV1-4 se amplió por medio de un doble híbrido especifico de proteínas de membrana (MYTH) basado en TRPV1, TRPV2 y TRPV4.

III) Abbreviations

2-APB	2-Aminoethoxydiphenyl borate
4 α-PDD	4α-Phorbol 12,13-didecanoate
6TBC	6-tert-butyl-m-cresol
80K-H	Protein Kinase C Substrate 80K-H
A	Amstrongs
AA	Arachidonic acid
aa	amino acid
ABR	Active BCR-related protein
ACBD3	Acyl-CoA binding domain containing 3
AKAP	A-Kinase anchoring protein
AKT	Protein Kinase B
AMPK	AMP-activated protein kinase
ANO1	Anoctamin-1
AQP	Aquaporin
ARD	Ankyrin Repeat Domain
ARL15	ADP-Ribosylation Factor -Like 15
AT1aR	Angiotensin receptor subtype 1a
ATP	Adenosine TriPhosphate
BAA	Bisandrographolide A
Bkca	Big potassium calcium channel
BRAC3	Brachylomia type 3
C-terminal	Protein carboxi-terminal, COOH-terminal
C-terminus	Protein carboxi-terminal, COOH-terminal
C. elegans	Caenorhabditis elegans
C. intestinalis	Ciona intestinalis

CA neuron	C and A fibers
Ca^{2+}	Calcium
CACNG3	Calcium Channel, Voltage-Dependent, Gamma Subunit 3
CAM	Calmodulin
CAMBS	Calmodulin Binding Site
CamKII	Calmodulin Kinase II
cAMP	Cyclic adenosine monophosphate
Cav	Calcium voltage-gated channels
CB1	Cannabinoid receptor 1
CBD1	Cannabinoid receptor 1
CBD2	Cannabinoid receptor 2
CCL	Choride channel
cdc2	Cyclin-dependent kinase 1
CDH	Cadherin family
CDK	Cyclin Dependent Kinase
cDNA	complementary Deoxyribonucleic acid
CFA	Carrageenan
CGRP	Calcitonin gene-related peptide
CHERP	Calcium homeostasis endoplasmic reticulum protein
clb	E3 ubiquitin- protein ligase
CMR1	Changed mutation rate protein 1
CMT2C	Charcot-Marie Tooth type 2C
CNG	Cyclic Nucleotide-Gated
CNGA	Cyclic Nucleotide-Gated A subunit
CNGB	Cyclic Nucleotide-Gated B subunit
CNS	Central Nervous System

COPD	Chronic Obstructive Pulmonary Disease
COX-2	Cyclooxygenase 2
Cryo-EM	Cryogenic Electron Microscopy
CTD	Protein carboxi-terminal, COOH-terminal
Cub	C-terminus of ubiquitin
CXCR	C-X-C chemokine receptor
D. melanogaster	Drosophila melanogaster
DAG	Diacylglycerol
DAP-150	Dynein-associated polypeptide
DAZAP2	DAZ-associated protein 2
DDX	Dead box helicase
DDX3X	Dead box helicase 3X
Ded1	DEAD-box protein 1
DGR	Dorsal Root Ganglion
DMD	Duchenne muscular dystrophy
DMEM	Dulbecco's modified Eagle's medium
DNA	Deoxyribonucleic acid
DPBA	2,4-dioxo-4-phenylbutanoic acid
DPPA	1,2-Dipalmitoyl-sn-glycero-3-phosphatidic acid
DPPC	Dipalmitoylphosphatidylcholine
EET	Epoxyeicosatrienoic acids
EGFP	Enhanced green fluorescent protein
EGFR	Epidermal Growth Factor Receptor
EIF	Eukaryotic translation initiation factor
EM	Electron microscopy
ENAC	Epithelial Sodium channel

eNOS	endothelial Nitric Oxide Synthase
ER	Endoplasmatic Reticulum
ERK	Extracellular signal–regulated kinases
FAF1	Fas Associated Factor 1
FFA	Fatty acid
Fl	Full length
FPP	Farnesyl pyrophosphate
GABA	?-aminobutyric acid
GABARAP	Gamma-aminobutyric acid receptor-associated protein
GCN5	Histone acetyltransferase GCN5
GEO	Genome expression Omnibus
GFP	Green fluorescent protein
GLTP	Glycolipid transfer protein
Gp120	Envelope glycoprotein GP120
GPCR	G Protein Coupled Receptor
h	Hour
H. sapiens	Homo sapiens
HAX-1	HCLS1 Associated Protein X-1
HBE	Human Bronchial Epithelial cells
HCK	Hematopoietic cell kinase
HCN	Hyperpolarization-activated Cyclic Nucleotide-gated
HEK293	Human Embrionic Kidney cells
HeLa	Henrietta Larks cells
His tag	Histidine tag
HIV	Human Immundeficiency Virus
HODE	Hydroxioctadecadienoic acid

HPETE	Hydroperoxyeicosatetraenoic acids
IB	Immunoblot
IFN	Interferon
IFNA	Interfeton typeI subunit A
IFNAR	Interferon receptor type 1
IFNB	Interfeton typeI subunit B
IGF-1	Insulin Growth Factor 1
IMP	Integral Membrane Protein
IP	Immunoprecipitation
IP3	Inositol trisPhosphate
IP3R	Inositol trisPhosphate Receptor
ITCH	E3 ubiquitin-protein ligase Itchy homolog
ITM2C	Integral Membrane Protein 2C
JMJD2C	Jumonji Domain-Containing Protein 2C
JNK	c-Jun N-terminal kinases
K+	Potassium
K2p	Potassium tandem pore domain
Kca	Potassium calcium- activated
KCNQ	Potassium voltage-gated channel subfamily KQT member
KCNQ10	inwardly rectifying K+ channel Kir 4.1
KIF13B	Kinesin Family Member 13B
KIF2A	Kinesin Family Member 2a
KIF2B	Kinesin Family Member 2B
Kir	Potassium inward rectifyig
Kv	Potassium Voltage-gated
LAC-Z	Lactose operon, β-galactosidase

LPC	lysophosphatidylcholine
LPI	Lysophosphatidylinositol
LPS	Lipopolysaccharides
LysoPC	lysophosphatidylcholine
M	Molar
M. brevicollis	Monosiga brevicollis
MAPK	Mitogen-activated protein kinases
MEF	Mouse embryonic fibroblasts
Mg^{2+}	Magnesium
MHR	High Homolog Region
Min	Minutes
MPD	Membrane Proximal Domain, between ARD and S1
mRNA	messenger RiboNucleic Acid
MTD	Metatropic dysplasia
MTT	3-(4,5-Dimethylthiazol-2-yl)-2,5- Diphenyltetrazolium Bromide
mV	mili Volt
MVK	Mevalonate kinase
MYH	Myosin
MYTH	Membrane Yeast Two Hybrid
N-terminal	Protein amino-terminal, NH2-terminal
N-terminus	Protein amino-terminal, NH2-terminal
Na^{+}	Sodium
Nav	Sodium voltage-gated channels
Nef	Negative Regulatory Factor
NF-KB	Nuclear factor kappa-light-chain-enhancer of activated B cells
NFAT	Nuclear factor of activated T-cells

NGF	Nerve Growth Factor
NHERF4	sodium-hydrogen exchanger regulatory factor 4
NKX2.2	NK Homeobox Protein NK-2
nM	nano Molar
NMDA	N-methyl-D-aspartate
NMDAR1	N-methyl-D-aspartate Receptor 1
NMDAR2B	N-methyl-D-aspartate Receptor 2B
NO	Nitric Oxide
NOMO1	Nodal Modulator 1
NTD	Protein amino-terminal, NH2-terminal
NTM	Neurotrimin
Nub	N-terminus of ubiquitin
NubG	N-terminus of ubiquitin mutated in Ile-13 to Gly
OCR	Osm-9/capsaicin receptor related
OCR-2	Osm-9 and Capsaicin receptor-Related
OS-9	Osteosarcoma Amplified 9
OSM-9	OSMotic avoidance abnormal family member 9
OVLT	Organum Vasculosum Lamina Terminalis
P-loop	Pore loop
PA	Phosphatidic acid
PACS-1	Phosphofurin Acidic Cluster Sorting Protein 1
PACSIN	Protein kinase C and casein kinase substrate in neurons
PAMPs	Pathogen associated molecular patterns
PAR2	Protease activated receptor 2
PC	Phosphatidyl choline
PDB	Protein Data Bank

PDZ	post synaptic density protein (PSD95), Drosophila disc large tumor suppressor (Dlg1), and zonula occludens-1 protein (zo-1)
PEX10	Peroxisomal Biogenesis Factor 10
PI	Phosphoinositol
PI3K	Phosphoinositide 3-kinase
PI4P	Phophoinositol-4-phosphate
PIP2	Phosphatidylinositol 4,5-bisphosphate
PIP2 BS	Phosphatidylinositol 4,5-bisphosphate Binding Ste
PKA	Protein Kinase A
PKARII	Protein Kinase A, RII Subunit
PKC	Protein Kinase C
PLA-2	Phospholipase A2
PLAG	Pleiomorphic adenoma gene 1 protein
PLC	PhosphoLipase C
PLP1	Proteolipid Protein 1
POLR2G	DNA-directed RNA polymerase II subunit G
POPC	1-palmitoyl-2-oleoylglycero-3-phosphocholine
POPG	1-palmitoyl-2-oleoyl-sn-glycero-3-phosphoglycerol
POPS	palmitoyl-2-oleoyl-sn-glycero-3-phospho-L-serine
PPAR	Peroxisome proliferator-activated receptor
PPI	Protein-protein Interaction
PPK	Palmoplantar keratoderma
PRD	Proline Rich Domain
pre-S1	Region prior to transmembrane helix 1
PRKA	Protein Kinase A
PRKD	Protein Kinase D
PRKD1	Protein Kinase D1

PRR	Pathogen recognition receptor
PS	Phosphatidylserine
PSTD	Parastremmatic dwarfism
RAB	Ras superfamily of monomeric G proteins
Rab11-FIP3	RAB11 Family Interacting Protein 3
RANBP	Ran Binding Protein
RGA	Recombinase Gene Activator protein
RLR	retinoic acid-inducible RIG-like receptors
RMs	Rough microsomes
RNA	RiboNucleic Acid
ROC	Receptor-operated channels
RPL12	Ribosomal Protein L12
RPS27A	Ribosomal Protein S27a
RTX	Resiniferatoxin
RyR1	Ryanodin receptor 1
S1-6	Transmembrane protein helices numbered from N- to C-terminal
S6K1	Ribosomal protein S6 kinase beta-1
SDS-Page	sodium dodecyl sulfate polyacrylamide gel electrophoresis
SEDM	Spondyloepiphyseal dysplasia Maroteaux
SGT	Small glutamine-rich tetratricopeptide repeat-containing protein
SMA	Smooth muscle actin
SMDK	Spondylometaphyseal dysplasia Kozlowski
SNAPIN25	Synaptosomal-associated protein 25
SNARE	SNAP (Soluble NSF Attachment Protein) REceptor
SNP	Single Nucleotide Polymorphism
SON	SupraOptic Nucleus

SPSMA	Scapuloperoneal spinal muscular atrophy
SRC	Non-receptor tyrosine kinases
Syne1	Spectrin Repeat Containing, Nuclear Envelope 1
SYT9	Synaptotagmin 9
T. rubripes	Takifugu rubripes
TAD1 and 2	Tetramerization Domain 1 and 2
TAK1	Transforming growth factor beta-activated kinase 1
TAP	transporter involved in antigen processing
Tat	trans-activating protein
TBK1	Tank binding kinase 1
TBS 1 and 2	Tubulin Binding sequence 1 and 2
TF	Transcription Factor
TG	Trigeminal ganglia
TGFB1	Transforming Growth Factor Beta
TGFα	Transforming Growth Factor Alpha
TGS1	Probable diacyglycerol O-acyltransferase
TLR	Toll-like Receptor
TM	Transmembrane
TM	TransMembrane
TMDs	TransMembrane Domain segments
TMEM	Transmembrane Protein
TMHMM	TM hidden Markov model
TNF	Tumor Necrosis Factor
TrKa	Tropomyosin receptor kinase A
TRP	Transient Receptor Potential
TRP box	Transient Receptor Potential box

TRPA	Transient Receptor Potential Ankyrin
TRPC	Transient Receptor Potential Canonical
TRPM	Transient Receptor Potential Melastin
TRPML	Transient Receptor Potential Mucolipin
TRPN	Transient Receptor Potential Non-mechanoreceptor
TRPP	Transient Receptor Potential Polycystic
TRPV	Transient Receptor Potential Vanilloid
UBC	Ubiquitin
UBP5	Ubiquitin carboxyl-terminal hydrolase 5
UTR	Untranslated region
VOC	Voltage-operated channels
WB	Western Blot
WT	Wild type
X-gal	5-Bromo-4-chloro-3-indolyl β-D-galactopyranoside
YVC1	Yeast Vacuolar Conductance 1
ZBTB17	Zinc Finger And BTB Domain Containing 17
Zo-1	Zona ocludens 1
Δ74-TRPV2	TRPV2 truncation lacking the N-terminal first 74 aminoacids
ΔARD-TRPV2	TRPV2 truncation lacking the Ankyrin Repeat Domain
µM	micro Molar

Table of contents

IV) List of figures

V) List of tables

Introduction

Living organisms, from the simpler unicellular form to the most complex multicellular being, face the challenge of adapting themselves to the highly variable environment. The membrane is the first and basic barrier to separate the cell and the environment, and from there, complexity begins towards optimal communication between two compartments at both sides the membrane. Along evolution biological organisms have developed several systems to evaluate crucial environmental parameters and generate the appropriate responses to adapt in such a changeful world, where membrane proteins are key players. The first atomic-level resolution membrane protein structure was reported in 1985 and since then only 308 unique membrane protein structures have been obtained, whereas there are over 80,000 PDB entries determined by diffraction methods for soluble proteins. Membrane proteins comprise 20-30% of all proteins in both prokaryotic and eukaryotic organisms but they represent less than 0.5% of all the known structures, with only 20 structures of human membrane proteins and less than 50 mammalian membrane proteins solved. They also represent around 50% of current drug targets. This fact should illustrate how important are membrane proteins and how scarce is our knowledge on them.

1. Membrane transport

Biological membranes are hydrophobic, thus impermeable to ions and molecules such as sugars and peptides. Transport of these molecules across the membrane, which is physiologically essential, is made possible by the existence of membrane transporters (uphill transport) and channels (downhill transport). In a general sense, both transporters and channels are membrane transporters but whereas channels are diffusion facilitators, the so called membrane transporters are active-transport proteins. Both types consist in general of bundles of hydrophobic transmembrane (TM) helices connected by inter-helical loops of very diverse length, structural characteristics shared with other membrane proteins such as GPCRs. The way in which membrane transporters make use of the available energy makes possible to classify them into ATP-powered pumps and secondary transporters. This thesis is going to focus in a specific set of ion channels.

2. Ion Channels

One of the early developed mechanisms by the cell to sense extracellular changes is based on ion channels and the generation of transmembranal ionic currents that will act as messengers [1, 2]. Ion channels are integral membrane proteins present in the membrane of several cellular and subcellular structures [3], assembled in such a way that they are embedded in the lipid bilayer forming pores and allowing the passive flux of ions upon changes in the environment [3]. Ion channels allow the permeation of a set of ion types, what is called ion selectivity, generally categorized into cationic and anionic channels. Ion flux through the cellular membranes mediates a tremendous variety of molecular processes essential for viability of living organisms, such as oocyte fertilization in humans [4], cell volume regulation or swimming behavior in unicellular organisms, movements of stomata pores in plants, muscle contraction, exocrine cell secretion, and the generation of neuronal excitability in higher animals [5]. Although ion channels are less divergent than other protein families, such as enzymes, there are still many types of channels opening and closing in concert to shape signals and responses to extracellular changes [3]. There are about 300 different ion channels depending on the cell type with specific amino acid fingerprint sequences, especially in the transmembrane domains [6]. This fact highlights their strong structural similarities and allows to talk about families of homologous channels that have evolved by successive gene duplication, mutation and selection (Fig. 1) [3]. The main ion channels subfamilies attending to their sequence identity and ion selectivity are listed here:

Potassium channels (K) are the largest family of ion channels [7]. They exist in nearly all life kingdoms [8] and they are mainly clustered attending to their structure and function into 4 main subfamilies: Voltage-gated (Kv), 6 transmembrane segments (TMs); Inward-rectifying (Kir), 2 TMs; calcium-activated (Kca), 6 TMs and Tandem-pore domain (K2p), 4 TMs (Fig. 1), (Table 1) [9].

Sodium channels voltage activated (Nav) comprise 10 proteins that are essential channels for action potential propagation. Mammalian genomes contain at least 8 voltage-gated Sodium channels (single polypeptide encoding for a 4-fold 6TMs subunit arrangement), (Fig. 1) that are mainly expressed in neurons, muscles, and glia [10]. Other sodium channels are eNAC or the nicotinic receptors.

Mammalian voltage-gated Calcium channels (Cav) are a diverse group of multimeric proteins (4-fold 6TMs subunit arrangement), (Fig. 1) classified attending to their biophysical and pharmacological profiles into L, P/Q/N, T and R subtypes (Table 1) [10]. The Cav subtypes are defined attending to the calcium currents they generate, according to physiological and pharmacological criteria. The L-type

current is defined as high voltage of activation, large single channel conductance and slow voltage-dependent inactivation. N-type currents were initially distinguished by their intermediate voltage dependence and intermediate rate of inactivation, much slower than T-type currents. The difference between P/Q/R types depends on the pharmacological sensitivity to several toxins.

Cyclic nucleotide-gated channel family (CNG) is composed of 6 members that are voltage-gated non selective ion channels (6 TMs), (Fig. 1) [11]. CNG channels are divided into two subfamilies attending to their sequence similarity: CNGA and CNGB (Table 1) [11]. In vertebrates, HCN channel family comprises 4 members of non selective calcium channels (HCN1-4), (Fig. 1) that are mainly expressed in heart and nervous system [12].

Finally other ion channel families, more distantly related but not less crucial for survival are the ligand gated ion channel receptors such as Glutamate or GABA receptors, the mechano-activated channels Piezo1 and Piezo2 [13] or the Chloride channel family that mediates in cell volume regulation (Table 1) [14].

Transient Receptor Potential channels (TRPs) (6 TMs) are the second more abundant family of ion channels [7], divided into 7 main subfamilies attending to their sequence identity: Melastatin (TRPM), Canonical (TRPC), Vanilloid (TRPV), Mucolipin (TRPML), Polycystic (TRPP), Ankyrin type (TRPA) and No-mechanoreceptor (TRPN) (Fig. 1), (Table 1) [15].

Family	Type	Number
Potassium channels (K)	Voltage-gated (Kv)	40
	Tandem-pore domain (K2p)	15
	Calcium activated (Kca)	8
	Inward rectifying (Kir)	15
TRP channels	TRPA (Ankyrin)	1
	TRPV (Vanilloid)	6
	TRPC (Cannonical)	7
	TRPP (Polycistic)	3
	TRPM (Melastin)	8
	TRPML (Mucolipin)	3
	TRPN (no-mechanoreceptor)	1
voltage-dependent	Nav1.1-1.9	9
	Nax	1
Voltage-dependent calcium (Cav)	L type	4
	P/Q/N type	2
	T type	3
	N type	1
HCN		4
CNG	CNGA	4
	CNGB	2
Mechano-activated channels	Piezo1, Piezo2	2
Chloride channels	CCLA	4
	CCLN	9
	CLIC	6

Table 1. Ion channel family diversity. Ion channel classification showing the channel families and number of genes clustered within each subfamily.

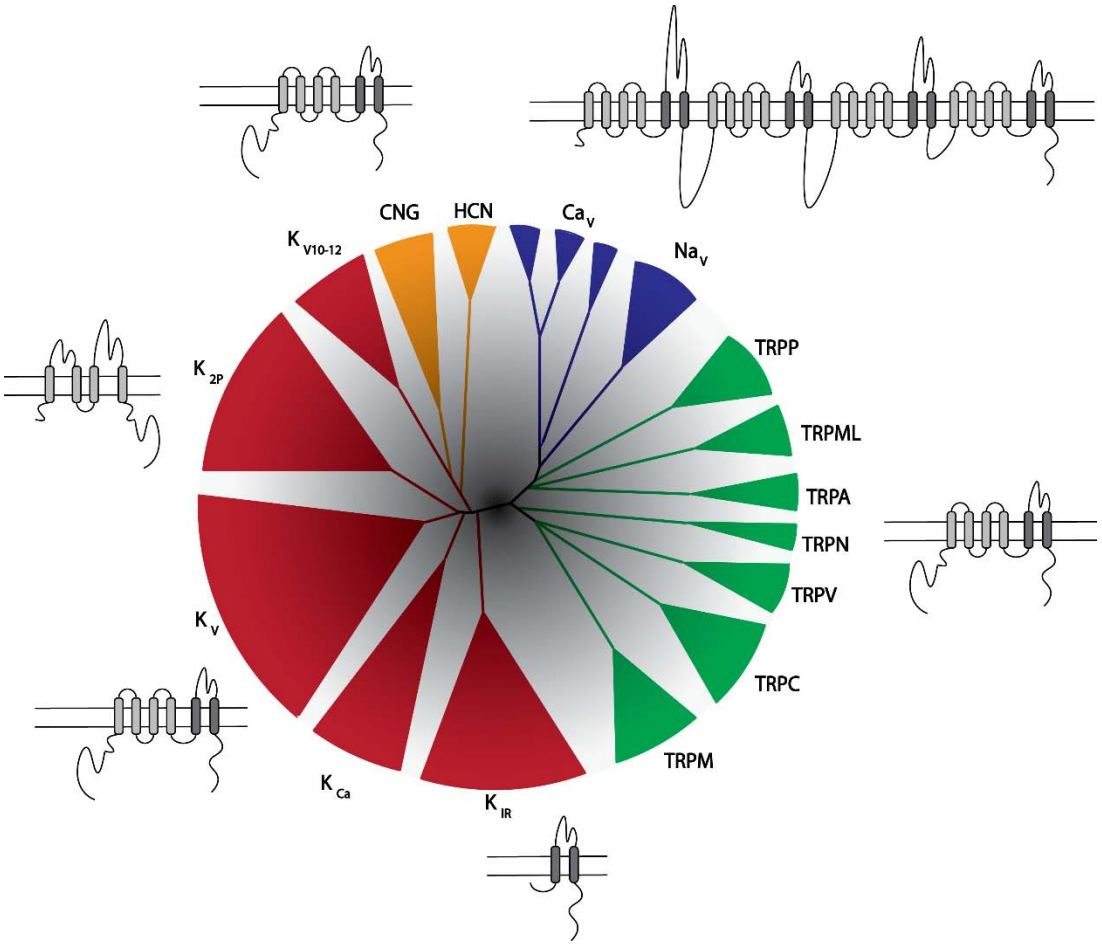

Figure 1. Cationic ion channel classification attending to sequence homology and ion permeability. Transmembrane topology is shown for each of the ion channel families. In red, Potassium channel family (K) with 4 main subfamilies: Voltage-gated (Kv), Calcium-activated (Kca), Inward-rectifying (Kir), and tandem-pore-domain (K2p). In green, Transient Receptor Potential (TRP) channel family, with 7 main subfamilies: Melastatin (TRPM), Canonical (TRPC), Vanilloid (TRPV), Mucolipin (TRPML), Polycystic (TRPP), Ankyrin type (TRPA) and No-mechanoreceptor (TRPN). In blue, Voltage-dependent calcium (Cav) and Voltage-dependent sodium (Nav) channels families. In yellow, Cyclic-nucleotide-gated (CNG) and Hyperpolarization-cyclic-nucleotide-gated (HCN) ion channels. Figure adapted from Frank H. yu et al [16].

Altogether, ion channels coordinate their gating to the extracellular conditions, generating intracellular ionic currents in response to changes in the environment and balancing cellular ion homeostasis as a first signaling of extracellular alterations. Ion channels rise important biomedical interest because their misregulation often leads to several pathological conditions, known as channelopathies, turning ion channels into potential molecular targets for diseases, such as dysplasias, cardiomyopathies, cancer, etc. [17, 18, 19].

3. Transient Receptor Potential Channels (TRP channels)

3.1. The TRP channel superfamily

TRP ion channels are a group of non-selective cation channels that act as polymodal cellular sensors for a wide spectrum of physical and chemical stimuli [15]. These channels were firstly discovered and described in 1960s in a mutant strain of *Drosophila melanogaster* [20, 21]. Since their discovery, TRP family has kept growing and nowadays they are the second widest ion channel family, where 28 members in mammals have been identified so far (Fig. 2a) [22]. TRP channels are present in a wide range of organisms from the yeast YVC1 (yeast vacuolar conductance 1) TRP channel to the 28 human TRPs [23]. Among life kingdoms, TRP channels have been mostly described in Fungi and Animalia. Despite this general distribution, extensive genomic studies have identified several distant homolog channels in the chlorophyte green algae, with at least some of them involved in calcium signaling such as TRP1 in *Chlamydomonas reinhardtii* or *Ostreococcus tauri* [24, 25]. The TRP family in Fungi, such as yeast, comprises only one member, YVC1, which encodes for a vacuolar membrane protein that function as a sensor of osmotic pressure [26] and generates intracellular calcium currents upon hypertonic shock stimulation [27]. Although homologous in structure and function, YVC1 is distantly related to mammalian TRPs and might be considered as a closer form to the ancestral TRPs [28].

	M. brevicollis	*D. Melanogaster*	*C. Elegans*	*C. Intestinalis*	*T. Rubripes*	*H.sapiens*
TRPV	1	3	5	2	4	6
TRPM	1	1	4	2	6	8
TRPC	1	3	3	8	8	7
TRPA	1	4	2	4	1	1
TRPML	-	4	1	9	2	3
TRPP	-	1	1	1	4	3
TRPN	1	1	1	1	-	-
Total	5	17	17	27	27	28

Table 2. TRP channel family distribution along evolution. Number of TRP channels corresponding to each of the subfamilies in several organisms: *Monosiga brevicollis* (*M. brevicollis*), the common ancestor of animal kingdom; *Drosophila melanogaster* (*D. melanogaster*), as member of Insecta; *Caenorhabditis elegans* (*C. elegans*), as member of Nematodes; *Ciona intestinalis* (*C. intestinalis*), as member of Ascidea; *Takifugu rubripes* (*T. rubripes*), as member of Chordata and Teleost fishes; and *Homo sapiens* (*H. sapiens*) as member of Mammals.

The origin of the actual diversity of TRP ion channels dates back to Choanoflagellates, unicellular and flagellated organisms considered to be the common ancestors of animals [29]. The Choanoflagellates present five homolog TRP channels, that would have expanded through gene duplication and generated the different TRP subfamilies present nowadays in animals (Table 2) [29].

Mammalian TRPs are clustered according to their sequence identity into 6 subfamilies: TRPA, TRPC, TRPM, TRPV, TRPML, and TRPP (Table 1, Table2 and Fig. 2a), as TRPN subfamily is lost in vertebrates (Table 2) [30]. The number of channels within each subfamily varies across species, depending on the number of gene duplications (Table 2) [30]. Most TRP subfamilies suffered a diversification, in parallel with the whole set of ion channels, maybe due to the need of higher organism to integrate more complex signals in order to maintain organism homeostasis.

3.2. TRP structural features

First approach to structure of TRPs was based on computational studies taking advantage of sequence homology to the close-related potassium channels [31, 32]. The first structural data available for TRPs came from the crystal structure of the soluble N-terminal ARD (Ankyrin Repeat Domain) of TRPV2, TRPV1 and TRPV6 [33, 34, 35], the C-terminal coiled-coil domains of TRPM7 [36], the C-terminal kinase domain of TRPM7 [37] and the coiled-coil C-terminal domain of TRPP2 [38]. Structure of full length TRP channels was revealed at low resolution using electron microscopy for TRPC3, TRPV1, and TRPV4 [39, 40, 41]. Structures have been challenging, due to the obvious difficulties with integral membrane proteins. Although available structures allowed for an interpretation on TRPs topology and conformational four-fold channel symmetry, the resolution did not allow the reliable location of transmembrane helices and specific folding of cytosolic domains.

A breakthrough in structural biology of large IMPs (Integral Membrane Proteins) has come altogether with TRPV1 and Cryo-EM [42]. Recently, the structural knowledge of IMP has suffered a revolution due to the improvement in Cryo-EM technology and the high resolution Cryo-EM structures for TRPV1, TRPA1 and TRPV2 (Fig. 2d) [42, 43, 44, 45].

With the current structural information we know that TRP family consists of a transmembrane domain formed by 6 transmembrane segments (S1-S6) and a pore loop between the segments 5 and 6 (S5-S6); with the N- and C-terminal domains facing the cytosol (Fig. 2b and d) [32]. TRPs are arranged in the membrane as tetramers, with the S5-S6 segments of the four subunits assembling the central pore

that coordinates the ion flux, and the S1-S4 transmembrane segments located surrounding the central S5-S6 core (Fig. 2b and d) [42]. Most TRP channels function as homotetramers, although the formation of heterotetrameric channels has been reported [46]. Channel heteromerization has been reported between members of the same subfamily or even between different subfamilies, such as TRPC and TRPV subfamilies, whose members are capable to heteromerize between them [46]. The formation of heterotetramers could potentially create a wider variety of TRP channels with differential gating properties and functional regulation, but functional implications are still under study and yet to be determined [46].

The N- and C-terminal domains, which together account for more than two thirds of the TRP channel sequence are located in the cytosolic intracellular environment (Fig. 2b). Although they are variable in length and domain distribution depending on the subfamily (Fig. 2c), these domains are supposed to carry out most part of the channel regulation [47]. The N-terminus of TRPC, TRPV and TRPA channels contain a different number of ankyrin repeats in the ARD, 4, 6 and 17 respectively (Fig. 2c). Similarly, TRPN subfamily contains a large ARD domain in the N-terminus (Fig. 2c). The ARD is a protein-protein recognition domain formed by two antiparallel alpha helices followed by a loop region linked to a β-hairpin structure [33]. ARD of TRPs is involved in several protein-protein interactions, mediates the binding of activating ligands and the gating by voltage and temperature in some TRP channels. In TRPV subfamily, ARD mediates the binding of compounds such as ATP, and the interaction with calmodulin and PI3K kinase [34, 48]. In TRPC subfamily ARD mediates the binding to phospholipase C (PLC) [49]. Alternatively, TRPM channels present 4 high homolog regions (MHRs) comprised along N-terminus [50] and some TRPM members present a calmodulin binding site similar to those found in TRPVs [51] (Fig. 2c). Distal N-terminus region, prior to ARD or MHR, is variable in length not just according to subfamilies, but even within each subfamily. Generally, distal N-terminus seems to be involved in channel trafficking regulation, although any consensus signal peptide or regulatory motif has been identified so far [52].

The C-terminal domain of TRP channels is mainly characterized by the presence of a highly conserved motif in the proximal region to the TMDs, called the TRP box or the TRP domain. TRP box can be found in TRPM, TRPV, TRPC and TRPA subfamilies (Fig. 2c). Being in close proximity to the pore region, the TRP box establishes several intra-subunits interactions, rendering to a correct channel assembly and playing an important role coupling the stimulus reception to the channel gating [53].

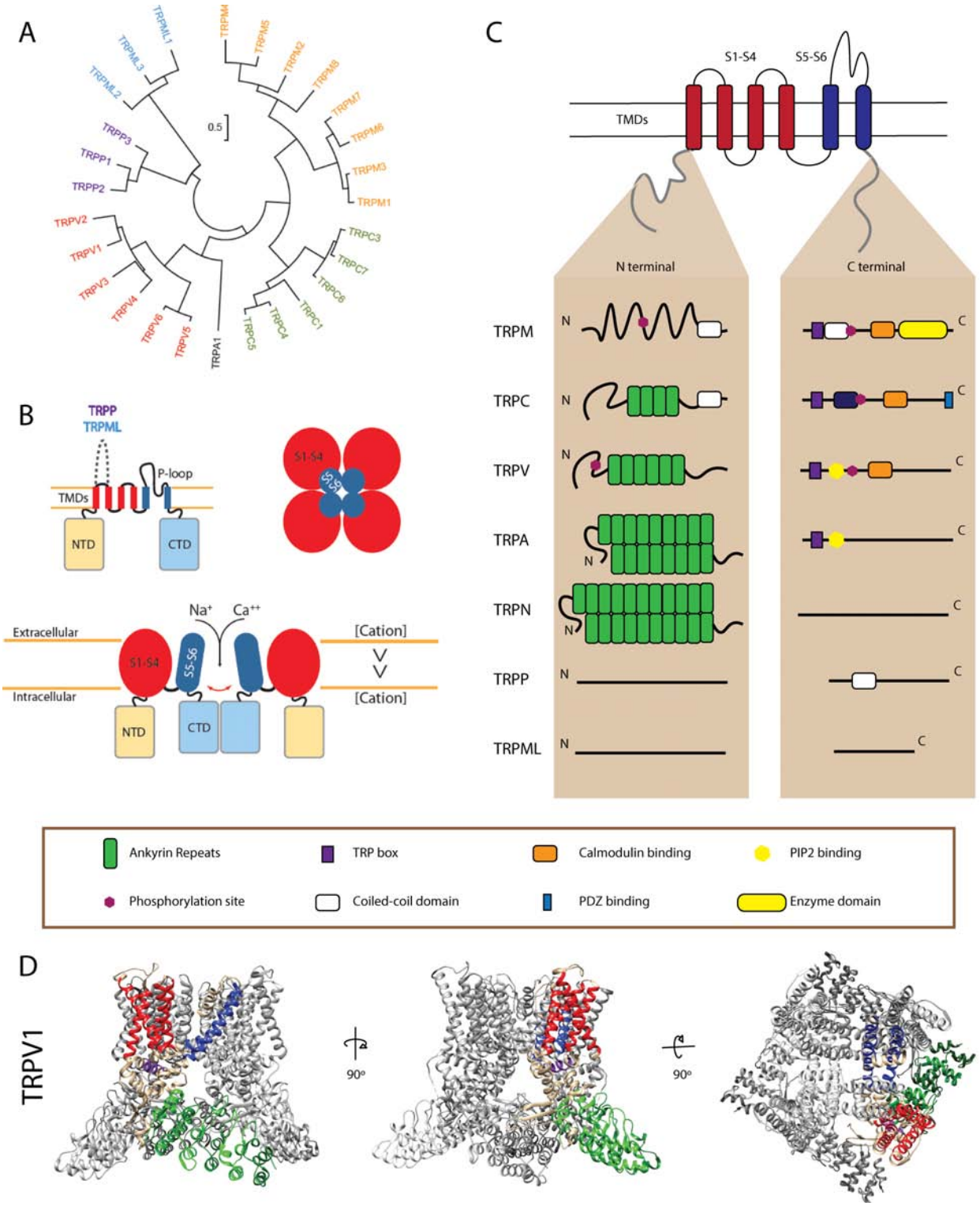

Figure 2. TRP channel subfamily evolution and structural features. A) Mammalian TRP channels associated by homology, showing the main 6 subfamilies TRPC, TRPV, TRPM, TRPA, TRPML, TRPP and the members within each subfamily. B) TRP general transmembrane structural features, showing the 6 transmembrane segments. In blue, S5-S6 transmembrane segments, clustered in the center of the channel and forming the ion gate. In red, S1-S4 transmembrane segments surrounding the channel gate. N-terminal (NTD) and C-terminal (CTD) are in the

intracellular side of the membrane. C) N- and C-terminal domain composition and structural features according to the TRP channel subfamily. D) TRPV1 Cryo-EM structure from different angles showing the transmembrane topology and the spatial arrangement of N- and C-terminal tails of TRPVs. The ARD domains (green), TM1-4 segments (red), TM5-6 segments (blue) and TRP box (magenta) have been highlighted in one of the four subunits to show general domain spatial distribution.

Phosphatidylinositol 4,5-bisphosphate (PIP2) binding has been mapped to close proximity of TRP box in TRPV and TRPA members [54, 55]. In general, the C-terminus is quite variable among subfamilies, either in length and domain composition. Calmodulin binding domains have been also characterized within the C-terminus of TRPM, TRPC and TRPV members (Fig. 2c), being crucial, as in the N-terminal calmodulin binding domains, for calcium dependent regulation of channel activity [56, 57, 58]. Other domains such as coiled-coil domains are present in the C-terminal of TRPM and TRPP subfamilies, being necessary for proper channel assembly [36, 38] (Fig. 2c). One peculiar trait among TRPM subfamily is the presence of an a-type serine/threonine kinase domain attached to the distal C-terminal tail of the channel [37], codifying on the same protein for an ion channel and a kinase (Fig. 2c).

Although general structure is maintained among TRPs and transmembrane region topology is quite homogeneous, TRPs are regulated in a very diverse manner and each of them present its particular traits. These differences are represented mainly by the diversity of functionally disparate domains present in the cytoplasmic N- and C-terminus (Fig. 2c).

3.3. TRP functional features

Generally, TRP channels are non-selective ion channels with a permeability ratio between calcium and sodium P_{Ca}/P_{Na} about ≤ 10, that trigger intracellular cation currents, mainly formed by Ca^{2+}, Mg^{2+}, and Na^{+}. Exceptionally, TRPM4 and TRPM5 are highly permeable to monovalent cations, TRPV5 and TRPV6 are highly permeable to calcium and TRPM6 and TRPM7 have a higher affinity for magnesium. Conversely, trivalent cations such as Lanthanum (La^{3+}) and Gadolinium (Gd^{3+}), act as pore blockers, inhibiting cation flux through the pore. TRP channels pore is formed by S5-S6 and the pore loop between these two segments, that contains a consensus sequence called selectivity filter which is variable among TRP subfamilies (Fig. 3) [42]. The pore is divided in upper and lower gates, the two regions that present a higher narrowing of the pore (Fig. 3).

TRPs trigger intracellular cationic currents upon ligand binding, either endogenous or exogenous agonists; or physical changes in temperature, osmolality or cell volume, mechanical stretch forces, or

voltage [59]. These heterogeneous ways to trigger channel gating can be integrated in an allosteric model, where several closed states are predicted and each stimuli: agonist, voltage or temperature; is able to trigger transition from one closed state to one open state, distinct from other open states mediated by other stimuli. The model implies that mechanisms responsible for integrating each stimuli to the pore opening are independent and differentially located within the channel [59]. Some TRPs are constitutively opened, generating a leak entry of cations though the plasma membrane and resulting in rising basal intracellular calcium and/or sodium levels. When open, TRPs generate a transient depolarization of the cells from their resting membrane potentials and provoke a further increase of intracellular Ca^{2+} and/or Na^{+}. This raise of calcium levels is further potentiated by phospholipase C (PLC) activity coupled to TRPs that triggers opening of IP3 receptor and release of the Endoplasmatic Reticulum (ER) calcium stores [60].

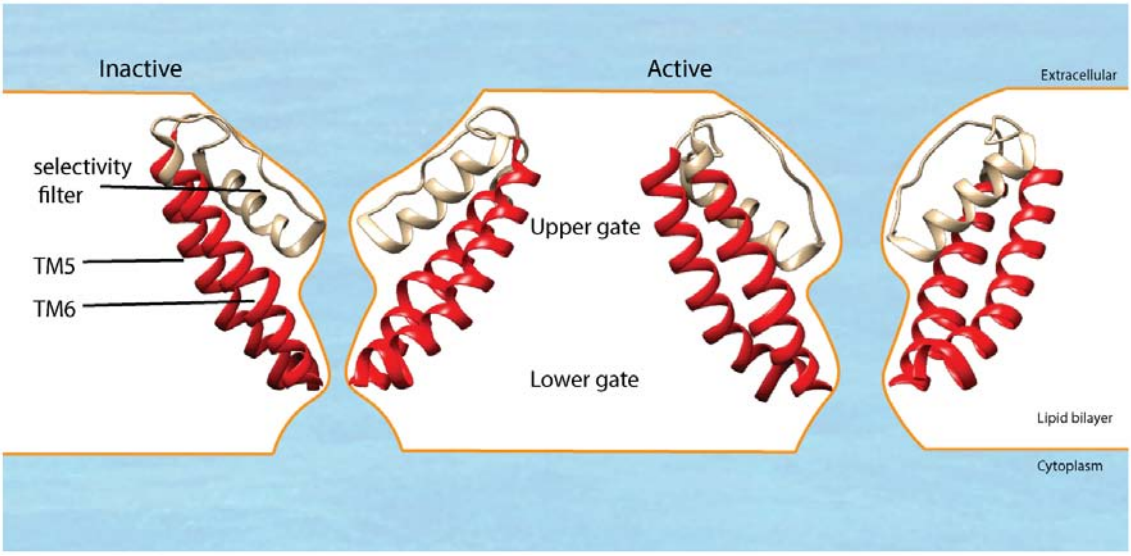

Figure 3. Pore model based on TRPV1 Cryo-EM structure. 2D representation of the pore region of TRPV1, with TM5 and TM6 highlighted in red [61]. Inactive state, closed pore, on the left; and active state upon Resiniferatoxin (RTX) and capsaicin addition, open pore, on the right. Blue area represents the water accessible area. It is visible the presence of two constriction areas named as gates, upper and lower gate. The upper gate is formed by the selectivity filter and the loop between TM5-TM6. Lower gate is determined by the bottom side of TM5 and TM6. The channel opening implies a movement to widen the water accessible area of the gates, either one or both of them, depending on the stimuli.

The TRP channels in general require participation of endogenous signaling proteins for their activation and regulation, such as binding to G-coupled protein receptors (GPCRs), PLC, calmodulin, protein kinases or phosphatases [62][63]. Of special interest is the regulation that the lipid metabolism

in general, and the cellular phosphoinositide lipid levels in particular play over channel gating. PIP2 has been shown to play a pivotal role in channel regulation, as its presence is needed in order to conform the channel in a sensitized state and PIP2 depletion generally leads to channel desensitization [64].

3.4. TRP and disease

TRP channels misregulation or malfunction has been linked to several diseases and pathological conditions. TRPs play an important role in keeping the cellular ion homeostasis. Calcium signaling has a high impact on many cellular processes and regulates transcription factors such as NFAT, that upon TRP channel gain of function, as increased gating and calcium entry, promotes cardiac hypertrophy [65] or other calcium dependent pathologies such as muscular dystrophies [66]. Nevertheless, TRPs integrate environmental changes and mediate in somatosensation processes such as thermoception, mechanoception, and even nociception [67]. TRP malfunction uncouples signaling cascades and leads to inadequate organism responses upon external insults. Ultimately, several TRP channels have been shown as capable to control cell growth, proliferation and cell cycle, leading to growth abnormalities or even cancer when not properly regulated [68].

4. Transient Receptor Potential Vanilloid (TRPV) subfamily

4.1. TRPV subfamily origin and evolution

The TRPV subfamily, vanilloid, was named after the first member characterization, the vanilloid/capsaicin receptor TRPV1 [69]. TRPV subfamily in mammals comprises 6 members that can be further divided into 2 subgroups attending to their sequence identity: TRPV1-4 and TRPV5-6. TRPV1-4 group is formed mainly by non-selective low calcium permeable channels that can be potentially activated by thermal stimuli, whereas TRPV5-6 group is characterized by a higher permeability to calcium (Table 3) [70], i.e. calcium specific.

TRPV subfamily in non-vertebrates comprises 2 member in *C. elegans,* named OSM-9 and OCR-2 and 2 members in *D. melanogaster*, named as Nanchung and Inactive [71], that are considered the closest to the ancestral TRPV channels. The TRPV subfamily diversity in mammals emerged from the common ancestor of teleost fishes and terrestrial vertebrates through repeated gene duplications; followed by sequence divergence that constitute the current TRPV repertoire, composed by 6 channels

of very diverse physiological properties [72]. In humans, TRPV5 and TRPV6 channels are clustered together and located in close genomic regions, within the 7th chromosome (Table 3), being the first to diverge from TRPV1-4 subgroup (Fig. 4). Although hierarchical clustering locates TRPV4 as closest to TRPV1-2 (Fig. 4), TRPV4 seem to have diverged earlier from TRPV1-3, according to genomic location (Table 3). TRPV4 is located within the 12th chromosome whereas TRPV1-3 are located in the 17th chromosome (Table 3), in such a close proximity that recent tandem gene duplication in common ancestors of fish and Tetrapods has been proposed to be the origin of these 3 genes. TRPV3 is present in all vertebrates but fish although the homology hierarchical clustering strongly indicates that TRPV1-2 genes in fishes appear after the divergence between TRPV3 and TRPV1-2 (Fig. 4). Thus, TRPV3 emerged before divergence of fish and Tetrapods and was lost in fish lineages [73]. Similarly, genomic location and hierarchical clustering of TRPV1 and TRPV2 genes revealed that both genes were already present in the common ancestor of tetrapod and fish and TRPV2 was lost through fish lineage (Fig. 4) [73].

Name	Chromosome location	Gene code	Uniprot code	Permeability Ca/Na
TRPV1	17p13.3	ENSG00000196689	Q8NER1	9.6
TRPV2	17p11.2	ENSG00000187688	Q9Y5S1	3
TRPV3	17p13.3	ENSG00000167723	Q8NET8	2.6
TRPV4	12q24.1	ENSG00000111199	Q9HBA0	6
TRPV5	7q35	ENSG00000127412	Q9NQA5	>100
TRPV6	7q33–q34	ENSG00000165125	Q9H1D0	>100

Table 3. TRPV subfamily features, based on Montell et al [70]. Genomic location, Ensembl and Uniprot codes are annotated for the 6 TRPV human channels. Permeability, indicating calcium selectivity was assessed for each channel, showing a clear difference in the ion selectivity between TRPV1-4 and TRPV5-6 groups.

TRPV subfamily folding and gating follow the same pattern described in general for TRPs, so we do not go into deeper detail as subfamily here and rather state the peculiarities when talking of each channel location and protein partners. Furthermore, as this thesis was focused on TRPV1, TRPV2 and TRPV4 we will further focus on the TRPV1-4 subgroup.

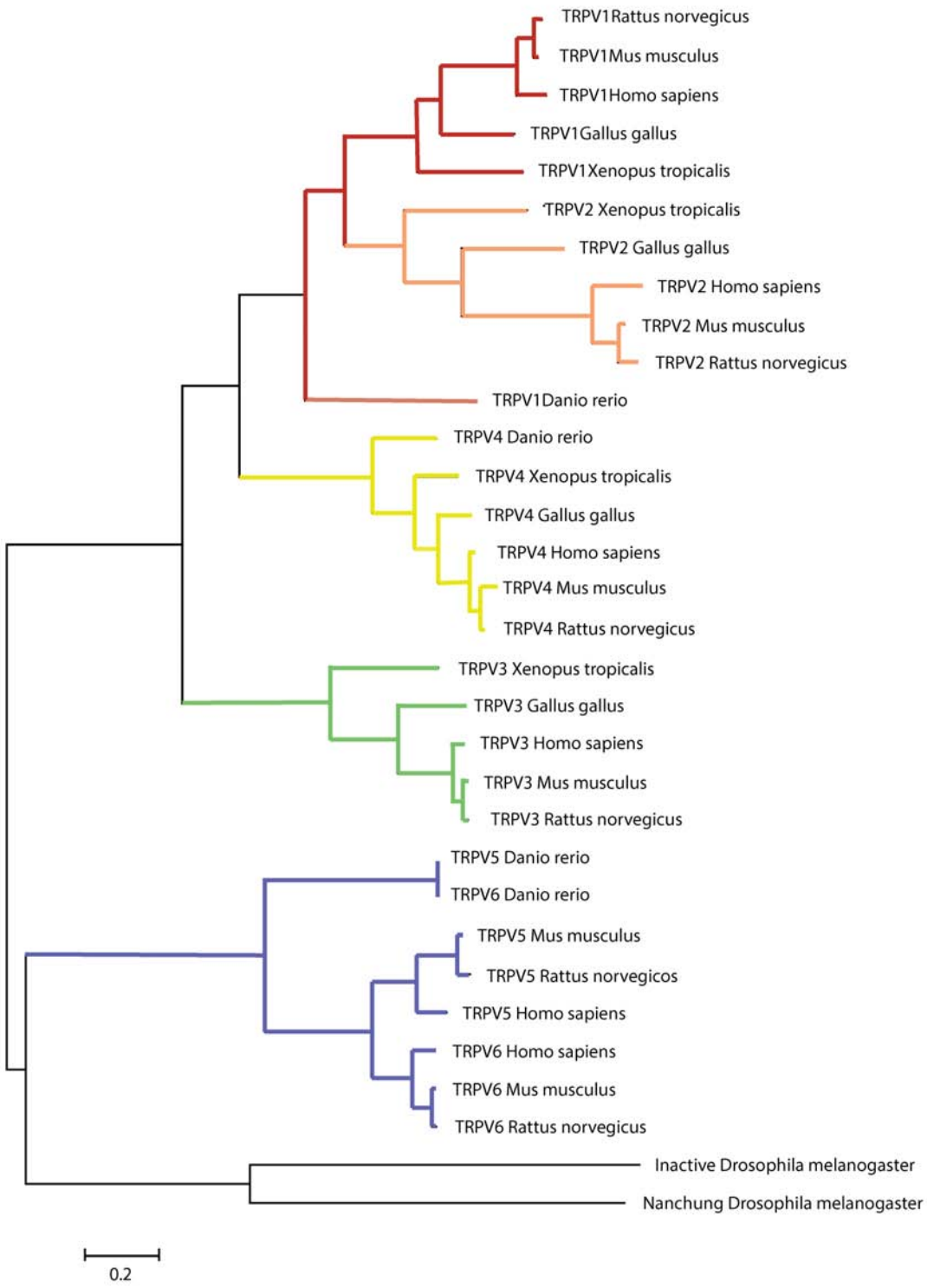

Figure 4. Maximum likelihood hierarchical clustering of TRPV subfamily. Main TRPV duplication points through vertebrate evolution, Inactive and Nanchung homolog TRPV genes from *D. melanogaster* were used as external point to root the tree for the clustering. Colored as follows: in blue TRPV5 and TRPV6 representatives, in green TRPV3, in yellow TRPV4, in red TRPV1 and in orange TRPV2.

4.2. TRPV1-4 channels physiology

TRPV channels are widely distributed within the body and mainly found in nervous system and epithelial tissues, where they exert their respective roles sensing environmental changes and generating intracellular responses mediated by cation flow.

TRPV1 is expressed in neuronal and non neuronal cell types. Outside the nervous system, TRPV1 mainly expresses in epithelial tissues of reproductive organs, spleen, stomach, intestine, kidney, pancreas, liver, lung, bladder, skin, skeletal muscle, and immune system mast cells, macrophages, and leukocytes (Fig. 5 and 6).

TRPV1 expression profiling was initially determined by capsaicin sensitivity, restricting its expression to primary sensory neurons and mainly located on the neurofilament negative small and medium sized dorsal root ganglion (DGR) cells [69, 74]. In central nervous system (CNS) TRPV1 was also found in the heat-sensing neurons from preoptic-anterior hypothalamus, suggesting a role in body temperature regulation [69]. TRPV1 mRNA expression and immunoreactivity confirm the presence of the channel in the hypothalamus [75]. Other brain structures such as neocortex or the C and Aδ fibers from spinal cord show also a high TRPV1 immunoreactivity [76]. Some reports indicate that TRPV1 is also expressed in glia cells such as astrocytes from the spinal cord and the circumventricular organs of mice brain [77, 78]. The heart, tooth pulp, extrinsic sensory nerves of the gastrointestinal tract, lung or the muscle and mucosa layers of urinary tract are innervated by TRPV1 fibers. TRPV1 seems to play a role in regulating correct functioning of all these organs. TRPV1 positive nerves are involved in the cardiogenic sympathoexcitatory reflex during myocardial ischemia, and activation of TRPV1 seems to play a role in cough and intestinal motility disorders [79, 75, 80, 81].

Outside the nervous system TRPV1 is also expressed in many non neuronal cell types. In skin, keratinocytes express TRPV1, and activation by capsaicin or RTX produced an upregulation of cyclooxygenase 2 (COX-2) followed by an increased release of interleukin-8 and prostaglandin E2, suggesting a role in inflammation [82]. TRPV1 was also found in arteriolar smooth muscle cells, and some channel agonists have been reported to cause vasodilatation when ectopically applied [83]. TRPV1 activation by dietary capsaicin increases nitric oxide (NO) production in endothelial cells, improving endothelium dependent vascular relaxation and preventing hypertension [84]. In the lungs, TRPV1 is present in epithelial cells and TRPV1 activation by pollutants, such as nanoparticles, induce apoptosis and mediates in the airways damage [85]. In the gastrointestinal tract, TRPV1 is also involved in

inflammatory processes while in the bladder mediates contraction of the epithelium and in pancreatic cells of rats regulates insulin secretion [86, 87, 88].

TRPV2 channel presents a ubiquitous body distribution. TRPV2 expression within the nervous system has been reported. Outside the nervous system TRPV2 is mainly found in skeletal muscle, heart, lung, skin, kidney, thyroid, testis and immune system cells (Fig. 5 and 6).

TRPV2 expression has been detected in rat, mouse and macaque brains [89, 90, 91], being the highest expressing TRPV channel in the neurons of mouse forebrain region [92]. TRPV2 presence in the brain is especially high in hypothalamic regions of the forebrain and correlates with several brain structures related to somatosensation and osmoregulation, suggesting a role of this channel in the maintenance of osmotic balance [93]. TRPV2 expression in neurons is concentrated in developing growth cones, where it has been described to promote the axon outgrowth during neuron morphogenesis [94]. Apart from neurons, glial cells such as astrocytes present functional TRPV2 in their plasma membranes [95]. TRPV2 from astrocytes is activated by lipidic compounds such as lysophosphatidylcholine (LPC), indicating a potential TRPV2 regulation of glial and neuronal activities in response to changes in lipidic composition [96]. In the peripheral nervous system, TRPV2 is mainly localized in developing mouse DRG and spinal motor neurons [94], although TRPV2 expression in adult rat DRG and trigeminal ganglia (TG) has been reported [97, 98]. Within this structures, TRPV2 is concentrated in primary afferents neurons, mainly in A and C fibers containing myelinated sensory neurons [99]. Intestine relaxation in mice seems to be inhibited by TRPV2 antagonist whereas agonist inhibited muscle contraction, suggesting that TRPV2 may play a role controlling the activity of sympathetic muscles like those of the intestinal track [100].

Outside of nervous system TRPV2 is also highly expressed in skeletal muscle, where it localizes mainly in intracellular pools and translocates to the plasma membrane upon Insulin Growth Factor (IGF-1) signaling (Fig. 5 and 6) [101]. In cardiomyocytes, TRPV2 participates in contractility under physiological conditions, regulating through its activity the IGF-1/PI3K/AKT pathway. Mechanical stretch sensed by TRPV2 promotes IGF-1 secretion and stimulation of cardiomyocytes, promoting their surveillance and functionality. The disruption of this positive feedback by TRPV2 loss results in impairments of cardiomyocyte function. Thus, TRPV2 plays an important role in the maintenance of cardiac structure and function [102, 103].

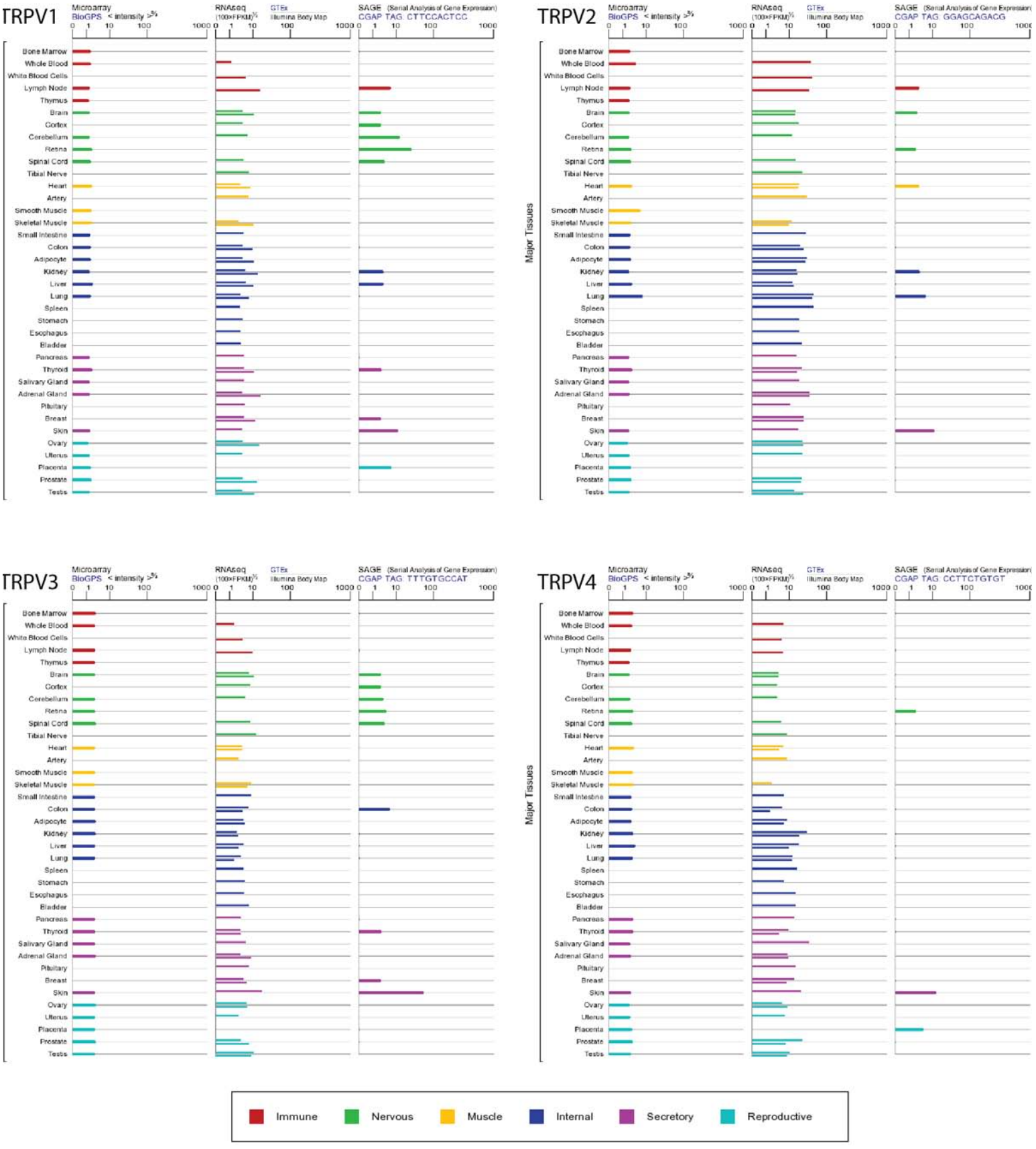

Figure 5. Gene expression profiles for TRPV1-4 channels. RNA expression levels from TRPV1 (top left), TRPV2 (top

right), TRPV3 (bottom left) and TRPV4 (bottom right) extracted from Gene Cards, human gene database (www.genecards.org). First row in each panel represents the expression profiling data from BioGPS, a dataset of 76 normal human tissues and compartments hybridized against HG-U133A. Second row contains the expression levels of 51 normal human tissues, cells and fluids, based on 2712 samples. Third row contain the estimated gene expression based on the data mining Serial Analysis of Gene Expression (SAGE) tool that cluster information from Hs.best_gene, Hs.best_tag and Hs_GeneData databases.

Furthermore, TRPV2 is over expressed and its activity produces an increase of stretch-induced cell damage in mice models of Duchenne muscular dystrophy (DMD) [66]. TRPV2 is also found in smooth muscle and endothelial cells of rabbit and human arteries [104, 105] and in smooth muscle cells of veins in rats [106], suggesting an additional role of TRPV2 in the circulatory system. TRPV2 is also expressed in intracellular compartments of pancreatic beta cells (Fig. 5 and 6). Similarly to the regulation in muscle cells, TRPV2 is translocated to the plasma membrane upon insulin stimulation and the activity of the channel promotes insulin secretion, indicating a crosstalk that might locate TRPV2 as a key player in metabolic processes and diabetic pathological conditions [107]. Immune organs, such as spleen contain TRPV2 expressing cells (Fig. 5 and 6). Many resident macrophage populations such as the lung alveolar express TRPV2 and the channel activity regulates phagocytic processes [108]. Finally, other immune cells as mast cells and lymphocytes in peripheral blood contain functional TRPV2 [109, 110]. In the mast cells, TRPV2 activation by mechanical stimuli produced calcium mediated degranulation [109].

TRPV3 is mainly located within the skin and the intestine, although its expression has been also reported in the brain (Fig. 5 and 6). TRPV3 is located and constitutively active at physiological temperature in dopaminergic neurons of *substantia nigra* of the rat brain and CA neurons from rat hippocampus and hypothalamus [111, 112]. TRPV3 presence in the brain, together with TRPV4, seems to contribute to ischemia induced membrane depolarization and intracellular calcium accumulation, pointing to these TRP channels as potential responsible for the neuroprotective effect of hypothermia in the brain [112, 113]. Furthermore, TRPV3 is found in neurons from hypoglossal nucleus and medial nucleus tractus solitarius, where it has been associated to development of hyperphagia and obesity in rats [114]. In the peripheral nervous system, TRPV3 colocalizes with TRPV1 in sensory neurons from DRG, potentially forming heterotetrameric channels [115]. TRPV3 expression was also detected at mRNA levels in spiral and vestibular ganglia [116], where it may play a role in hearing sensation.

TRPV3 is mainly found in skin keratinocytes where it exerts a role in direct peripheral somatosensation (Fig 5 and 6). Indeed, TRPV3 in the mostly expressed TRPV in human skin and there is a

growing evidence of the channel participation in multiple cutaneous processes [117]. Human and mouse keratinocytes arrest their proliferation and enter in apoptosis upon TRPV3 activation [118]. TRPV3 participates in migration and wound healing by promoting nitric oxide (NO) synthesis via nitrite dependent pathway [119], which controls keratinocyte differentiation and inflammation. Furthermore, TRPV3 is highly involved in the formation and maintenance of the skin barrier and TRPV3 deletion leads to impaired epidermal barrier structure [120]. This effect is mediated by interaction of TRPV3 with epidermal growth factor receptor (EGFR) that enhances channel activity and stimulates transforming growth factor alpha (TGFα), which promotes cell proliferation, differentiation and development. [120]. Altogether, TRPV3 activation ultimately regulates hair morphogenesis and follicle cycling in human and mice, driving to hair loss and a hairless phenotype in rodents [121, 122]. Finally, TRPV3 channel is also expressed and functional in the epithelial cells throughout the gastrointestinal tract, in the distal colon, jejunum and ileum, where it is involved in pro-inflammatory responses (Fig. 5 and 6) [123, 124].

TRPV4 is ubiquitously expressed and found in brain, heart, arteries, intestine, pancreas bladder, kidney, liver and female reproductive tract (Fig. 5 and 6) [125]. TRPV4 is expressed in the DRG neurons and the osmosensory neurons from organum vasculosum lamina terminalis (OVLT) and supraoptic nucleus (SON), two regions responsible of keeping osmotic balance within the body [126]. TRPV4 in the hippocampal neurons is active at physiological brain temperatures and thereby controls their excitability in a temperature dependent manner [127], suggesting potential implications of TRPV4 in memory development. A part from neuronal expression, TRPV4 is found in glia cells and its expression controls glia cell volume, maturation and activation. About 30% of astrocytes express TRPV4 and this subpopulation is responsible for initiating excitatory gliotransmitter release of glutamate and enhance synaptic transmission [128]. In the peripheral nervous system sensory organs, TRPV4 is also found in the epithelial cells of the human cornea [129].

Outside the nervous system TRPV4 is mainly expressed in epithelial tissues (Fig. 5 and 6). In the skin, TRPV4 is found in keratinocytes, where it interacts with β-catenin, playing an important role in the formation and functioning of the intercellular junction-dependent barrier [130]. TRPV4 is found in the epithelial cells of the bronchiae, the trachea and the larynx [131, 132], where it is activated upon insult of the airways by pollutant particles and contributes to inflammation and airflow obstruction [133, 134]. Indeed, TRPV4 is involved in promotion of chronic obstructive pulmonary disease (COPD) and several single nucleotide polymorphisms of TRPV4 have been associated to COPD [135]. In the intestine TRPV4 participates by its activation in the serotonin and histamine induced visceral hypersensitivity (Fig. 5 and

6) [136]. Nevertheless, high levels of TRPV4 were detected in epithelial cells of human and mice colon, and TRPV4 expression was upregulated in inflamed colons from mice. Activity of TRPV4 produced an intracellular calcium increase and chemokine release, contributing to pro-inflammatory responses and arguing for a role of TRPV4 in colitis and other inflammatory bowel diseases [137]. In the urothelium TRPV4 is present in the urothelial cell layer and senses the filling state of the urinary bladder. Inhibition of the channel by knockdown or antagonist targeting proved the potential of this channel as molecular target for the treatment of bladder dysfunction [138]. In the pancreas, TRPV4 is highly expressed in beta cells and activation of the channel enhances glucose stimulated insulin secretion [139]. Finally, TRPV4 is found in many other epithelial tissues such as mammary gland [140], oviduct [141], bile duct [142], in smooth and skeletal muscle [143, 144], immune cells [145, 146] and chondrocytes [147] (Fig. 4 and 5).

TRPV5 and **TRPV6** have both a similar pattern in terms of distribution, being mainly found in intestine and kidney, where they regulate calcium passive reabsorption in the luminar or apical nephrite membrane and act as key players in organism calcium homeostasis [148, 149]. TRPV5 seems to be the major isoform in kidney, whereas TRPV6 is also found in the prostate, stomach, brain or lung.

As a summary, although TRPV1-4 channels have a distinct pattern of expression, they are widely spread within the body and found within most part of tissues and organs (Table 3 and Fig. 5), where they exert very diverse roles to assure correct organism functioning. In general, TRPV1-4 expression profile, together with the rest of channels and receptors, determine the sensitivity and responsiveness of each cellular type and organ to the challenge by different stimuli. Thus, TRPV1-4 expression profile partially determines the distinct responses generated by each cellular type. TRPV1-4 misregulation leads in most part of cases to pathophysiological conditions due to the decoupling of the environmental changes and the right cellular responses, leading to imbalance of intracellular signaling cascades downstream of these channels.

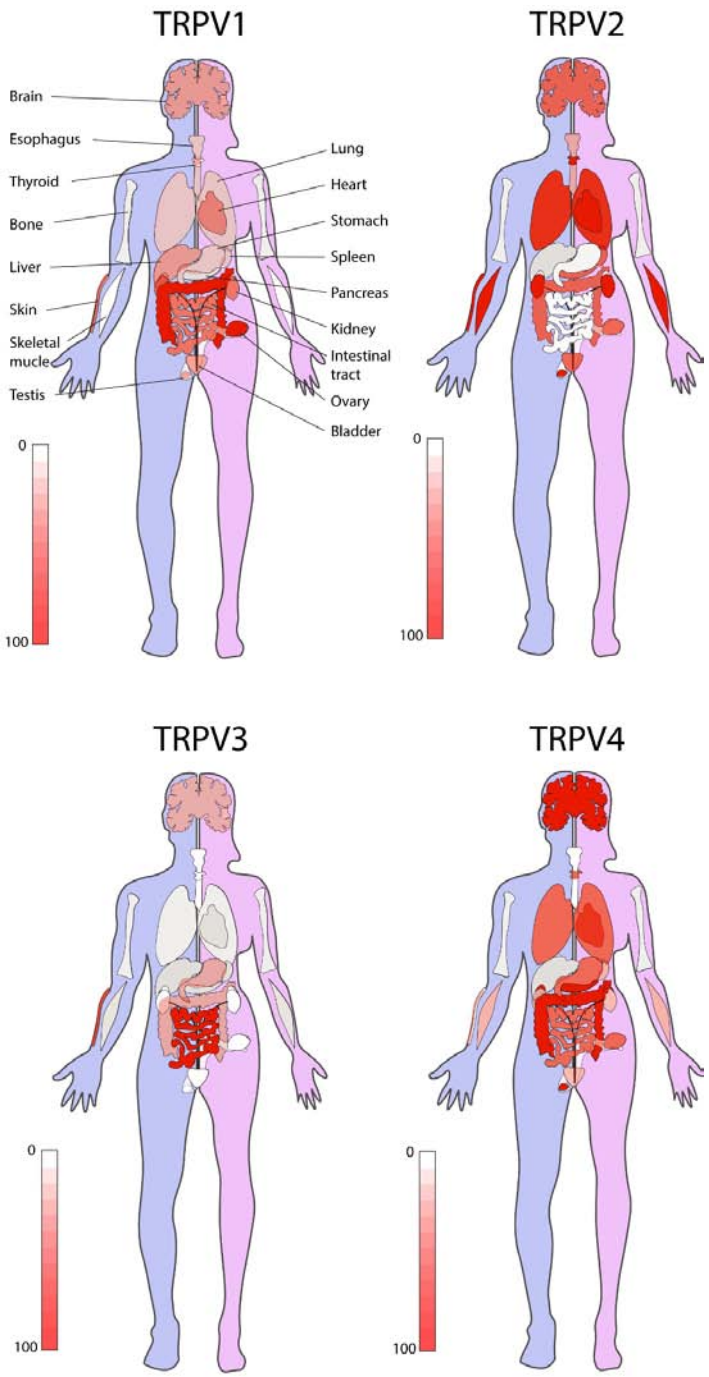

Figure 6. TRPV1-4 tissue expression based on The Human Protein Atlas. The channel expression levels were represented in a gradient of red color, showing the distribution and relative abundance of each channel among the human body. The expression level values for each channel within each tissue were extracted from The Human Protein Atlas webpage (http://www.proteinatlas.org), normalized from 100 (maximum expression level, intense red) to 0 (minimum expression level, white) and the tissues were colored according to the red scale. The levels were normalized independently for each channel, just allowing the comparison between the protein levels of each channel among the different tissues. Although levels are not comparable between channels the overall pattern of channel expression can be compared.

4.3. TRPV1-4 channels pharmacology

The pharmacology of TRPV channels has been extensively reviewed [150, 151]. Here we just focused in some of the main agonist and antagonist for each channel, as the TRPV channel pharmacology is wide and diverse.

TRPV1 was the first described member of the TRPV subfamily and up to date is the better pharmacologically characterized TRPV. TRPV1 channel and, subsequently the family were named due to the activation by vanilloid and endovanilloid compounds. TRPV1 is an integrator of multiple signals, capable to be activated by capsaicin, the pungent compound of chili peppers and other noxious stimuli such as heat (≥43°C) [69], or toxins from Jelly fish or tarantula (Annex table 1) [69]. TRPV1 evoked currents are potentiated by low pH, similar to those acidic conditions described during tissue acidosis or injuries [152]. Exposure to ethanol, nicotine or pro-inflammatory cytokines promotes a further sensitization of the channel (Annex table 1) [153, 154, 155]. Lipidic compounds such as anandamide or hydroxioctadecadienoic acid (HODE) also stimulate TRPV1 and generate intracellular calcium currents (Annex table 1) [156, 157]. Lipidic compounds play a pivotal role regulating TRPVs, while some have shown to activate TRPV1 others, specially PIP2, directly bind the channel and maintain a sensitized state that upon PIP2 depletion produces a de-sensitization of the channel [158]. Finally, capsaicin-like compounds such as hydroperoxyeicosatetraenoic acids (HPETE) promote TRPV1 activation (Annex table 1) [159]. Apart from already known wide spectrum antagonists, such as ruthenium red or trivalent cations, some specific TRPV1 inhibitory compounds have been developed. Capsazepine, a competitive capsaicin antagonist, has been known for decades, even before TRPV1 was firstly cloned (Annex table 1) [160]. More recently other TRPV1 antagonists such as JNJ17203212 and JNJ39729209 have been described (Annex table 1) [161, 162]. Further antagonists such as SB 705498 and XEN-DO501 have been generated and tested in clinical trials of cough models, showing a reduction in TRPV1 activity (Annex table 1) [163, 164].

TRPV2 was firstly described as a thermosensor of noxious heat temperatures, with an activation threshold higher than 52ºC [165], but its role in sensing temperatures has been controversial. TRPV2 pharmacology is limited, as most known activators show species dependency and few of them are specific. TRPV2 is activated by Δ9-tetrahydrocannabinol, cannabidiol, and Δ9-tetrahydrocannabivarin (Annex table 1) [166]. Although they modulate TRPV2 activity, cannabinoid derivatives are not specific and they trigger also activation of cannabinoid receptors (CBD1 and CBD2) as well as other TRP channels

as TRPV1 and TRPA1 [166]. 2-APB, one of the first identified agonist of TRPV2, also shows unspecificity and is able to activate to some extent TRPV1 and TRPV3 (Annex table 1) [167]. Furthermore, It has been described that 2-APB is species-specific and does not activate human TRPV2 [167]. Similar to TRPV1, ruthenium red and trivalent cations are able to work as unspecific TRPV2 channel blockers. Probenecid, another TRPV2 non-specific activator, shows higher affinity for this channel compared to other TRPs, being a promising candidate to use as TRPV2 agonist (Annex table 1) [168]. Although not highly specific, SKF96365, Amiloride and Tranilast can work as TRPV2 antagonists (Annex table 1) [169, 100].

TRPV3 was firstly cloned attending to its sequence identity to other heat-activated TRPV channels, sharing 40% identity with TRPV1. First TRPV3 characterization determined channel activation by temperature in the physiological range of 32 to 39°C and by agonist binding such as Camphor and 2-APB (Annex table 1) [115, 170, 171]. A broad spectrum of natural compounds has been reported to induce TRPV3 gating, including extracts from spices such as Camphor, Carvacrol, Thymol and Eugenol (Annex table 1). All these chemicals act as non specific channel agonists with potencies that range from high µM to low mM [172]. Farnesyl pyrophosphate (FPP), an intermediate metabolite in the mevalonate pathway, has been identified as endogenous ligand for TRPV3 [173], while synthetic chemicals such as 2-APB, DPBA, 6TBC and Incensole acetate, an incense component, have been developed to improve channel agonist specificity (Annex table 1) [174, 172, 175]. Finally lipids such as Arachidonic acid (AA) have been shown to sensitize TRPV3 [176]. Concerning antagonists, TRPV3 can be blocked by non selective ruthenium red and synthetic compounds HC-001403, GRC 15133, GRC 17173 and 17(R)-resolvin D1 that display a higher affinity for the channel but low specificity (Annex table 1) [177, 178]. Although TRPV3 abundance of agonist and antagonist, specificity still remains an issue and further drug screens will have to be carried out to accomplish a fine targeting of this channel.

TRPV4 was firstly identified as a sensor of hypotonic cell swelling [179], although later on the channel has shown a surprising gating promiscuity, being activated by physical and chemical stimuli. TRPV4 is a thermosensitive channel, active at physiological temperatures, generating a cation leakage within the cell. Furthermore, its activity is potentiated with temperatures higher than 38ºC [180]. TRPV4 evoked currents upon osmotic cell swelling seem to be mediated by Phospholipase A2 (PLA-2) release of Arachidonic acid and further metabolization of AA by cytochrome P450 epoxygenase, leading to the formation of epoxyeicosatrienoic acids (EETs) (Annex table 1) [181]. Phorbol esters such as 4 α-PDD bind TRPV4 with a high specificity (Annex table 1) [182]. Based on a mutagenesis screen of TRPV4, interaction with 4 α-PDD was mapped to the TM3-TM4 region. The length of the phorbol ester fatty acid chain is

determinant for the ligand binding affinity, being 6 and 10 carbons the optimal length [182]. TRPV4 is also activated by the dimeric diterpenoid bisandrographolide A (BAA) (Annex table 1), from the plant *Andrographys paniculata*, and mutants in the same binding pocket between TM3 and TM4 seem to impair response to this compound [182]. GSK1016790A, a synthetic compound, has demonstrated to be a potent and specific TRPV4 activator, working on the low nM range (Annex table 1) [183]. Besides agonist, TRPV4 channel can be sensitized by several physiological conditions, such as inflammation and the generation of proteases like Protease-activated receptor 2 (PAR2) [184], interaction with IP3 receptor and PIP2 binding [185]. Concerning channel antagonists, general unspecific channel blockers as ruthenium red, gadolinium or lanthanum have been used [186]. Citral, a chemical from lemongrass oil, is able to inhibit TRPV4 in a voltage independent manner (Annex table 1) [187]. More specific channel blockers, RN-1734 and RN-9893 have been generated and show an efficient TRPV4 inhibition at the µM and nM range respectively (Annex table 1) [188]. Recently other specific channel blockers such as GSK2193874 and HC 067047 have been developed and tested in animal models, showing higher efficiency in blocking TRPV4 (Annex table 1) [189, 190].

4.4. TRPV1-4 channels interactors

TRPV1-4 channels have been described in the formation of several complexes with proteins of very different nature within the cell through interactions of strong and/or transient nature. Thus, TRP channels may not solely act as ion channels allowing the pass of ions but may also directly interact and contribute to the activation of intracellular signalling pathways, establishing complexes surrounding the channels that couple channel activity to the intracellular enzymatic activity (Fig. 7). The regulatory processes could work in both directions, forming a crosstalk between channels and signalling cascades. Then, TRP channels would be influenced by and influence over the intracellular enzymatic and metabolic state. The main already described signalling cascades acting over TRPV channel function are related to Protein kinase A (PKA), Protein kinase C (PKC), Phosphoinositide 3 kinase (PI3K) and calmodulin (CAM)/calmodulin kinase (CamKII) (Fig. 7).

Scaffolding proteins such as AKAP target pro-inflammatory kinases PKC and PKA to TRPVs [191]. AKAP targeting of PKC promotes TRPV1 trafficking to the plasma membrane, sensitization of the channel and TRPV1-mediated hyperalgesia [192, 193]. TRPV1 is directly phosphorylated by PKC at the S502, T704 and S800 residues. TRPV1 PKC mediated phosphorylation at these residues does not activate the channel but sensitizes it to activation by capsaicin (Fig. 7) [194]. Similarly, PKA reduces TRPV1

desensitization by directly phosphorylating S116 of TRPV1 N-terminus, resulting in an increase in channel activity (Fig. 7) [195]. In the case of TRPV2, PKA mediates in vitro phosphorylation of the channel in a process that is mediated by ACBD3 protein, which recruits PKA to the TRPV2-AKAP complex (Fig. 7) [196].

Calmodulin has been related to all TRPV1-4 channels, as well as to other TRPs. Mostly, TRPVs bind calmodulin on their N-terminal ARD domain in a calcium dependent manner and in their C-terminal domain (Fig. 7) [197, 198]. TRPV1 N-terminal binding pocket mediates in channel desensitization (Fig. 7) [199]. Conversely, TRPV2 is not able to bind calmodulin in the N-terminus but the binding pocket on the C-terminus is kept, dependent on basic amino acids within this region, mainly R679 and K681 [58]. TRPV4 calmodulin binding pocket in the C-terminus potentiates channel activity and its depletion results in functional inhibition of the channel (Fig. 7) [198, 200].

GPCRs and ionotropic receptors such as NMDA trigger TRPV1 serine phosphorylation via PKC and CamKII [201]. Activation of these receptors promotes activation of phospholicase C (PLC) and release of DAG and IP3. Lately, DAG potentiates PKC activity directly and IP3 promotes the gating of IR3R and the calcium release from ER, which will act over calmodulin/CamKII complex and thus, over channel activity (Fig.7). NGF, acting on the TrkA receptor, activates PI3K signalling pathway and promotes the phosphorylation of TRPV1, potentiating channel activity in a process mediated by PLC (Fig. 7) [202]. Lipid metabolism is also crucial for TRPV regulation. PIP2 binds directly to TRPV channels and sensitizes them to their respective specific agonist (Fig. 7).

TRPV channels further modulate their activity by regulating the number of channels present in the membrane. The cells keep a balance between channel export and import. Channel delivery to the plasma membrane is mediated by different exocytosis mechanisms that are carried out by a set of proteins (Fig. 8). The constitutive exocytosis pathway keeps membrane protein and TRPVs turnover, whereas the regulated exocytosis promotes the mobilization of intracellular vesicles located near the plasma membrane upon cell stimulation, recruiting TRPVs to the membrane (Fig. 8). Trafficking of TRPVs to the plasma membrane is mediated by phosphorylation processes and interaction with SNAP (Soluble NSF Attachment Protein) Receptor (SNARE) complex proteins (Fig. 7 and 8). Cyclin dependent kinase 5

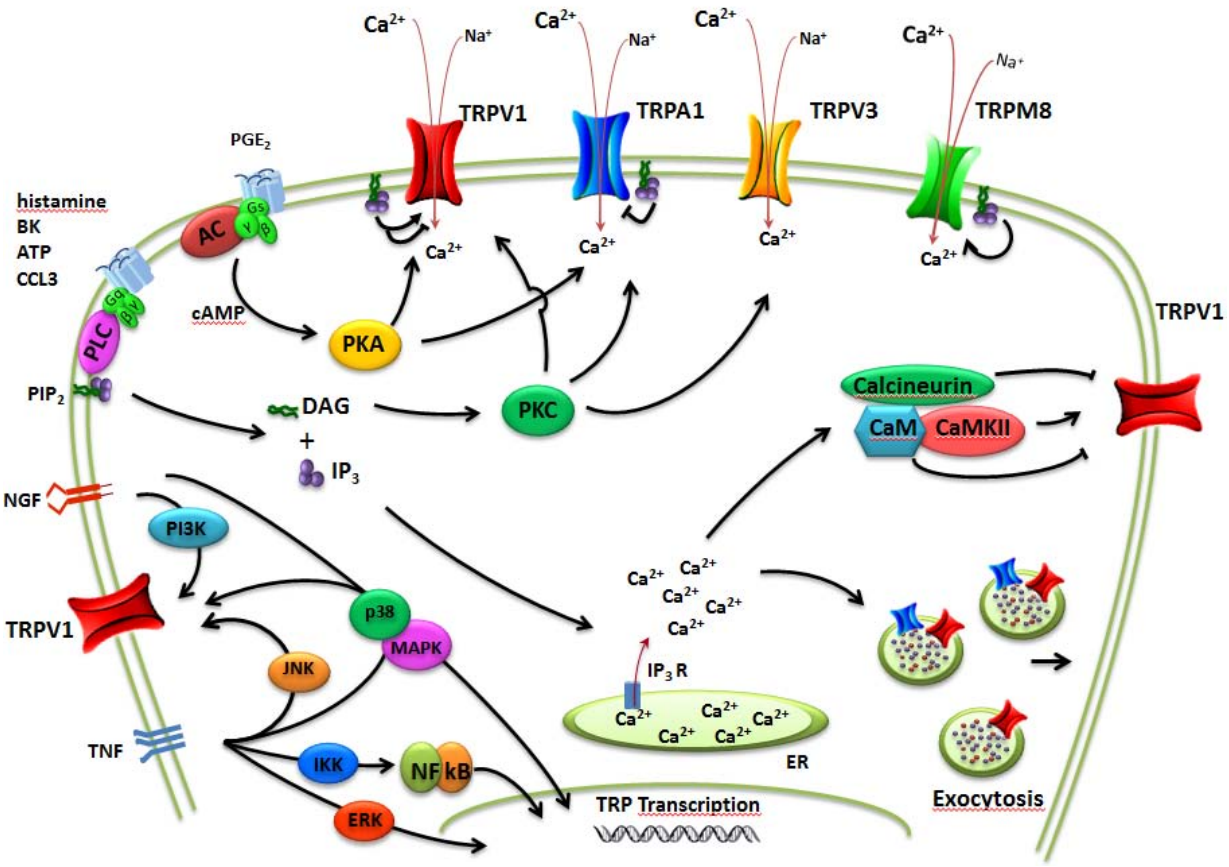

Figure 7. Signalling cascades coupled to the members of TRP family. TRPV1-4 main described cellular regulatory signalling cascades are related to IP3R, calmodulin (CAM) and Calmodulin kinase 2 (CamKII), Phosphoinositide 3 kinase (PI3K), Protein kinase C (PKC) and Protein kinase A (PKA). Figure from Fernandez-Carvajal et al. 2011 [203].

(CDK5), PKC and PKA mediated phosphorylation of TRPV1 promotes the recruitment of the channel to the plasma membrane [204, 205, 206]. Similarly SNARE complex, a large family of proteins that regulates vesicle fusion, mediates TRPV1 recruitment to the plasma membrane upon PKC activation, leading to a potenciation of TRPV1 activity [205]. TRPV1 interacts with SNAPIN25 and Synaptotagmin IX on its N-terminus [205], and this interaction links TRPs to regulated exocytosis processes that might have impact in channel functioning.

TRPV1-4 interactors extracted from www.TRPchannel.org were listed as follows: TRPV1 related proteins are listed in annex table 2. TRPV2 related proteins are listed in annex table 3. TRPV3 related proteins are listed in annex table 4. TRPV4 related proteins are listed in annex table 5.

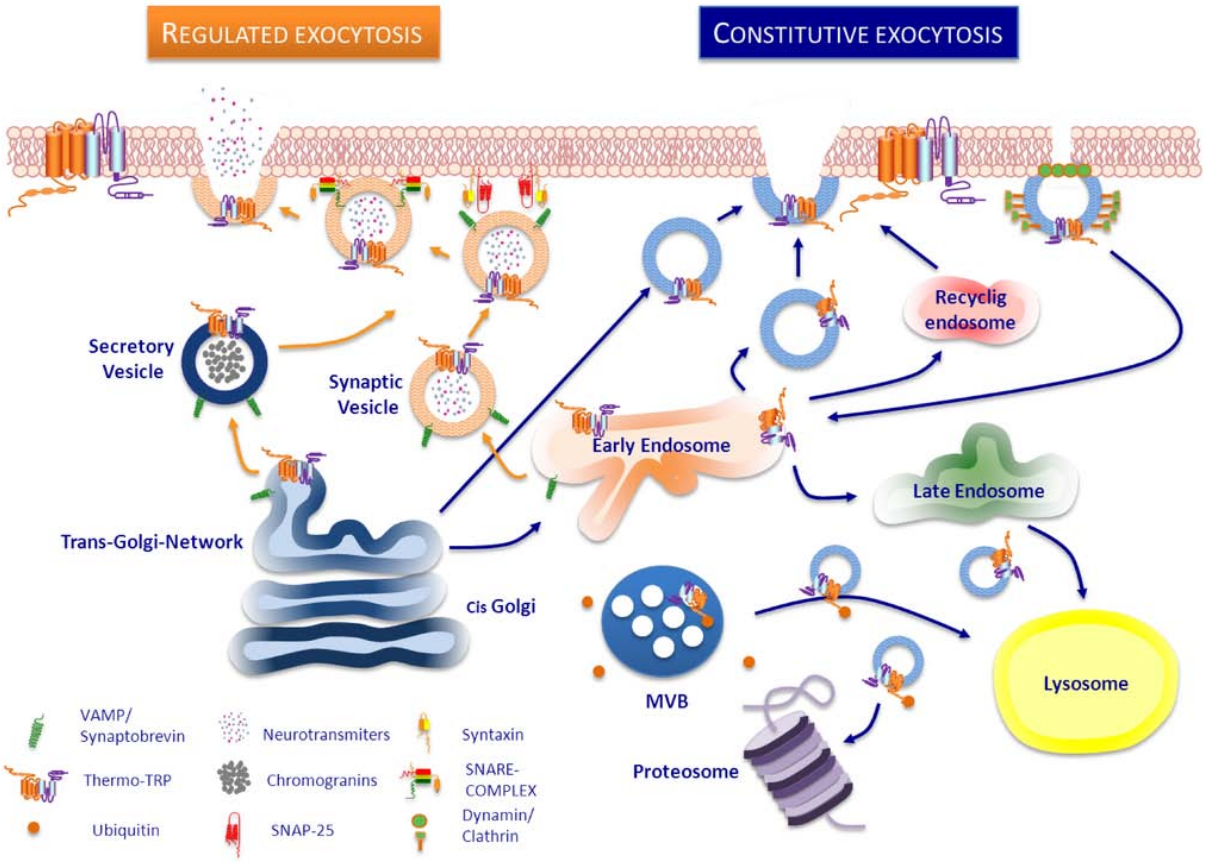

Figure 8. Trafficking pathways of TRPV channels to the plasma membrane. TRPVs are targeted to the membrane by two main exocytosis pathways. Secretory vesicles, the system used by neurons to release neurotransmitters, could contain TRP channels that are delivered to the plasma membrane upon neuron stimulation in a process mediated by calcium and SNARE protein complex. Constitutive exocytosis constantly delivers TRPVs to the plasma membrane from the Golgi or through the endosomes. TRPV membrane levels are modulated by clathrin-dependent endocytosis pathway, which targets TRPVs to the endosomes and degradation. Figure from Ferrandiz-Huertas et al 2014 [207].

Interactors and regulatory mechanisms determined to date are mainly related to TRPV1 and TRPV4 whereas TRPV2 and TRPV3 remain almost orphans in terms of protein partners (Fig. 9). The intersection between TRPV1-4 channel partners reveals potential processes that might regulate TRPV subfamily, which are mainly related to association with scaffolding proteins such as AKAP5 or calcium mediators such as calmodulin (Fig. 9). This central protein cluster also includes the binding to the cytoskeleton by proteins such as Tubulin and the potential regulation of all these channels by phosphorylation events that might be mediated by protein kinases such as PRKA (PKA) (Fig. 9).

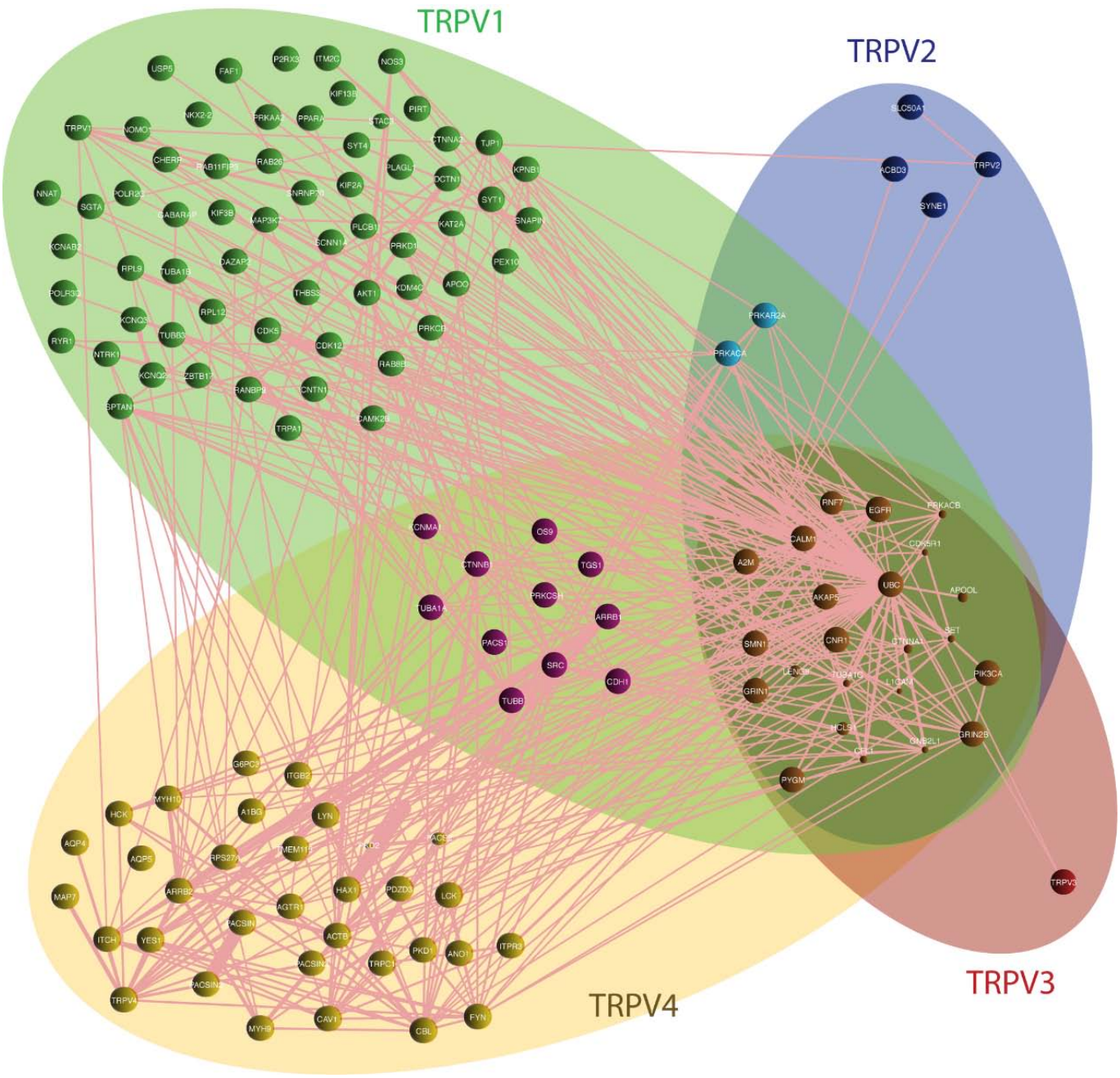

Figure 9. Interactomic representation of TRPV1-4 partners. TRPV1 exclusive interactors are coloured in green, TRPV2 in dark blue, TRPV3 in red and TRPV4 in yellow. Common interactors between TRPV1 and TRPV2 are coloured in cyan blue and common interactors between TRPV1 and TRPV4 are coloured in purple. Common interactors between more than two channels are clustered in the overlapping area of the 4 proteins and coloured in brown. The lines binding the TRPV1-4 partners represent physical interactions according to Cytoscape Genemania plugin (Human genome). For further detail on specific interactors check annex tables 2, 3, 4 and 5.

4.5. TRPV1-4 channels mutations and Disease

TRPV1, as previously described, is highly expressed in the sensory neurons of the nervous system, where it has been linked to the pain transduction circuitry [69]. Sensory neurons are depolarized upon activation of TRPV1 by several painful stimuli that can potentially evoke pain responses in the brain [208]. In fact, TRPV1 knock out (ko) mice present impairment in pain sensation and nociception [209]. Additionally, TRPV1 ko mice DRG neurons loose their ability to develop thermal hyperalgesia, pointing to TRPV1 as potential mediator of inflammatory sensitization to noxious thermal stimuli [210]. TRPV1 evoked thermal hyperalgesia in mice is mediated by the sensitization of the channel upon protease-activated receptor 2 (PAR2) cleavage. PAR2 is cleaved by pro-inflammatory proteases and activates PKC and PKA, which in turn will sensitize TRPV1 [184]. This mechanism may link inflammatory processes with pain and hyperalgesia.

Furthermore, TRPV1 participates in several inflammatory pathological conditions. In the mouse knee joint, TRPV1 promotes the CFA mediated acute and chronic inflammation [211], while in the gastrointestinal tract upregulation of TRPV1 expression and function correlates with several inflammatory pathologies such as inflammatory bowel disease [212]. In the epithelial airways, TRPV1 activation by capsaicin promotes chronic cough and the upregulation of TRPV1 expression has been reported in cough and asthma [213, 214]. In concordance with this findings, two single nucleotide polymorphism (SNP) contained in the non coding 3´UTR of TRPV1, rs4790521 and rs4790522, have been associated with childhood asthma in Asian population [215]. Moreover, TRPV1 mutant at I585V residue codifies for a dysfunctional channel that lowers the risk of childhood asthma (Fig. 10) [216]. Disease related bioinformatics analysis through Disgenet revealed highest association of TRPV1 with the described pathological conditions: Hyperalgesia, inflammation, pain or obesity (Annex table 6).

Conversely, TRPV1 activation may prevent some pathological conditions. TRPV1 activation by dietary capsaicin prevents adipogenesis, obesity and hypertension in mice and human [84, 217]. Two SNP in TRPV1 sequence, P322A and D734E, were found to be associated with a mice model of diabetes (Fig. 10). These mutations provoked a channel loss of function in the sensory neurons that innervates beta cells [218].

TRPV2 play important roles in physiological conditions and its activity is important for the correct functioning of many tissues and organs. TRPV2 misregulation has been linked with dystrophic cardiomyopathy, rheumatoid arthritis or cancer (Annex table 7). By instance, TRPV2 in dystrophic

cardiomyocites presents an increase in plasma membrane levels and channel activity [66], whereas TRPV2 activation decreases fibroblast invasiveness and inflammation, leading to a protective effect in arthritis [219]. Despite the evidence of TRPV2 role in several pathological conditions, any missense mutation of this channel has been linked as potential etiological cause of disease (Fig. 10).

Mainly pathological associations with TRPV2 according to Disgenet are related to cancer, although with a very poor score (Annex table 7). Indeed, some neoplasms such as prostate cancer cell migration and invasion require increased TRPV2 translocation to plasma membrane and the subsequent rise in resting calcium level (Annex table 7). Among the top 10 diseases we found muscular dystrophies and cardiomyopathies (Annex table 7). TRPV2 in muscular tissue represents one of the main entry routes for calcium, and its misregulation leads to calcium sustained increase, a toxicity effect in myocytes and muscle degeneration [220].

TRPV3 is mainly expressed in the skin, where it plays important roles controlling skin barrier formation [120]. Besides from regulatory mechanisms of TRPV3 expression levels, several natural variants of TRPV3 have been associated to skin disorders. By instance, mutation at G573C/S and W692G in TRPV3 are associated with Olmsted syndrome (Fig. 10) [221], a rare congenital disorder characterized by bilateral mutilating palmoplantar keratoderma and periorificial keratotic plaques with severe itching at all lesions. Functional characterization of TRPV3 mutants determine a clear gain of function, produced by the channel constitutively open; which leads to an increase in apoptosis rate that may be considered as the etiological cause of the disease [221]. Recently, several studies determined other TRPV3 missense mutations in Olmster syndrome patients such as L673P, T521S or M672I residues (Fig. 10) [222, 223, 224]. Besides hereditary Olmsted syndrome, TRPV3 is also involved in the development of itching, inflammatory and acquired skin diseases. Indeed, TRPV3 expression is upregulated in rosacea, a chronic inflammatory skin disease [225]. According to Disgenet, TRPV3 is associated with skin diseases and migraine disorders although association scores are very low (Annex table 8).

TRPV4 is widely spread and plays important roles in all the tissues where it is expressed. Some naturally occurring mutants have been identified for TRPV4, mainly missense and nonsense point mutations, that are linked with the development of genetic disorders in humans [125].

As osmosensor, TRPV4 plays an important role controlling systemic water balance. A SNP located at the distal N-terminus (P19S) is associated with serum sodium concentration and hyponatremia (Fig. 10) [226]. Functional studies of this mutant showed a diminished response to

hypotonic stress and to the EETs compared to that in wild type TRPV4 [226]. In the bronchiae, TRPV4 activation controls airway epithelial cell volume and epithelial-endothelial permeability under physiological conditions. It also participates in bronquial smooth muscle contraction and mucosal ciliary transport. Impairment of TRPV4 function in this tissue may lead to chronic obstructive pulmonary disease (COPD), which is characterized by airway epithelial damage, bronchoconstriction and mucus hyper secretion. In fact, P19S SNP is also associated with COPD patients (Fig. 10) [135].

Other TRPV4 missense mutation, specifically at positions R616Q or V620I are associated with patients affected with brachylomia type 3 (BRAC3), a heterogeneous type of skeletal dysplasia mainly characterized by a short trunk, scoliosis, and mild short stature (Fig. 10) [227]. These two mutants generate a gain of function in TRPV4, increasing basal channel activity, which is a key determinant in the severity of TRPV4 mediated skeletal dysplasias [227, 228]. Indeed, TRPV4 misregulation has been associated with several types of dysplasia. For instance, dominant mutations in TRPV4 gene seem to lead to metatropic dysplasia (MTD), ranging in severity from mild to lethality [229]. Metatropic dysplasias are characterized by short extremities and trunk accompanied by progressive scoliosis, and craniofacial abnormalities. TRPV4 mutations at I331F and P799L induce MTD by increasing intracellular calcium in chondrocytes, that in turn alters chondrocyte differentiation in the growth plate and leads to the MTD phenotype (Fig. 10) [229]. Genetic mapping of patients affected by Spondyloepiphyseal dysplasia Maroteaux (SEDM) showed missense mutations in TRPV4, either E183K, Y602C, or E797K (Fig. 10). Functional studies of E797K mutant determined that it is constitutively active, pointing to a gain of function in TRPV4 as the etiological cause of SEDM (Fig. 8) [230]. Parastremmatic dwarfism (PSTD) and Spondylometaphyseal dysplasia Kozlowski (SMDK), another types of dysplasia, are associated with TRPV4 missense mutation at the TM4 R594H residue (Fig. 10). This mutation produces a gain of function and a rise in intracellular calcium levels, similar to those on MTD and SEDM [230, 231]. Finally, Charcot-Marie Tooth type 2C (CMT2C), an axonal form of this peripheral nervous system pathology, and scapuloperoneal spinal muscular atrophy (SPSMA) have been linked to TRPV4. Genetic studies identified missense mutations in TRPV4 associated to these nervous system pathologies [232]. Mutations at the R269H, R315W, and R316C residues of TRPV4 produce a channel gain of function and cytotoxicity, thus, promoting these neurodegenerative pathologies (Fig. 10) [233].

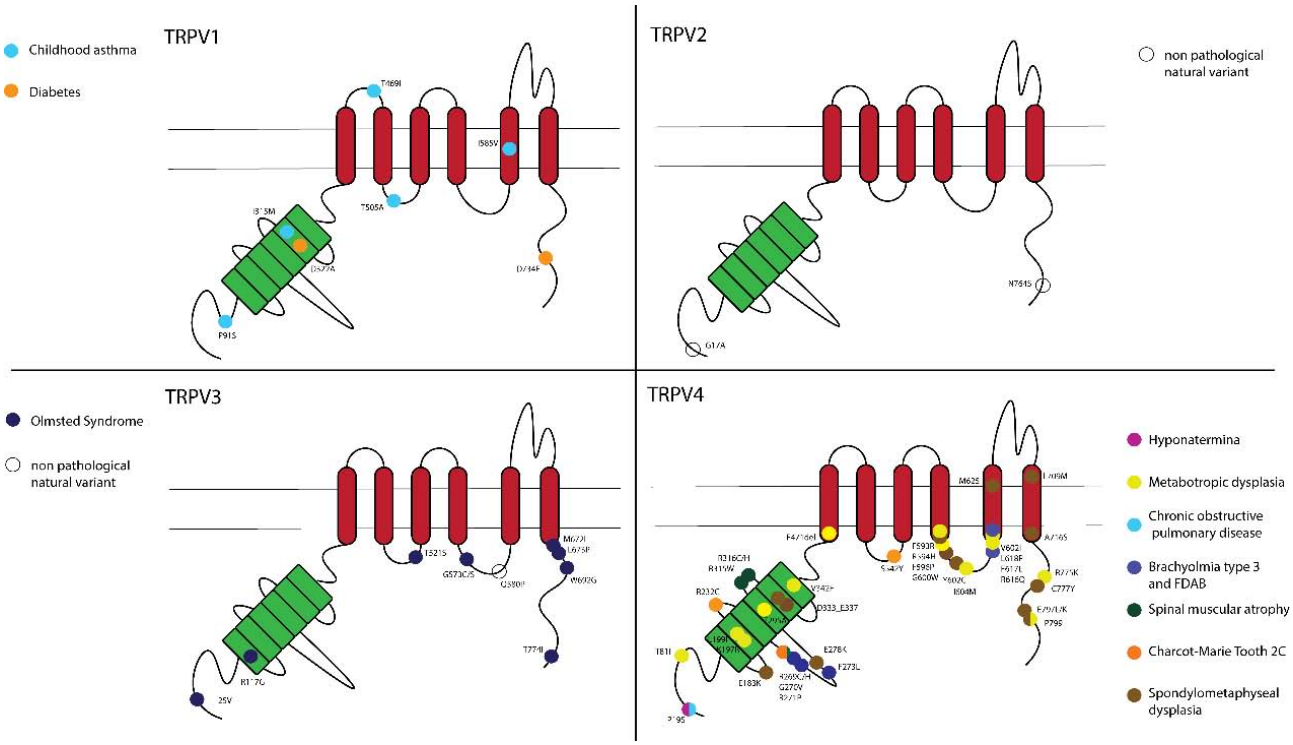

Figure 10. TRPV1-4 natural variants associated with disease. Natural occurring mutations have been position over a 2D representation of each of the TRPV1-4 channels to allow the visualization of the regions containing pathological associated mutations.

As we have reported here, TRPV channels are key players in organism homeostasis and their misregulation leads to pathological conditions, being proteins of great interest from a biomedical perspective. Although we have knowledge about TRPVs structure and folding properties, body distribution, pharmacology, regulatory mechanisms and associated diseases (reviewed during this introduction); many questions still remain to be addressed when trying to understand in detail TRPV functioning. Broadening the basic knowledge about TRPV molecular mechanisms and modulation should constitute the first step in order to fully understand and effectively treat TRPV mediated pathologies. Within this context, the thesis presented here will try to compile previous knowledge of TRPVs that will establish our departure point **(Chapter I)** and analyse TRPV primary sequence to understand common molecular processes and key structural and functional features for this subgroup of channels **(Chapter II)**. From this point, we will address several key aspects of TRPV functioning, from folding and trafficking **(Chapter III)** to protein protein interactions and their physiological and pathological implications **(Chapter IV and V)**.

Objectives

Objectives

NOTE: It is worthy to mention that the chronological development of this thesis coincides with the Cryo-EM structural biology breakthrough started with TRPV1 [42], diminishing the impact of part of the results presented here, such as: the identification of structural motifs and the structural modelling of the TRPV1-4 subgroup (Chapter II) [234]; the identification of the transmembrane topology of TRPV2 as representative for the TRPV1-4 subgroup (Chapter III) [235]. This constitutes an example that might serve as an indicator of the importance and competitiveness of the TRP field.

The main aim of this Thesis is to widen the knowledge of TRPV1-4 channel subfamily. We intend to characterize new potential mechanisms that mediate in folding, structure, trafficking, regulation and functionality, as well as the physiological implications that these issues might entail.

Specific Objectives

Chapter I

- Review the available bibliography concerning TRPV2, the least understood TRPV channel and the focus of a large part of our work.

Chapter II

- Deepen into TRPV1-4 subgroup evolution and domain conservation to gain structural insight into the multidomain organization and conservation of these channels.
- Determine TRPV1-4 conserved regions that may be crucial domains for structure and function.

Chapter III

- Characterize the implications of N-terminus of TRPV2 in protein trafficking and folding.
- Study the transmembrane folding modules and determinant properties of TRPV2 membrane insertion.
- Map the transmembrane alpha helices distribution of TRPV2 and analyse the potential conservation in TRPVs.

Chapter IV

- Identify potential interactors for TRPV2 to widen the knowledge on the regulation of this channel.
- Determine potential TRPV2 roles from the identified partners and characterize the potential implications of these roles over TRPV2 function.
- Determine domains of TRPV channels involved in lipid binding.

Chapter V

- Identify potential interactors for TRPV4 to broaden the knowledge on the regulation of this channel.
- Determine the main roles carried out by TRPV4 interactome.
- Identify functional implications of newly described TRPV4 interactions.

Results

Chapter I

What do we know about the transient receptor potential vanilloid 2 (TRPV2) ion channel?

Specific Objectives

- Review the available bibliography concerning TRPV2, the least understood TRPV channel and the focus of a large part of our work.

the FEBS Journal
REVIEW ARTICLE

What do we know about the transient receptor potential vanilloid 2 (TRPV2) ion channel?

Alex Perálvarez-Marín[1], Pau Doñate-Macian[1] and Rachelle Gaudet[2]

1 Centre d'Estudis en Biofísica, Departament de Bioquímica i de Biologia Molecular, Universitat Autònoma de Barcelona, Cerdanyola del Vallés, Spain
2 Department of Molecular and Cell Biology, Harvard University, Cambridge, MA, USA

Keywords
calcium signalling; cancer; endocrinology; immunology; ion channels; muscle physiology; neuroscience; pharmacology; somatosensation; TRPV2

Correspondence
A. Perálvarez-Marín, Centre d'Estudis en Biofísica, Unitat de Biofísica, Departament de Bioquímica i de Biologia Molecular, Edifici M, Universitat Autònoma de Barcelona, 08193 Cerdanyola del Vallés, Spain
Fax: +34 9358 11907
Tel: +34 93581 4504
E-mail: peralvarezmarin@gmail.com

(Received 27 January 2013, revised 22 March 2013, accepted 14 April 2013)

doi:10.1111/febs.12302

Transient receptor potential (TRP) ion channels are emerging as a new set of membrane proteins involved in a vast array of cellular processes and regulated by a large number of physical and chemical stimuli, which involves them with sensory cell physiology. The vanilloid TRP subfamily (TRPV) named after the vanilloid receptor 1 (TRPV1) consists of six members, and at least four of them (TRPV1–TRPV4) have been related to thermal sensation. One of the least characterized members of the TRP subfamily is TRPV2. Although initially characterized as a noxious heat sensor, TRPV2 now seems to have little to do with temperature sensing but a much more complex physiological profile. Here we review the available information and research progress on the structure, physiology and pharmacology of TRPV2 in an attempt to shed some light on the physiological and pharmacological deorphanization of TRPV2.

Introduction

The transient receptor potential (TRP) superfamily is a multifunctional set of membrane proteins that function as ion channels and extend communication lines between the cell and its environment, what may be called sensory physiology or somatosensation. TRP channels in cellular membranes are modulated by a vast array of physical or chemical stimuli, including radiation (in the form of temperature, infrared radiation or light), pressure (osmotic or mechanical) and natural compounds. Excellent reviews about TRP channels are available [1–7], and thus an overview of the TRP superfamily is beyond the scope of the present review. The subject of discussion here is the transient receptor potential vanilloid 2 (TRPV2) channel, one of the most mysterious and intriguing members of this superfamily, with a paucity of data concerning the endogenous function of the channel. The intention of the review is to shed some light on the controversies

Abbreviations
2-APB, 2-aminoethoxydiphenyl borate; ARD, ankyrin repeat domain; DRG, dorsal root ganglion; IGF-1, insulin growth factor 1; LPS, lipopolysaccharide; OCR, osm-9/capsaicin receptor related; OSM-9, osmotic avoidance abnormal family member 9; PI3K, phosphatidylinositol 3-kinase; PIP_2, phosphatidylinositol 4,5-bisphosphate; RGA, recombinase gene activator; TMD, transmembrane domain; TNF, tumor necrosis factor; TRPA, TRP subfamily ANKTM1; TRPC, TRP subfamily canonical; TRPML, TRP subfamily mucolipin; TRPM, TRP subfamily melastatin; TRPN, TRP subfamily NompC; TRPP, TRP subfamily polycystin; TRP, transient receptor potential; TRPV2, transient receptor potential vanilloid 2; TRPV, TRP subfamily vanilloid.

concerning TRPV2 by integrating the latest reports on TRPV2 with historical data on this ion channel towards understanding the TRPV molecular mechanism from a more structural perspective.

The TRP channel superfamily

TRP channels were originally identified within the rhabdomeres of the photoreceptor in *Drosophila* [8] and the first member was cloned in the late 1980s [9]. TRP channels constitute an extensive ion channel superfamily represented across the phylogenetic tree from yeast to human. They are indeed the second largest family of voltage-gated-like ion channels after the potassium channel family [10]. Many TRP channels are polymodal signal integrators that trigger cellular signalling pathways via non-selective cation flux (e.g. Ca^{2+}, Mg^{2+} and Na^{+}). Different TRP channels show different permeability and selectivity to cations, both monovalent and divalent, whereas most trivalent cations act as channel blockers. The specifics of cation permeability are physiologically important since cations play roles in cell function regulation, such as fertilization, muscle contraction or exocytosis.

As a relevant example of TRP channel function in mammals, several TRP channels located in the dorsal root ganglion (DRG) nociceptive sensory neurons respond to nociceptive stimuli to cause pain. From a pharmaceutical and biomedical point of view, there are vast and diverse implications including some still to be determined. For instance, TRPs are lead targets in the treatment of acute and chronic pain [11,12]. Nevertheless the role of TRP channels is not limited to the pain field. TRP channels have been implicated in several physiological and pathological processes such as cancer, genetic disorders and other rare diseases, and not only restricted to somatosensation.

A set of common sequence features among TRPs translates to shared structural features. Mainly, these channels share a membrane topology of six transmembrane segments (S1–S6), with a pore-forming loop between S5 and S6. Similarly to the tridimensional structure of potassium channels, TRPs are arranged in the membrane as tetramers as the basic functional unit. The S1–S4 segments and the N- and C-terminal cytoplasmic domains are modulating domains important to the gating of the channel, with the S5 andS6 segments defining the pore and selectivity filter (Fig. 1A).

TRPs are not classified by their functional role but based on amino acid sequence identity and similarity. The mammalian TRP channel superfamily is classified into six subfamilies with significant sequence similarity within the transmembrane domains (TMDs) but very low similarity in their N- and C-terminal cytoplasmic regions (Fig. 1B). The six subfamilies are named based on founding members: TRPA (ANKTM1); TRPC (canonical); TRPM (melastatin); TRPML (mucolipin); TRPP (polycystin); and TRPV (vanilloid). A seventh subfamily, TRPN (NompC), is present in invertebrates and some vertebrates, although it is absent in mammals. Here we focus on the TRPV subfamily and how TRPV2 distinguishes itself from its closest TRPV homologs.

TRPV2 within the TRPV subfamily

The first identified TRP channel of the TRPV family was OSM-9 (osmotic avoidance abnormal family member 9) from *Caenorhabditis elegans* [13]. OSM-9 is required for olfaction, mechanosensation and olfactory adaptation. OCR-1 to OCR-4 (osm-9/capsaicin receptor related) are the other TRPV channels in *C. elegans*, for a total of five [14]. In *Drosophila melanogaster* the TRPV members are Nanchung and Inactive, which are involved in sensory perception [15]. The TRPV mammal subfamily is divided into two groups based on sequence homology, TRPV1–4 and TRPV5–6 (Fig. 1B). The group formed by TRPV5 and TRPV6 shares high sequence identity (~ 75%) but low identity with the TRPV1–4 group (~ 20%) [6,16]. TRPV5 and TRPV6 are calcium-selective channels important for general Ca^{2+} homeostasis and heterotetramers between them have been described [17]. All four channels within the TRPV1–4 group show temperature-invoked currents when expressed in heterologous cell systems, ranging from activation at ~ 25 °C for TRPV4 to activation at ~ 52 °C for TRPV2. However, a physiological role in temperature sensing has not been demonstrated for TRPV2, and the thermal responses of TRPV2 knockout mice have been shown to be similar to those of wild-type mice [18]. In contrast, TRPV1 has been convincingly shown to play an important role in thermosensation using knockout mice [19]. The original characterization of the TRPV3 knockout mice [20] and TRPV4 knockout mice [21] showed some impairment in thermosensation. However, more recent work showed that any thermosensory defects in the TRPV3 and TRPV4 knockout mice are minor and strain-dependent [22]. Therefore, a physiological thermosensory role is the exception (TRPV1) rather than the rule for TRPV channels.

As detailed below, there is increasing support for a role of TRPV2 in various osmosensory or mechanosensory mechanisms. The mechanosensory function of select TRPV channel family members seems to have

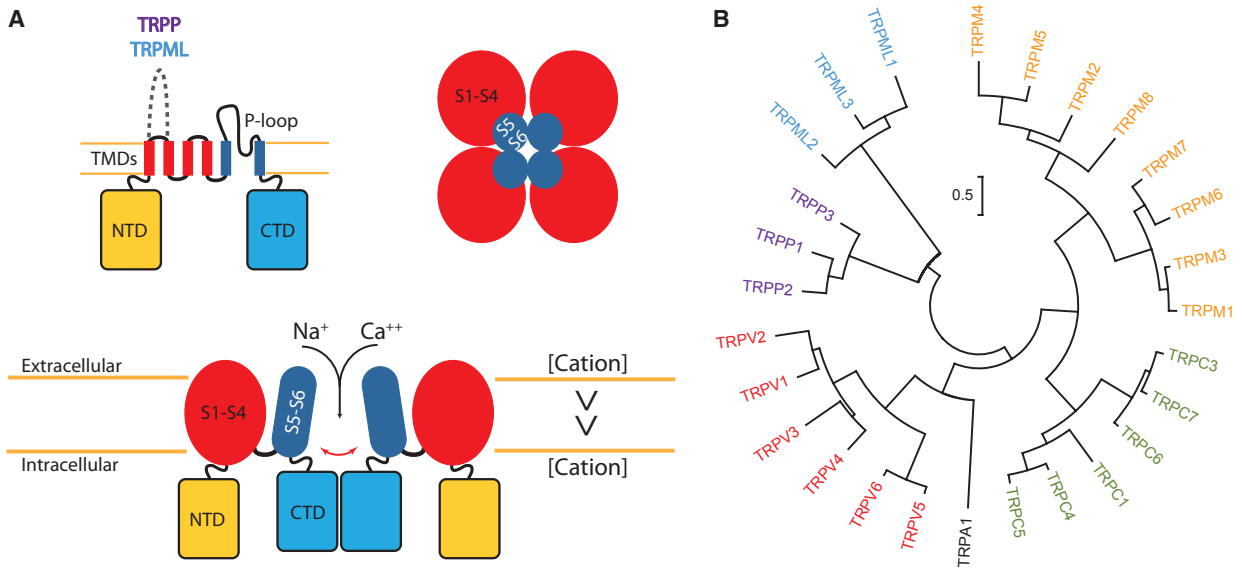

Fig. 1. The TRP channel molecular mechanism and classification. (A) The six-transmembrane segment topology of the monomer and tetrameric functional unit of TRP channels. The cytoplasmic N- and C-terminal domains and the transmembrane domain constituting the pore are indicated. The long loop present between S1 and S2 in TRPP and TRPML is indicated by a dashed line. The transmembrane domain comprises segments 1–4 (red), distal to the pore of the channel, and segments 5 and 6 (blue) proximal to the pore of the channel. (B) Human classification of the TRP family representative of the mammal TRP subfamilies classification. Notice that in humans TRPC2 is a non-coding pseudogene and it is not represented.

been maintained through evolution. For instance, the *C. elegans* TRPV channels OSM-9 and OCR-2 are essential for osmosensation and mechanosensation [23]. Similarly, Nanchung and Inactive, the TRPV-related proteins in *D. melanogaster*, located in the mechanosensitive Johnston's organ in the fly antennae, are responsible for the sense of hearing [15,24].

Two laboratories nearly simultaneously cloned TRPV2 orthologs. Human and rat TRPV2 were cloned based on their homology to TRPV1, and accordingly named vanilloid-receptor-like protein 1 (VRL-1) [25]. Mouse TRPV2 was cloned and named growth-factor -regulated channel (GRC) based on the fact that it induces calcium currents upon stimulation of cells by insulin growth factor 1 (IGF-1) [26]. Of note, TRPV2 has also infrequently been referred to as Osm-9-like TRP channel 2 (OTRPC2) [27]. TRPV2 mediates cationic currents with higher divalent permeability (P) ($Ca^{2+} > Mg^{2+} > Na^{+} \sim Cs^{+} \sim K^{+}$; $P_{Ca^{2+}}/P_{Na^{+}} = 2.94$; $P_{Mg^{2+}}/P_{Na^{+}} = 2.40$) [25]. The sequence identity among the best characterized orthologs (human, rat and mouse) ranges from 75% to 90% (Fig. 2). TRPV2 shares 50% sequence identity with TRPV1, the best characterized member of this subfamily. TRPV1 is a polymodal channel activated by anandamide, capsaicin, resiniferatoxin, heat, low pH and eicosanoids [28]. TRPV3 is a thermosensor for non-noxious heat and responds to natural compounds found in plants such as oregano, camphor and thyme [29]. TRPV4 is a constitutively active Ca^{2+}-permeable channel modulated by non-noxious heat [21] and also by pressure and hypotonicity [30,31]. TRPV4 has also been associated with hearing loss [32].

Heteromerization of TRPV1–4 channels has been documented, although mostly in heterologous expression systems. Heterotetramerization of TRPV2 with TRPV1 has been described *in vitro* in HEK cells [17,33,34]. TRPV1 and TRPV2 have also been shown to tightly colocalize *in vivo* in rat DRG [17,33,35]. However, physiological roles of any TRPV2 heterotetramerization have yet to be identified.

TRPV2 structure and evolution

TRPV2 presents a high conservation level of identity within mammalian orthologs (see Fig. 2 for human, rat and mouse sequence alignment). Specific TRPV2 orthologs are only found in tetrapod vertebrates, but not in fish where there is a TRPV1/2 isoform. One evolutionary hypothesis is that a common ancestor between TRPV1 and TRPV2, referred to as TRPV1/2, duplicated generating two genes [36]. This gene duplication is ambiguous in time. One hypothesis is that it could have occurred in the common ancestor between fishes and tetrapods and then the copy for TRPV2 was lost in fishes. The second possibility argues for the

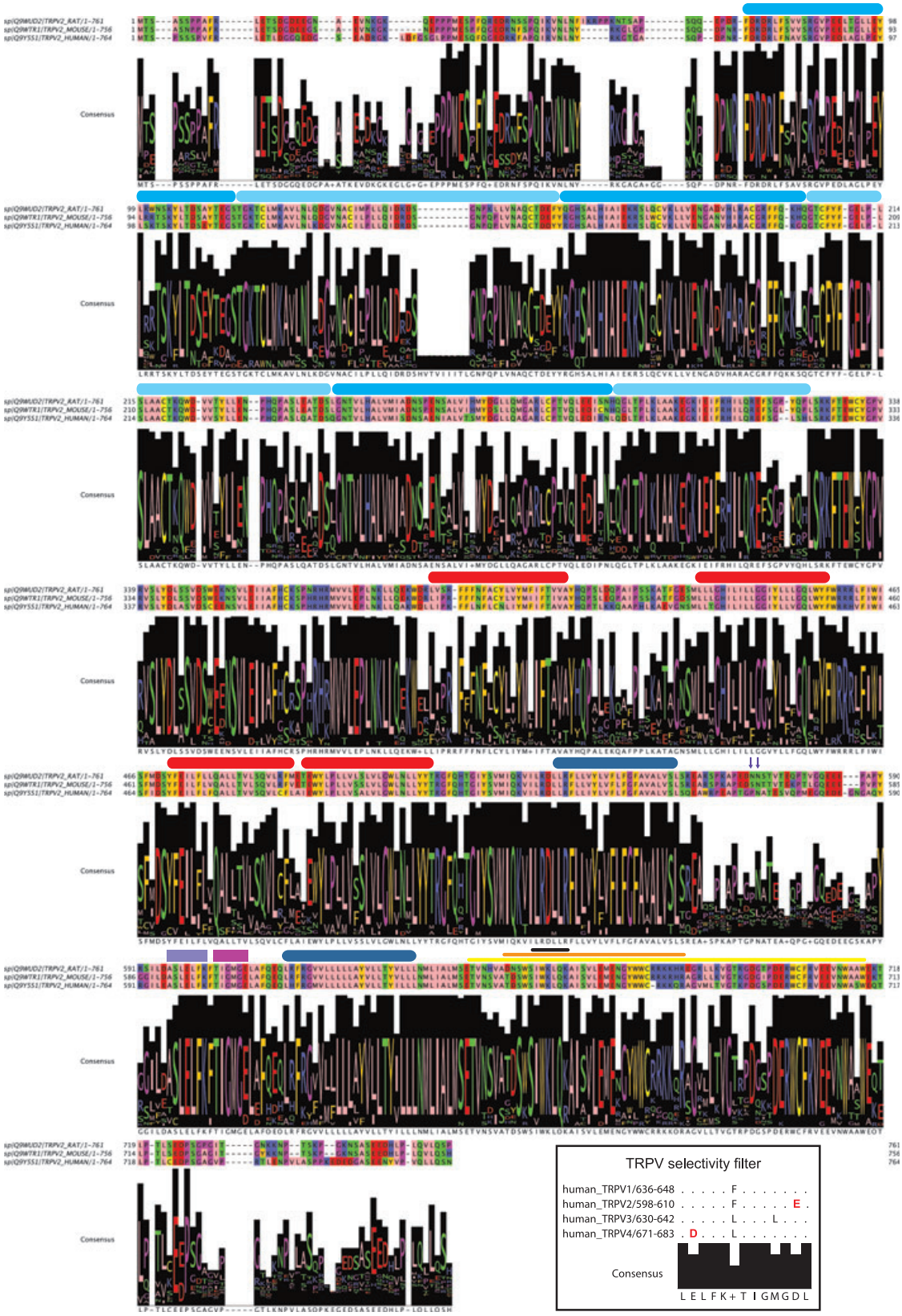
TRPV selectivity filter
human_TRPV1/636-648 . . . . . F . . . . . .
human_TRPV2/598-610 . . . . . F . . . . . E .
human_TRPV3/630-642 . . . . . L . . . L . . .
human_TRPV4/671-683 . D . . . L . . . . . .
Consensus
L E L F K + T I G M G D L

Fig. 2. TRPV2 sequence conservation and structural features. Alignment of rat (rTRPV2), mouse (mTRPV2) and human (hTRPV2) orthologs. The most relevant sequence features are indicated using the following color code: ARD (light blue); S1–S4 (red); S5–S6 (dark blue); pore (violet); selectivity filter (magenta); PIP_2 binding domain (yellow); calmodulin binding domain (orange); TRP box (black). The N-glycosylation sites between S5 and S6 are indicated by black arrows. For details see the text. The alignment consensus indicates the conservation degree obtained by aligning the following UNIPROT codes: Q9WUD2, Q9WTR1, Q9Y5S, E2RLX8, F6WJB2, F7BDA4, F7A622, G1RXC4, G1SNM3, F1SDE4, G3T6Z2, G3GVL1, Q5EA32, G3WJU0, F6RMV4, F7A8J8, G1N455, F1NPJ9, F6UY90. The alignment has been built in MAFFT [136] and plotted using JALVIEW [137] and the functional ZAPPO profile. Inset, the human TRPV1–4 pore region aligned highlighting the differences in respect to the pore and selectivity filter consensus sequence.

gene duplication occurring after the divergence between tetrapods and vertebrates. Saito and Shingai argue that based on genomic organization of TRPVs the first possibility is more likely [36].

TRPV2 sequence features are best understood through comparisons with the other TRPV subfamily members. Excellent reviews on the structural organization of TRPV channels are available [7,37,38]. Briefly, TRPV2 consists of a large N-terminal cytoplasmic domain (~ 390 residues), followed by six transmembrane segments (~ 250 residues) containing a pore-forming loop, and a C-terminal cytoplasmic domain (~ 100 residues). Specific TRPV2 sequence features are summarized in Fig. 2.

The N-terminal cytoplasmic region of TRPV2 can be further subdivided into a distal N-terminal region, an ankyrin repeat domain (ARD) and a membrane-proximal linker region. The distal N-terminal cytoplasmic region comprises the first ~ 60–70 residues, which were not ordered and therefore not visible in the first crystal structure obtained for a human TRPV2 N-terminal region [39]. This distal N-terminal region is rather divergent in length, sequence and function for different TRPV channels. For instance, the TRPV4 N-terminus is longer, ~ 130 residues, and contains a proline-rich segment that interacts with the SH3 domain of PACSIN [40]. In rat TRPV2, deletion of up to 65 N-terminal residues did not significantly alter channel function as assessed *in vitro*, whereas deletion of 83 or more residues greatly reduced plasma membrane expression in HEK293 cells [41], supporting the assignment of a domain boundary around 60–70 residues from the N-terminus.

Residues ~ 70–320 of TRPV2 form the ARD, which contains six ankyrin repeats. This soluble domain has yielded the only piece of atomistic tridimensional information currently available for TRPV2: the crystal structures of the human and rat TRPV2-ARD were published nearly simultaneously [39,42]. ARDs are common protein–protein recognition domains, and although by no means unique to TRP channels they are clearly important for the modulation of TRP channels from the TRPA, TRPC, TRPN and TRPV

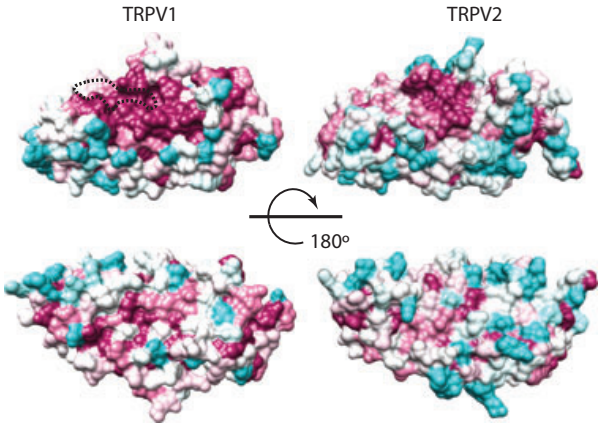

Fig. 3. The TRPV2-ARD concave surface has a small conserved region. The sequence conservation of TRPV1 and TRPV2 orthologs is mapped onto the crystal structures of the TRPV1-ARD (left) [70] and TRPV2-ARD (right) [42], respectively, using CONSURF [138]. The degree of conservation follows a gradient from magenta, most conserved, to cyan, least conserved. The ATP binding region in TRPV1-ARD is indicated by a dashed outline.

subfamilies [43]. Each TRPV2 ankyrin repeat (ANK1–6) is defined by two antiparallel helices (inner and outer) followed by a loop region linking to a β-hairpin structure (named Fingers 1–5). These motifs are arranged linearly, with repeats packing side-by-side and the β-hairpin structures projecting out ~ 90° relative to the helical axes. Each ankyrin repeat is typically rotated a few degrees counterclockwise relative to the previous repeat, leading to an overall helical arrangement of the repeats [44]. The concave surface thus generated is often used in protein–ligand interactions to modulate the function of ARD-containing proteins. This is an important observation when comparing the sequence conservation profiles of the ARDs of TRPV1 and TRPV2 (Fig. 3). When the sequence conservation within a set of orthologous sequences is mapped onto the molecular surface of the ARD, TRPV2 shows a lower degree of conservation than TRPV1. The most conserved region on the TRPV2-ARD surface does map to the concave surface, partially overlapping with the larger conserved region on

the TRPV1-ARD. As detailed below, the TRPV1-ARD binds to ATP, but the ATP binding region, highly conserved in TRPV1, is not present in TRPV2 (Fig. 3). Overall, the different conserved surface profiles of TRPV1 and TRPV2 suggest that their ARDs bind to a different set of regulatory ligands.

Connecting the TRPV2-ARD to the first transmembrane segment (S1) is a highly conserved ~ 65-residue segment, which has been referred to as the membrane proximal domain. Functional analyses of modular chimeras between TRPV1 and TRPV2, and their functional analyses expressed in HEK cells, suggest that the membrane proximal domain is an important structural module for the temperature sensitivity of TRPV channels [45].

As mentioned above, the TMD (residues ~ 390 and ~ 640) of TRPV2 is predicted to contain six transmembrane segments (S1–S6) and a pore-forming loop between S5 and S6 (predictions by TMHMM [46] and ΔGPRED [47]). Accordingly, we have experimentally refined the position of the TMD for rat TRPV2 to be between residues 389 and 638 (unpublished results) as shown in Fig. 2. Heat, pH, voltage sensitivity and agonist binding sites for TRPV1 have been related to residues in the TMD (both at transmembrane segments and loops) but none of the results obtained for TRPV1 could be translated for TRPV2 [48]. For example, residues in the S4–S5 linker region may be important for voltage sensitivity of TRPV1; however, no effect has been observed when mutating analogous residues in the TRPV2 S4–S5 linker [49].

An interesting feature in the TRPV2 TMD is the presence of an N-glycosylation consensus motif (NXT/S) in the S5–S6 loop (Fig. 2). While the first asparagine is only found in rat and hamster TRPV2, the second one is conserved in nearly all TRPV2 orthologs. This glycosylation site is analogous to the N604 glycosylation site for TRPV1 [50]. An interesting study showed that, in rat F11 DRG cells, heterologously expressed rat and mouse TRPV2 are mostly expressed in the plasma membrane in a glycosylated form, whereas the endogenous TRPV2 isoform (rat) remains in the cytoplasm in a non-glycosylated form [51]. These results suggest that glycosylation plays a role in TRPV2 trafficking towards the plasma membrane, as has been shown for other TRPs [52,53]. Recent reports indicate that the glycosylation of TRPV2 may play an anchoring role under the modulation of the Klotho factor [54] (further discussed below).

The TRPV2 pore-forming domain and selectivity filter, located in the S5–S6 region, is highly conserved (Fig. 2). Although the selectivity filter does not show a clear consensus sequence across the TRP channel superfamily [55,56], the TRPV1–4 group shows high overall conservation (Fig. 2, inset). TRPV2 does differ in divalent/monovalent cation permeability from the rest of the non-selective TRPV subfamily members (TRPV1, TRPV3 and TRPV4), with the lowest $P_{Ca^{2+}}/P_{Na^{+}}$ at 2.94 (TRPV1 ~ 10, TRPV3 ~ 10, TRPV4 ~ 6) [3]. This difference in selectivity could be due to the conserved aspartate-to-glutamate substitution in TRPV2 (highlighted in Fig. 2, inset). TRPV4 shows a similar aspartate-to-glutamate substitution at a different location in the selectivity filter, which may similarly account for somewhat lower $P_{Ca^{2+}}/P_{Na^{+}} \sim 6$ selectivity compared with $P_{Ca^{2+}}/P_{Na^{+}} \sim 10$ for TRPV1 and TRPV3. Mutagenesis studies in the pore-forming region have indicated that mouse TRPV2 heterologously expressed in HEK cells may be constitutively active, inducing high cytotoxicity, since a change of charge mutant (E594K) reduced cytotoxicity [57].

The C-terminal cytoplasmic domain spanning residues 639–761 in rat TRPV2 contains relevant features for the assembly of the channel, such as oligomerization (TRP domain), phosphatidylinositol 4,5-bisphosphate (PIP_2) binding and calmodulin binding domains [58–60]. Although the sequence determinants driving TRPV2 oligomerization have not been proven directly, studies on TRPV4 [61] and TRPV1 [60] provide strong arguments for the role of a C-terminal coil-coiled domain in the homotetramerization of the channels. The predicted coil-coiled domain in TRPV1 overlaps with the TRP domain, just after the S6 segment. The TRP domain consists of ~ 20 amino acids, and for TRPV1 it has been shown that it participates in channel oligomerization and gating transduction [60,62,63].

TRPV2 regulatory interactions

Several regulatory interactions between TRPV2 cytoplasmic domains and various signalling molecules have been investigated. A two-hybrid screening using the first ~ 390 residues of human TRPV2, corresponding to the whole N-terminal cytoplasmic region, identified an interaction of TRPV2 with recombinase gene activator (RGA) [64] in the RBL2H3 mast cell line. Although it was later demonstrated that a physiological complex containing both TRPV2 and RGA is crucial for the cAMP-driven trafficking of TRPV2 to the plasma membrane, it remains unclear whether RGA and TRPV2 interact directly [65].

The TRPV2 N-terminal region has also been implicated in another protein–protein interaction. Mouse TRPV2 residues 1–167 were used as bait to identify the human GSRP-56 (Golgi-localized spectrin-repeat containing protein 56), which is an alternative splicing

isoform of Syne-1 (synaptic nuclear envelope protein 1) [66]. A physiological role for this interaction has yet to be elucidated.

The N-terminal ARD plays important roles in the regulation of the TRPV channels. For instance, mutations to its concave surface affect the activity of TRPV1, TRPV3 and TRPV4 [67–70]. In the case of TRPV1, the channel activity can be modulated by ATP or calmodulin, and these two ligands were found to bind competitively to the TRPV1-ARD concave surface [70]. This finding was extended to TRPV3 and TRPV4, although the details of the modulatory effects differ [68]. Intriguingly, TRPV2 is the only member of the TRPV1–4 group that shows no binding of ATP or calmodulin to its ARD and is insensitive to changes in intracellular ATP concentration [67–70].

The TRPV2 Ca^{2+}-dependent desensitization is dependent on PIP_2 depletion from the membrane [58]. The C-terminal TRP domain contains the TRP box (I_{695}WKLQR$_{701}$ in rat TRPV1, I_{659}WKLQK$_{664}$ in rat TRPV2), which has been implicated in PIP_2 and calmodulin binding. Alanine mutagenesis of TRPV1 residues I696, W697 and R701 (K in TRPV2) severely affected channel gating, raising the free energy of channel activation [62]. Mercado *et al.* defined a PIP_2 binding domain in TRPV2 within the C-terminal proximal residues 647–715 [58] (Fig. 2). It has been proposed that the phospholipase C hydrolysis of PIP_2 is the main regulatory process for TRPV2 and other TRP channels [71]. Recently, Julius and his team have shown compelling evidence that TRPV1 is intrinsically temperature sensitive by using an extremely elegant TRPV1 reconstitution model [72]. Besides being the first published report for TRPV1 activity in a biochemically defined reconstituted membrane system, they describe the inhibition of TRPV1 by C-terminal binding of phosphoinositides. A number of studies had previously provided evidence favoring a sensitizing role of phosphoinositides [58,71]. In contrast, the Julius laboratory had already previously described PIP_2-mediated inhibition of TRPV1 in cells [73], and they now provided strong evidence of a similar inhibitory role in a reconstituted system. Julius and colleagues present a comprehensive and testable model of how the physiology of phosphoinositide levels can regulate TRPV1 activity, which may be a conserved mechanism for TRPV2.

A C-terminal TRPV2 calmodulin binding domain was initially predicted and later characterized *in vitro* by the Gordon laboratory [58,74]. This calmodulin binding domain was further characterized and restricted to the 654–683 region of human TRPV2, almost fully overlapping with the TRP domain [59]. Despite showing binding of calmodulin to a C-terminal fragment of TRPV2 (residues 684–753, Fig. 2) in a Ca^{2+}-dependent manner, the Gordon laboratory could not show that calmodulin is a major player in TRPV2 desensitization [58].

A few additional predicted and/or characterized TRPV2 interacting proteins have been cataloged in the TRP channel interacting protein (TRIP) database [75,76], some of which are further detailed in later sections.

TRPV2 physiology and signalling pathways

TRPV2 is a homotetrameric N-glycosylated protein that translocates from intracellular membrane compartments to the plasma membrane after stimulation of the phosphatidylinositol 3-kinase (PI3K) and other kinase signalling pathways. TRPV2 proteins expressed heterologously in HEK293 cells show a species-dependent variability in thermal sensing and ligand activation (further described below in TRPV2 modulation and pharmacology). From a physiological perspective, TRPV2 has been associated with several functions depending on the considered tissue. Although originally described as a noxious heat thermosensor, several reports point towards TRPV2 functioning instead as a mechanoreceptor and/or osmosensor. Strikingly, TRPV2 knockout mice display normal thermal and mechanical nociception responses [18]. Analysis of sensory ganglia development (DRG and trigeminal ganglia) resulted in no significant differences comparing wild-type and knockout tissues. The acute nociception and hyperalgesia responses to thermal and mechanical stimuli in the knockout mice were normal. To discard compensation effects of other heat-gated channels on the TRPV2 knockout mice, the authors studied TRPV1/TRPV2 double knockout mice and the thermal phenotype was statistically indistinguishable from the single TRPV1 knockout. From a chemical ligand perspective, in contrast to most studies where TRPV2 was expressed heterologously, studies of TRPV2-null cultured neurons showed no differential calcium responses dependent on cannabinoid, probenecid or 2-aminoethoxydiphenyl borate (2-APB) compared with wild-type, although the wild-type responses were highly inconsistent [18]. Therefore, the TRPV2 knockout mouse analyses indicate that TRPV2 is not sensitive to these compounds under physiological conditions.

The most distinctive features of the knockout mice are reduced perinatal viability and embryo and adult body weight. Although the study of the knockout mice

has thus far shed little light on the physiological roles of TRPV2, studies derived from culturing knockout mice cells indicate that macrophage function is clearly affected [77], which may correlate with perinatal lethality relating TRPV2 to immune activity (discussed below and excellently reviewed recently in [78]). In summary, the physiological role of TRPV2 is probably one of the most unsettled and controversial among TRP channels. Below we discuss the available data on TRPV2 physiology and signalling pathways, but first we introduce the pharmacological agents that have been shown to modulate TRPV2. The sparse pharmacology toolkit available to study TRPV2 is important for evaluating our knowledge of TRPV2 physiology.

TRPV2 modulation and pharmacology

The pharmacology of TRP and TRPV channels has been extensively and excellently reviewed [2,28,79]. Several compounds have been shown to modulate TRPV2. However, few of them are specific, and most show species dependence in their effectiveness on TRPV2 (Table 1). The fact that TRPV2 was initially proposed as a noxious heat thermosensor involved in nociception may have misled the TRPV2 deorphanizing attempts to find endogenous and/or specific modulators. Other more physiological modulators will be described in subsequent sections. Here, we focus on the main chemical modulators for TRPV2 (listed in Table 1).

Cannabis sativa derivatives have proved to be the most potent TRPV2 activators thus far with EC_{50} in the micromolar range, although they are not specific for TRPV2 [80,81]. In a comparison of a panel of cannabinoids, TRPV2 is most strongly activated by (−)-trans-Δ9-tetrahydrocannabinol, cannabidiol and Δ9-tetrahydrocannabivarin, whereas cannabinoic acids are least potent [81]. However, cannabinoids can also activate other TRP channels, e.g. cannabidiol is a potent activator of TRPV1 and TRPA1 [81]. Therefore, one has to be cautious in assigning the effect of these compounds to TRPV2 in a physiological context – in studies using live animal or native tissues, for example. Indeed, proof of direct interaction between TRPV2 and cannabidiol from biochemical and structural perspectives would promote better understanding of TRPV2's activity.

2-APB was one of the first activators identified for TRPV2, with an EC_{50} of 129 μM in transfected HEK293 cells [82]. Later reports showed that human TRPV2 was insensitive to 2-APB, indicating species-dependent variability in 2-APB sensitivity [41,83]. Dyphenylboronic anhydride (DPBA) also activates mouse but not human TRPV2 [83,84]. After testing the activation by 2-APB and DPBA on chimeric TRPV2 constructs, Juvin *et al.* speculated that the 2-APB sensitivity region could be located in the cytoplasmic domains [83].

Blockers have been identified that can affect TRPV2 function, although most are promiscuous compounds that therefore have to be used with caution. The activation of mouse TRPV2 by 2-APB helped identify SKF96365 and amiloride as TRPV2 blockers [83]. Ruthenium Red, trivalent cations and citral have also been identified as non-specific TRPV2 channel blockers [82,85,86].

Table 1. TRPV2 pharmacology. NA, not available.

Effect	Compound	Class	Concentration	System/species	Reference
Agonist	2-APB[a]	Diphenyl compound	129 μM	HEK-293/rat	[82]
Agonist	Diphenylboronic anhydride	Diphenyl compound	100 μM	HEK-293/rat	[84]
Agonist	Cannabidiol[a]	Cannabinoid	1.25 μM	HEK-293/rat	[81]
Agonist	Cannabigerol	Cannabinoid	1.72 μM	HEK-293/rat	[81]
Agonist	Cannabinol	Cannabinoid	39.9 μM	HEK-293/rat	[81]
Agonist	Cannabidivarin	Cannabinoid	7.3 μM	HEK-293/rat	[81]
Agonist	Cannabigivarin	Cannabinoid	1.41 μM	HEK-293/rat	[81]
Agonist	Δ^9-tetrahydrocannabinol[a]	Cannabinoid	0.65 μM	HEK-293/rat	[81]
Agonist	Tetrahydrocannabinol acid	Cannabinoid	18.4 μM	HEK-293/rat	[81]
Agonist	Tetrahydrocannabivarin	Cannabinoid	4.11 μM	HEK-293/rat	[81]
Agonist	Lysophosphatidyl choline	Lysophospholipid	3.37 μM	HEK-293/rat	[81,132]
Agonist	Lysophosphatidyl inositol	Lysophospholipid	NA	HEK-293/rat	[132]
Agonist	Probenecid	Uricosuric compound	31.9 μM	HEK-293/rat	[87]
Antagonist	Ruthenium Red	Inorganic dye	0.6 μM	HEK-293/rat	[25]
Antagonist	SKF96365	Alkylated imidazole	100 μM	CHO-K1/mouse	[83]
Antagonist	Tranilast	Diphenyl compound	10–100 μM	MCF-7/human	[89]

[a] Species dependence [41].

From a specificity perspective, two compounds have shown promising results as more specific modulators of TRPV2: probenecid and tranilast, as activator and inhibitor respectively. Probenecid (*p*-(di-*n*-propylsulfamyl)-benzoic acid), although not exclusive for TRPV2, showed high specificity for this TRP channel, compared with TRPV1, TRPV3, TRPV4, TRPA1 and TRPM8, with an EC_{50} = 32 μM in transiently transfected TRPV2-expressing HEK293 cells [87]. A recent report has shown the effect of probenecid on TRPV2 *in vivo* and *ex vivo* [88]. As an inhibitor, tranilast is an antiallergic drug described as an ion channel blocker by the Kojima laboratory [89]. Tranilast has been used recently in several reports as a TRPV2-specific antagonist [90–92], although it has not to our knowledge been fully validated as a direct TRPV2 blocker.

TRPV2 in the nervous system

During neural development, TRPV2 is expressed in developing mouse DRG and spinal motor neurons from embryonic day 10.5 and sustained until embryonic day 13.5 [93]. This expression pattern and the localization of TRPV2 in developing growth cones pointed to the possible involvement of TRPV2 in axon outgrowth. Tominaga and his colleagues indeed observed membrane-stretch-induced TRPV2 activation and subsequent intracellular Ca^{2+} elevation exerted by axon outgrowth in developing neurons [93]. Of note, a role for TRPV2 in the developing nervous system could help explain the reduced perinatal viability observed in TRPV2 knockout mice.

There is also evidence for TRPV2 expression in the adult peripheral and central nervous systems. In DRG [25,94] and trigeminal ganglia [95], TRPV2 expression is concentrated in a population of medium- and large-diameter primary afferents that do not express TRPV1, primarily in myelinated A- and C-fiber sensory neurons [96–102]. Many of the neurons expressing TRPV2 are peptidergic neurons. For instance, in mice TRPV2 colocalized with substance P [96]. Another study found that one-third of TRPV2-expressing cultured rat DRG neurons were calcitonin-gene-related peptide positive, and activation of TRPV2 cannabinoid derivatives led to calcitonin-gene-related peptide release [80]. In primary cultures of myenteric neurons, TRPV2-like currents were invoked by 2-APB, probenecid or lysophospholipids and stretch [92]. The same study also found that intestine relaxation is inhibited by nitric oxide synthase inhibitors and TRPV2 antagonists like tranilast. Furthermore, TRPV2 agonists inhibited muscle contraction, but not in the presence of a nitric oxide synthase inhibitor, indicating that TRPV2 is activated downstream of nitric oxide. This last study therefore suggests that TRPV2 may be important in controlling the activity of sympathetic muscles like those of the intestinal track, and that the nitric oxide signalling pathway may be an important pathway that modulates TRPV2 function *in vivo*. One overarching conclusion, previously highlighted by the Basbaum and Julius groups, is that in contrast to TRPV1 the widespread distribution of TRPV2 in the spinal cord suggests that TRPV2 is a player in several physiological roles besides nociception [98].

A number of studies have also observed broad TRPV2 expression in important regions in rat, mouse and macaque brains [35,103–105]. A systematic approach analyzing the transcriptome of developing and mature mouse forebrain has identified TRPV2 as the highest expressing TRPV channel in the neurons of this brain region [106]. This is in contrast to TRPV1 for which a thorough study with green fluorescent protein reporter transgenic lines found that TRPV1 expression is essentially restricted to the hypothalamus within the mouse brain [107]. Recently, a thorough characterization of the expression and distribution of TRPV2 in rat forebrain and hindbrain has been published [108]. In this study, they observe TRPV2 expression in a number of brain structures relevant to osmoregulation and other autonomic functions. This detailed work provides important clues on TRPV2 function suggesting, along with the previous studies, that TRPV2 is important in various osmosensory mechanisms, including osmotic balance, autonomous regulation, somatosensation, food and fluid intake, and cardiovascular functions [104,105,108].

TRPV2 in the endocrine system

TRPV2 has also been implicated in the endocrine system, more specifically in pancreas and insulin secretion. In early studies, the Kojima laboratory cloned TRPV2 as a calcium-permeable channel that translocates from intracellular pools towards the plasma membrane in response to IGF-1 [26]. More recently [91], the same laboratory determined that TRPV2 is highly expressed in the β-type insulinoma cell line MIN-6 and in the core of mouse pancreatic islets but not in α-cells. Using various inhibitors, knockouts and knockdowns, they determined that TRPV2 translocation is downstream of insulin signalling and upstream of insulin secretion and cell growth, suggesting that TRPV2 is part of an autocrine positive feedback loop for insulin secretion. Furthermore, glucose-induced insulin exocytosis is mediated by the TRPV2-dependent intracellular increase of Ca^{2+} concentration [90].

Of note, these studies have relied on the blocking effects of tranilast on TRPV2.

In β-cells, TRPV2 levels in the plasma membrane are also affected by Klotho, an antiaging protein, with TRPV2 downstream of Klotho and upstream of insulin secretion [54]. Interestingly, Klotho has a similar effect on the plasma membrane localization of TRPV5 in the kidney [109]. Klotho cleaves the terminal sialic acid in the glycan moiety of TRPV5, promoting the binding of galectin-1 to the processed glycan and thereby anchoring TRPV5 in the plasma membrane [110]. It is interesting to speculate whether TRPV2 translocation to the plasma membrane could be similarly mediated through modification of TRPV2 glycosylation (Fig. 2).

TRPV2 in immunity

TRPV2 is expressed in immune-related tissues such as the spleen [25], but additionally TRPV2 transcripts have been detected in many resident macrophage populations such as liver Kupffer cells, skin epidermal Langerhans cells and lung alveolar macrophages [77]. TRPV2 expression has also been identified in mast cell populations [65,111,112] and in lymphocytes [113].

There are several lines of evidence suggesting that TRPV2 function is important in various immune cell types. Studies from the Turner laboratory [65,112] show that physical stimuli leading to mast cell degranulation involve TRPV2 activation and calcium entry. They demonstrated a direct interaction of TRPV2 with an A-kinase-adapter-protein (AKAP)-like protein, ACBD3 (acyl CoA binding domain protein), and that TRPV2 can be phosphorylated by protein kinase A *in vitro*, suggesting that TRPV2 activation in mast cells could be mediated by a protein kinase A signalling pathway. Zhang *et al.* [111] show TRPV2-mediated mast cell degranulation in a human cell line (HMC-1) in response to several stimuli such as temperature (> 50 °C), red light and mechanical stress. Of note, this TRPV2-mediated thermal response in a human cell line contradicts previous observations that human TRPV2 does not respond to noxious heat temperatures [41].

A study of TRPV2-deficient macrophages led to the conclusions that TRPV2 is involved in phagocytosis and that TRPV2 recruitment towards the phagosome is driven by PI3K signalling, Src kinases, akt kinase and protein kinase C, but not by phospholipase C nor the Syk kinases [77]. A previous study had similarly shown the translocation of TRPV2 from the endoplasmic reticulum to the plasma membrane in macrophages after activation of the PI3K signalling pathway activated by the fMetLeu chemotactic peptide [114], similarly to the effect of the neuropeptide head activator in neuronal and neuroendocrine cell cultures [115]. Further studies on TRPV2 in macrophages showed that TRPV2 translocated to the podosome [116], where the plasma membrane calcium concentration seems to play a crucial role on the podosome assembly, an indispensable cytoskeleton tool for migration of cells such as macrophages, neutrophils, endothelial cells and malignant tumor cells [117].

Like most of TRPV2's physiology, the role in immunity is not exempt from controversy. Comparing wild-type and TRPV2-deficient macrophages led to the conclusion that lipopolysaccharide (LPS)-induced tumor necrosis factor (TNF) release in macrophages is not mediated by TRPV2 [77]. However, Yamashiro *et al.* [118] showed evidence that TRPV2 was involved in TNF and interleukin-6 production induced by LPS in the RAW macrophage cell line. These authors argue that the differences between the Link *et al.* [77] and Yamashiro *et al.* [118] studies may derive from experimental conditions.

TRPV2 in circulatory organs and muscle function

TRPV2 is expressed in smooth muscle and endothelial cells of arteries in both rabbit [119] and human [120], and in smooth muscle cells of veins in rats [121], suggesting a role of TRPV2 in circulatory organs. Muraki *et al.* [105] found that Ruthenium Red and antisense oligos against TRPV2 decreased both the nonselective cation channel current and Ca^{2+} influx induced by hypotonic swelling of aortic myocytes. In contrast, inhibitors of L-type voltage-dependent calcium channels or treatment with caffeine had no effect, indicating that TRPV2 is activated by hypotonic induced cell swelling in arteries.

Studies in striated muscle are also providing new insights into the pathophysiological role of TRPV2. The Shigekawa laboratory identified TRPV2 as the predominant TRP channel in heart [122]. Comparing the skeletal to cardiac muscle expression of TRPV2, it has been shown that the expression in cardiac muscle is 10-fold higher [122]. In skeletal muscle, the expression of TRPV2 in normal tissue is mostly located in the cell interior, and it is translocated towards the sarcolemma by addition of IGF-1. In dystrophic striated muscle, TRPV2 increases its expression level in the sarcolemma. This deregulated overexpression of TRPV2 in the sarcolemma may account for abnormal or leaky Ca^{2+} influx in dystrophic phenotypes [123]. Duchenne's muscular dystrophy's hallmark is the lack of expression of dystrophin disrupting the link between

the extracellular matrix and the cytoskeleton, which is mediated by the interaction between dystrophin and dystroglycans and sarcoglycans (forming the dystrophin–glycoprotein complex, DGC) [124]. This DGC disruption affects stretch-modulated channels such as TRPV2. This hypothesis has been studied in eccentric contractions (lengthening) in dystrophic muscle where the endogenous expression of TRPV2 has been reduced by the use of dominant-negative TRPV2 transgenic mice [122,123,125].

TRPV2 in cancer

Overexpression of TRPV2 at the mRNA and protein levels has been observed in several cancer types and cell lines [126]. Nevertheless the role, if any, of TRPV2 in cancer remains poorly understood. With regard to liver cancers, TRPV2 shows high expression levels in human hepatocarcinoma cells (HepG2) [127]. Another study found high TRPV2 levels in cirrhotic liver and well-differentiated hepatic tumors compared with poorly differentiated tumors, suggesting a potential role for TRPV2 as a prognostic marker [128].

TRPV2 has also been linked to bladder cancers. TRPV2 mRNA and protein levels were detected in both normal tissue and urothelial carcinoma patients and cell lines [129]. Intriguingly, mRNA was also detected for a short splice variant (s-TRPV2) in which removal of exons 10–11 produced a protein without residues 529–663 – corresponding to the S5–S6 segments – although the presence of the corresponding protein was not confirmed. In non-tumor patients, mRNAs for both the full-length and short splice variants were found, but the s-TRPV2 variant was less abundant and the full-length mRNA more abundant in late-stage tumors [129]. A second study similarly observed higher TRPV2 mRNA levels in a poorly differentiated bladder cancer cell line compared with a well-differentiated line [130]. Furthermore, the carcinoma cells that expressed high levels of TRPV2 underwent apoptosis when exposed to the TRPV2 agonist cannabidiol, arguing for TRPV2 as a potential therapeutic target for the treatment of bladder cancer.

In prostate cancer, TRPV2 expression levels are higher in metastatic cancers compared with solid tumors, defining TRPV2 as a potential marker for advanced prostate cancer [131]. Lysophospholipids mediated the translocation of TRPV2 to the plasma membrane, stimulating prostate cancer cell migration but not cell growth [132]. This suggests that TRPV2 plays a role in cancer cell migration that is analogous to its role in macrophages.

The Santoni group has investigated the expression of TRPV2 in gliomas. In primary glioma cells, mRNA TRPV2 expression is reduced compared with benign astrocyte control tissues, with a progressive reduction in high grade gliomas [133]. Furthermore, TRPV2 silencing favors cell proliferation and survival of the U87MG cell line [133], whereas overexpressing TRPV2 in the MCZ glioma cell line resulted in reduced tumor diameter and glioma viability [134]. Altogether, the results suggest that TRPV2 functions as a negative regulator of glioma cell survival and proliferation. A very recent study similarly points to TRPV2 as an important therapeutic target for the treatment of glioblastoma, showing that cannabidiol enhances TRPV2 expression and activity, inducing apoptosis of human glioma cell lines [135]. The authors also suggest a role for TRPV2 in the uptake of chemotherapeutic agents, showing that a TRPV2 pore-less variant (deleting residues 572–609) reduces doxorubicin uptake in a dominant-negative manner [135]. Strikingly, a short TRPV2 splice variant (Δ551–663, corresponding to the pore region and the sixth transmembrane segment) has been identified in human leukemic cell lines [114], similar to the s-TRPV2 variant observed in bladder cells [129]. Nagasawa *et al*. speculate that short variants can act as dominant-negative mutant, forming heteromers with full-length TRPV2 that do not traffic to the plasma membrane [114]. This hypothesis also fits the glioma results [135], as an explanation for chemotherapy resistance in tumor cell lines, and points to TRPV2 as a promising therapeutic target in several cancer types.

Conclusions and future perspectives

We have reviewed the current information about the sequence determinants and physiology of the TRPV2 ion channel. The TRPV2 tissue distribution is quite broad and the cellular signalling pathways that regulate its function seem to show some tissue-specific variations. *In vivo*, the knockout TRPV2 mouse model argues against the role of TRPV2 as a mechanosensor and thermosensor. The fact that TRPV1/TRPV2 double knockout mice show a thermal phenotype that is indistinguishable from the single TRPV1 knockout should discourage future classification of TRPV2 as a thermosensor, at least in mice. Most *in vitro* cellular studies have shown TRPV2 to be activated downstream of physical stimuli such as mechanical stretch, heat, osmotic swelling, and endogenous and exogenous chemical modulators such as hormones, growth factors, chemotactic peptides (fMetLeu, neuropeptide head activator etc.), lysophospholipids and cannabinoids. Depending on the cell type, TRPV2 is regulated by general or

specific signalling pathways involving phospholipase C, the PI3K pathway or other kinases. However, an important theme is emerging that TRPV2 is regulated through translocation and trafficking from internal cytosolic pools towards the plasma membrane, where the levels of PIP_2 in the surroundings of TRPV2 seem to play a crucial role in TRPV2-mediated Ca^{2+} signalling. Concerning the translocation mechanism, heterologous expression studies of recombinant TRPV2 in HEK cells have shown that PI3K activation of TRPV2 does not drive TRPV2 trafficking towards the cell surface [57] in contrast to other studies [26,77,114,116,122]. The set of controversies related to TRPV2, such as thermosensation, translocation, LPS dependence etc., should call for extra attention on drawing definitive conclusions, since experimental conditions (e.g. expression systems, antibodies, detection tags/epitopes) seem to be a major source of conflicting observations for TRPV2 activation. Another major limitation in TRPV2 biochemistry and physiology studies is the scarcity of specific endogenous ligands and/or pharmacological drugs, making TRPV2 essentially an orphan TRP channel. The most reliable pharmacological modulators for TRPV2 are probenecid [87] and cannabidiol [135], as agonists, which are also known to activate/inhibit other TRP channels (e.g. TRPV1, TRPA1, TRPM8 [81,87]), which can lead to complications in interpreting experiments in physiological systems coexpressing several TRP channels. Regarding inhibition, tranilast has been identified, so far, as a TRPV2-specific antagonist [89].

To deorphanize TRPV2 and to understand TRPV2's molecular mechanisms, a combination of several approaches can be taken. First, integrating the current physiological knowledge of TRPV2 with structural biology approaches will open new perspectives on how this polymodal tetrameric channel is modulated. New structural knowledge on TRPV2 will also provide more general knowledge on the TRPV subfamily, including its closest homolog TRPV1, and the TRP superfamily. For example, the structural characterization of the N-terminal ARD has already yielded information about differential TRPV2 regulation compared with the rest of the TRPV subfamily. In line with the structural biology aspect, biochemical and/or structural evidence for TRPV2 modulator binding would be ideal for a better understanding of TRPV2 molecular mechanisms. Second, obtaining information on the TRPV2 interactome has already provided insightful information such as protein–protein interactions implicated in regulation, translocation and trafficking. Further studies on the TRPV2 interactome may open new physiological perspectives on TRPV2's elusive role(s). Finally, the development of methods to identify modulators of TRPV2 in a high-throughput screening fashion should open new therapeutic perspectives for a channel with potential implications in several types of cancer and other disorders such as muscular dystrophies, diabetes and central nervous system disorders. Interestingly, several pharmaceutical companies have started to patent compounds and methods to screen properties of TRPV2 (reviewed in [28]). We can therefore anticipate some synergy in which pharmacological advances will enable experiments to deepen our understanding of TRPV2 physiology.

Acknowledgements

The authors want to acknowledge the funding from Spanish Government Young Researcher Grant (MICINN-SAF2010-21385 to A.P.-M.), a Marie Curie International Outgoing Fellowship within the 7th European Community Framework Programme (PIOF-GA-2009-237120 to A.P.-M.) and the National Institutes of Health (R01GM081340 to R.G.).

References

1 Nilius B & Owsianik G (2011) The transient receptor potential family of ion channels. *Genome Biol* **12**, 218.
2 Ramsey IS, Delling M & Clapham DE (2006) An introduction to TRP channels. *Annu Rev Physiol* **68**, 619–647.
3 Venkatachalam K & Montell C (2007) TRP channels. *Annu Rev Biochem* **76**, 387–417.
4 Wu L-J, Sweet T-B & Clapham DE (2010) International Union of Basic and Clinical Pharmacology. LXXVI. Current progress in the mammalian TRP ion channel family. *Pharmacol Rev* **62**, 381–404.
5 Montell C, Birnbaumer L & Flockerzi V (2002) The TRP channels, a remarkably functional family. *Cell* **108**, 595–598.
6 Montell C (2005) The TRP superfamily of cation channels. *Sci STKE* **272**, re3.
7 Latorre R, Zaelzer C & Brauchi S (2009) Structure–functional intimacies of transient receptor potential channels. *Q Rev Biophys* **42**, 201–246.
8 Minke B (1977) Drosophila mutant with a transducer defect. *Eur Biophys J* **3**, 59–64.
9 Montell C & Rubin GM (1989) Molecular characterization of the Drosophila trp locus: a putative integral membrane protein required for phototransduction. *Neuron* **2**, 1313–1323.
10 Almén MS, Nordström KJV, Fredriksson R & Schiöth HB (2009) Mapping the human membrane proteome: a majority of the human membrane proteins can be classified according to function and evolutionary origin. *BMC Biol* **7**, 50.

11 Levine JD & Alessandri-Haber N (2007) TRP channels: targets for the relief of pain. *Biochim Biophys Acta* **1772**, 989–1003.
12 Chung M-K, Jung SJ & Oh SB (2011) Role of TRP channels in pain sensation. *Adv Exp Med Biol* **704**, 615–636.
13 Colbert HA, Smith TL & Bargmann CI (1997) OSM-9, a novel protein with structural similarity to channels, is required for olfaction, mechanosensation, and olfactory adaptation in *Caenorhabditis elegans*. *J Neurosci* **17**, 8259–8269.
14 Xiao R & Xu XS (2010) *C. elegans* TRP Channels. *Adv Exp Med Biol* **704**, 323–339.
15 Kim J, Chung YD, Park D-Y, Choi S, Shin DW, Soh H, Lee HW, Son W, Yim J, Park C-S *et al.* (2003) A TRPV family ion channel required for hearing in Drosophila. *Nature* **424**, 81–84.
16 Clapham DE (2007) Mammalian TRP channels. *Cell* **129**, 220.
17 Hellwig N, Albrecht N, Harteneck C, Schultz G & Schaefer M (2005) Homo- and heteromeric assembly of TRPV channel subunits. *J Cell Sci* **118**, 917–928.
18 Park U, Vastani N, Guan Y, Raja SN, Koltzenburg M & Caterina MJ (2011) TRP vanilloid 2 knock-out mice are susceptible to perinatal lethality but display normal thermal and mechanical nociception. *J Neurosci* **31**, 11425–11436.
19 Caterina MJ (2000) Impaired nociception and pain sensation in mice lacking the capsaicin receptor. *Science* **288**, 306–313.
20 Moqrich A (2005) Impaired thermosensation in mice lacking TRPV3, a heat and camphor sensor in the skin. *Science* **307**, 1468–1472.
21 Lee H, Iida T, Mizuno A, Suzuki M & Caterina MJ (2005) Altered thermal selection behavior in mice lacking transient receptor potential vanilloid 4. *J Neurosci* **25**, 1304–1310.
22 Huang SM, Li X, Yu Y, Wang J & Caterina MJ (2011) TRPV3 and TRPV4 ion channels are not major contributors to mouse heat sensation. *Mol Pain* **7**, 37.
23 Sokolchik I, Tanabe T, Baldi PF & Sze JY (2005) Polymodal sensory function of the *Caenorhabditis elegans* OCR-2 channel arises from distinct intrinsic determinants within the protein and is selectively conserved in mammalian TRPV proteins. *J Neurosci* **25**, 1015–1023.
24 Gong Z, Son W, Chung YD, Kim J, Shin DW, McClung CA, Lee Y, Lee HW, Chang D-J, Kaang B-K *et al.* (2004) Two interdependent TRPV channel subunits, inactive and Nanchung, mediate hearing in Drosophila. *J Neurosci* **24**, 9059–9066.
25 Caterina MJ, Rosen TA, Tominaga M, Brake AJ & Julius D (1999) A capsaicin-receptor homologue with a high threshold for noxious heat. *Nature* **398**, 436–440.
26 Kanzaki M, Zhang YQ, Mashima H, Li L, Shibata H & Kojima I (1999) Translocation of a calcium-permeable cation channel induced by insulin-like growth factor-I. *Nat Cell Biol* **1**, 165–170.
27 Harteneck C, Plant TD & Schultz G (2000) From worm to man: three subfamilies of TRP channels. *Trends Neurosci* **23**, 159–166.
28 Ferrer-Montiel A, Fernández-Carvajal A, Planells-Cases R, Fernández-Ballester G, González-Ros JM, Messeguer A & González-Muñiz R (2012) Advances in modulating thermosensory TRP channels. *Expert Opin Ther Pat* **22**, 999–1017.
29 Xu H, Delling M, Jun JC & Clapham DE (2006) Oregano, thyme and clove-derived flavors and skin sensitizers activate specific TRP channels. *Nat Neurosci* **9**, 628–635.
30 Suzuki M, Mizuno A, Kodaira K & Imai M (2003) Impaired pressure sensation in mice lacking TRPV4. *J Biol Chem* **278**, 22664–22668.
31 Mizuno A, Matsumoto N, Imai M & Suzuki M (2003) Impaired osmotic sensation in mice lacking TRPV4. *Am J Physiol Cell Physiol* **285**, C96–101.
32 Tabuchi K, Suzuki M, Mizuno A & Hara A (2005) Hearing impairment in TRPV4 knockout mice. *Neurosci Lett* **382**, 304–308.
33 Rutter AR, Ma Q-P, Leveridge M & Bonnert TP (2005) Heteromerization and colocalization of TrpV1 and TrpV2 in mammalian cell lines and rat dorsal root ganglia. *NeuroReport* **16**, 1735–1739.
34 Cheng W, Yang F, Takanishi CL & Zheng J (2007) Thermosensitive TRPV channel subunits coassemble into heteromeric channels with intermediate conductance and gating properties. *J Gen Physiol* **129**, 191–207.
35 Liapi A & Wood JN (2005) Extensive co-localization and heteromultimer formation of the vanilloid receptor-like protein TRPV2 and the capsaicin receptor TRPV1 in the adult rat cerebral cortex. *Eur J Neurosci* **22**, 825–834.
36 Saito S & Shingai R (2006) Evolution of thermoTRP ion channel homologs in vertebrates. *Physiol Genomics* **27**, 219–230.
37 Li M, Yu Y & Yang J (2011) Structural biology of TRP channels. *Adv Exp Med Biol* **704**, 1–23.
38 Gaudet R (2008) TRP channels entering the structural era. *J Physiol* **586**, 3565–3575.
39 McCleverty CJ, Koesema E, Patapoutian A, Lesley SA & Kreusch A (2006) Crystal structure of the human TRPV2 channel ankyrin repeat domain. *Protein Sci* **15**, 2201–2206.
40 Cuajungco MP, Grimm C, Oshima K, D'hoedt D, Nilius B, Mensenkamp AR, Bindels RJM, Plomann M & Heller S (2006) PACSINs bind to the TRPV4 cation channel. PACSIN 3 modulates the subcellular localization of TRPV4. *J Biol Chem* **281**, 18753–18762.

41 Neeper MP, Liu Y, Hutchinson TL, Wang Y, Flores CM & Qin N (2007) Activation properties of heterologously expressed mammalian TRPV2: evidence for species dependence. *J Biol Chem* **282**, 15894–15902.
42 Jin X, Touhey J & Gaudet R (2006) Structure of the N-terminal ankyrin repeat domain of the TRPV2 ion channel. *J Biol Chem* **281**, 25006–25010.
43 Gaudet R (2008) A primer on ankyrin repeat function in TRP channels and beyond. *Mol BioSyst* **4**, 372–379.
44 Michaely P, Tomchick DR, Machius M & Anderson RGW (2002) Crystal structure of a 12 ANK repeat stack from human ankyrinR. *EMBO J* **21**, 6387–6396.
45 Yao J, Liu B & Qin F (2011) Modular thermal sensors in temperature-gated transient receptor potential (TRP) channels. *Proc Natl Acad Sci USA* **108**, 11109–11114.
46 Krogh A, Larsson B, Von Heijne G & Sonnhammer EL (2001) Predicting transmembrane protein topology with a hidden Markov model: application to complete genomes. *J Mol Biol* **305**, 567–580.
47 Hessa T, Meindl-Beinker NM, Bernsel A, Kim H, Sato Y, Lerch-Bader M, Nilsson I, White SH & Von Heijne G (2007) Molecular code for transmembrane-helix recognition by the Sec61 translocon. *Nature* **450**, 1026–1030.
48 Jordt S-E & Julius D (2002) Molecular basis for species-specific sensitivity to 'hot' chili peppers. *Cell* **108**, 421–430.
49 Boukalova S, Marsakova L, Teisinger J & Vlachova V (2010) Conserved residues within the putative S4–S5 region serve distinct functions among thermosensitive vanilloid transient receptor potential (TRPV) channels. *J Biol Chem* **285**, 41455–41462.
50 Wirkner K, Hognestad H, Jahnel R, Hucho F & Illes P (2005) Characterization of rat transient receptor potential vanilloid 1 receptors lacking the N-glycosylation site N604. *NeuroReport* **16**, 997–1001.
51 Jahnel R, Bender O, Münter LM, Dreger M, Gillen C & Hucho F (2003) Dual expression of mouse and rat VRL-1 in the dorsal root ganglion derived cell line F-11 and biochemical analysis of VRL-1 after heterologous expression. *Eur J Biochem* **270**, 4264–4271.
52 Morenilla-Palao C, Pertusa M, Meseguer V, Cabedo H & Viana F (2009) Lipid raft segregation modulates TRPM8 channel activity. *J Biol Chem* **284**, 9215–9224.
53 Erler I, Al-Ansary DMM, Wissenbach U, Wagner TFJ, Flockerzi V & Niemeyer BA (2006) Trafficking and assembly of the cold-sensitive TRPM8 channel. *J Biol Chem* **281**, 38396–38404.
54 Lin Y & Sun Z (2012) Antiaging gene Klotho enhances glucose-induced insulin secretion by up-regulating plasma membrane levels of TRPV2 in MIN6-cells. *Endocrinology* **153**, 3029–3039.
55 Voets T & Nilius B (2003) The pore of TRP channels: trivial or neglected? *Cell Calcium* **33**, 299–302.
56 Owsianik G, Talavera K, Voets T & Nilius B (2006) Permeation and selectivity of TRP channels. *Annu Rev Physiol* **68**, 685–717.
57 Penna A, Juvin V, Chemin J, Compan V, Monet M & Rassendren F-A (2006) PI3-kinase promotes TRPV2 activity independently of channel translocation to the plasma membrane. *Cell Calcium* **39**, 495–507.
58 Mercado J, Gordon-Shaag A, Zagotta WN & Gordon SE (2010) Ca^{2+}-dependent desensitization of TRPV2 channels is mediated by hydrolysis of phosphatidylinositol 4,5-bisphosphate. *J Neurosci* **30**, 13338–13347.
59 Holakovska B, Grycova L, Bily J & Teisinger J (2011) Characterization of calmodulin binding domains in TRPV2 and TRPV5 C-tails. *Amino Acids* **40**, 741–748.
60 García-Sanz N, Fernández-Carvajal A, Morenilla-Palao C, Planells-Cases R, Fajardo-Sánchez E, Fernández-Ballester G & Ferrer-Montiel A (2004) Identification of a tetramerization domain in the C terminus of the vanilloid receptor. *J Neurosci* **24**, 5307–5314.
61 Becker D, Müller M, Leuner K & Jendrach M (2008) The C-terminal domain of TRPV4 is essential for plasma membrane localization. *Mol Membr Biol* **25**, 139–151.
62 Valente P, García-Sanz N, Gomis A, Fernández-Carvajal A, Fernández-Ballester G, Viana F, Belmonte C & Ferrer-Montiel A (2008) Identification of molecular determinants of channel gating in the transient receptor potential box of vanilloid receptor I. *FASEB J* **22**, 3298–3309.
63 García-Sanz N, Valente P, Gomis A, Fernández-Carvajal A, Fernández-Ballester G, Viana F, Belmonte C & Ferrer-Montiel A (2007) A role of the transient receptor potential domain of vanilloid receptor I in channel gating. *J Neurosci* **27**, 11641–11650.
64 Barnhill JC, Stokes AJ, Koblan-Huberson M, Shimoda LMN, Muraguchi A, Adra CN & Turner H (2004) RGA protein associates with a TRPV ion channel during biosynthesis and trafficking. *J Cell Biochem* **91**, 808–820.
65 Stokes AJ, Wakano C, Del Carmen KA, Koblan-Huberson M & Turner H (2005) Formation of a physiological complex between TRPV2 and RGA protein promotes cell surface expression of TRPV2. *J Cell Biochem* **94**, 669–683.
66 Kobayashi Y, Katanosaka Y, Iwata Y, Matsuoka M, Shigekawa M & Wakabayashi S (2006) Identification and characterization of GSRP-56, a novel Golgi-localized spectrin repeat-containing protein. *Exp Cell Res* **312**, 3152–3164.
67 Phelps CB, Procko E, Lishko PV, Wang RR & Gaudet R (2007) Insights into the roles of conserved

and divergent residues in the ankyrin repeats of TRPV ion channels. *Channels (Austin)* **1**, 148–151.
68 Phelps CB, Wang RR, Choo SS & Gaudet R (2010) Differential regulation of TRPV1, TRPV3, and TRPV4 sensitivity through a conserved binding site on the ankyrin repeat domain. *J Biol Chem* **285**, 731–740.
69 Myers BR, Bohlen CJ & Julius D (2008) A yeast genetic screen reveals a critical role for the pore helix domain in TRP channel gating. *Neuron* **58**, 362–373.
70 Lishko PV, Procko E, Jin X, Phelps CB & Gaudet R (2007) The ankyrin repeats of TRPV1 bind multiple ligands and modulate channel sensitivity. *Neuron* **54**, 905–918.
71 Rohacs T, Thyagarajan B & Lukacs V (2008) Phospholipase C mediated modulation of TRPV1 channels. *Mol Neurobiol* **37**, 153–163.
72 Cao E, Cordero-Morales JF, Liu B, Qin F & Julius D (2013) TRPV1 channels are intrinsically heat sensitive and negatively regulated by phosphoinositide lipids. *Neuron* **77**, 667–679.
73 Prescott ED & Julius D (2003) A modular PIP2 binding site as a determinant of capsaicin receptor sensitivity. *Science* **300**, 1284–1288.
74 Gordon-Shaag A, Zagotta WN & Gordon SE (2008) Mechanism of Ca(2+)-dependent desensitization in TRP channels. *Channels (Austin)* **2**, 125–129.
75 Shin Y-C, Shin S-Y, So I, Kwon D & Jeon J-H (2011) TRIP database: a manually curated database of protein–protein interactions for mammalian TRP channels. *Nucleic Acids Res* **39**, D356–D361.
76 Shin Y-C, Shin S-Y, Chun JN, Cho HS, Lim JM, Kim H-G, So I, Kwon D & Jeon J-H (2012) TRIP database 2.0: a manually curated information hub for accessing TRP channel interaction network. *PLoS One* **7**, e47165.
77 Link TM, Park U, Vonakis BM, Raben DM, Soloski MJ & Caterina MJ (2010) TRPV2 has a pivotal role in macrophage particle binding and phagocytosis. *Nat Immunol* **11**, 232–239.
78 Santoni G, Farfariello V, Liberati S, Morelli MB, Nabissi M, Santoni M & Amantini C (2013) The role of transient receptor potential vanilloid type-2 ion channels in innate and adaptive immune responses. *Front Immunol* **4**, 34.
79 Vriens J, Appendino G & Nilius B (2009) Pharmacology of vanilloid transient receptor potential cation channels. *Mol Pharmacol* **75**, 1262–1279.
80 Qin N, Neeper MP, Liu Y, Hutchinson TL, Lubin ML & Flores CM (2008) TRPV2 is activated by cannabidiol and mediates CGRP release in cultured rat dorsal root ganglion neurons. *J Neurosci* **28**, 6231–6238.
81 De Petrocellis L, Ligresti A, Moriello AS, Allarà M, Bisogno T, Petrosino S, Stott CG & Di Marzo V (2011) Effects of cannabinoids and cannabinoid-enriched Cannabis extracts on TRP channels and endocannabinoid metabolic enzymes. *Br J Pharmacol* **163**, 1479–1494.
82 Hu H-Z, Gu Q, Wang C, Colton CK, Tang J, Kinoshita-Kawada M, Lee L-Y, Wood JD & Zhu MX (2004) 2-Aminoethoxydiphenyl borate is a common activator of TRPV1, TRPV2, and TRPV3. *J Biol Chem* **279**, 35741–35748.
83 Juvin V, Penna A, Chemin J, Lin YL & Rassendren FA (2007) Pharmacological characterization and molecular determinants of the activation of transient receptor potential V2 channel orthologs by 2-aminoethoxydiphenyl borate. *Mol Pharmacol* **72**, 1258–1268.
84 Chung MK, Güler AD & Caterina MJ (2005) Biphasic currents evoked by chemical or thermal activation of the heat-gated ion channel, TRPV3. *J Biol Chem* **280**, 15928–15941.
85 Leffler A, Linte RM, Nau C, Reeh P & Babes A (2007) A high-threshold heat-activated channel in cultured rat dorsal root ganglion neurons resembles TRPV2 and is blocked by gadolinium. *Eur J Neurosci* **26**, 12–22.
86 Stotz SC, Vriens J, Martyn D, Clardy J & Clapham DE (2008) Citral sensing by transient [corrected] receptor potential channels in dorsal root ganglion neurons. *PLoS One* **3**, e2082.
87 Bang S, Kim KY, Yoo S, Lee S-H & Hwang SW (2007) Transient receptor potential V2 expressed in sensory neurons is activated by probenecid. *Neurosci Lett* **425**, 120–125.
88 Robbins N, Koch SE, Tranter M & Rubinstein J (2011) The history and future of probenecid. *Cardiovasc Toxicol* **12**, 1–9.
89 Nie L, Oishi Y, Doi I, Shibata H & Kojima I (1997) Inhibition of proliferation of MCF-7 breast cancer cells by a blocker of Ca(2+)-permeable channel. *Cell Calcium* **22**, 75–82.
90 Aoyagi K, Ohara Imaizumi M, Nishiwaki C, Nakamichi Y & Nagamatsu S (2010) Insulin/phosphoinositide 3-kinase pathway accelerates the glucose-induced first-phase insulin secretion through TrpV2 recruitment in pancreatic β-cells. *Biochem J* **432**, 375–386.
91 Hisanaga E, Nagasawa M, Ueki K, Kulkarni RN, Mori M & Kojima I (2009) Regulation of calcium-permeable TRPV2 channel by insulin in pancreatic beta-cells. *Diabetes* **58**, 174–184.
92 Mihara H, Boudaka A, Shibasaki K, Yamanaka A, Sugiyama T & Tominaga M (2010) Involvement of TRPV2 activation in intestinal movement through nitric oxide production in mice. *J Neurosci* **30**, 16536–16544.
93 Shibasaki K, Murayama N, Ono K, Ishizaki Y & Tominaga M (2010) TRPV2 enhances axon outgrowth

through its activation by membrane stretch in developing sensory and motor neurons. *J Neurosci* **30**, 4601–4612.

94 Ahluwalia J, Rang H & Nagy I (2002) The putative role of vanilloid receptor-like protein-1 in mediating high threshold noxious heat-sensitivity in rat cultured primary sensory neurons. *Eur J Neurosci* **16**, 1483–1489.

95 Ichikawa H & Sugimoto T (2000) Vanilloid receptor 1-like receptor-immunoreactive primary sensory neurons in the rat trigeminal nervous system. *Neuroscience* **101**, 719–725.

96 Yamamoto Y & Taniguchi K (2005) Immunolocalization of VR1 and VRL1 in rat larynx. *Auton Neurosci* **117**, 62–65.

97 Ma Q-P (2001) Vanilloid receptor homologue, VRL1, is expressed by both A- and C-fiber sensory neurons. *NeuroReport* **12**, 3693.

98 Lewinter RD, Skinner K, Julius D & Basbaum AI (2004) Immunoreactive TRPV-2 (VRL-1), a capsaicin receptor homolog, in the spinal cord of the rat. *J Comp Neurol* **470**, 400–408.

99 Koike S, Uno T, Bamba H, Shibata T, Okano H & Hisa Y (2004) Distribution of vanilloid receptors in the rat laryngeal innervation. *Acta Otolaryngol* **124**, 515–519.

100 Hamamoto T, Takumida M, Hirakawa K, Takeno S & Tatsukawa T (2008) Localization of transient receptor potential channel vanilloid subfamilies in the mouse larynx. *Acta Otolaryngol* **128**, 685–693.

101 Hamamoto T, Takumida M, Hirakawa K, Tatsukawa T & Ishibashi T (2009) Localization of transient receptor potential vanilloid (TRPV) in the human larynx. *Acta Otolaryngol* **129**, 560–568.

102 Gibbs JL, Melnyk JL & Basbaum AI (2011) Differential TRPV1 and TRPV2 channel expression in dental pulp. *J Dent Res* **90**, 765–770.

103 Wainwright A, Rutter AR, Seabrook GR, Reilly K & Oliver KR (2004) Discrete expression of TRPV2 within the hypothalamo-neurohypophysial system: implications for regulatory activity within the hypothalamic-pituitary-adrenal axis. *J Comp Neurol* **474**, 24–42.

104 Nedungadi TP, Carreño FR, Walch JD, Bathina CS & Cunningham JT (2012) Region-specific changes in transient receptor potential vanilloid channel expression in the vasopressin magnocellular system in hepatic cirrhosis-induced hyponatraemia. *J Neuroendocrinol* **24**, 642–652.

105 Muraki K, Iwata Y, Katanosaka Y, Ito T, Ohya S, Shigekawa M & Imaizumi Y (2003) TRPV2 is a component of osmotically sensitive cation channels in murine aortic myocytes. *Circ Res* **93**, 829–838.

106 Cahoy JD, Emery B, Kaushal A, Foo LC, Zamanian JL, Christopherson KS, Xing Y, Lubischer JL, Krieg PA, Krupenko SA *et al.* (2008) A transcriptome database for astrocytes, neurons, and oligodendrocytes: a new resource for understanding brain development and function. *J Neurosci* **28**, 264–278.

107 Cavanaugh DJ, Chesler AT, Jackson AC, Sigal YM, Yamanaka H, Grant R, O'Donnell D, Nicoll RA, Shah NM, Julius D *et al.* (2011) Trpv1 reporter mice reveal highly restricted brain distribution and functional expression in arteriolar smooth muscle cells. *J Neurosci* **31**, 5067–5077.

108 Nedungadi TP, Dutta M, Bathina CS, Caterina MJ & Cunningham JT (2012) Expression and distribution of TRPV2 in rat brain. *Exp Neurol* **237**, 223–237.

109 Chang Q, Hoefs S, van der Kemp AW, Topala CN, Bindels RJ & Hoenderop JG (2005) The beta-glucuronidase klotho hydrolyzes and activates the TRPV5 channel. *Science* **310**, 490–493.

110 Cha S-K, Ortega B, Kurosu H, Rosenblatt KP, Kuro-O M & Huang C-L (2008) Removal of sialic acid involving Klotho causes cell-surface retention of TRPV5 channel via binding to galectin-1. *Proc Natl Acad Sci USA* **105**, 9805–9810.

111 Zhang D, Spielmann A, Wang L, Ding G, Huang F, Gu Q & Schwarz W (2012) Mast-cell degranulation induced by physical stimuli involves the activation of transient-receptor-potential channel TRPV2. *Physiol Res* **61**, 113–124.

112 Stokes AJ, Shimoda LMN, Koblan-Huberson M, Adra CN & Turner H (2004) A TRPV2-PKA signaling module for transduction of physical stimuli in mast cells. *J Exp Med* **200**, 137–147.

113 Saunders CI, Kunde DA, Crawford A & Geraghty DP (2007) Expression of transient receptor potential vanilloid 1 (TRPV1) and 2 (TRPV2) in human peripheral blood. *Mol Immunol* **44**, 1429–1435.

114 Nagasawa M, Nakagawa Y, Tanaka S & Kojima I (2007) Chemotactic peptide fMetLeuPhe induces translocation of the TRPV2 channel in macrophages. *J Cell Physiol* **210**, 692–702.

115 Boels K, Glassmeier G, Herrmann D, Riedel IB, Hampe W, Kojima I, Schwarz JR & Schaller HC (2001) The neuropeptide head activator induces activation and translocation of the growth-factor-regulated Ca(2+)-permeable channel GRC. *J Cell Sci* **114**, 3599–3606.

116 Nagasawa M & Kojima I (2012) Translocation of calcium-permeable TRPV2 channel to the podosome: its role in the regulation of podosome assembly. *Cell Calcium* **51**, 186–193.

117 Linder S & Aepfelbacher M (2003) Podosomes: adhesion hot-spots of invasive cells. *Trends Cell Biol* **13**, 376–385.

118 Yamashiro K, Sasano T, Tojo K, Namekata I, Kurokawa J, Sawada N, Suganami T, Kamei Y,

Tanaka H, Tajima N *et al.* (2010) Role of transient receptor potential vanilloid 2 in LPS-induced cytokine production in macrophages. *Biochem Biophys Res Commun* **398**, 284–289.
119 Park KS, Kim Y, Lee Y-H, Earm YE & Ho W-K (2003) Mechanosensitive cation channels in arterial smooth muscle cells are activated by diacylglycerol and inhibited by phospholipase C inhibitor. *Circ Res* **93**, 557–564.
120 Fantozzi I, Zhang S, Platoshyn O, Remillard CV, Cowling RT & Yuan JXJ (2003) Hypoxia increases AP-1 binding activity by enhancing capacitative Ca^{2+} entry in human pulmonary artery endothelial cells. *Am J Physiol Lung Cell Mol Physiol* **285**, L1233–45.
121 Peng G, Lu W, Li X, Chen Y, Zhong N, Ran P & Wang J (2010) Expression of store-operated Ca^{2+} entry and transient receptor potential canonical and vanilloid-related proteins in rat distal pulmonary venous smooth muscle. *Am J Physiol Lung Cell Mol Physiol* **299**, L621–L630.
122 Iwata Y, Katanosaka Y, Arai Y, Komamura K, Miyatake K & Shigekawa M (2003) A novel mechanism of myocyte degeneration involving the Ca^{2+}-permeable growth factor-regulated channel. *J Cell Biol* **161**, 957–967.
123 Iwata Y, Katanosaka Y, Arai Y, Shigekawa M & Wakabayashi S (2009) Dominant-negative inhibition of Ca^{2+} influx via TRPV2 ameliorates muscular dystrophy in animal models. *Hum Mol Genet* **18**, 824–834.
124 Gailly P (2012) TRP channels in normal and dystrophic skeletal muscle. *Curr Opin Pharmacol* **12**, 326–334.
125 Zanou N, Iwata Y, Schakman O, Lebacq J, Wakabayashi S & Gailly P (2009) Essential role of TRPV2 ion channel in the sensitivity of dystrophic muscle to eccentric contractions. *FEBS Lett* **583**, 3600–3604.
126 Lehen'kyi V & Prevarskaya N (2012) TRPV2 (transient receptor potential cation channel, subfamily V, member 2). *Atlas Genet Cytogenet Oncol Haematol* **16**, 563–567.
127 Vriens J, Janssens A, Prenen J, Nilius B & Wondergem R (2004) TRPV channels and modulation by hepatocyte growth factor/scatter factor in human hepatoblastoma (HepG2) cells. *Cell Calcium* **36**, 19–28.
128 Liu G, Xie C, Sun F, Xu X, Yang Y, Zhang T, Deng Y, Wang D, Huang Z, Yang L *et al.* (2010) Clinical significance of transient receptor potential vanilloid 2 expression in human hepatocellular carcinoma. *Cancer Genet Cytogenet* **197**, 54–59.
129 Caprodossi S, Lucciarini R, Amantini C, Nabissi M, Canesin G, Ballarini P, Di Spilimbergo A, Cardarelli MA, Servi L, Mammana G *et al.* (2008) Transient receptor potential vanilloid type 2 (TRPV2) expression in normal urothelium and in urothelial carcinoma of human bladder: correlation with the pathologic stage. *Eur Urol* **54**, 612–620.
130 Yamada T, Ueda T, Shibata Y, Ikegami Y, Saito M, Ishida Y, Ugawa S, Kohri K & Shimada S (2010) TRPV2 activation induces apoptotic cell death in human T24 bladder cancer cells: a potential therapeutic target for bladder cancer. *Urology* **76**, 509.e1–7.
131 Monet M, Lehen'kyi V, Gackiere F, Firlej V, Vandenberghe M, Roudbaraki M, Gkika D, Pourtier A, Bidaux G, Slomianny C *et al.* (2010) Role of cationic channel TRPV2 in promoting prostate cancer migration and progression to androgen resistance. *Cancer Res* **70**, 1225–1235.
132 Monet M, Gkika D, Lehen'kyi V, Pourtier A, Abeele FV, Bidaux G, Juvin V, Rassendren F, Humez S & Prevarsakaya N (2009) Lysophospholipids stimulate prostate cancer cell migration via TRPV2 channel activation. *Biochim Biophys Acta* **1793**, 528–539.
133 Nabissi M, Morelli MB, Amantini C, Farfariello V, Ricci-Vitiani L, Caprodossi S, Arcella A, Santoni M, Giangaspero F, De Maria R *et al.* (2010) TRPV2 channel negatively controls glioma cell proliferation and resistance to Fas-induced apoptosis in ERK-dependent manner. *Carcinogenesis* **31**, 794–803.
134 Morelli MB, Nabissi M, Amantini C, Farfariello V, Ricci-Vitiani L, di Martino S, Pallini R, Larocca LM, Caprodossi S, Santoni M *et al.* (2012) The transient receptor potential vanilloid-2 cation channel impairs glioblastoma stem-like cell proliferation and promotes differentiation. *Int J Cancer* **131**, E1067–E1077.
135 Nabissi M, Morelli MB, Santoni M & Santoni G (2013) Triggering of the TRPV2 channel by cannabidiol sensitizes glioblastoma cells to cytotoxic chemotherapeutic agents. *Carcinogenesis* **34**, 48–57.
136 Katoh K, Misawa K, Kuma KI & Miyata T (2002) MAFFT: a novel method for rapid multiple sequence alignment based on fast Fourier transform. *Nucleic Acids Res* **30**, 3059–3066.
137 Waterhouse AM, Procter JB, Martin DMA, Clamp M & Barton GJ (2009) Jalview Version 2 – a multiple sequence alignment editor and analysis workbench. *Bioinformatics* **25**, 1189–1191.
138 Ashkenazy H, Erez E, Martz E, Pupko T & Ben-Tal N (2010) ConSurf 2010: calculating evolutionary conservation in sequence and structure of proteins and nucleic acids. *Nucleic Acids Res* **38**, W529–33.

Chapter II

Dissecting domain-specific evolutionary pressure profiles of transient receptor potential vanilloid subfamily members 1 to 4.

Specific Objectives

- Deepen into TRPV1-4 subgroup evolution and domain conservation to gain structural insight into the multidomain organization and conservation of these channels.
- Determine TRPV1-4 conserved regions that may be crucial domains for structure and function.

Dissecting Domain-Specific Evolutionary Pressure Profiles of Transient Receptor Potential Vanilloid Subfamily Members 1 to 4

Pau Doñate-Macián, Alex Perálvarez-Marín*

Unitat de Biofísica, Centre d'Estudis en Biofísica, Departament de Bioquímica i de Biologia Molecular, Universitat Autònoma de Barcelona, Bellaterra, Spain

Abstract

The transient receptor potential vanilloid family includes four ion channels–TRPV1, TRPV2, TRPV3 and TRPV4–that are represented within the vertebrate subphylum and involved in several sensory and physiological processes. These channels are related to adaptation to the environment, and probably under strong evolutionary pressure. Using multiple sequence alignments as source for evolutionary, bioinformatics and statistical analysis, we have analyzed the evolutionary profiles for TRPV1, TRPV2, TRPV3 and TRPV4. The evolutionary pressure exerted over vertebrate TRPV2 sequences compared to the other channels argues for a positive selection profile for TRPV2 compared to TRPV1, TRPV3 and TRPV4. We have analyzed the selective pressure on specific protein domains, observing a common selective pressure trend for the common TRPV scaffold, consisting of the ankyrin repeat domain, the membrane proximal domain, the transmembrane domain, and the TRP domain. Through a more detailed analysis we have identified evolutionary constraints involved in the subunit contact at the transmembrane domain level. Performing evolutionary comparison, we have translated specific channel structural information such as the transmembrane topology, and the interaction between the membrane proximal domain and the TRP box. We have also identified potential common regulatory domains among all TRPV1-4 members, such as protein-protein, lipid-protein and vesicle trafficking domains.

Citation: Doñate-Macián P, Perálvarez-Marín A (2014) Dissecting Domain-Specific Evolutionary Pressure Profiles of Transient Receptor Potential Vanilloid Subfamily Members 1 to 4. PLoS ONE 9(10): e110715. doi:10.1371/journal.pone.0110715

Editor: Mandë Holford, The City University of New York-Graduate Center, United States of America

Received February 25, 2014; **Accepted** September 18, 2014; **Published** October 21, 2014

Funding: The authors want to acknowledge the funding from Spanish Government Young Researcher Grant (MICINN-SAF2010-21385 to A.P.-M.), a Marie Curie International Outgoing Fellowship within the 7th European Community Framework Programme (PIOF- GA-2009-237120 to A.P.-M.), and a Predoctoral Fellowship from the Generalitat de Catalunya (2013FIB00251 to P.D.-M.). The funders had no role in study design, data collection and analysis, decision to publish, or preparation of the manuscript.

Competing Interests: The authors have declared that no competing interests exist.

* Email: peralvarezmarin@gmail.com

Introduction

TRP channel superfamily consists of a set polymodal non-selective oligomeric membrane cationic channels, with large cytoplasmic regulatory domains [1,2]. These channels are predicted to share a common tetrameric membrane topology around the formation of a pore in the membrane to allow the flux of cations, but there are several differential regulatory domains that allow/block the cation flux through the membrane [2]. These domains are very specialized, and follow an evolutionary pattern that has been reflected in the subfamily classification of the large TRP superfamily. The vanilloid subfamily (TRPV) in vertebrates consists of at least six members (TRPV1-6) [3]. From an evolutionary perspective, there are two subgroups within this subfamily, first, TRPV1-4 which are non-selective cation channels, and second, TRPV5 and TRPV6, which are calcium selective ion channels. Another classification identifies the TRPV1-4 subgroup as thermosensors in mammals: TRPV1 and TRPV2 act as noxious heat sensors (T>43°C), and TRPV3 and TRPV4 as physiological temperature sensors.

Evolutionary studies on TRPV channels, have attempted to gain information on the evolution profile of the family [4,5], or on the identification of specific domains in TRPV1 [6]. Understanding how evolution drives specialization of functional and structural domains has been and is a bioinformatics challenge [7,8], especially when the study focus is multi-domain oligomeric membrane proteins, such as TRP channels. When considering membrane proteins, one should take into account protein-protein and lipid-protein contacts, internal transmembrane polar clusters, etc. Evolution information derived from the primary sequence may provide important hints about how a membrane protein is integrated in its environment. Biologically significant positions in a protein can be inferred by identifying directional selection in comparison to neutral selection. Neutral selection indicates low evolutionary pressure and directional selection indicates high evolutionary pressure that can follow two ways: positive selection *versus* negative (purifying) selection events. Purifying selection acts towards function conservation, whereas positive selection argues for environment adaptation or species/tissue dependent function variability, thus selective pressure defines the evolutionary history of a protein. Some studies have used evolutionary constrains to provide general information, such as domain organization and spatial interaction, and even mapping the evolutionary constrains for automated modeling of membrane proteins [9–12]. However, to understand specific issues, such as topology, selective pressure on biologically significant residues, or domain conservation, a detailed study and characterization of the system of interest is required.

In this study, we provide a comprehensive depiction of the evolutionary profile of the non-selective cation channels from the TRPV subfamily, i.e. TRPV1, TRPV2, TRPV3, and TRPV4 channels. We analyze the global evolutionary selective pressure for TRPV1-4 channels and the selective pressure exerted on specific domains as a candidate force driving function differentiation.

Results

Identifying evolutionary traits among TRPV1-4 channels

To dissect the common evolutionary features among TRPV1-4 sequences, we carried out a computational phylogenetic analysis. First, we retrieved the different sequences for TRPVs available in public databases. We also inspected specific genomes to get the complete protein sequence from some fragment TRPV sequences available in the UNIPROT database [13]. All the protein sequences used in this study are available as Dataset S1. Specifically, from the UNIPROT and NCBI databases (2011) we could curate the TRPV1 full sequence for: *Equus caballus, Salmo salar, Monodelphis domestica, Sarcophilus harrisii* and *Putorius furo*; and the TRPV2 full sequence for: *Tursiops truncatus*, *Dipodormys ordii* and *Gasterosteus aculeatus*.

With all sequences available, we performed the multiple sequence alignment (MSA) that depicted a phylogenetic tree (Fig. 1A). This tree revealed a clear distribution of the channels within the corresponding evolutionary distribution in four defined groups. To provide a more illustrative depiction (Fig. 1B), we clustered the sequences using principal component analysis in JalView [14]. Some TRPV2 fragment sequences (*Melopsittacus undulatus* and *Anolis carolinensis*) were clustered in the TRPV1 subgroup (Fig. 1A). TRPV3 and TRPV4 clusters were clearly identified (Fig. 1B) and originated from the divergent node that defines the fish TRPV1/2 cluster (Fig. 1A).

TRPVs evolutionary pressure

Using a subset of TRPV channels sequences we compared the conservation distribution for TRPV1 (25 sequences), TRPV2 (28 sequences), TRPV3 (21 sequences), and TRPV4 (22 sequences). We used the directional selection algorithm (FADE) of the HyPhy package [15,16] to analyze the MSAs for each channel and detect differences in the substitution rate as a rough indicator of positive selection among TRPVs (Table 1). The substitution rate in sequences for vertebrates was TRPV2>TRPV1>TRPV4> TRPV3, however, TRPV4 has a higher number of sites under positive selection (177, Table 1), i.e. positive selected residues compared to the other TRPVs. In the case of mammalian sequences, the substitution rate was TRPV2>TRPV1>TRPV3> TRPV4, and TRPV2 is the channel with higher number of residues under positive selection, whereas TRPV4 shows a strong purifying selective pressure in mammals. To measure the variability within each channel set of sequences we computed the pairwise distances among all sequences for a specific channel and represented them in box plots for divergence frequency distribution (Fig. 1C). We compared all available sequences for each channel depicting the sequence variability in the vertebrate subset (Fig. 1C). The level of sequence divergence among species was highest for TRPV2 (median at 0.34), followed by TRPV4 (0.20), TRPV1 (0.14), and the least divergent is TRPV3 (0.13). There was a bias on the number of sequences available for TRPV channels in the databases depending on the phylogenetic group, where mammals are the most represented. In Fig. 1D, we show the sequence variability for each channel only considering mammals information. Although at lesser extent, the level of sequence divergence was still highest for TRPV2 (median at 0.19), followed by TRPV1 (0.12), TRPV3 (0.11) and TRPV4 (0.04). Results for sequence divergence in Fig. 1C and Fig. 1D agree reasonably well with the directional selection analysis of the MSAs carried out in HyPhy (Table 1).

To determine whether divergence variance among TRPVs could fit into any of these directional evolutionary pressure hypothesis, we performed a pairwise statistical analysis. Divergence among mammals and vertebrates TRPVs was not the same (p-value $<2.2\cdot10^{-16}$). In mammals, divergence was extremely different between TRPV1-TRPV2, TRPV1-TRPV4, TRPV2-TRPV3, TRPV2-TRPV4 and TRPV3-TRPV4 (p-value $<2.2\cdot10^{-16}$), while divergence between TRPV1-TRPV3 was less dissimilar (p-value = 0.003). In vertebrates, divergence was extremely different between TRPV1-TRPV2, TRPV2-TRPV3 and TRPV2-TRPV4 (p-value $<2.2\cdot10^{-16}$), divergence was different between TRPV1-TRPV3 (p-value = 0.017) and there was no difference in divergence between TRPV1-TRPV4 and TRPV3-TRPV4 (p-value = 0.999).

In Fig. 2A we show the evolutionary pressure exerted on specific domains (box plot for each domain, Table 2 for the list of domains) for mammalian TRPVs compared to the median of the evolutionary pressure exerted on the full-length mammalian TRPV sequences (dashed line). A statistically significant difference in the divergence of a specific domain compared to the full-length sequence is indicated with an asterisk (Fig. 2A). For clarity, we provide an additional representation highlighting the differences between positive *versus* purifying evolutionary pressures exerted over the different TRPV domains for mammals as a comparison of medians (Fig. 2B). Defining as a zero level the median value for the full-length TRPV sequence, we provide a ratio to identify the median positive values as divergent, and negative values as conserved for specific protein domains when compared to the full-length sequence (see Methods section for details). We indicate with an arrow the domains that show statistical differences (divergence/conservation) for all channels derived from the information in Fig. 2A. Since the high-resolution partial structure of TRPV1 has been solved [17], we had the opportunity to map the conservation profiles for the different channels onto the 3D TRPV1 structure or onto models based on this structure (Fig. 3).

For TRPV1, the domains accounting for higher divergence than the full-length protein (positive selection) are the N-terminus, the 1st extracellular loop, the TM3, the 5th extracellular loop, the PIP2 binding domain and the distal C-terminus (Fig. 2A and Fig. 3). For TRPV2, the positive selection pressure is focused in the N-terminus, the 1st extracellular loop, the 5th extracellular loop, and the very distal C-terminus (Fig. 2A and Fig. 3). For TRPV3, which shows a high conservation profile, the positive selection pressure is focused in the first ankyrin repeat and in the 5th extracellular loop (Fig. 2A and Fig. 3). For TRPV4, the lowest selection pressure is focused in the N-terminus (Fig. 2A and Fig. 3). In TRPVs the positive evolutionary pressure is exerted on the N-terminus and the loop 5 (although is not statistically significant for all the channels, Fig. 2B), while purifying evolutionary pressure is exerted over the membrane proximal domain (MPD), the 2nd intracellular loop, the very short 3rd extracellular loop, the 4th transmembrane segment, the 4th intracellular loop, the 6th transmembrane segment, the TRP box linker (post TM6 segment) and the TRP box.

The TRPV1 structure and the TRPV2-4 models lack information on the N-terminus domain, the 5th extracellular loop and the very distal C-terminus domain. Strikingly, to obtain the high-resolution structure of TRPV1, the 5th extracellular loop (under positive selection) was removed from the sequence as part of the experimental design [17]. The very distal C-terminus domain of

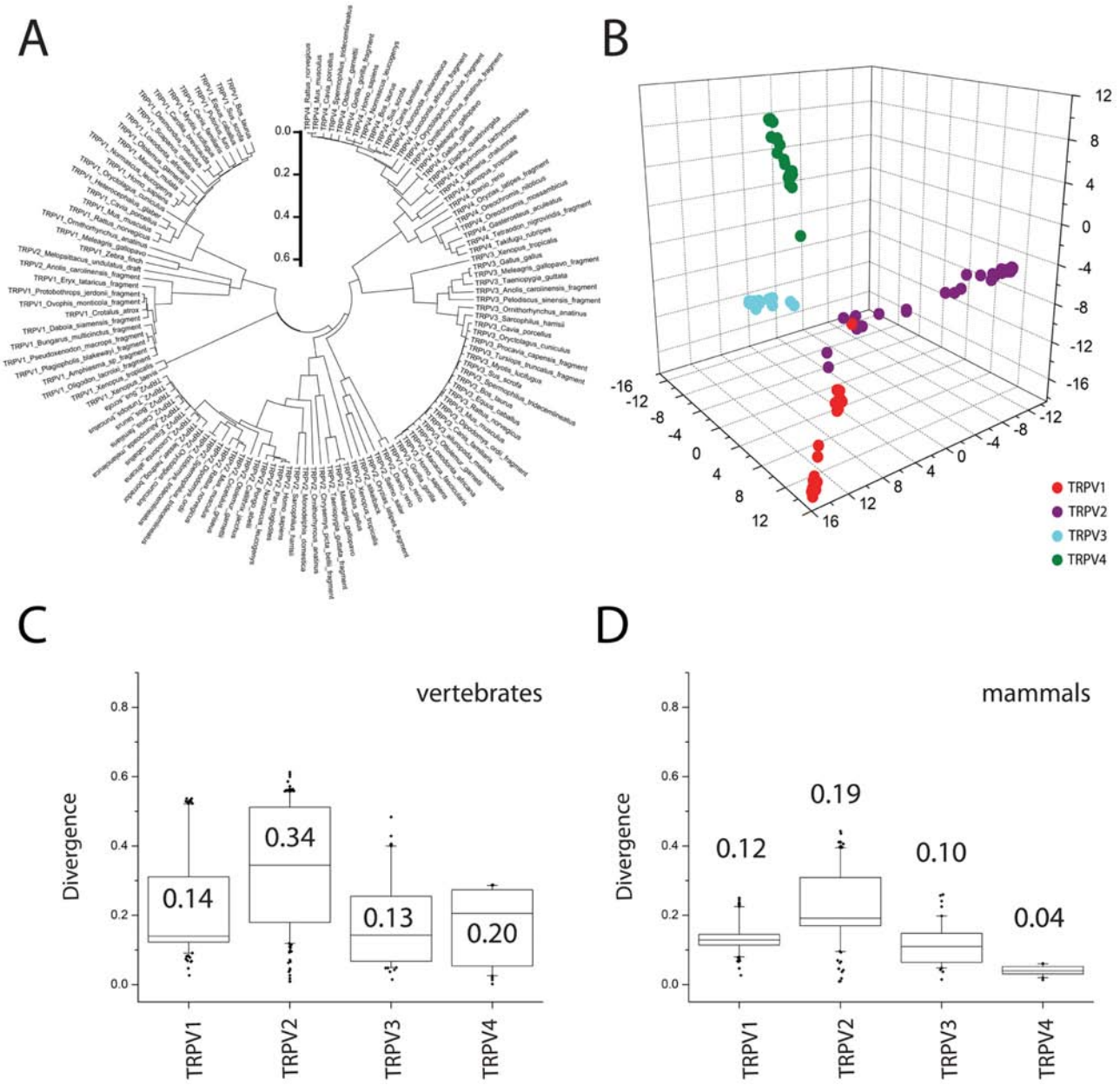

Figure 1. TRPVs phylogeny. A. Radial phylogenetic tree for TRPVs. The scale bar indicates evolutionary time in arbitrary units. **B.** Clustering by PCA analysis for TRPVs. Attending to their evolutive distances TRPV1-4 could be clustered into 4 subgroups corresponding to each of the four channels. **C.** Sequence divergence profile for vertebrate TRPVs. **D.** Sequence divergence profile for mammalian TRPVs. The box plots represent the divergence of sequences distribution for each channel. The median value is indicated for each box plot. Refer to the text for specific statistical comparison of the medians.
doi:10.1371/journal.pone.0110715.g001

TRPV1 (also under positive selection) was not solved, probably because of protein proteolysis, indicating that these domains are not crucial in the TRPV scaffold.

The transmembrane domain

The main oligomerization contacts for TRPV channels happen in the transmembrane domain (TMD). The contacts between the different subunits along the TM1-TM6 define the four-fold symmetry, the ion pore, and the selectivity filter. To map evolutionary traits on the TMD we have used EVcouplings [18] using the rat TRPV1 sequence as reference to compare the evolutionary constrains with the TRPV1 tridimensional structure. We have analyzed the evolutionary constraints (EC) on the TMD and the overlapping of the ECs (color dots) and the actual contacts (grey shaded area) in the tridimensional structure (Fig. 4A, Table S1 for a full set of ECs). The cloud of ECs is more disperse than the contacts defined by the tridimensional structure, indicating that the evolutionary traits in TRPV channels not only define the physical contacts. In Fig. 4B we have classified the ECs within the TMD domain. The TM5–TM6 region shows the highest number of ECs, followed by the TM2-loop 2 region. The TM1 and TM3 regions showed a similar number of ECs. To discriminate the

Table 1. Evolutionary analysis of TRPV1-4 channels for directional positive selection based on multiple sequence alignments.

	Vertebrates			
	TRPV1	**TRPV2**	**TRPV3**	**TRPV4**
substitution/site	4.49	8.57	2.43	3.21
residues in alignment	964	915	829	906
sequences	25	28	21	22
sites under positive selection*	100	158	69	177
	Mammals			
	TRPV1	**TRPV2**	**TRPV3**	**TRPV4**
substitution/site	1.88	3.66	1.19	0.33
residues in alignment	875	821	811	872
sequences	20	22	18	11
sites under positive selection*	72	106	37	13

*considering as significant the top 5% sites in the FADE analysis (0.95 posterior filter).
doi:10.1371/journal.pone.0110715.t001

residues involved in monomer-to-monomer contacts, we have mapped the subunit A (inter-chain) contacts from the PDB file (3J5P) in Fig. 4C. The contacts between chain A and B and chain A and chain C, are the same (in black and grey respectively). However, the contacts between chain A and chain D (open circles) are fewer and are located in the pore-forming region. Assuming four-fold symmetry, these contacts are equally defined for all subunit interactions (Table S2 for the full set of contacts for the TRPV1 TMD structure). The distribution of the inter-chain contacts corresponds to the TM1–TM5, TM4–TM5, TM4–TM6, TM5–TM6 and TM6–TM6 segments. The segments showing higher number of contacts are between TM4–TM5 and TM6–TM6 segments.

Cytosolic domains

Recently the high-resolution structure for rat TRPV1 has been solved providing relevant tridimensional information [17]. The structure provides an exceptional illustration of intra-domain interaction, showing the interaction between the MPD and the TRP box depicted in Fig. 5A. Significantly, these two regions are highly conserved among all TRPVs, and not only within a TRPV isoform (Fig. 2 and 3), indicating a common molecular mechanism (Fig. 5A). From the tridimensional perspective, the membrane proximal region of the MPD domain acts as a fork where the TRP box slides during the gating mechanism. Considering the residue conservation (Fig. 5B and C) this seems to be a highly conserved mechanism among vertebrate TRPV1-4 channels. The MPD domain has been studied for TRPV1 and TRPV2, as a potential thermosensing module [19]. From the conservation perspective, biophysical features arise (Fig. 5B) such as the high consensus conservation of positive residues (R/K/H) close to conserved aromatic residues prone to partitioning at the water-membrane interface and promote protein-membrane interactions, thus acting as a lipid-binding domain. In this domain there are at least four highly conserved S/T/Y residues potentially phosphorylated (score over 0.5 by NetPhos algorithm [20]) indicating regulatory sites.

The C-terminus domain, comprising residues after TM6 until the end of the sequence, do not show the same level of conservation among channels as the N-terminus. Nevertheless, the C-terminal region of TRPV1 is one of the most characterized and some information can be cross-related among the different TRPV channels (Fig. 5C). TRPV1 contains two tubulin-binding sequences (TBS1 and TBS2). TBS1 falls within a TRPV1-4 rich positive-residue conserved region, whereas TBS2 is within a very low conservation region (TBS in Fig. 5C) [6,21]. TRPV4 has been shown to bind microtubule-associated protein 7 in the last ~60 C-terminal residues [22]. The tetramerization domains (TAD) are present in all TRPVs, overlapping with the highly conserved TRP box within the TRP domain [23,24]. Derived from the recent structural information, the TRP domain has a tight relationship with the MPD. Concerning the PIP2 binding domain although initially described for TRPV1 [25], it was later described for TRPV2 [26] within the C-terminus. Due to the level of conservation of this region (which also includes the TRP box) and focusing on the conserved aromatic and positively-charged residues, the PIP2 domain may be easily defined for TRPV3 and TRPV4 as well [27].

Another protein-protein interaction region defined in TRPV1 is the one for the binding of AKAP79 protein [28], which can be easily translated into TRPV2, TRPV3 and TRPV4 because of the consensus sequence conservation (Fig. 5C). Finally, in Fig. 5C a gap appears in the middle of the highly conserved TRP box hallmark (IWKLQR consensus), indicating that one should be cautious about the poor quality of some non-reviewed sequences (outliers in Fig. 1C and D), which may introduce artifacts in the MSA.

Discussion

Experimental structural data is essential for the understanding of membrane proteins' molecular mechanisms. Bioinformatics provides tools to depict some functional/structural details using evolutionary information in the absence of structural data. Considering TRP channels as the subject for a bioinformatics approach represents a major challenge because the large number of protein members and the diverse functions. Here we have restricted our analysis to the TRPV1-4 evolutionary subset of TRP channels to gain structural insight into the multidomain organization and conservation of these channels. In addition, we have taken advantage on the recently solved structure for TRPV1 to validate specific evolutionary traits [17].

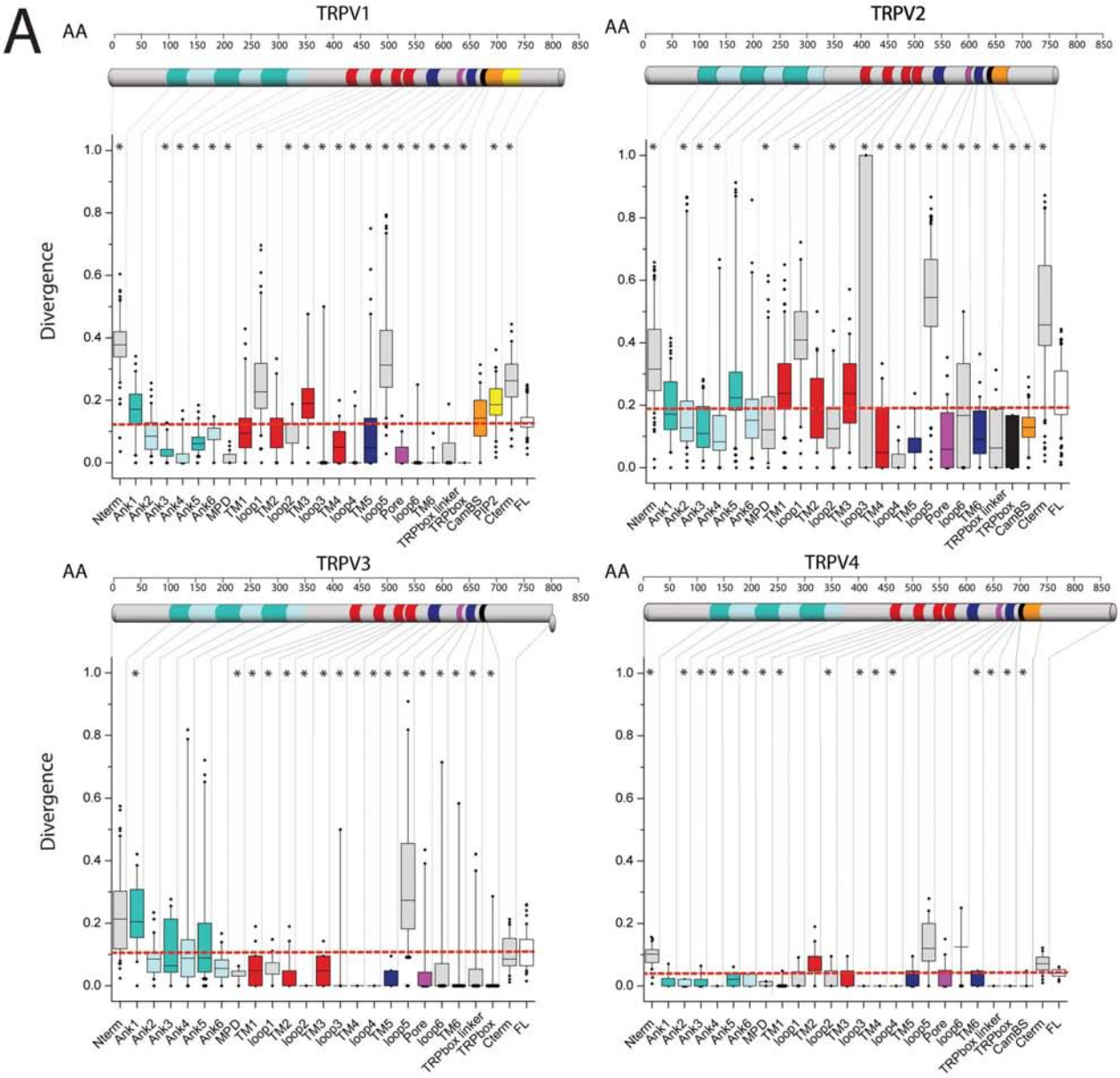
A
TRPV1
TRPV2
TRPV3
TRPV4
AA
Divergence
Nterm
Ank1
Ank2
Ank3
Ank4
Ank5
Ank6
MPD
TM1
loop1
TM2
loop2
TM3
loop3
TM4
loop4
TM5
loop5
Pore
loop6
TM6
TRPbox linker
TRPbox
CamBS
PIP2
Cterm
FL

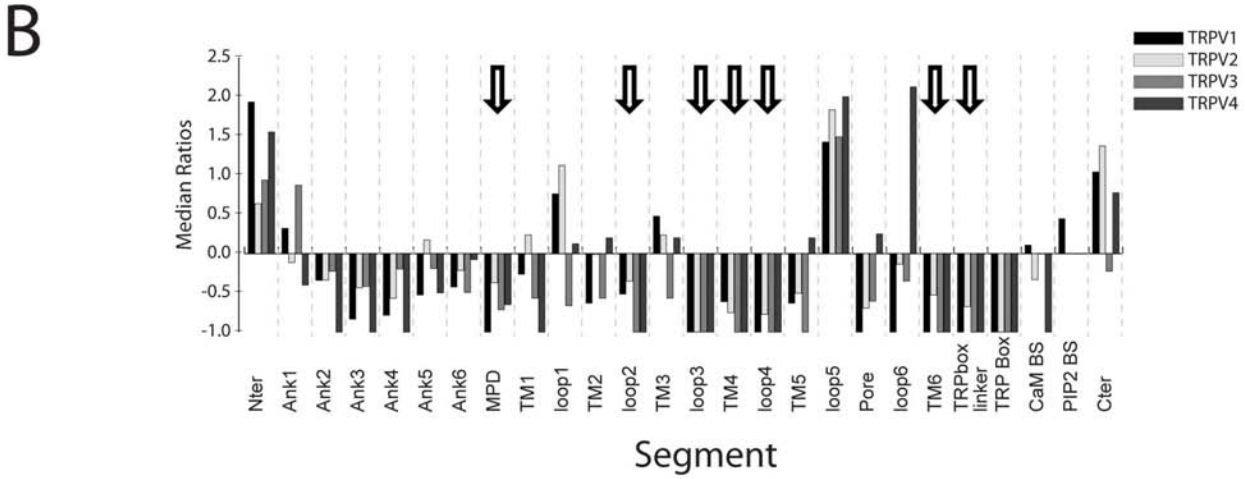
B
TRPV1
TRPV2
TRPV3
TRPV4
Median Ratios
Nter
Ank1
Ank2
Ank3
Ank4
Ank5
Ank6
MPD
TM1
loop1
TM2
loop2
TM3
loop3
TM4
loop4
TM5
loop5
Pore
loop6
TM6
TRPbox
linker
TRP Box
CaM BS
PIP2 BS
Cter
Segment

Figure 2. Domain-specific conservation profile for TRPV channels. A. Box plots showing the sequence divergence for specific domains of TRPV1-4 channels. The domain topology for the channels is indicated as a cartoon bar. The color-coding for each domain in the cartoon bar is represented in the box plot coloring. **B.** Plot of the normalized ratio for the medians for each domain segment. The Y-axis indicates the conservation (negative values) or divergence (positive values) of the domain in respect to the full-length protein conservation (value 0).
doi:10.1371/journal.pone.0110715.g002

Considering the evolution time and sequence divergence parameters (Fig. 1), we can estimate the rate of evolutionary pressure. The purifying evolutionary pressure on TRPV1, TRPV3, and TRPV4 sequences is higher than on TRPV2 sequences, which are more divergent, either comparing mammals or vertebrates. Considering pressure across taxonomy, the highest purifying pressure has been exerted over TRPV4, although at very similar levels to TRPV1 and TRPV3. TRPV2 selective pressure indicates the possibility that TRPV2 channels are under positive selection, compared to TRPV1, TRPV3 and TRPV4. Another interesting hypothesis is that TRPV2 appeared as gene duplication from TRPV1 and positive selection on TRPV2 acts towards defining new physiological roles; thus, both channels (TRPV1 and TRPV2) may still have redundant roles on specific tissues/organisms. This hypothesis fits with the chromosome location of TRPV1, TRPV2 and TRPV3 in human (Chr17) and mouse (Chr11) for example, that indicates that a TRPV gene duplicated first originating TRPV2, and a more recent gene duplication generated the ancestor of TRPV1 and TRPV3 genes [29]. TRPV4 is located in chromosomes 12 and 5 in human and mouse, respectively, indicating an earlier/distinct genetic variation events.

TRPV1-4 subset is represented in the tree of life starting from teleosts [5] (Fig. 1), although representative TRPV ancestors are found in *Caenorhabditis elegans* and in *Drosophila melanogaster* [5,30–32]. The late onset of these channels on the evolutionary tree of life argues for a very specific function requirement. Our analysis indicates that regions such as the distal N-terminus, some extracellular loops (such as the loop 5), and the distal C-terminus of TRPV1-4 channels are highly divergent, probably under positive selection, and very specific for each one of the channels. The putifying evolutionary pressure trend on specific domains, such as ARD, MPD, TMD and TRP domain (TRP box linker and TRP box) indicates that TRPV1-4 channels share a common minimal functional scaffold unit, comprising the ARD to the TRP domain, which corresponds to solved the high resolution tridimensional structure [17].

Table 2. Segment definition for human TRPV1-4 channels based on UNIPROT details*.

Segment	hTRPV1	hTRPV2	hTRPV3	hTRPV4
Nterm	1–110	1–71	1–116	1–147
Ank1*	111–153	72–114	117–166	148–189
Ank2*	154–200	115–161	167–213	190–236
Ank3*	201–247	162–207	214–260	237–282
Ank4*	248–283	208–243	261–295	283–319
Ank5*	284–332	244–292	296–338	320–367
Ank6*	333–359	293–319	339–366	368–395
MPD	360–433	320–390	367–439	396–465
TM1	434–454	391–411	440–460	466–486
loop1	455–476	412–434	461–487	487–508
TM2	477–497	435–455	488–508	509–529
loop2	498–513	456–471	509–523	530–550
TM3	514–534	472–492	524–544	551–571
loop3	535	493	545	572
TM4	536–556	494–514	546–566	573–593
loop4	557–579	515–537	567–589	594–616
TM5	580–600	538–558	590–610	617–637
loop5	601–635	559–595	611–621	638–662
pore	636–647	596–609	622–641	663–682
loop6	648–659	610–621	642–649	683–690
TM6	660–680	622–642	650–670	691–711
C-loop	681–696	643–654	671–690	712–731
TRPbox	697–702	659–664	691–697	732–738
Cam BS	768–802	655–686		812–831
PIP2	778–793			
Cterm	803–839	687–764	698–790	832–871
Total length	839	764	790	871

**Ankyrin repeats were defined according to the crystal structure.*
doi:10.1371/journal.pone.0110715.t002

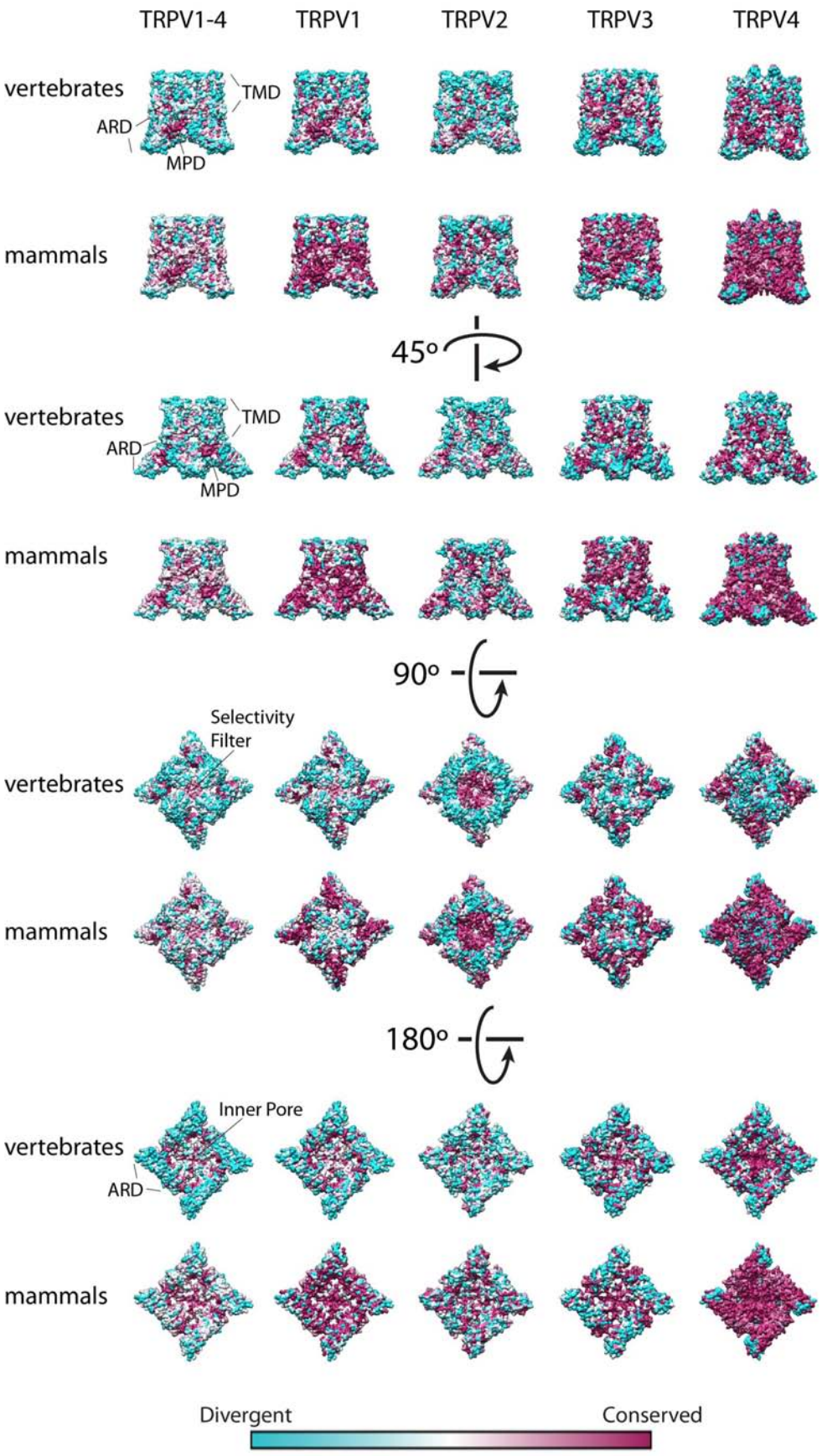
TRPV1-4
TRPV1
TRPV2
TRPV3
TRPV4
vertebrates
TMD
ARD
MPD
mammals
45°
vertebrates
TMD
ARD
MPD
mammals
90°
Selectivity Filter
vertebrates
mammals
180°
Inner Pore
vertebrates
ARD
mammals
Divergent
Conserved

Figure 3. Tridimensional Conservation plots for TRPV1-4 comparing vertebrate and mammalian sequences. Conservation degree for each amino acid position was plotted on the solved structure for TRPV1 (pdb code 3J5P) for the MSAs for TRPV1-4 and TRPV1. For the conservation plot of TRPV2, TRPV3 and TRPV4 homology models were built based on the coordinates of TRPV1 (pdb code 3J5P). The conservation ranges from cyan (divergent) to magenta (conserved). Specific domains are indicated: TMD, transmembrane domain; ARD, ankyrind repeat domain; MPD, membrane proximal domain.
doi:10.1371/journal.pone.0110715.g003

We have taken special consideration into the TMD of these channels, mainly because the channel gating that allows the cation flux through the pore, but also because the conservation profile of this domain will provide hints about homo/heteromer contacts, transmembrane topology and ligand binding. To get structural insight into the TMD we have analyzed the TMD residual coevolution pattern. Taken altogether, the evolutionary pressure on TM4–TM6 region is the highest, while the ECs in the TM1–TM3 region are not so represented (Fig. 4B). The evolution profile correlates with the inter-chain structure contacts: most of the inter-chain contacts in the TMD are located in the TM4–TM6 region, with the exception of the TM1–TM5 contacts (Fig. 4D). Analyzing the residues that may have co-evolved provides and interesting approach to understand the residues that may be in close vicinity. In the case of transmembrane proteins, the residual coevolution information can be cross-related to predict contacts between transmembrane segments involved in the folding/oligomerization of TPRV channels.

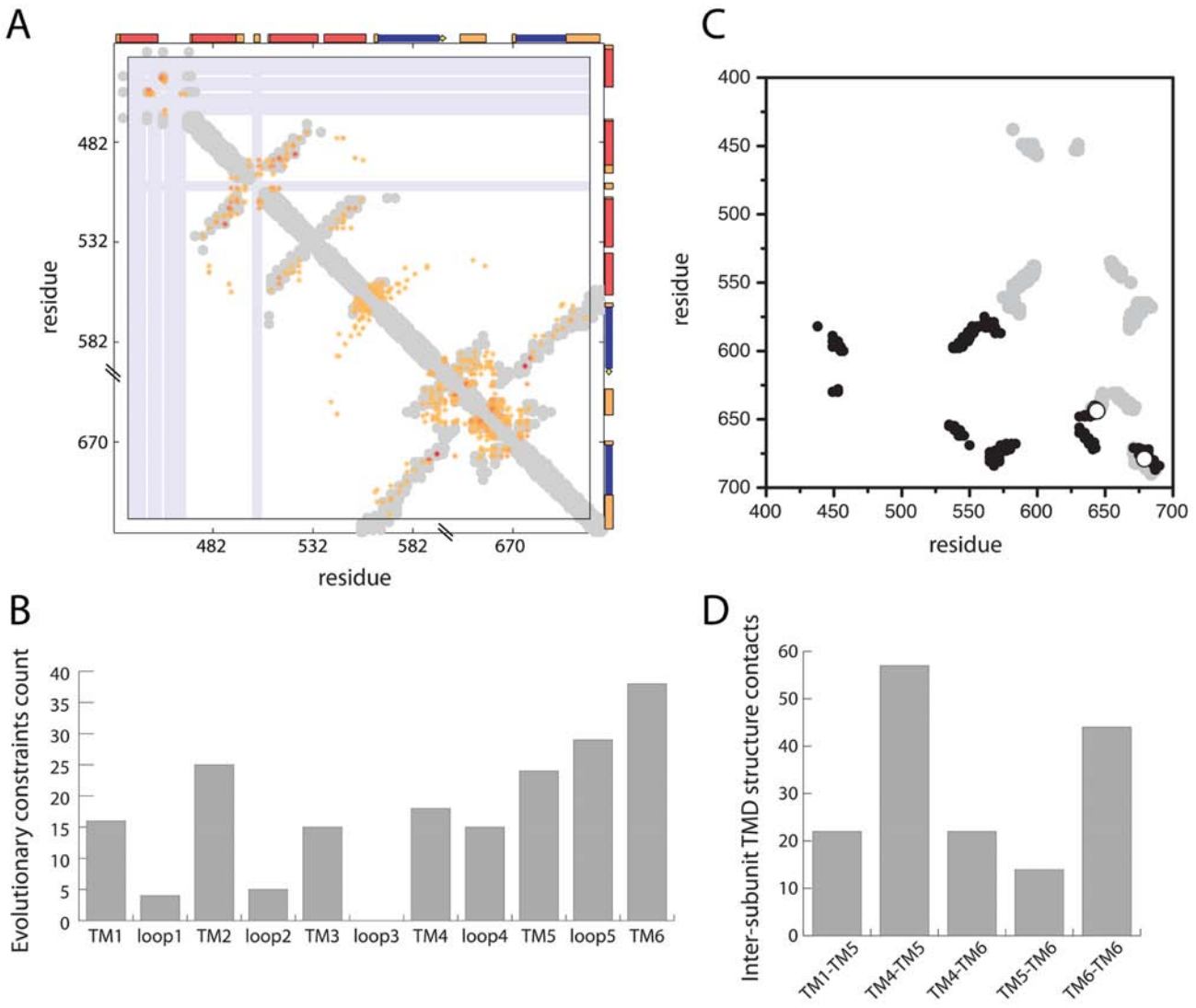

Figure 4. Transmembrane domain analysis for TRPV1-4. A. Evolutionary constraints heat map for the TMD of TRPVs using rat TRPV1 as reference sequence. The colored dots indicate the evolutionary constraints. The grey shaded area indicates the tridimensional structure contacts (3J5P). **B.** Histogram indicating the number of evolutionary constraints for each TMD region. **C.** Inter-chain structure contacts for chains A–B, black, for chains A–C, grey, and chains A–D, open circles. **D.** Histogram indicating the number of inter-chain structure contacts for chain A against chain B, C, and D between the indicated transmembrane segments.
doi:10.1371/journal.pone.0110715.g004

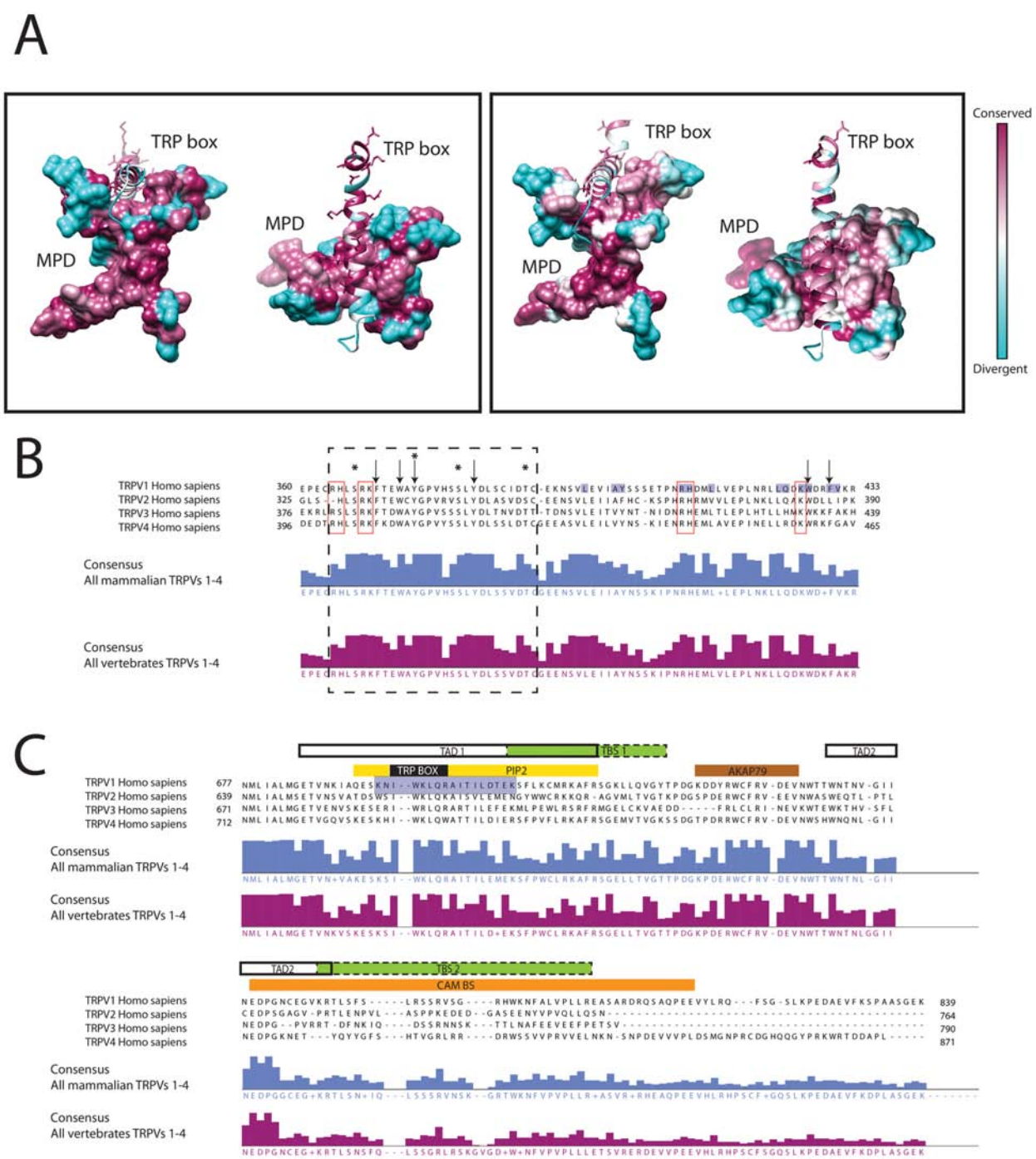

Figure 5. Cytosolic domains of TRPV channels. A. Conservation plot for the TRPV1 N-terminus (surface representation) and C-terminus (ribbon representation) interaction region. The residues involved in the MPD and TRP box interaction have been selected using a 5Å threshold. The specific residues are indicated in the alignments in Fig. 5B and 5C. The left plot represents the conservation scores obtained by ConSurf [46] for all TRPV1 sequences in this study. The plot in the right represents the conservation scores for all TRPV sequences used in this study. **B.** MSA for the membrane proximal domain of human TRPVs. The consensus sequence and the confidence score for the whole set of mammalian and vertebrate sequences are indicated. The black dashed line box delimits a conserved domain with predicted phosphorylation sites (asterisks, see text for details). Conserved residues are highlighted, positively charged residues are framed in red, and black arrows indicate aromatic residues. Shaded residues in the TRPV1 sequence represent the contacts between the MPD and the TRP box, represented in Fig. 5A. **C.** MSA of the C-terminal domain of human TRPV1-4 channels. Fragment showing the alignment of the C-terminal region from the human TRPV1-4 channels. The consensus sequence and the confidence score for the whole set of mammalian and vertebrate sequences are indicated. Specific structural/regulatory domains are indicated; TAD, tetramerization domain, commonly known as TRP domain; TBS, tubulin-binding sequence; PIP2, Phosphatidylinositol 4,5-bisphosphate binding sequence; AKAP79; CAM BS, calmodulin binding sequence. The alignments were plotted using JalView 2.8 [14]. Shaded residues in the TRPV1 sequence represent the contacts between the MPD and the TRP box, represented in Fig. 5A.
doi:10.1371/journal.pone.0110715.g005

Using the primary sequence information we have delimited some conserved sequence determinants in the TRPV MPD domain that may be protein-protein and/or protein-lipid interaction modules (Fig. 5A and B). Although the MPD has been postulated to be the thermal sensing domain of the TRPV thermosensors [19], other roles for the MPD become evident, such as a lipid binding domain or a vesicle trafficking domain. Interestingly, the LKRSF consensus in the MPD sequence of TRPVs, with a highly likely phosphorylation serine site (Fig. 5) is also present near the coil domain of mammalian syntaxins 1,2, and 3, which also interact with the C2A domain of synaptotagmins [33]. The conserved LKRSF in TRPVs sequence is a predicted motif for PKC phosphorylation and it could be also involved in the regulation of syntaxin-binding proteins involved in vesicle-mediated transport. Vesicle trafficking may lead to translocation of TRPVs from internal membrane pools towards the plasma membrane, essential for TRPVs activity [34–36].

Similarly, the conservation of some functional features located in the C-terminus segment, allows the inference of domains such as the tetramerization, PIP2 binding and AKAP79 binding domains for all TRPVs 1–4 (Fig. 5C). It is noteworthy the importance of these domains for the correct assembly of the tetramer in the membrane, the gating and the regulation of the channel, respectively.

Conclusions

Concerning TRPV1-4, we find that TRPV2 is under positive selection. The evolutionary pressure on specific domains is positive on the N-terminal and most extracellular loops, but negative in the ARD, TMD and the TRP domain. Taking advantage of the recently solved structure for TRPV1, we have been able to map specific evolutionary traits in the TMD that are relevant for the structure of the channel. We have also used the conservation profiles in the cytosolic domains to extrapolate functions of one channel to the rest, such as the AKAP interaction of TRPV1, the PIP2 binding of TRPV1 and TRPV2, etc.

From this study we find that evolutionary pressure is exerted differentially on different TRPVs but similarly on specific TRPV domains, arguing for a strong physiology/tissue-dependence/environment adaptability of these channels. From a methodological perspective, we provide a workflow for dissecting complex multidomain membrane proteins through their primary sequences, integrating and adapting state-of-the-art algorithms specifically for membrane proteins. In summary, our study highlights the relevance of evolutionary primary sequence analysis of membrane proteins towards predicting potential functional and structural sequence hallmarks, which may obviously require experimental validation.

Materials and Methods

Sequence retrieval and revision of draft sequences

We retrieved all the available sequences for TRPV1, TRPV2, TRPV3 and TRPV4 channels available from UNIPROT [13,37]. The complete sequences from UNIPROT were used without further modifications. The fragment sequences were used as primers in genome databases NCBI [38] and UCSC [39] by BLAST and BLAT algorithms, respectively. Sequences identified in genomes were completed and used for further analysis. The fragment sequences that could not be completed, either because the genomic region was not covered or because they were not found, were not modified and the original UNIPROT retrieved fragments were used. The total set of sequences consisted of: TRPV1 (35 sequences), TRPV2 (35 sequences), TRPV3 (27 sequences), and TRPV4 (28 sequences). To avoid biased information, we used only the full-length sequences for the divergence analysis and conservation plots (Table 1 and Supplementary Information). Preliminary sequence analysis was carried out using the computational phylogenetics HyPhy software package [15]. To detect directional selection we performed a two-step process: first, we run the "Model Selection Tool" and the best model for our data was Jones-Taylor-Thornton (JTT). Second we performed a FADE analysis for each TRPV channel MSA (rooting the alignment in the *Homo sapiens* sequence) to detect sites under evolutionary directional positive selection (output in Table 1). As a measure of positive selection we chose the residues with a posterior confidence interval >0.95.

Multiple sequence alignment

All the sequences were aligned using ClustalW algorithm with a gap opening penalty of 10 and a gap extension penalty of 0.1 [40]. For validation of the alignments, we have also used MAFFT alignments [41]; there were no major differences between the generated MSAs. We defined two subsets of MSAs, to discriminate between mammalian and vertebrate sequences for TRPV1, TRPV2, TRPV3 and TRPV4.

Phylogenetic tree generation

Trees were generated by maximum likelihood algorithm (Nearest-Neighbour-interchange heuristic method). A JTT model with uniform rates was used to calculate amino acid substitutions. Bootstrapping method with 250 iterations was used to improve the phylogenetic tree confidence value.

Box plot generation

Using the full protein or the specific segment MSAs we build a pairwise sequence divergence matrix in MEGA5.0. Considering one specific TRPV channel, all species sequences within the specific member were compared in a pairwise fashion obtaining a divergence matrix. Specifically, we applied a p-distance model, where the pairwise divergence among all the sequences in one TRPV member subset is calculated considering the number of substitutions per total number of residues considered (full length protein or specific segment). Any amino acid substitution is scored with equal distance (uniform rate), and alignment gaps are considered partial deletions sites and are removed from any calculations, i.e. sites present in all sequences are considered.

Medians of divergence in mammal and vertebrate TRPVs were compared with Kruskal-Wallis test. Divergence of each TRPV was compared with divergence of the other TRPVs using Wilcoxon rank sum test. p-values were adjusted for multiple comparisons using the Bonferroni correction and considered significant (*) when p-value<0.05. Statistical analysis was performed with R Statistical Package (Version 2.15.1) [42].

The sequences of human TRPV1, TRPV2, TRPV3 and TRPV4 were used as references for domain definition. MSAs were truncated into different segments attending to UNIPROT topology definition for the different transmembrane segments and functional domains. The ankyrin repeats were defined attending to the crystal structures already available [43–45]. The divergence matrices for specific segments were generated as previously indicated for the full-length sequences. The distances (divergence) within the box represent the first three quartiles and the line corresponds to the median (second quartile). The whiskers indicate the values within 1.5 times the interquartile range from the lowest and highest quartile, respectively. Diamonds represent outliers. For statistical analysis of the divergence of specific segments, we

used a Mann-Whitney comparison of two medians (segment *versus* full-length).

Boxplots were generated both for full sequences and for specific domains. We have used a normalized ratio of medians (Fig. 2B) to provide a qualitative comparison for the analysis of divergence between full-length sequences and specific domains, among the different channels:

(Segment median – Full length median)/(Full length median).

Evolutionary constraints and conservation plots

To map residue and domain conservation on the specific domains, we used the ConSurf server [46] using the 3J5P TRPV1 structure as template. Evolutionary constraints of the TRPVs TMD domain were predicted using the EVcouplings server [18] and the inter-chain crystal contacts for rat TRPV1 structure, PDB code 3J5P [17] were analyzed using the contact map analysis tool from the SPACE suite [47].

Tridimensional representations and modeling

All structural representations have been performed using UCSF Chimera [48]. The modeling of TRPV2, TRPV3, and TRPV4 in Figure 3 has been carried out using the MODELLER suite [49] included in UCSF Chimera.

Supporting Information

Table S1 Output file from the EVcouplings algorithm indicating the evolutionary constraints for rat TRPV1 transmembrane domain segment.
(CSV)

Table S2 Inter-chain structure contacts for chain A obtained for the rat TRPV1 transmembrane domain segment high-resolution structure (PDB code 3J5P).
(CSV)

Dataset S1 Full list of sequences used in this analysis.
(PDF)

Acknowledgments

We thank Dr. Mireia Olivella and Dr. Ute Hellmich for critical reading of the manuscript. The authors want to thank Dr. Irene R. Dégano for the assistance on the statistical analysis and on the preparation of the manuscript. The authors want to acknowledge the Generalitat de Catalunya for the recognition of the "Membrane Proteins Structural and Computational Biology Research Group" as an emerging research group (GRE 2014 SGR 1628).

Author Contributions

Conceived and designed the experiments: PD-M AP-M. Performed the experiments: PD-M AP-M. Analyzed the data: PD-M AP-M. Contributed reagents/materials/analysis tools: AP-M. Wrote the paper: AP-M. Commented on and edited the manuscript: PD-M.

References

1. Nilius B, Owsianik G (2011) The transient receptor potential family of ion channels. Genome Biol 12: 218.
2. Ramsey IS, Delling M, Clapham DE (2006) An introduction to trp channels. Annu Rev Physiol 68: 619–647.
3. Gunthorpe M, Benham C, Randall A (2002) The diversity in the vanilloid (TRPV) receptor family of ion channels. Trends Pharmacol 23: 183–191.
4. Montell C (2001) Physiology, Phylogeny, and Functions of the TRP Superfamily of Cation Channels. Sci STKE 2001: 1re–1.
5. Saito S, Shingai R (2006) Evolution of thermoTRP ion channel homologs in vertebrates. Physiol Genomics 27: 219–230.
6. Sardar P, Kumar A, Bhandari A, Goswami C (2012) Conservation of Tubulin-Binding Sequences in TRPV1 throughout Evolution. PLoS One 7: e31448.
7. Andrade MA, Sander C (1997) Bioinformatics: from genome data to biological knowledge. Curr Opin Biotechnol. 8 : 675–683.
8. Edwards YJK, Cottage A (2003) Bioinformatics Methods to Predict Protein Structure and Function: A Practical Approach. Mol Biotechnol 23: 139–166.
9. Arinaminpathy Y, Khurana E, Engelman DM, Gerstein MB (2009) Computational analysis of membrane proteins: the largest class of drug targets. Drug Discov Today 14: 1130–1135.
10. Fuchs A, Martin-Galiano AJ, Kalman M, Fleishman S, Ben-Tal N, et al. (2007) Co-evolving residues in membrane proteins. Bioinformatics 23: 3312–3319.
11. Gromiha MM, Ou Y-Y (2013) Bioinformatics approaches for functional annotation of membrane proteins. Brief Bioinform. in press.
12. Lundstrom K (2006) Structural genomics for membrane proteins. Cell Mol Life Sci 63: 2597–2607.
13. The UniProt Consortium (2014) Activities at the Universal Protein Resource (UniProt). Nucleic Acids Res 42: D191–198.
14. Waterhouse AM, Procter JB, Martin DMA, Clamp M, Barton GJ (2009) Jalview Version 2–a multiple sequence alignment editor and analysis workbench. Bioinformatics 25: 1189–1191.
15. Kosakovsky Pond SL, Frost SDW, Muse S V. (2005) HyPhy: Hypothesis testing using phylogenies. Bioinformatics 21: 676–679.
16. Delport W, Poon AFY, Frost SDW, Kosakovsky Pond SL (2010) Datamonkey 2010: A suite of phylogenetic analysis tools for evolutionary biology. Bioinformatics 26: 2455–2457.
17. Liao M, Cao E, Julius D, Cheng Y (2013) Structure of the TRPV1 ion channel determined by electron cryo-microscopy. Nature 504: 107–112.
18. Marks DS, Hopf TA, Sander C (2012) Protein structure prediction from sequence variation. Nat Biotechnol 30: 1072–1080.
19. Yao J, Liu B, Qin F (2011) Modular thermal sensors in temperature-gated transient receptor potential (TRP) channels. Proc Natl Acad Sci 108: 11109–11114.
20. Blom N, Gammeltoft S, Brunak S (1999) Sequence and structure-based prediction of eukaryotic protein phosphorylation sites. J Mol Biol 294: 1351–1362.
21. Goswami C, Hucho TB, Hucho F (2007) Identification and characterisation of novel tubulin-binding motifs located within the C-terminus of TRPV1. J Neurochem 101: 250–262.
22. Suzuki M, Hirao A, Mizuno A (2003) Microtubule-associated [corrected] protein 7 increases the membrane expression of transient receptor potential vanilloid 4 (TRPV4). J Biol Chem 278: 51448–51453.
23. Becker D, Müller M, Leuner K, Jendrach M (2008) The C-terminal domain of TRPV4 is essential for plasma membrane localization. Mol Membr Biol 25: 139–151.
24. García-Sanz N, Fernández-Carvajal A, Morenilla-Palao C, Planells-Cases R, Fajardo-Sánchez E, et al. (2004) Identification of a tetramerization domain in the C terminus of the vanilloid receptor. J Neurosci 24: 5307–5314.
25. Prescott ED, Julius D (2003) A modular PIP2 binding site as a determinant of capsaicin receptor sensitivity. Science (80−) 300: 1284–1288.
26. Mercado J, Gordon-Shaag A, Zagotta WN, Gordon SE (2010) Ca2+-dependent desensitization of TRPV2 channels is mediated by hydrolysis of phosphatidylinositol 4,5-bisphosphate. J Neurosci 30: 13338–13347.
27. Gambhir A, Hangyás-Mihályné G, Zaitseva I, Cafiso DS, Wang J, et al. (2008) Electrostatic Sequestration of PIP2 on Phospholipid Membranes by Basic/Aromatic Regions of Proteins. Biophys J 86: 2188–2207.
28. Fischer MJM, Btesh J, McNaughton PA (2013) Disrupting sensitization of transient receptor potential vanilloid subtype 1 inhibits inflammatory hyperalgesia. J Neurosci 33: 7407–7414.
29. Abramowitz J, Birnbaumer L (2007) Know thy neighbor: a survey of diseases and complex syndromes that map to chromosomal regions encoding TRP channels. Handb Exp Pharmacol: 379–408.
30. Gong Z, Son W, Chung YD, Kim J, Shin DW, et al. (2004) Two interdependent TRPV channel subunits, inactive and Nanchung, mediate hearing in Drosophila. J Neurosci 24: 9059–9066.
31. Kim J, Chung YD, Park D-Y, Choi S, Shin DW, et al. (2003) A TRPV family ion channel required for hearing in Drosophila. Nature 424: 81–84.
32. Sokolchik I, Tanabe T, Baldi PF, Sze JY (2005) Polymodal sensory function of the Caenorhabditis elegans OCR-2 channel arises from distinct intrinsic determinants within the protein and is selectively conserved in mammalian TRPV proteins. J Neurosci 25: 1015–1023.
33. Shao X, Li C, Fernandez I, Zhang X, Südhof TC, et al. (1997) Synaptotagmin-syntaxin interaction: the C2 domain as a Ca2+-dependent electrostatic switch. Neuron 18: 133–142.
34. Morenilla-Palao C, Planells-Cases R, García-Sanz N, Ferrer-Montiel A (2004) Regulated exocytosis contributes to protein kinase C potentiation of vanilloid receptor activity. J Biol Chem 279: 25665–25672.

35. Nagasawa M, Nakagawa Y, Tanaka S, Kojima I (2007) Chemotactic peptide fMetLeuPhe induces translocation of the TRPV2 channel in macrophages. J Cell Physiol 210: 692–702.
36. Penna A, Juvin V, Chemin J, Compan V, Monet M, et al. (2006) PI3-kinase promotes TRPV2 activity independently of channel translocation to the plasma membrane. Cell Calcium 39: 495–507.
37. Consortium U (2013) Update on activities at the Universal Protein Resource (UniProt) in 2013. Nucleic Acids Res 41: D43–47.
38. Benson DA, Karsch-Mizrachi I, Lipman DJ, Ostell J, Wheeler DL (2005) GenBank. Nucleic Acids Res 33: D34–38.
39. Dreszer TR, Karolchik D, Zweig AS, Hinrichs AS, Raney BJ, et al. (2012) The UCSC Genome Browser database: extensions and updates 2011. Nucleic Acids Res 40: D918–923.
40. Larkin MA, Blackshields G, Brown NP, Chenna R, McGettigan PA, et al. (2007) Clustal W and Clustal X version 2.0. Bioinformatics 23: 2947–2948.
41. Katoh K, Misawa K, Kuma K ichi, Miyata T (2002) MAFFT: a novel method for rapid multiple sequence alignment based on fast Fourier transform. Nucleic Acids Res 30: 3059–3066.
42. Team RDC (2008) R: A Language and Environment for Statistical Computing. R Foundation for Statistical Computing, Vienna, Austria. ISBN 3–900051–07–0.
43. Inada H, Procko E, Sotomayor M, Gaudet R (2012) Structural and biochemical consequences of disease-causing mutations in the ankyrin repeat domain of the human TRPV4 channel. Biochemistry 51: 6195–6206.
44. Jin X, Touhey J, Gaudet R (2006) Structure of the N-terminal ankyrin repeat domain of the TRPV2 ion channel. J Biol Chem 281: 25006–25010.
45. Lishko P V, Procko E, Jin X, Phelps CB, Gaudet R (2007) The ankyrin repeats of TRPV1 bind multiple ligands and modulate channel sensitivity. Neuron 54: 905–918.
46. Ashkenazy H, Erez E, Martz E, Pupko T, Ben-Tal N (2010) ConSurf 2010: calculating evolutionary conservation in sequence and structure of proteins and nucleic acids. Nucleic Acids Res 38: W529–533.
47. Sobolev V, Eyal E, Gerzon S, Potapov V, Babor M, et al. (2005) SPACE: a suite of tools for protein structure prediction and analysis based on complementarity and environment. Nucleic Acids Res 33: W39–43.
48. Pettersen EF, Goddard TD, Huang CC, Couch GS, Greenblatt DM, et al. (2004) UCSF Chimera–a visualization system for exploratory research and analysis. J Comput Chem 25: 1605–1612.
49. Fiser A, Sali A (2003) Modeller: generation and refinement of homology-based protein structure models. Guid to Yeast Genet Funct Genomics, Proteomics, Other Syst Anal 374: 461–491.

Supporting information

http://journals.plos.org/plosone/article?id=10.1371/journal.pone.0110715

Table S1

Output file from the EVcouplings algorithm indicating the evolutionary constraints for rat TRPV1 transmembrane domain segment.

Table S2

Inter-chain structure contacts for chain A obtained for the rat TRPV1 transmembrane domain segment high-resolution structure (PDB code 3J5P).

Dataset S1

Full list of sequences used in this analysis.

Chapter III

Molecular and topological membrane folding determinants of transient receptor potential vanilloid 2 channel.

Specific Objectives

- Characterize the implications of N terminus of TRPV2 in protein trafficking and folding.
- Study the transmembrane folding modules and determinant properties of TRPV2 membrane insertion.
- Map the transmembrane alpha helices distribution of TRPV2 and analyse the potential conservation in TRPVs.

Biochemical and Biophysical Research Communications 462 (2015) 221–226

Contents lists available at ScienceDirect

Biochemical and Biophysical Research Communications

journal homepage: www.elsevier.com/locate/ybbrc

Molecular and topological membrane folding determinants of transient receptor potential vanilloid 2 channel

Pau Doñate-Macian [a, 1], Manuel Bañó-Polo [b, 1], Jose-Luis Vazquez-Ibar [a], Ismael Mingarro [b, **], Alex Perálvarez-Marín [a, *]

[a] Departament de Bioquímica i de Biologia Molecular, Unitat de Biofísica, Universitat Autònoma de Barcelona, 08193 Bellaterra, Spain
[b] Department of Biochemistry and Molecular Biology, ERI BioTecMed, University of Valencia, Dr. Moliner 50, 46100 Burjassot, Spain

ARTICLE INFO

Article history:
Received 22 April 2015
Available online 5 May 2015

Keywords:
Ion channels
TRP channels
Membrane protein trafficking
Membrane protein folding and biogenesis
Calcium signaling

ABSTRACT

Transient Receptor Potential (TRP) channels are related to adaptation to the environment and somatosensation. The transient receptor potential vanilloid (TRPV) subfamily includes six closely evolutionary related ion channels sharing the same domain organization and tetrameric arrangement in the membrane.

In this study we have characterized biochemically TRPV2 channel membrane protein folding and transmembrane (TM) architecture. Deleting the first N-terminal 74 residues preceding the ankyrin repeat domain (ARD) show a key role for this region in targeting the protein to the membrane. We have demonstrated the co-translational insertion of the membrane-embedded region of the TRPV2 and its disposition in biological membranes, identifying that TM1-TM4 and TM5-TM6 regions can assemble as independent folding domains. The ARD is not required for TM domain insertion in the membrane. The folding features observed for TRPV2 may be conserved and shared among other TRP channels outside the TRPV subfamily.

1. Introduction

Transient Receptor Potential (TRP) channels are polymodal cation channels with physiological key roles represented in six subfamilies in mammals [1]. The vanilloid subfamily in mammals consists of 6 members (TRPV1-6) with a very defined topology of two cytosolic domains flanking a membrane-embedded region. The TRPV1-4 subgroup has been defined as non-selective cation channels, whereas TRPV5-6 are calcium selective. The closest homologs are TRPV5 and TRPV6, sharing a 75% sequence identity [2]. The most studied member of the TRPV subfamily is TRPV1, the capsaicin receptor, which structure has been recently solved at high resolution. This structure showed a tetrameric arrangement of 6 transmembrane (TM) helices per monomer in TRPV1 with a topology and tetrameric arrangement similar to sodium channels [3], which is likely to be shared among the different TRPV members. The TRPV1-4 subgroup has a low sequence identity (TRPV1 and TRPV2 are the closest homologs with about 50% sequence identity), although evolutionary pressure patterns are similar [4].

Translocation of TRPV2 towards the plasma membrane has been observed in the presence of physical stimuli, growth factors or chemotactic peptides [5]. Recently, the possibility has arisen that TRPV2 functions as an intracellular or plasma membrane ion channel in a cell type/tissue dependent manner [6]. Thus it is key to define which TRPV2 domains are in charge for the sub-cellular localization and the proper folding of the channel.

Most membrane-embedded proteins are inserted and assembled in the ER membrane at sites termed translocons [7]. During this process, the translocon mediates the integration of TM sequences into the non-polar core of the membrane and delivers hydrophilic cytoplasmic and luminal domains to the appropriate

Abbreviations: ARD, ankyrin repeat domain; EGFP, enhanced green fluorescent protein; TM, transmembrane; TMD, transmembrane domain; TMHMM, TM hidden Markov model; TRP, transient receptor potential; TRPV, transient receptor potential vanilloid subfamily.

* Corresponding author. Centre d'Estudis en Biofísica/Unitat de Biofísica, Edifici M, Universitat Autònoma de Barcelona, 08193 Bellaterra, Barcelona, Spain. Fax: +34 935811907.
** Corresponding author. Department of Biochemistry and Molecular Biology/ERI BioTecMed, Dr. Moliner 50, University of Valencia, 46100 Burjassot, Spain. Fax: +34 963544635.
E-mail addresses: Ismael.Mingarro@uv.es (I. Mingarro), peralvarezmarin@gmail.com (A. Perálvarez-Marín).
[1] These authors contributed equally to this work.

http://dx.doi.org/10.1016/j.bbrc.2015.04.120
0006-291X/

compartments. Simultaneously, the nascent protein may undergo covalent modifications (e.g. *N*-glycosylation) and fold properly to eventually adopt its native state. *N*-glycosylation is cotranslationally performed in the lumen of the ER by the enzyme oligosaccharyltransferase, which is adjacent to the translocon [8]. TRPV2 has canonical *N*-glycosylation sites, $N_{571}N_{572}ST$, thus integration of the protein into ER-derived membranes can be monitored by *N*-glycosylation.

In this study we have applied a combination of biochemical approaches focusing on key molecular aspects of the TRPV2 channel related to membrane location, transmembrane architecture and folding. Some of the conclusions derived from this study can be relevant for the other members of the TRPV subfamily and other ion channels.

2. Materials and methods

2.1. Plasmids

cDNA sequences for rat TRPV2 were cloned into a pCDNA3 vector. The TRPV2 ORF was encoded in frame with an EGFP tag and an 8XHis-tag at the C-terminus. The N-terminus truncations for TRPV2 were obtained by classical PCR cassette reaction and ligated into pCDNA3 within NdeI and NotI sites.

2.2. Cell culture and transfection

HEK293 cells were cultured in Dulbecco's modified Eagle's medium (DMEM) supplemented with 10% FBS, 100 units/mL penicillin and 100 μg/mL streptomycin. Transfection was performed using polyethyleneimine (PEI, Polysciences, 23966). HEK293 cells overexpressing the transfected constructs were harvested 48 h after transfection and cells were lysed and membrane proteins solubilized for 15 min at 4 °C in detergent-containing buffer (50 mM Tris–HCL pH 7.4, 150 mM NaCl, 2 mM EDTA, 1% Triton, 5% glycerol, 1 mM benzamidine and EDTA-free protease inhibition cocktail, ROCHE 11873580001). The total fractions were centrifuged at 14000 g for 10 min. The supernatant was labeled as soluble (S) and the non-solubilized pellet was dissolved using a volume of buffer equal to the supernatant's volume and labeled as non-solubilized (P). EGFP-containing cell extracts could be visualized in an SDS-PAGE using a blue light box to monitor EGFP emission. Quantification of bands has been carried out using ImageJ gel analyzer tool [9].

2.3. MTT viability assay

24 h after transfecting HEK293T cells, cells were plated at 40,000 cells/well density in a 96 well plate. 48 h transfected cells were incubated with 3-(4,5-Dimethylthiazol-2-yl)-2,5-Diphenyltetrazolium Bromide (MTT) reagent (Invitrogen, M6494) for 3.5 h at 37 °C and the absorbance at 590 nm was measured with a FluoStar Optima microplate reader (BMG Labtech).

2.4. Biotinylation assay

Transfected HEK293 cells were washed with phosphate buffered saline (PBS) and incubated with sulfo-NHS biotin (0.5 mg/ml) for 30 min at 4 °C in an orbital shaker. After incubation cells were washed with PBS, quenched with a solution of 50 mM glycine and 50 mM ammonium chloride in PBS and washed with PBS. Cells were lysed in IP buffer pH = 7.4 (PBS, 1% Triton, 5% glycerol, 2.5 mM calcium chloride, 1 mM magnesium chloride, 5 mM EDTA, 5 mM EGTA, 10 mM sodium pyrophosphate, 50 mM sodium fluoride, 1 mM NaVO3, 1 mM benzamidine and EDTA-free protease inhibition cocktail, ROCHE). Cell extracts were incubated for 15 min at 4 °C and centrifuged at 14,000× *g* for 10 min. 500 μg of total protein from the cell extracts were incubated for 3 h at 4 °C with 50 μL neutravidin beads. Immunoprecipitated complexes were denatured with SDS-PAGE sample buffer (90 °C for 5 min), separated by SDS-PAGE and analyzed by immunoblotting. Scanned films were quantified using ImageJ gel analyzer tool [9]. For exocytosis inhibition, transfected HEK293 cells were treated with 50 μM Exo1 (SantaCruz, sc-200752) 2 h prior to biotinylation treatment. To allow the comparison of protein levels between the samples, all samples were loaded into the same gel.

2.5. Immunoblotting

Lysates and inmunoprecipitates were loaded into SDS-PAGE and transferred to a nitrocellulose membrane. Membranes were blocked in TBS-T with 5% (w/v) non-fat dry milk powder and incubated with primary anti His-Tag antibody from Developmental Studies Hybridoma Bank (DHSB mouse P5A11) at 1:1000 dilution and secondary antibody (Santa Cruz, anti mouse sc-2031) at 1:3000 dilution. Detection was carried out with Crescendo reagent (Millipore, WBLUR0100).

2.6. Microscopy and image analysis

Transfected cells on glass bottom microwell dishes (MATTEK) were in vivo visualized using a Leica TCS SP5 confocal microscope with a lens PL APO 40x/1.25–0.75. Cells were incubated 5 min with CellMask Deep Red Plasma Membrane (Life Technologies, C-10046) and HOESCH dyes (Life Technologies, H1399) before visualization. At least five fields were captured for each sample, yielding a total of ≥40 cells visualized.

2.7. Transmembrane topology experiments

TRPV2 truncated constructs were obtained by using forward primers that include the SP6 promotor sequence at the 5′ end and reverse primers at defined positions with an N-glycosylation C-terminal tag followed by tandem stop codons (Table S1) [10]. *In vitro* transcription and translation were performed as previously reported [11]. After membrane pelleting, samples were analyzed by SDS-PAGE, and gels were visualized on a Fuji FLA3000 phosphorimager using the ImageGauge software. The membrane insertion efficiency of a given truncated form was calculated as the quotient between the intensity of the singly glycosylated band divided by the summed intensities of the non-glycosylated and singly glycosylated bands.

2.8. TRPV2 modeling and docking into the TRPV2 EM map

The rat TRPV2 homology model was built using the Modeller [12] built-in in UCSF Chimera [13] using the rat TRPV1 coordinates (PDB code 3j5p). The membrane-embedded domain of TRPV2 was restrained to the topology experiments. TRPV2 homology model docking into the electron microscopy (EM) map of TRPV2 (code EMDB-5688, [14]) was carried out in UCSF Chimera. The TRPV2 EM map was flipped horizontally to show the same handedness of the TRPV1 structure.

3. Results and discussion

3.1. N-terminus of TRPV2 is involved in cell membrane localization

To characterize structural and physiological aspects related to the N-terminus of TRPV2 we studied two N-terminal truncations of

rat TRPV2 (rTRPV2); first, a deletion involving the 74 residues preceding the ARD (ΔN74-rTRPV2), and second, a truncation involving the entire ARD (ΔARD-rTRPV2), i.e. a rat TRPV2 protein variant with the first 336 residues deleted (Fig. 1A). Taking advantage of rTRPV2-EGFP fusions, we analyzed the protein expression levels by in-gel fluorescence of the full-length and truncated forms for rTRPV2 in HEK293T cells (Fig. 1B). Complete solubilization was not achieved using Triton X-100, but the full length and truncated forms were observed at similar levels in the non-solubilized (P) and the solubilized (S) fractions (Fig. 1B). Due to the heterologous expression of the different isoforms, we needed to verify that no observable differences arose from toxicity effects derived from protein overexpressions in HEK293T cells. The toxicity associated to the expression of GFP fused proteins was evaluated by means of an MTT assay, comparing to non-transfected cells, and to the EGFP alone (vector). No significant toxicity effects on HEK293T cells related to the presence of rat TRPV2 could be observed (Fig. 1C), as compared to another study showing cytotoxic effects in mouse TRPV2-transfected cells [15]. We also evaluated the cellular distribution of the full-length TRPV2 compared to the truncated forms. In Fig. 2A we provide an illustrative representation for the TRPV2 subcellular localization of the different constructs, all of them resulting in an internal-membrane rich TRPV2 localization. Image analysis of co-localization shows that the deletion of either the first 74 or 336 residues (ΔN74 or ΔARD constructs) of TRPV2 leads to a strong reduction of TRPV2 in the plasma membrane of HEK293T cells (Fig. 2A). To quantitate the localization of TRPV2 in the plasma membrane we performed a surface biotinylation assay [6,16]. TRPV2 was precipitated from biotinylated HEK293T cells (Fig. 2B) indicating that a fraction of TRPV2 is present in the plasma membrane of the transfected cells. The percentage of membrane-localized TRPV2 is significantly decreased either by the ΔN74 or ΔARD truncations (first 74 or 336 amino acids, respectively) (Fig. 2C). As a control, we inhibited TRPV2 targeting from the ER to the membrane by treating HEK293T transfected cells with an exocytosis inhibitor, 2-(4-Fluorobenzoylamino)-benzoic acid methyl ester (Exo1) (Fig. 2C), which induces a rapid collapse of the Golgi [17].

In sequence length, TRPV2 is the shortest within the TRPV1-4 subgroup (e.g. human sequences for TRPV1, TRPV2, TRPV3, and TRPV4 are 839, 764, 790, and 871 residues, respectively), displaying the shortest N-terminal region compared to TRPV1, TRPV3, and TRPV4. We observe that the first N-terminal 74 residues of TRPV2 play a role in the subcellular localization of the protein, such as targeting to the plasma membrane, since the deletion of this region leads to strong intracellular accumulation of the protein channel (Fig. 2).

3.2. Cotranslational insertion of TRPV2 membrane-embedded domain

To address that the N-terminus truncations do not yield intracellular accumulation of the channel due to improper packing/folding of the TRPV2 membrane-embedded domain we have performed further membrane protein topology studies.

TRPV2 lacking the first 336 residues and defining the membrane-embedded domain (residues 337–654) was translated *in vitro* in reticulocyte lysate in the presence of rough microsomes (RM). Most of this protein was glycosylated, which is detected by an increase in molecular mass of about 2.5 kDa (Fig. 3, lane 3). The TRPV2 membrane-embedded sequence contains an endogenous acceptor site for *N*-linked glycosylation: $N_{571}N_{572}ST$. No glycosylation was observed when a double mutant harbouring the consecutive Asn residues replaced by serines was translated in the presence of RMs (Fig. 3, lane 5). Therefore, the acceptor site

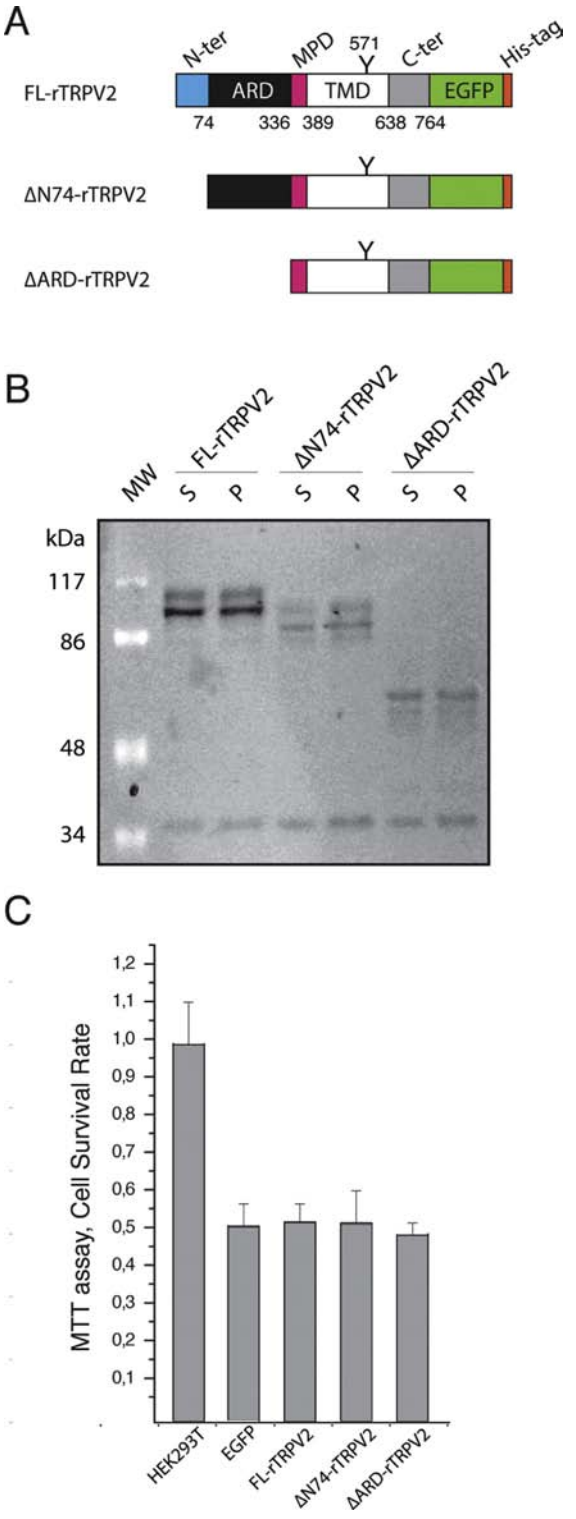

Fig. 1. Heterologous expression of TRPV2 N-terminal constructs. A. The domain organization of a TRPV2 monomer is displayed as a color-coded cartoon: N-terminus, blue; ARD, black; pre-TMD, pink; TMD, white; C-terminus, grey; EGFP, green; His-tag, orange. The *N*-glycosylation site is highlighted by a Y-shaped symbol. B. In-gel fluorescence indicating the expression of the truncations in HEK293T cells. TRPV2 wild type and truncations were extracted from membranes and present in the soluble fraction. C. MTT assay to determine the survival rate of HEK cells transfected with the defined rat TRPV2 truncations. (For interpretation of the references to color in this figure legend, the reader is referred to the web version of this article.)

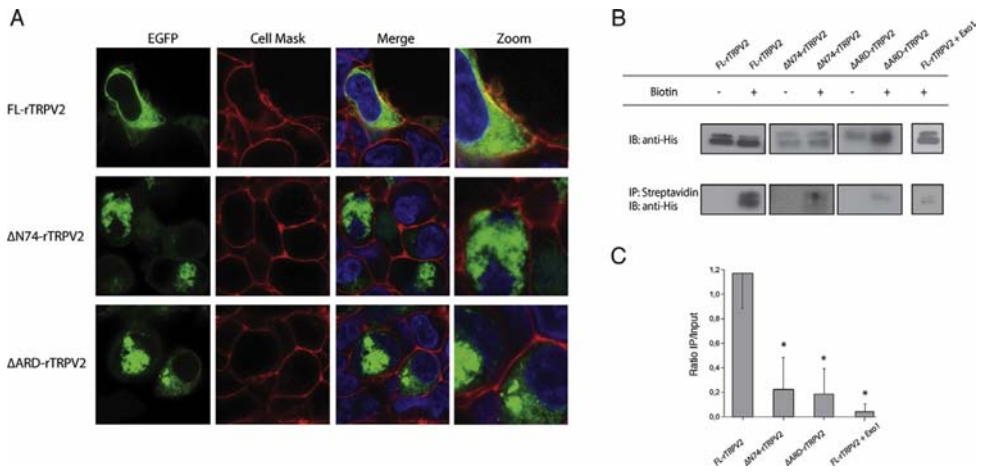

Fig. 2. TRPV2 cellular localization. A. Confocal imaging for HEK293T cells transfected with rat TRPV2 truncations. The left panel corresponds to the EGFP signal; the middle panel corresponds to the CellMask dye. The two right panels (merge) overlays the EGFP and CellMask channels also including the HOESCH channel to mark nuclei. B. Biotinylation assay for TRPV2 and the N-terminal truncations determining the amount of protein present in the plasma membrane. For each biotinylation experiment (N = 3), and for quantification purposes, samples were loaded in the same gel, and analyzed in the same film. C. Quantification of 3 independent biotinylation assays.

$N_{571}N_{572}$ST is cotranslationally glycosylated *in vitro*, suggesting that the cytosolic N-terminus comprising the first 336 residues (ΔN74 and ΔARD constructs) is not required for membrane packing/folding of the protein.

3.3. Ordered membrane insertion of TRPV2 membrane-embedded domain

Next, we predicted the topology of TRPV2 membrane-embedded region using two commonly used prediction algorithms, i.e. the TM hidden Markov model (TMHMM) [18] and the experimentally based ΔG Predictor [19] methods to assess the segments with the higher probabilities to span biological membranes. As seen in Fig. 4A both methods roughly agree in their prediction outputs. Nevertheless, the membrane-buried segment of TM3 does not coincide in both predictions.

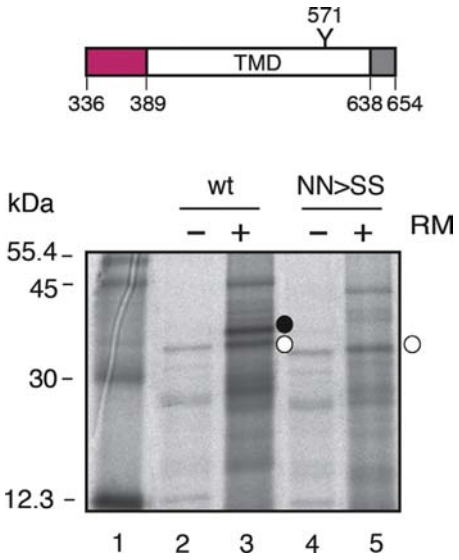

Fig. 3. TRPV2 is cotranslationally inserted into RMs and glycosylated at $N_{571}N_{572}$ST acceptor site. Full-length TRPV2 membrane-embedded region and TRPV2-derived construct NN > SS containing the mutations Asn571Ser and Asn572Ser. Both constructs were translated *in vitro* in the presence of [^{35}S]Met/Cys and in the absence (−) and in the presence (+) of dog pancreas RMs. Bands of non-glycosylated proteins are indicated by a white dot and glycosylated proteins are indicated by a black dot. Molecular weight markers are shown on the left (lane 1).

Since *N*-linked glycosylation occurs in a compartment-specific manner, this modification can provide valuable topological information [20]. Thus, to experimentally map the membrane-embedded domain of the TRPV2, we used *N*-glycosylation as a topological reporter [21]. We prepared a series of protein truncates containing an added C-terminal glycosylation tag (NSTMGM) that has been proven to be efficiently modified in the *in vitro* translation system [10]. As shown in Fig. 4B, translation products containing residues 336–432 (truncated 96-mer polypeptides) of TRPV2, including the first predicted TM segment (TM1), were efficiently glycosylated in the presence of RMs (52 ± 4% of glycosylation), supporting the expected N-terminal cytoplasmic orientation for TM1. Truncated 134-mer polypeptides, which include residues 336–470 (Fig. 4A), were not glycosylated (6 ± 3% of glycosylation), indicating that the second predicted TM segment (TM2) efficiently integrates into the membrane (see Fig. 4B top for an illustrative scheme). The precise location of the third predicted TM segment was tested by translating a 159-residue truncation (residues 336–495). According to the TMHMM prediction, TM3 would span from residue 462 to residue 484, whilst according to the ΔG Predictor TM3 would end at residue 492. It has been previously reported that glycosylation occurs when the acceptor Asn is ~11–13 residues away from the membrane [22,23]. Therefore, since 159-mer polypeptides are not glycosylated (see Fig. 4B, lane 6), TM3 may extend up to Met492. To corroborate TM3 positioning, we added a previously used flexible amino acid linker [24] to extend the Asn glycosylation acceptor site farther away from the membrane ((159 + 10)-mer). Translation *in vitro* of this construct in the presence and in the absence of RMs (Fig. 4B, lanes 7 and 8) rendered glycosylated forms, placing the C-terminal end of the membrane-embedded TM3 segment around residue 492, in perfect agreement with the segment predicted by the ΔG Predictor (residues 471–492).

Furthermore, insertion of TM4 was analyzed by translating a 200-residue truncation (residues 336–536). The low level of glycosylation observed (26 ± 4%, Fig. 4B lane 10) indicates that the predicted fourth TM segment was significantly inserted. Truncated polypeptides encompassing residues 336–609, which include the native potential glycosylation site $N_{571}N_{572}$ST, were doubly

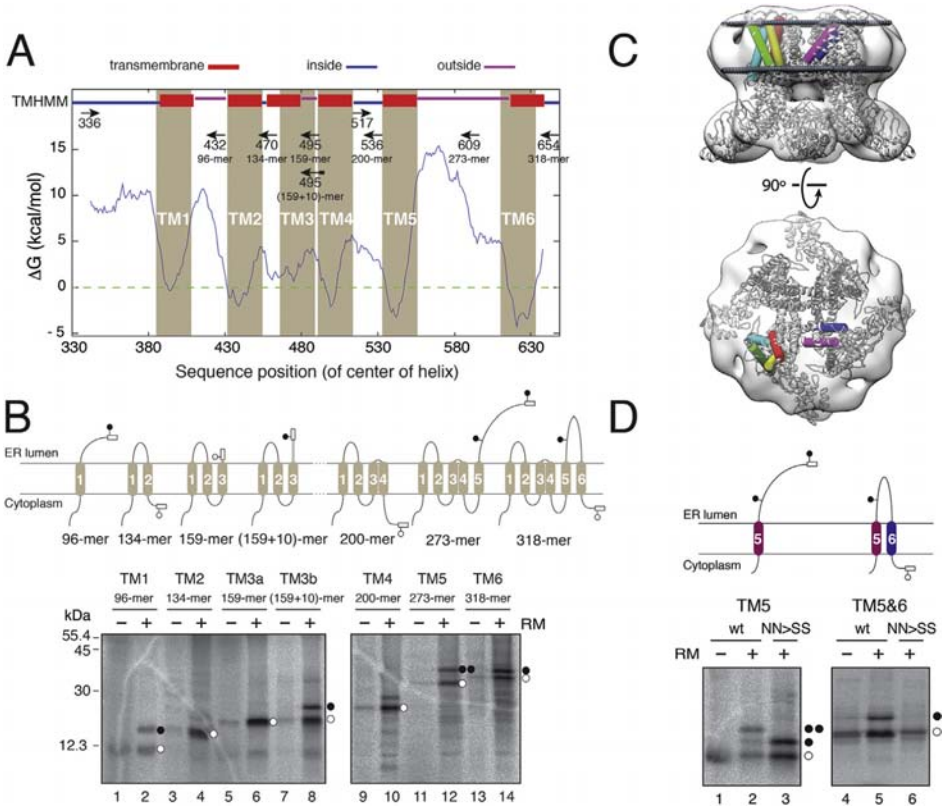

Fig. 4. TRPV2 TM segments are sequentially inserted into the ER membrane. A. Topology prediction for full-length TRPV2 membrane-embedded region using TMHMM [18] and the experimentally based ΔG Predictor [19] methods. In the TMHMM prediction method (top line), TM domains (red rectangles), cytoplasmic loops (blue lines) and luminal loops (pink lines) are indicated. In the ΔG Predictor, the ΔG graph (blue line) shows the predicted membrane-insertion efficiency along the sequence and the predicted TM domains are highlighted in brown. A set of oligonucleotides (arrows) was designed to generate TRPV2-truncated forms, which are indicated by the length of the truncated polypeptide (-mer) and the starting and ending residue in the TRPV2 sequence. B. *In vitro* expression and representative SDS-PAGE analysis of TRPV2 truncates. The presence of RMs and non-glycosylated and glycosylated polypeptides (empty and black dots, respectively) is indicated. Models of the membrane topology of truncated TRPV2 constructs are illustrated, in which a fused C-terminal *N*-glycosylation tag (rectangle) provides a simple readout for topology determination. C. Homology model of the tetrameric TRPV2 has been built using the membrane-embedded domain topology resulting from this study and docked into the TRPV2 EM map at 13.6 Å [14]. A monomer of the channel has been depicted using colored cylinders using the following color code: TM1, cyan; TM2, green; TM3, yellow; TM4, red; TM5, purple; TM6, blue. The spheres displayed in the top view indicate the limits of the lipid bilayer estimated using the OPM database [28]. D. *In vitro* translation of C-terminal-tagged mRNAs encoding TRPV2 and TRPV2-derived (NN > SS) constructs including TM5 (residues 517–609) and TM5-6 hairpin (residues 517–654) was performed in the presence (+) and absence (−) of membranes as indicated. Bands of non-glycosylated polypeptides are indicated by a white dot and singly- and doubly-glycosylated proteins are indicated by one and two black dots, respectively. (For interpretation of the references to colour in this figure legend, the reader is referred to the web version of this article.)

glycosylated, indicating that TM5 efficiently integrates into the membrane. Finally, the single glycosylation of 318-mer construct (residues 336–654) carrying the C-terminal glycosylation tag, combined with the absence of glycosylation in the mutated version (NN > SS) of TRPV2 membrane-embedded region (Figs. 3 and 4B), supports the presence of an inserted sixth TM segment.

3.4. Fitting of a homology model of TRPV2 into the TRPV1 solved structure

Next, we built a homology model of rat TRPV2 based on the recently solved structure of rat TRPV1 (PDB code 3j5p, [3]) using the ΔG Predictor [19] predicted TM segments and the present experimental results as constraints (represented by ribbons in Fig. 4C). The TRPV2 membrane-embedded domain sequence prediction satisfies the TM helix disposition of TRPV2 built on the coordinates of the TM1-TM6 of TRPV1 (Fig. 4C, coloured cylinders). In addition, we fitted the homology model of TRPV2 on the low resolution EM map of TRPV2 (code EMDB-5688, [14]) (not shown).

Both the TRPV2 model and the 3D structure of TRPV1 show a large spatial gap between the TM1-4 and the TM5-6 segments due to a relatively long membrane interface domain between TM4 and TM5. This fact suggested the possibility of TM1-4 and TM5-6 acting as independent folding/assembly subunits.

3.5. Membrane insertion of TM5-TM6 hairpin

TRPV2 channel functions as a tetramer. As shown in Fig. 4C, in each monomer TM5 and TM6 seem to cluster away from the rest of the membrane-embedded domain (TM1-4) as an α-helical hairpin. This simple structural motif is thought to occur relatively frequently in integral membrane proteins and may serve as an important structural and/or functional element [25]. In the TRPV1 case, this helical hairpin has been implicated in the formation of the central ion-conducting pore of the tetramer [3]. To explore the possibility that TRPV2 TM5 and TM6 region could integrate into the membrane as an independent folding motif, we translated from Arg517 to Glu609 (Fig. 4D), a region that includes the extra-membranous loop connecting TM4 to TM5, the fifth TM segment and the native glycosylation site $N_{571}N_{572}ST$. As shown in Fig. 4D (lanes 1–3), doubly glycosylated forms were observed, suggesting that TM5 isolated from the rest of the membrane-embedded region is able to direct its integration into the ER membrane through the translocon. Furthermore, translation of truncated C-terminal

reporter tag fusions encompassing from Arg517 to Asp654, which extended the polypeptide to include TM6, show singly glycosylated forms, suggesting α-helical hairpin insertion (Fig. 4D, lane 5). Notably, single glycosylation and no glycosylation were observed when the native glycosylation acceptor site was mutated in these two constructs (Fig. 4D, lanes 3 and 6). Combined, these results support the independent α-helical hairpin motif integration into biological membranes.

Taking into account our experimental topological analysis, together with TRPVs evolutionary information [4] and the recent TRPV1 and TRPV2 structures [3,14], it is evident that the membrane-embedded domain of the TRPV1-4 shares a common membrane disposition. Interestingly, the insertion into the bilayer of TRPV channels is cotranslational and does not require the cytosolic N-terminal region (first 74 residues and the ARD), since our translation/insertion experiments were carried out in the absence of this domain. We have also identified that the TM1-TM4 and the TM5-TM6 regions of TRPV2 are capable of assembling separately in the membrane, acting as independent folding units. Thus, an independent folding of the TM1-TM4 and TM5-TM6 can be assumed for TRPV1-4 channels, and it cannot be ruled out for the equivalent region of other ion channels with similar topology such as potassium and/or sodium channels [26,27].

Conflict of interest

None declared.

Acknowledgments

The cDNA sample for rat TRPV2 was kindly provided by Prof. Rachelle Gaudet. The authors acknowledge the skillful assistance of Elodia Serrano, the funding from Spanish Government (MICINN-SAF2010-21385 to A.P.-M. and BFU2012-39482 to I.M.), a Marie Curie International Outgoing Fellowship within the 7th European Community Framework Programme (PIOF-GA-2009-237120 to A.P.-M.), the Generalitat de Catalunya research program (AGAUR, 2014-SGR-1628 to A.P.-M.) and the Generalitat Valenciana (PROMETEOII/2014/061 and ACOMP/2014/245 to I.M.). P.D.-M. is a recipient of an FI fellowship from Generalitat de Catalunya (FI–2013FIB00251); M.B.-P. was the recipient of an FPU fellowship from the Spanish Ministry of Education. A.P.-M. is a recipient of the Universitat Autònoma de Barcelona-Programa Banco de Santander Fellowship.

Appendix A. Supplementary data

Supplementary data related to this article can be found at http://dx.doi.org/10.1016/j.bbrc.2015.04.120.

Transparency document

Transparency document related to this article can be found online at http://dx.doi.org/10.1016/j.bbrc.2015.04.120.

References

[1] B. Nilius, G. Owsianik, The transient receptor potential family of ion channels, Genome Biol. 12 (2011) 218.
[2] M.J. Gunthorpe, C.D. Benham, A. Randall, J.B. Davis, The diversity in the vanilloid (TRPV) receptor family of ion channels, Trends Pharmacol. Sci. 23 (2002) 183–191, http://dx.doi.org/10.1016/S0165-6147(02)01999-5.
[3] M. Liao, E. Cao, D. Julius, Y. Cheng, Structure of the TRPV1 ion channel determined by electron cryo-microscopy, Nature 504 (2013) 107–112.
[4] P. Doñate-Macián, A. Perálvarez-Marín, Dissecting domain-specific evolutionary pressure profiles of transient receptor potential vanilloid subfamily members 1 to 4, PLoS One 9 (2014) e110715, http://dx.doi.org/10.1371/journal.pone.0110715.
[5] A. Perálvarez-Marín, P. Doñate-Macian, R. Gaudet, What do we know about the transient receptor potential vanilloid 2 (TRPV2) ion channel? FEBS J. 280 (2013) 5471–5487, http://dx.doi.org/10.1111/febs.12302.
[6] M.R. Cohen, K.W. Huynh, D. Cawley, V.Y. Moiseenkova-Bell, Understanding the cellular function of TRPV2 channel through generation of specific monoclonal antibodies, PLoS One 8 (2013) e85392, http://dx.doi.org/10.1371/journal.pone.0085392.
[7] L. Martínez-Gil, A. Saurí, M.A. Marti-Renom, I. Mingarro, Membrane protein integration into the endoplasmic reticulum, FEBS J. (2011) 3846–3858, http://dx.doi.org/10.1111/j.1742-4658.2011.08185.x.
[8] I. Nilsson, D.J. Kelleher, Y. Miao, Y. Shao, G. Kreibich, R. Gilmore, et al., Photocross-linking of nascent chains to the STT3 subunit of the oligosaccharyltransferase complex, J. Cell Biol. 161 (2003) 715–725, http://dx.doi.org/10.1083/jcb.200301043.
[9] W.S. Rasband, ImageJ, U. S. Natl. Institutes Heal, Bethesda, Maryland, USA, 2012, pp. 1997–2012. http//imagej.nih.gov/ij/.
[10] M. Bañó-Polo, F. Baldin, S. Tamborero, M.A. Marti-Renom, I. Mingarro, N-glycosylation efficiency is determined by the distance to the C-terminus and the amino acid preceding an Asn-Ser-Thr sequon, Protein Sci. 20 (2011) 179–186, http://dx.doi.org/10.1002/pro.551.
[11] A. Saurí, S. Tamborero, L. Martínez-Gil, A.E. Johnson, I. Mingarro, Viral membrane protein topology is dictated by multiple determinants in its sequence, J. Mol. Biol. 387 (2009) 113–128, http://dx.doi.org/10.1016/j.jmb.2009.01.063.
[12] A. Fiser, A. Sali, Modeller: generation and refinement of homology-based protein structure models, Methods Enzymol. 374 (2003) 461–491.
[13] E.F. Pettersen, T.D. Goddard, C.C. Huang, G.S. Couch, D.M. Greenblatt, E.C. Meng, et al., UCSF Chimera–a visualization system for exploratory research and analysis, J. Comput. Chem. 25 (2004) 1605–1612, http://dx.doi.org/10.1002/jcc.20084.
[14] K.W. Huynh, M.R. Cohen, S. Chakrapani, H.A. Holdaway, P.L. Stewart, V.Y. Moiseenkova-Bell, Structural insight into the assembly of TRPV channels, Structure 22 (2014) 260–268, http://dx.doi.org/10.1016/j.str.2013.11.008.
[15] A. Penna, V. Juvin, J. Chemin, V. Compan, M. Monet, F.-A. Rassendren, PI3-kinase promotes TRPV2 activity independently of channel translocation to the plasma membrane, Cell Calcium 39 (2006) 495–507.
[16] C. Morenilla-Palao, R. Planells-Cases, N. García-Sanz, A. Ferrer-Montiel, Regulated exocytosis contributes to protein kinase C potentiation of vanilloid receptor activity, J. Biol. Chem. 279 (2004) 25665–25672.
[17] Y. Feng, S. Yu, T.K.R. Lasell, A.P. Jadhav, E. Macia, P. Chardin, et al., Exo1: a new chemical inhibitor of the exocytic pathway, Proc. Natl. Acad. Sci. U. S. A. 100 (2003) 6469–6474, http://dx.doi.org/10.1073/pnas.0631766100.
[18] A. Krogh, B. Larsson, G. von Heijne, E.L. Sonnhammer, Predicting transmembrane protein topology with a hidden Markov model: application to complete genomes, J. Mol. Biol. 305 (2001) 567–580, http://dx.doi.org/10.1006/jmbi.2000.4315.
[19] T. Hessa, N.M. Meindl-Beinker, A. Bernsel, H. Kim, Y. Sato, M. Lerch-Bader, et al., Molecular code for transmembrane-helix recognition by the Sec61 translocon, Nature 450 (2007) 1026–1030.
[20] L. Martínez-Gil, A.E. Johnson, I. Mingarro, Membrane insertion and biogenesis of the turnip crinkle virus p9 movement protein, J. Virol. 84 (2010) 5520–5527, http://dx.doi.org/10.1128/JVI.00125-10.
[21] I. Nilsson, G. von Heijne, Fine-tuning the topology of a polytopic membrane protein: role of positively and negatively charged amino acids, Cell 62 (1990) 1135–1141, http://dx.doi.org/10.1016/0092-8674(90)90390-Z.
[22] I. Nilsson, G. Von Heijne, Determination of the distance between the oligosaccharyltransferase active site and the endoplasmic reticulum membrane, J. Biol. Chem. 268 (1993) 5798–5801.
[23] M. Orzáez, J. Salgado, A. Giménez-Giner, E. Pérez-Payá, I. Mingarro, Influence of proline residues in transmembrane helix packing, J. Mol. Biol. 335 (2004) 631–640, http://dx.doi.org/10.1016/j.jmb.2003.10.062.
[24] S. Tamborero, M. Vilar, L. Martínez-Gil, A.E. Johnson, I. Mingarro, Membrane insertion and topology of the translocating chain-associating membrane protein (TRAM), J. Mol. Biol. 406 (2011) 571–582, http://dx.doi.org/10.1016/j.jmb.2011.01.009.
[25] M. Bañó-Polo, L. Martínez-Gil, B. Wallner, J.L. Nieva, A. Elofsson, I. Mingarro, Charge pair interactions in transmembrane helices and turn propensity of the connecting sequence promote helical hairpin insertion, J. Mol. Biol. 425 (2013) 830–840, http://dx.doi.org/10.1016/j.jmb.2012.12.001.
[26] X. Tao, J.L. Avalos, J. Chen, R. MacKinnon, Crystal structure of the eukaryotic strong inward-rectifier K+ channel Kir2.2 at 3.1 A resolution, Science 326 (2009) 1668–1674, http://dx.doi.org/10.1126/science.1180310.
[27] J. Payandeh, T. Scheuer, N. Zheng, W.A. Catterall, The crystal structure of a voltage-gated sodium channel, Nature 475 (2011) 353–358, http://dx.doi.org/10.1038/nature10238.
[28] M.A. Lomize, A.L. Lomize, I.D. Pogozheva, H.I. Mosberg, OPM: orientations of proteins in membranes database, Bioinformatics 22 (2006) 623–625, http://dx.doi.org/10.1093/bioinformatics/btk023.

Chapter IV

TRPV2 channel interactomics reveals association with proteins crucial for neuronal development and lipid metabolism.

Specific objectives

- Identify potential interactors for TRPV2 to widen the knowledge on the regulation of this channel.
- Determine potential TRPV2 roles from the identified partners and characterize the potential implications of these roles over TRPV2 function.
- Determine domains of TRPV channels involved in lipid binding.

TRPV2 channel interactomics reveals association with proteins crucial for neuronal development and lipid metabolism.

Doñate-Macian P, Viader-Godoy M, Martins M, Álvarez-Marimon E, Del Valle-Pérez B, Barnadas R, Perálvarez-Marín A.
Unitat de Biofisica, Departament de Bioquimica i Biologia Molecular, Fac. Medicina, UAB. Barcelona 08190

SUMMARY

TRPV2 is a non-selective ion channel that is almost ubiquitously expressed in human tissues. In the nervous system TRPV2 plays an important role in somatosensation and axon outgrowth, although the molecular mechanisms by which TRPV2 exerts its function and regulates its activity are unkown.
From literature mining we have identified two interactions for TRPV1 (Snapin25 and Synaptotagmin IX), which we have validated and mapped further for TRPV2. The interaction between TRPV1 and TRPV2 with Snapin25 and Synaptotagmin IX requires of the conserved membrane proximal domain (MPD) in both channels. Further in vitro characterization of the MPD domain of TRPV1 and TRPV2 reveals a phosphatidic acid binding domain with potential implications in channel activity.
To expand the TRPV2 interactome in CNS we have performed a membrane yeast two hybrid (MYTH) screening and identified 20 new potential interactors of TRPV2. Bioinformatic analysis of TRPV2 interactome shows high association with neuronal development and lipid metabolism.
This study establishes the first interactomics approach for TRPV2 to define regulatory pathways for this channel in the central nervous system (CNS).

INTRODUCTION

TRP channels are the second most represented family (28 members in human) after potassium channels family (1). TRPs are somatosensory proteins that can be modulated by a wide range of stimuli, such as temperature (2), pH, shear or mechanical stress (3) or endogenous ligands and exogenous agonists or antagonists (4). The switch of TRPs to open state upon stimuli exposure generate inward cationic currents that trigger intracellular responses (5). Being activated by such a wide range of stimuli, TRPs carry out very diverse functions in the human body and play crucial roles in nociception, cell communication and adaptation to the environment (5). Knowledge about TRPs function is increasing, but most part of the molecular mechanisms by which they exert their function and regulate their activity are still unknown. For instance, TRPV2 is one of the least understood TRP channels.
Structurally TRPV2 is arranged as a homotetramer in the plasma membrane, as shown by its 3D structure that has been recently solved (6, 7). TRPV2 activity is modulated by several molecular processes such as calmodulin binding (8), lipid binding (9), trafficking to the plasma membrane (10) or phosphorylation (11).
TRPV2 is present in most human tissues (12), showing higher expression levels in the CNS(13, 14), where it plays a role in somatosensation (12). TRPV2 is also implicated in nervous system development, where it promotes axon outgrowth upon mechanical stimulation (15). Furthermore, TRPV2 has been associated with pathological conditions such as muscular dystrophy, cardiomyopathies (16) or cancer (17).
TRPV2 known interactors network is a small set of proteins, most of them shared with other TRPV members. Calmodulin binds to the C-terminus of the channel (K661 and K664 residues) (8), coupling the channel to calcium transduction pathways. Similar to other TRPVs, TRPV2 binds to A-kinase Ancoring Protein 79 (AKAP-79), an scaffolding protein that binds PKC, PKA and calcineurin (18) and ACBD3, an adaptor protein linked to PKA (11). Plasma membrane trafficking of TRPV2 is mediated by its interaction with Recombinase Gene Activator protein (RGA) in the ER/Golgi (19), and further potentiated by cAMP or Insulin growth factor (IGF-1) (20, 10). Finally, TRPV2 activity is linked to lipid metabolism, being sensitized by Phosphatidylinositol 4,5-Bisphosphate (PIP_2)(9) and activated by endogenous lysophospholipids such as lysophosphatidylcholine (LPC) and lysophosphatidylinositol (LPI) (21).
Although huge efforts to elucidate TRPV2 and TRP channel regulation have been carried out during the last decades, most described mechanisms have been focused on channel gating and trafficking. From the regulatory perspective several key questions arise: i) how the protein reaches its specific membrane compartment and which are the specific pathways or key elements? ii) Which regulatory pathways affect indirectly TRPV2 through protein post-translational modifications such as glycosylation and/or phosphorylation? iii) Which are the key

protein-protein interactions that modulate TRPV2 function?
There is still plenty of information to gather about how TRPV2 or TRPs function is coupled to specific cellular processes. To gain knowledge on TRPV2 channel regulation, here we used a stepwise approach combined with a high throughput screening technique, a yeast two hybrid specific for membrane proteins (MYTH) (22) and further bioinformatics analysis.

RESULTS

TRPV2 shares common interaction partners with its closer relative TRPV1

Our first attempt to determine potential binding partners was to identify conserved interaction areas in TRPV2 already described in closest related proteins. TRPV1 ion channel is the closest relative to TRPV2, with a 50% of sequence identity Structural arrangement and functional domain features are conserved between these two ion channels (23). TRPV1 and TRPV2 have a highly conserved N-terminus (23), and it has been already described that TRPV1 is able to interact with proteins from the SNARE complex such as Snapin25 and Synaptotagmin IX through its N-terminal region (24). SNARE complex is involved in driving vesicle-regulated exocytosis, which is a highly relevant process in nervous synaptic events. Attending to the high sequence similarity found in this region and the TRPV2 expression levels in the CNS we decided to test whether TRPV2 was also able to form complexes with SNARE proteins.
The full length sequence of rat TRPV1 and TRPV2 tagged with GFP, and the full length Snapin25 and Synaptotagmin tagged with myc were overexpressed in mammalian HEK293T cells. When, either Snapin25 or Synaptotagmin IX, were immunoprecipitated using an anti-myc tag antibody; a band corresponding to the molecular weight of TRPV1 and TRPV2 (around 90 and 80 kDa, respectively) appeared using an anti-GFP tag antibody for immunoblotting (Fig. 1a). TRPV1 and TRPV2 bands only appear when anti-myc antibody was added to the reaction (Fig. 1a), showing that the precipitation of TRPV1 and TRPV2 is specific and only occurs when Snapin25 or Synaptotagmin IX are immunoprecipitated.
In order to test whether the binding of the SNARE proteins happens in the C-terminus of TRPV2 channel, the same co-immunoprecipitation was repeated but using a TRPV2 deletion of the N-terminal ankyrin repeat domain (ARD) ΔARD-TRPV2 tagged with GFP (Fig. 1b). As in the previous experiment ΔARD-TRPV2 was precipitated when we immunoprecipitated either Snapin25 or Synaptotagmin IX (Fig. 1b).
The only region in common between previous reports (24) and our experiment with ΔARD-TRPV2 was the membrane proximal domain (MPD), a fragment of around 60 amino acids in the N-terminal region, located between the ARD domain and the transmembrane domain, which is highly conserved among TRPV1-4 (23). The purified MPD from TRPV1 and TRPV2 were pulled down in the presence of Snapin25 and Synaptotagmin IX and both SNARE proteins were precipitated (Fig. 1c). Free GFP, used as negative control did not precipitate SNARE proteins (Fig. 1c), pointing to MPD as responsible for the specifically binding of Snapin25 and Synaptotagmin IX (Fig. 1c).

TRPV2 yeast two hybrid assay reveals new potential TRPV2 partners

Validation of interactions based on sequence similarity between TRPV1 and TRPV2 has proven useful in the case of experimental validation of TRPV2 interaction with Snapin25 and Synaptotagmin IX. We have validated other interactions using pure bioinformatics analysis (23). However, the sequence similarity validation approach has a key limitation, it will not identify novel specific interactions for TRPV2 and its specific regulatory processes.
To discover novel interactions for TRPV2 we performed a split-ubiquitin-based membrane yeast two hybrid screen (MYTH) (22, 25), which has obvious advantages for identifying membrane protein interactions (see Box1 for details).
As protein baits we generated TRPV1 and TRPV2 fused to the MYTH cassette (NubG-VP16-LexA) on N- and C-terminus. Although the expression of all the baits was confirmed by immunoblot (Box1B), TRPV1 N-terminal bait expression was not detected under confocal fluorescence microscopy (Box1C). Baits tagged in the N-terminus in general seem to be less eficient in the case of TRPV1 and TRPV2, with lower expression levels under confocal fluorescence microscopy.
After the transformation of yeast reporter strain with a 10^7 potential preys human brain cDNA library, N-terminus TRPV1 bait showed no positive transformants, in line with the lack of expression of this construct observed by confocal fluorescence microscopy. TRPV1 C-terminal bait (TRPV1-VP16-LexA) had two positive interactors that were identified by sequencing as CNTN2 and ABCA2 (Fig. 2a). Attending to the properties of the MYTH assay, CNTN2 showed the highest growing over selective media and strongest blue colour staining in the presence of X-Gal from TRPV1 hits (Fig. 2a), indicating a more constitutive nature of the interaction (22).
Human brain cDNA library screen gave a total of 20 positive transformants for TRPV2 (Fig. 2a). N-terminal TRPV2 bait showed positive interaction with NTM and FGF1, being NTM interaction the strongest among them (Fig. 2a). C-terminal TRPV2 bait showed 18 positive transformants (Fig. 2a), being the most efficient bait among the baits used in this study.
The positive interactors for TRPV2 tagged at the C-terminus that had highest growth over selective media and strongest blue colour intensity in the presence of Xgal were: ABR, ARL15, Opalin, ST18 and SACM1L (Fig. 2a). These properties in MYTH assay performance point to a more tight potential interaction between TRPV2 and these proteins. The transformants that showed the lowest blue colour intensity from TRPV2 bait taged on the C-terminus were identified as: PIP4K2B, INPP5F, SDC3 or ALDH1A3 (Fig. 2a). These interactors are able to grow under selective conditions, although they do not turn intensively blue in presence of Xgal (Fig. 2a); pointing to a more transient nature of the interaction.

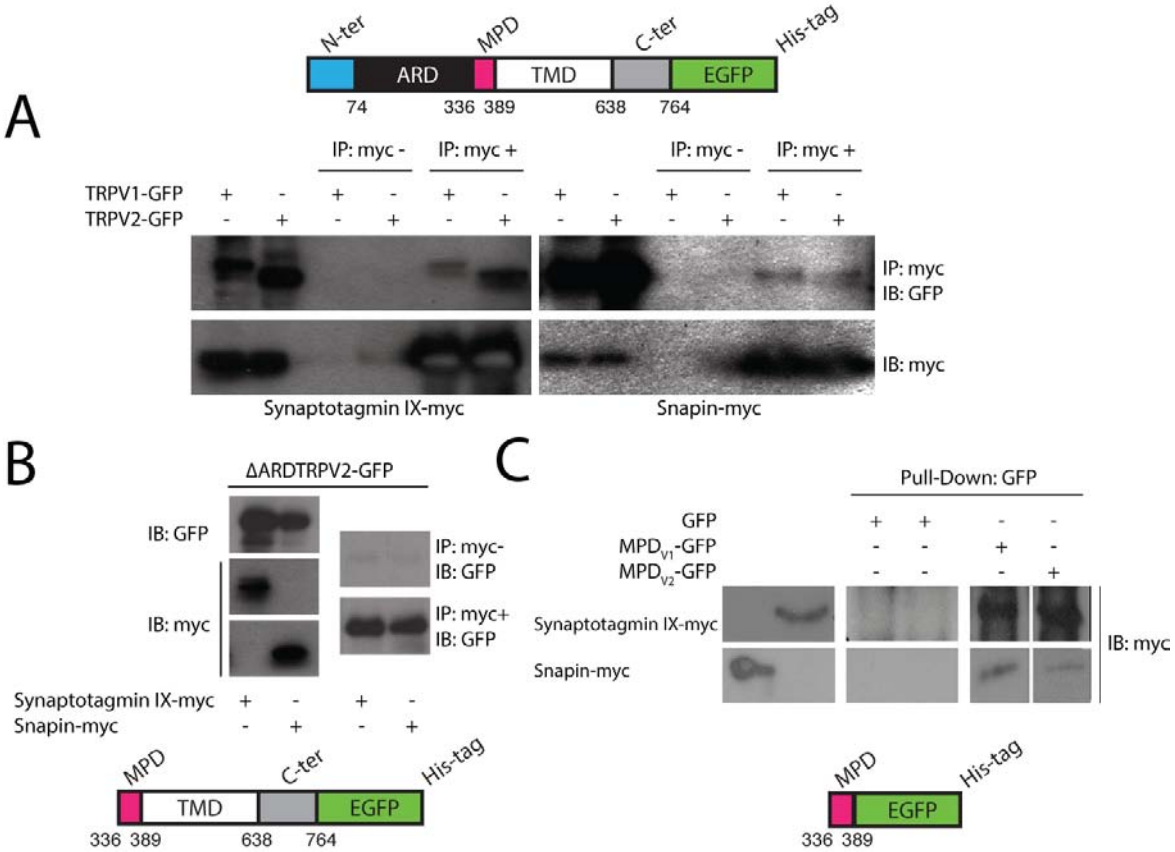

Figure 1. Mapping TRPV2 interaction with SNARE proteins, Snapin25 and Synaptotagmin IX by Co-IP. A) Full length TRPV1 and TRPV2 are able to co-precipitate with Snapin25 and Synaptotagmin IX. B) TRPV2 lacking N-terminal ARD domain, ΔARD-TRPV2, is still able to co-precipitate with Snapin25 and Synaptotagmin IX. C) The MPD region of TRPV1 and TRPV2 is still able to precipitate both proteins of the SNARE complex.

All identified interaction partners were listed with their UNIPROT codes, cell location and annotated function in order to have a broad vision of TRPV1-2 interactome (Fig. 2b).

TRPV2 interactome associates with nervous system development and lipid metabolism

To gain a global insight of TRPV2 interaction-based physiological role, we performed a molecular systems biology approach. TRPV2 partners determined by MYTH assay and Co-IPs were used to construct a putative protein-protein interaction network using closest related genes (Fig. 3a and supplementary information). Gene enrichment based on protein co-localization, gene co-expression, genetic interactions and domain conservation was used to construct the network. TRPV2 interactors were easily connected within the network (Fig. 3a and supplementary information). Structural features of the network were evaluated: the number of neighbours (nodes) and the number of connections (edges) were counted. Edges:nodes ratio was used as estimation of network interconnectivity. To determine whether TRPV2 interaction network is more interconnected than randomly generated networks, edges:nodes ratios were compared by means of a T-test (Fig. 3b). TRPV2 network had a edges:nodes ratio of 12.52 whereas randomly generated networks have a mean edges:nodes ratio of 4.4 and a standard deviation of 1.46 (Fig. 2b). Thus, TRPV2 gene enriched network is statitstically more interconnected than mean random networks over the whole human interactome, with a p-value lower than 10^{-4} (Fig.3b and supplementary information).

Enriched network was used to determine gene ontology (GO)-Terms associated with TRPV2. Statistically significant GO-terms (Benjamini and Hochberg corrected p-value lower than 0.05) were functionally associated manually and clustered as cellular processes. The main cellular processes represented by the proteins within the network are related to lipid metabolism, cell development and nervous system development, neurotransmitter and synaptic regulation, cell signaling, ion transport and vesicle transport (Fig. 3b, Fig. 3c and supplementary information).

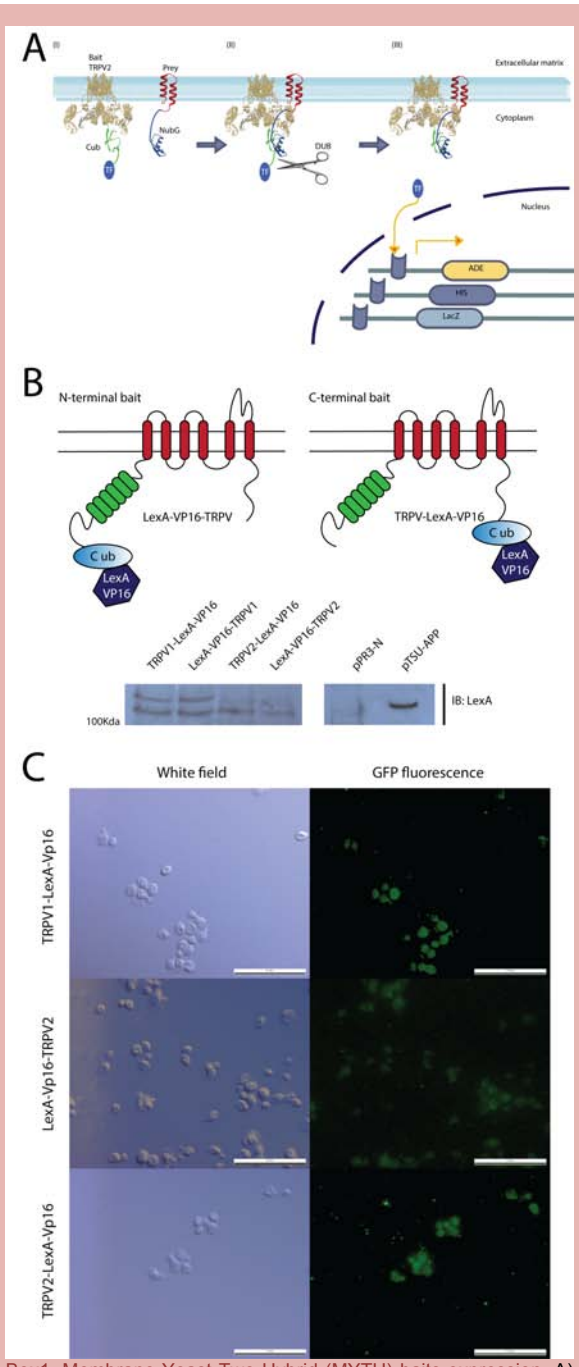

Box1. Membrane Yeast Two Hybrid (MYTH) baits expression. A) MYTH workflow showing that only when bait and prey interact Transcription Factor (TF, LexA-VP16) is released and go to the nucleus to start reporter gene expression. B) Representation of N- and C-terminal TRPV baits (LexA-VP16-TRPV and TRPV-LexA-Vp16 respectively). Western blot against LexA tag showing the expression levels of TRPV1 and TRPV2 fused to MYTH cassette on the N- anc C-terminus. pTSU-APP was used as positive control for WB and pPR3-N as negative C) Fluorescence microscopy images of NMY51 yeast cells expressing TRPV1 and TRPV2 baits fused to GFP.

The MYTH system is Split-ubiquitin based, and it allows the location of the TRPV2 bait in its natural environment, with the channel embeded in the membrane (Box1A). Furthermore, the N-terminus of ubiquitin is mutated in order to hinder spontaneous refolding of ubiquitin, that only will be possible if bait and prey proteins interact (Box 1A). Once the interaction occurs and ubiquitin is refolded, the degradation ubiquitin complex (DUB) will cleave bait constructs and release the Transcription Factor LexA-VP16 (TF)(Box 1A). TF will traffic to the nucleus and start the expression of reporter genes that will allow cells to grow in selective media lacking Histidine (His) or Adenine (Ade) (Box 1A). Furthermore, LacZ reporter gene will be activated upon interaction, so the colonies carrying a putative interactor will become blue stained in the presence of X-Gal (Box 1A). The blue colour intensity could be used to determine whether interactions are stronger or constitutive (intense blue colour staining) or more transient (low blue colour intensity)(22). Therefore, the system used is more accurate for detection of occurring interactions than regular two hybrid assays, as it allows the location of full sequence proteins in a similar environment than the native protein, and the ubiquitin spontaneous refolding is prevented.

Using MYTH system, full length TRPV1 and TRPV2 baits carrying the MYTH C-ubiquitin (Cub), and transcription factor LexA-VP16 (TF) fusion cassette at N- or C-terminus of both channels, were transformed into NMY51 strain. To confirm the correct expression of the tagged TRPV1 and TRPV2, a western blot against LexA tag was used. Two bands corresponding to the tagged TRPV1 and TRPV2 baits molecular weights are observed (Box 1B), pointing to a proper expression of TRPV1-2 baits fused to the LexA tag. The presence of 2 bands is characteristic of the TRPV channels. It has been reported that the upper band corresponds to the glycosylated form of the channels (43). APP tagged with the MYTH fusion cassette was used as positive control for the western blot, and pPR3-N was used as negative control (Box 1B). The expression of the baits was further checked by fluorescence microscopy. TRPV1 and TRPV2 baits tagged with GFP were visualized under the microscope (Box 1C). TRPV1 N-terminal bait was not visible under the microscope (data not shown). Baits generated with the MYTH cassette on the C-terminus seem to have a higher intensity when observed under the microscope (Box 1C).

The functionality and self-activation of the generated MYTH baits was tested. To this end, we transformed two different prey constructs into NMY51 strain expressing our baits. First prey is composed of an unrelated protein fused to N-ubiquitin tag not mutated (Nub), so self-activation of bait is allowed. All baits showed potential functionality for MYTH assay. Second, self-activation with a prey carrying the N-ubiquitin tag mutated (NubG) was tested as previously described (P01401-P01429)(22). The prey carrying mutated NubG is supposed to do not interact with the bait, so as a result the background signal for each bait was assessed and the selectivity media for each bait was established. From this moment N and C terminal baits of TRPV1 were plated in SD-His containing 7,5mM 3AT, N terminal TRPV2 bait in SD-His 10mM 3AT and C terminal TRPV2 bait in SD-His 5mM 3AT.

A

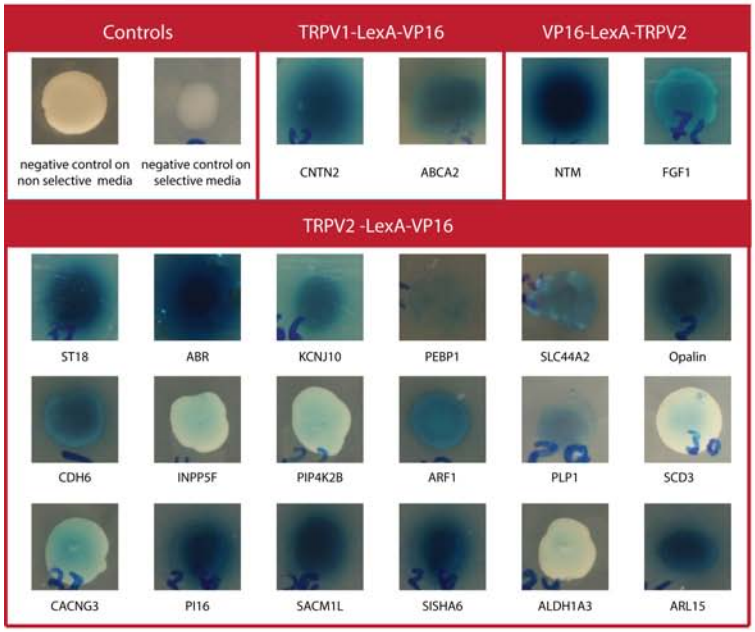

Figure 2. MYTH TRPV1 and TRPV2 interaction partners. A) Potential interactors isolated from the MYTH screen growing under selective conditions and in the presence of Xgal. NMY51 strain without transformation was used as negative control. Those colonies showing strongest blue colour represent the strongest and more constitutive potential interactors. Those with lighter blue colour represent potential interactions of a more transient nature. B) List of isolated interactors. Once identified by sequencing the interactors determined by MYTH were annotated for whole name, Uniprot code, cellular location and protein function.

B

Interactor	Bait	Full name	Uniprot code	Location	Function
CNTN2	TRPV1-LexA-VP16	Contactin 2	Q02246	plasma membrane	maintain voltage-gated K channels in ranvier nodes. Cell adhesion
ABCA2	TRPV1-LexA-VP16	ATP-binding cassette A member 2	Q9BZC7	Endosome and lysosome membrane	potential transporter, may have a role in lipid metabolism and neural development
NTM	VP16-LexA-TRPV2	neurotrimin	Q9P121	plasma membrane	neural cell adhesion
FGF1	VP16-LexA-TRPV2	fibroblast growth factor 1	P05230	cytoplasm and secreted	regulates cell survival, cell division, angiogenesis, cell differenciation and migration
ST18	TRPV2-LexA-VP16	suppression of tumorigenicity 18 protein	O60284	nucleus	represses basal transcription activity from target promoters
ABR	TRPV2-LexA-VP16	Active breakpoint cluster region-related protein	Q12979	cytoplasm	GTPase-activating protein for RAC and CDC42.
KCNJ10 (KIR4.1)	TRPV2-LexA-VP16	ATP-sensitive inward rectifier K Channel	P78508	plasma membrane	voltage-gated K buffering action of glial cells in the brain
PEBP1	TRPV2-LexA-VP16	phosphatidylethanolamine binding protein 1	P30086	cytoplasm	Binds ATP, opioids and phosphatidylethanolamine. Inhibits the kinase activity of RAF/MEK complex
SLC44A2	TRPV2-LexA-VP16	Choline transporter-like protein 2	Q8IWA5	plasma membrane	Transports choline
Opalin	TRPV2-LexA-VP16	opalin	Q96PE5	plasma membrane of CNS	Involved in temporal lobe epilepsy and spastic paraplegia
CDH6	TRPV2-LexA-VP16	cadherin 6	P55285	plasma membrane	Calcium dependent cell adhesion proteins
INPP5F	TRPV2-LexA-VP16	phosphatidylinositide phosphatase SAC2	Q9Y2H2	cytoplasm	Hydrolyzes phosphatidylinositol 4,5-bisphosphate
PIP4K2B	TRPV2-LexA-VP16	phosphatidylinositol 5 phosphate 4 kinase type 2 beta	P78356	plasma membrane	Participates in the biosynthesis of phosphatidylinositol 4,5-bisphosphate
ARF1	TRPV2-LexA-VP16	ADP ribosylation factor 1	P84077	cytoplasm	GTP-binding protein, an ADP-ribosyltransferase. Involved in protein trafficking among different compartments
PLP1	TRPV2-LexA-VP16	myelin proteolipid protein	P60201	plasma membrane	Cause of leukodystrophy hypomyelinating type 1 and spastic paraplegia X-linked type 2
SDC3	TRPV2-LexA-VP16	syndecan 3	O75056	plasma membrane	Cell surface proteoglycan that may bear heparan sulfate
CACNG3	TRPV2-LexA-VP16	voltage dependent calcium channel gamma 3 subunit	O60359	plasma membrane	Voltage gated channel, Calcium channel
PI16	TRPV2-LexA-VP16	peptidase inhibitor 16	Q6UXB8	plasma membrane	Putative serine protease inhibitor. Highly expressed in cardiac hypertrophy
SACM1L	TRPV2-LexA-VP16	phsphatidylinositide phosphatase SAC1	Q9NTJ5	plasma membrane/RE	Phosphoinositide phosphatase that hydrolyzes $PtdIns_3P$ and $PtdIns_4P$
SHISA6	TRPV2-LexA-VP16	protein shisa6 homolog	Q6ZSJ9	plasma membrane	Antagonistic to Wnt and Fgf signalings. Regulates short term membrane plasticity
ARL15	TRPV2-LexA-VP16	ADP ribosylation factor like protein 15	Q9NXU5	cytoplasm	GTP-binding protein, an ADP-ribosyltransferase. Involved in protein trafficking among different compartments
ALDH1A3	TRPV2-LexA-VP16	aldehyde dehydrogenase family 1 member A3	P47895	cytoplasm	Recognizes as substrates free retinal and cellular retinol-binding protein-bound retinal

Lipid metabolic processes related to the network involve proteins such as SACM1L INPP5F, PIP4K2B or ALDH1A3 (Fig. 2b and Fig. 3c), enzymes related to metabolism of phosphoinositides. Main TRPV2 partners related to cell development and nervous system development were: SNAP25, NTM, PEBP1, PLP1, FGF1, ALDH1A3 (Fig. 2b and Fig. 3c). This group includes proteins related to cell metabolism like ALDH1A3, other proteins related to vesicle trafficking, such as SNAP25, and proteins that form part of nervous system structures. This is the case of PLP1, a protein marker of myelin sheath; or NTM, mediator in neuronal adhesion and neurite outgrowth. Neurotransmitter and synaptic regulation group is formed by: SYT9, SNAP25, PEBP1, PLP1, ABR, ARL15 and INPP5F (Fig. 2b and Fig. 3c). The proteins within this group are mostly related to vesicle transport such as SYT9, SNAP25, ABR or ARL15. Proteins representing ion transport processes were mainly the ion channels and transporters determined by the MYTH assay: TRPV2, CACNG3, KCNJ10 and SLC44A2 (Fig. 2b and Fig. 3c). Signaling processes were mainly related to PEBP1, SYT9, SNAP25, INPP5F, PIP4K2B, PLP1, ARF1. This is a heterogeneous group that contains genes related to neuronal development as PLP1, lipid metabolism as PIP4K2B or INPP5F, SNARE complex proteins such as SYT9 and SNAP25 or GTP binding proteins such as ARF1, that mediate vesicle trafficking (Fig. 2b and Fig. 3c).

TRPV2 interaction validation and mapping

Interactors showing highest intensity in the X-gal assay and related to enriched pathways of the interactome, mainly cell development, nervous system development, vesicle trafficking, ion channels and lipid metabolism were chosen for further validation. Utrophin (an spectrin domain molecule) was used as brain protein external control. Purified rat TRPV2 and rat ARD domain were inmobilized on nitrocellulose membranes and rat brain protein extracts were then incubated with the membranes. Immunoblotting against the selected interactors was carried out (Fig. 4). Among the interactors tested 6 of them, PLP1, NTM, CACNG3, ABR, Opalin and ARL15 were able to bind to TRPV2, whereas Utrophin and KCNJ10 did not show any binding (Fig. 4). In the case of NTM, CACNG3, ABR and Opalin we could determine that the binding happens in the ARD domain of TRPV2, as they are also able to bind to this domain when expressed isolatedly (Fig. 4).

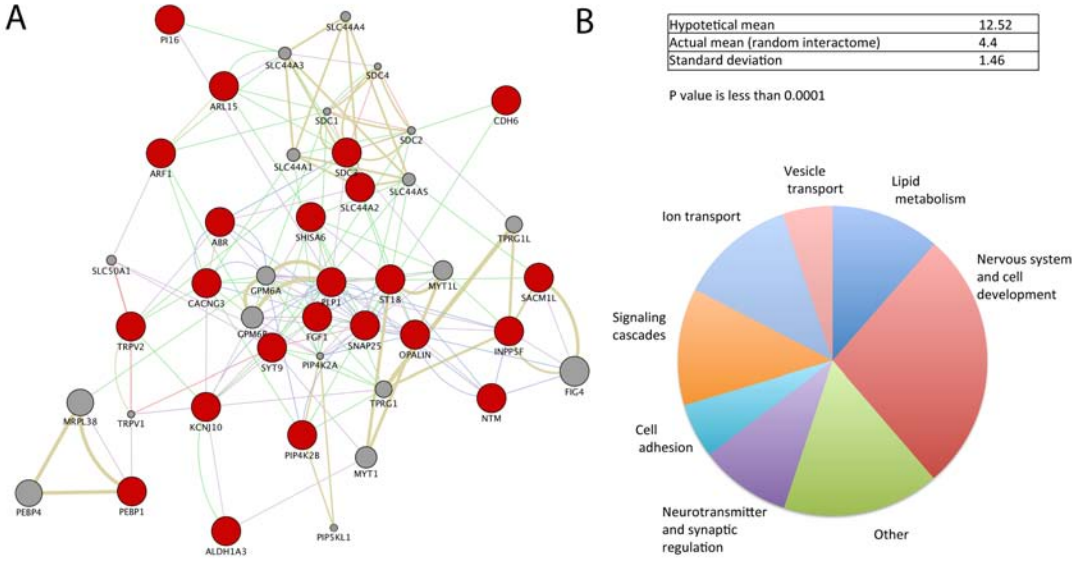

C

Process	Genes	pValue (highest association)
Lipid metabolism	SACM1L, PLP1, PIP4K2B, INPP5F, ALDH1A3	5.83 10E-11
Nervous system and cell development	SNAP25, NTM, PEBP1, PLP1, FGF1, ALDH1A3	1.19 10E-8
Neurotransmitter and synaptic regulation	SYT9, SNAP25, PEBP1, PLP1, ABR, ARL15, INPP5F	2.68 10E-5
Cell adhesion	CDH6, NTM, SCD3	2.01 10E-4
Signaling cascades	PEBP1, SYT9, SNAP25, INPP5F, PIP4K2B, PLP1, ARF1	2.56 10E-4
Ion transport	TRPV2, CACNG3, KCNJ10, SLC44A2	8.37 10E-4
Vesicle tansport	SYT9, SNAP25, ARF1	3.36 10E-3

Figure 3. TRPV2 interactome gene enrichment analysis. A) TRPV2 interactome gene enrichment of 100 closest related genes. Simplification scheme showing the main 20 closest related proteins to TRPV2 partners (red dots). B) TRPV2 interactome is statistically more interconected than random interactomes. Main cellular processes related to TRPV2 using a gene enrichment of 100 closest related genes. Representation of the number of genes within the TRPV2 interactome that are related to each cellular process. C) Main Cellular processes related to TRPV2 interactome and genes from TRPV2 MYTH assay that are associated with each process. p-values represent the highest association of Go-terms included in each process.

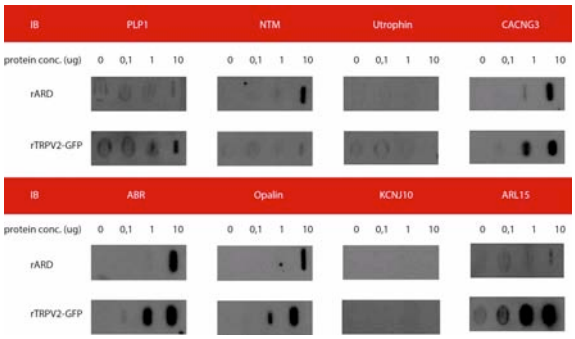

Figure 4. Validation of TRPV2 MYTH interactors. Rat TRPV2 full length protein and the rat ARD domain of TRPV2 were inmobilized on membranes and tested against interactor partners present in rat brain extracts.

MPD of TRPV1 and TRPV2 is a lipid binding domain in vitro.

TRPV2 interactome shows a potential relationship of TRPV2 with lipid metabolism, agreeing with bioinformatics predictions based on TRPVs primary sequence (23). To check the protein-lipid interaction capability, lipids were immobilized in nitrocellulose membranes at increasing concentrations and full length TRPV1, TRPV2 and MPD domain of TRPV1 and TRPV2, all tagged with GFP, were incubated and monitored for lipid binding (Fig. 5a). MPD domains were tested due to its proximity to the membrane bilayer surface and high conservation among TRPV1-4 subfamily (23), that argues for a potential importance of this domain in protein function or assembly. Indeed MPD interaction with the C-terminus is esential for proper channel folding and trafficking of TRPV4 (26). GFP was used as negative protein control.

The proteins were tested against phosphoinositol (PI), phosphatidic acid (PA), phophoinositol-4-phosphate (PI4P), phosphatidylserine (PS), 1-palmitoyl-2-oleoyl-sn-glycero-3-phosphocholine (POPC) and 1-palmitoyl-2-oleoyl-sn-glycero-3-phosphoglycerol (POPG)(Fig. 5a). The screen showed a binding of PA to the MPD region of TRPV1 and TRPV2. Despite the use of the full length TRPV1 or TRPV2, these channels did not show binding to any of the lipids tested (Fig. 5a). MPD domain of TRPV1 and TRPV2 do not bind to any other lipids or the negative control, containing only buffer (Fig. 5a). MPD domains bind to PA in a concentration dependent manner (Fig. 5a). In our experiment, GFP alone, used as protein negative control, is not able to bind to any of the lipids tested (Fig. 5a).

To confirm the observed binding to PA of the heterologously expressed MPD, Tryptophan (Trp) fluorescence quenching experiments were carried out. The binding of molecules to a protein masks the tryptophan endogenous fluorescence of the protein and this reduction on the fluorescent signal can be quantified. The MPD domains of TRPV1 and TRPV2, together with GFP as protein negative control, were incubated with increasing concentrations of several lipids (Fig. 5b). The lipids tested were: DPPA, DPPC, POPG and POPS. First, emision spectrum at 495nM excitation wavelength was acquired for each of the 3 proteins (Fig. 5b top left). GFP alone showed no significant decrease of trp fluorescence signal upon adition of any of the tested lipids (Fig. 5b top right). Lipid addition produced an increase in the Trp fluorescence, especially DPPC (Fig. 5b top right). MPD domains of TRPV1 and TRPV2 show a significant decrease in Trp fluorescence upon adition of PA, while no decrease was observed upon adition of DPPC, POPG or POPC. Trp quenching showed a PA concentration dependent effect (Fig. 5b bottom left and right). The study of Trp fluorescence confirmed that the isolated MPDs of TRPV1 and TRPV2 expressed heterologously are able to interact with PA. As PA binding to full length TRPV1 or TRPV2 was not observed (Fig. 5a), we used a genetically encoded PA reporter (Raf-mCherry) to study whether full length TRPV1 and TRPV2 share the same subcellular distribution or not. Raf-mCherry is a protein capable to bind to PA-rich domains (27). HEK293 transiently transfected with TRPV1 or TRPV2 and Raf-PA-mCherry were visualized by epifluorescence imaging. Either TRPV1 or TRPV2 full length proteins tagged with GFP (green channel) showed strong colocalization with raf-PA-mCherry (red channel) (Fig. 5c).

Phosphatidic acid is able to modulate TRPV2 channel activity

TRPV2 activity can be modulated by several lipidic compounds. LPC and LPI can activate TRPV2 (21). We wonder whether PA binding to TRPV2 might affect TRPV2 activity or not. To address this issue, we carried out a yeast membrane-based calcium influx assay (To be published). Briefly, TRPV2 was expressed in yeast, cells were disrupted and membranes collected, and extruded through a 100 nm pore size filter in the presence of Fura8 to obtain TRPV2 containing vesicles, loaded with Fura8. Increasing concentrations of lipid were added and the Fura fluorescence recorded. An increase in Fura8 excitation ratio correlates with a calcium entry in the liposomes. Using this technique we were able to see an increase in Fura8 ratio upon adition of LPC, an already known activator of TRPV2 (Fig. 6). A similar increase was observed when DPPA was added, indicating that DPPA mediates calcium entry to the TRPV2 containing liposomes (Fig. 6). Vesicles without TRPV2 protein showed no significant changes in Fura8 ratio upon addition of LPC or DPPA, indicating that the changes observed in calcium levels inside the liposomes were TRPV2 channel mediated (Fig. 6).

DISCUSSION

The identification of TRPV2's interactome should open new research perspectives to understand this channel and its pathophysiological processes.

First, we studied known interactions for TRPV1 and validated them experimentally for TRPV2. Snapin25 and Synaptotagmin IX are proteins of the SNARE

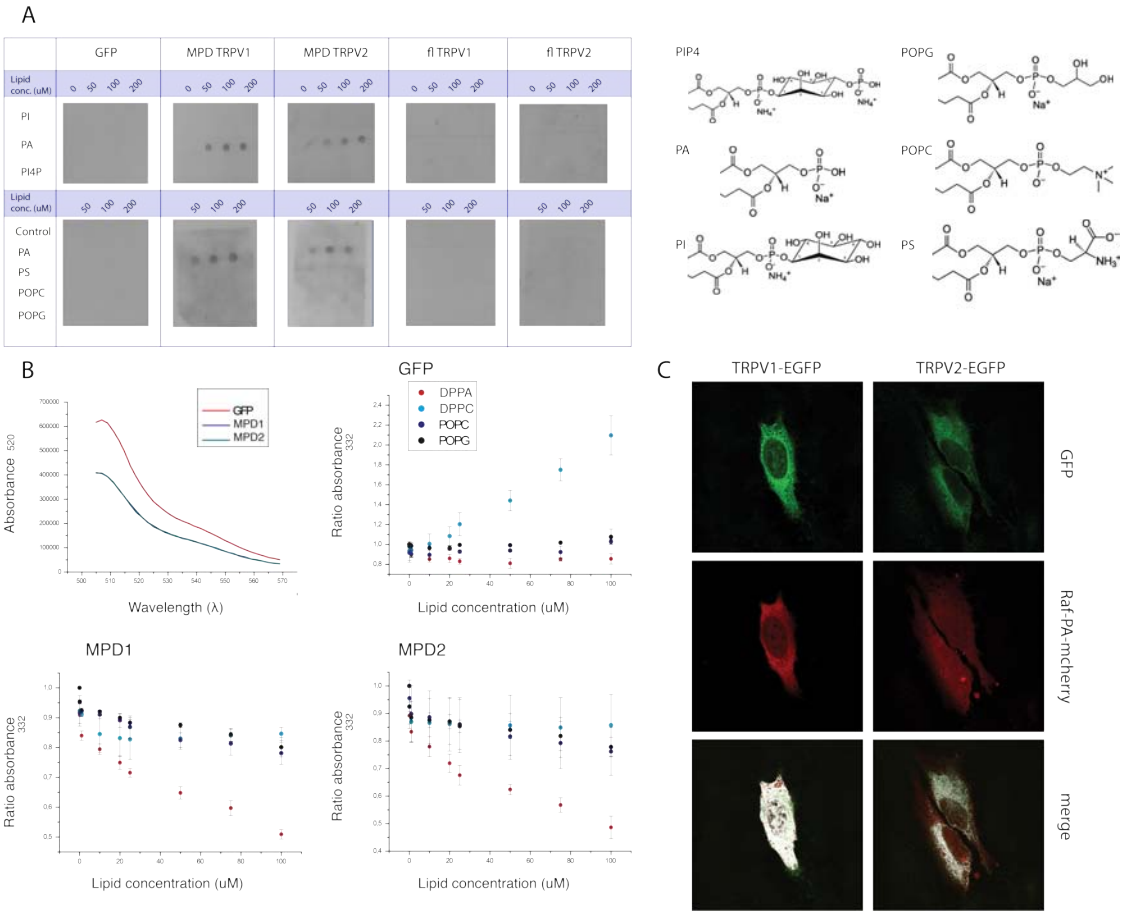

Figure 5. Lipid binding screen for TRPV1 and TRPV2. A) Lipid strips screening the binding of TRPV1, TRPV2 and MPD domain from TRPV1 and TRPV2 (MPD1 and MPD2 respectively) to the lipids inmobilized in the membranes. Structures of lipids used during this assay. B) Tryptophan fluorescence quenching experiments. Fluorescence spectrum of the proteins used is shown on the top left panel. GFP tryptophan fluorescence in the presence of increasing concentration of lipids is shown on the top right panel. MPD1 and MPD2 tryptophan fluorescence in the presence of increasing concentration of lipids is shown in the bottom panels. C) Fluorescent confocal imaging of HEK293 cells showing TRPV1 and TRPV2 location within the cell (Green) and raf-PA location (Red). Merge channel shows colocalization of green and red channels highlighted in white.

complex that mediate TRPV1 trafficking (24). TRPV2 also interacts with Snapin25 and Synaptotagmin IX, and we have further mapped the interaction to the MPD of TRPV1 and TRPV2 (Fig. 1). The interactions with SNARE complex proteins such as Snapin25 and Synaptotagmin IX relates TRPV channels to processes where exocytosis is key. The MPD is a highly conserved motif in TRPVs (23) which may indicate that SNARE-mediated exocytosis is a conserved mechanism. In fact, this domain has been related to thermosensation (28) and it is essential for folding, assembly and trafficking in the case of TRPV4 (26).

To deepen into the neural physiology of TRPV2, a MYTH assay using a brain cDNA library was performed in order to screen TRPV2 potential partners. Although there have been previous studies using the yeast two hybrid technique to analyze TRP channels regulation (24, 19), our study is the first yeast two hybrid assay performed with a full length TRPV channel as bait and the second one with a TRP (29). The screening for TRPV1 and TRPV2 yielded a list of 2 positive interactors and 20 positive interactors, respectively.

Protein-protein interactions can be classified into stable and transient, i.e. strong and weak. The MYTH screening provides a colorimetric indication on the nature of the interaction, however one always must assume that the detected interaction is a false positive. The biochemical validation step is necessary to validate the interaction, but it can also be possible that the interaction can not be detected/validated either *in vitro* or *in vivo*.

To understand the physiological processes where TRPV2 is related we took a bioinformatics approach, rather than a classical biochemical validation approach. The potential interactions detected by MYTH are related to specific biological processes and regardless of the nature of the interaction they will point towards relevant biological processes, which should be validated by themselves through statistical enrichment.

One of the enriched biological processes is transport across membranes, represented by the interaction of

TRPV2 with SLC44A2, KCNJ10 and CACNG3, a choline transporter, a potassium channel and the regulatory subunit of a calcium channel, respectively (Fig. 2b and Fig. 3). It has been previously shown that ion channels act coordinately because of their co-existence in specific membrane domains (30).
Another biological process that has been enriched by using the MYTH interactome is phospholipid metabolism, mainly represented by the INPP5F and PIP4K2B genes (Fig. 2b and Fig. 3). These two proteins are enzymes involved in PIP2 phosphorylation processes. It has been described that TRPV2 colocalizes with PIP2 in the same plasma membrane microdomains (9). Furthermore, other TRP channels such as TRPV1 and TRPV4 do also bind PIP2 (31, 32). PIP2 enzymes interacting with TRPV2 indicate that PIP2 is metabolized in close proximity to the channel or even docked in the channel, what has been already proposed (9). Interactions between TRPV2 and lipid metabolism proteins might also imply a crosstalk between channel functioning and regulation of phosphoinositide synthesis.
The other main set of interactors is related to cell developmental processes, comprising proteins such as Opalin, PLP1, NTM or ABR (Fig. 2b and Fig. 3). Two components of myelin sheaths, a GPI-adhesion molecule and a GTP-ase activating protein from Rho family, respectively. These genes are mostly expressed and related to the formation of myelin sheaths around the neuron axons or in the ranvier nodes structural arrangement (33). Furthermore, NTM, a protein anchored to the membrane by a lipid binding anchor, controls neurite outgrowth, promoting the outgrowth of DRG neurons (34). Interestingly, TRPV2 is expressed in this same type of neurons and the channel expression and activity are crucial for axon and neurite outgrowth (15, 35). TRPV2 might interact directly with proteins present in the myelin sheath and the regulation of the channel may promote cation-dependent processes in CNS development.

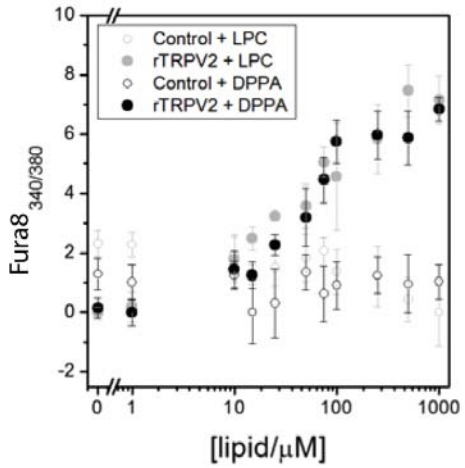

Figure 6. TRPV2 activation by phosphatidic acid (PA). Fluorescence ratio at 340 and 380, measuring Fura8. Lipids LPC and DPPA were added at increasing concentrations to liposomes containing TRPV2 (grey and black dots respectively) and to empty liposomes (grey and black circles respectively).

Gene enrichment analysis of the network generated by TRPV2 MYTH assay and Co-IPs was conducted to assess potential interatomics based functional roles for TRPV2 (Fig. 3a and supplementary). The network generated is statistically more interconnected than randomly generated networks (p-value less than 0.0001), arguing for a good accuracy of our study, as it determined proteins that are significantly related with each other, and not randomly interconnected. Furthermore, the network shows a statistically significant association with cell processes such as cell development, lipid metabolism or ion transport (Fig. 3b and c). These assocaitions are coherent for TRPV2, that has already been described to play these potential roles as already discussed.
Among the interactors discovered by the MYTH assay, 8 were chosen for further validation (Fig. 4). Using biochemical methods we could confirm the physical interaction potential of ARB, ARL15, CACNG3, Opalin, NTM and PLP1. These 6 proteins were able to interact with TRPV2 full length (Fig. 4). ABR, CACNG3, Opalin and NTM were even able to bind to the N-terminal ARD domain of TRPV2 (Fig. 4), indicating that the interaction of these proteins with TRPV2 needs the ARD domain. Although promising, experimental validation is required to undercover if the hability of TRPV2 to bind ABR, ARL15, CACNG3, Opalin, NTM and PLP1 is conserved under physiological conditions. Accordingly, KCNJ10 interactor, which has not been detected by immunoblotting, cannot be ruled out.
TRPV2 partners network analysis showed a strong correlation with lipid metabolism (Fig. 3). TRPV channels are known to interact with different phosphoinositides, such as LPA or PIP2, and the binding of lipids regulates channel activity (9, 36, 32). We tested lipid binding for TRPV2 and TRPV1 and we show that the MPD domain of both channels bind to DPPA *in vitro* (Fig. 5). The lipid screening showed that the MPD binding to PA is determined by the nature of the polar head of the lipid, as PC, POPG or POPC, that have the same hydrophobic tail, were not bound. Binding is not due to an electrostatic effect, since PG and PA are both negatively charged. Generation of point mutants of the MPD domain positively charged residues would further determine the specific residues for PA, however it has been shown that mutagenesis in the MPD can lead to deleterious effects on protein expression, oligomerization and/or trafficking (26). The binding of PA to the full length TRPV1 or TRPV2 channels was not detected, maybe because the binding region is not exposed by the detergents used to solubilize TRPVs during purification, or because lipids are tightly bound to specific sites through the purification process. Although PA binding was not observed, TRPV1 and TRPV2 overexpressed in a mammalian cell system showed strong colocalization with PA. This fact points to a shared membrane micro-domain of both, TRPVs and PA. Nevertheless, TRPV2 contained in vesicles is activated upon PA adition (Fig. 6). This fact points to a direct binding of PA on TRPV2 that triggers channel opening. The interaction with PA might be interesting also to understand TRPV2 potential association with neuronal development, as PA is one of the most abundant

lipids in myelin sheaths (37) and PA accumulation has been asociated with processes related to demyelination (38, 39).

EXPERIMENTAL PROCEDURES

DNA plasmids and clonings

TRPV1 and TRPV2 cDNA were cloned into a pcDNA3 vector containing an eGFP tag and a 8XHis-tag at the C-terminus. The N-terminus truncation for TRPV2, ΔARD-TRPV2 (Δ1-336 rat TRPV2) was obtained by classical PCR and ligated into the same pcDNA3 vector within NdeI and NotI sites.
Full length rat TRPV2 GFP tagged was cloned into pPICz vector for expression in *P.pastoris*. The rat TRPV2 Ankyrin repeat domain ARD GFP tagged was cloned into a PET21 vector for expression in *E. coli*. Membrane Proximal Domain of TRPV1 and TRPV2 (MPD) sequences were purchased from GenScript and cloned into pTTQ18-GFP plasmid within EcoRI-PstI sites.
pBT3-STE vector (P03233), control bait protein pTSU-APP, control prey pPR3-N (P01401-P01429) and cDNA library from human brain (P12227,) were purchased from Dualsystems. Human TRPV1 and TRPV2 full length, with or without GFP C-terminus tag, were cloned into pPR3-N and pBT3-STE within SfiI sites.

Cell cultures and transfection

HEK293 cells were cultured in Dulbecco's modified Eagle's medium (DMEM) supplemented with 10% FBS, 100 units/mL penicillin and 100 µg/mL streptomycin. Transfection was performed using polyethyleneimine (PEI, Polysciences, 23966). HEK293 cells overexpressing the transfected constructs were lysed 48 hours after transfection and membrane proteins solubilized for 30 min at 4°C in lysis buffer (50mM Tris-HCL pH 7.4, 150mM NaCl, 2mM EDTA, 1% Triton, 5% glycerol, 1mM benzamidine and EDTA-free protease inhibition cocktail, ROCHE 11873580001). Cell extracts were centrifuged at 14000g at 4ºC for 10 min to remove agregates.

Western blot

Lysates and immunoprecipitates were loaded into SDS-page gels and run at 100mV for 90 min. Gels were transfered to nitrocellulose membranes into a semi-dry cast at 100mA for 1hour. Membranes were blocked in blocking buffer (5% non-fat-dry milk TTBS 1x) ON at 4ºC. Primary antibodies were incubated in blocking buffer for 1 hour RT. Primary antibodies were diluted as follows: anti Lex A tag (sc-107150, SantaCruz) 1:1000, anti His tag (P5A11, DSHB) 1:1000, anti myc tag (551101, Pharmigen) 1:1000, anti GFP tag (GFP-G1, DSHB) 1:1000, anti NTM (sc-98979, SantaCruz), anti PLP1 (sc-98781, SantaCruz), anti CACNG3 (c-164818, SantaCruz), anti ABR (sc-54558, SantaCruz), anti ARL15 (sc107150, SantaCruz), anti Opalin (sc-163187, SantaCruz), anti Utrophin (Mancho3, DSHB) and anti KCNJ10 (sc23637, SantaCruz) 1:200. Secondary antibodies were incubated for 1 hour at RT. Anti mouse (sc-2031, SantaCruz) and anti rabbit (sc-2030, SantaCruz) were used at 1:2000 diluition in blocking buffer. Membranes were developed with Luminata crescendo reagent (WBLUR0100, Millipore).

Co-Immunoprecipitations

Soluble fractions from cell lysis were used as input for co-immunoprecipitations. Cell extracts at 1ug/ul (500ug total protein) were incubated ON at 4ºC with anti myc antibody (551101, Pharmigen). Immuno-complexes were then incubated with 50uL of sepharose beads (17-0618-01, GE) for 2 hours at 4ºC. After incubation complexes were washed with lysis buffer 3 times. Immunoprecipitated complexes were denatured with SDS-PAGE sample buffer (90ºC for 5 min), separated by SDS-PAGE and analyzed by western blotting.

Membrane Yeast Two Hybrid Assay (MYTH)

MYTH assay was previously described by Snider and coleagues (22). MYTH reporter strain NMY51, containing reporter genes HIS3, ADE2, and lacZ downstream of lexA operators, was purchased from Dualsystems Biotech (P01401-P01429). Western blot against LexA tag was used to confirm the correct expression of the generated baits. NMY51 yeast cells expressing GFP tagged baits were fixed and visualized using a Leica TCS SP5 confocal microscope. The MYTH assay was performed essentially following the provider instructions (P01401-P01429). Transformation eficiency of the human brain cDNA library into NMY51 carrying the bait constructs was higher than $2x10^6$. Transformants were plated into SD selective agar plates. pBT3-N TRPV1 and pBT3-STE TRPV1 were plated in 7,5mM 3-aminotriazole (3AT) SD-His, pBT3-N TRPV2 was plated in 10mM 3AT SD-His and pBT3-STE in 5mM 3AT SD-His. After incubation at 30 °C for 3–5 days, transformants were transfered into selective plates whit same stringency but containing 5-bromo-4-chloro-3-indolyl-β,d-galactopyranoside (X-Gal). Prey plasmids were then recovered by miniprep kit, transformed into Dh5a *E. coli* competent cells, purified from *E. coli*, and sequenced. Isolated prey plasmids carrying a putative interaction partner were then re-transformed into NMY51 strain containing the original bait to confirm the interaction.

Gene enrichment and network analysis

Genes determined by the MYTH assay for TRPV2 (21 hits) and validated Co-IP hits were used to construct a network in Cytoscape (40) with Genemania algorithm (41). The network was constructed using as template the Genemania Human genome and adding the 100 closest related genes based on colocalization, co-expression, physical interactions and domain conservation. Randomized genes from human genome were used to construct networks using the same Genemania parameters. Nodes and edges within each network were quantified and the ratio Edges/nodes was used as a measure of network connectivity. Mean human network connectivity was estimated by randomly obtained networks and compared to the TRPV2 generated network using T-test. Bingo Cytoscape app (42) was used to find Go-Term categories statistically enriched within the TRPV2 network. P-values of Go-terms were calculated with the hypergeometric test and corrected with the

Benjamini&Hochberg FDR algorithm. Go-Terms were manually clustered by their function as cellular processes. Each cellular process includes a series of functionally related Go-Terms from Bingo analysis. TRPV2 partners associated to each cellular process were quantified and represented as a pie chart.

TRPV2 and TRPV2 fragments purification

Rat TRPV2 full length tagged with a C-terminal GFP and a 8xHis tag was overexpressed in yeast *P. Pastoris*. Yeast carrying the construct of interest was grown in YPD Zeocin at 30ºC. Cells were harvested and cultured in Minimal Glycerol Yeast media (MGY) for 48 hours, till an Od_{600} of 10. Protein expression was induced by metanol, culturing the cells in Minimal Methanol media (MM) at 30ºC for 24 hours. Cells were lysed using a bead beater. Lysates centrifuged and pellet was solubilized for 1 hour at 4ºC in 1%DDM, 0.2% colesterol 50mM Tris-HCl (pH 7.4), 150mM NaCl buffer complemented with EDTA-free protease inhibitor. Lysates were centrifuged 45min at 25000g and supernatant collected and purified using Ni-NTA resin (30210, Qiagen).

MPD and ARD domain purification

MPD domains from TRPV1 and TRPV2 tagged with GFP and 8xHis tag in the C-terminus were heterologously expressed in *E. Coli*. ARD domain of rat TRPV2 was also expressed in *E.coli*. Expression of the protein was induced with 200 µM IPTG when the culture reached an OD_{600} of 0.6. After 5-6 hours at 37ºC cells were collected and lysed using a sonicator in 50mM Tris-HCl (pH 7.4), 150mM NaCl, 10% glicerol and EDTA-free protease inhibitors. Lysates were centrifuged 45min at 25000g and supernatant collected and purified using Ni-NTA resin.

TRPV2 strips

Full length rat TRPV2 and ARD TRPV2 domain, were purified and placed into nitrocellulose membranes using a dot blot and a vacuum. Membranes were dried for 30min at RT and kept at 4ºC. For interaction screen the TRPV2 membranes were blocked with blocking buffer (2%BSA PBS1x) and incubated with a lysate from rat brain tissue at 1 µg/ml in blocking buffer for 1 hour at RT. After incubation membranes were washed 3 times in TTBS 1x and further analyzed by western blot against the desired interaction partner.

Lipid strips

Lipids were resuspended in a 1:2:1 parts Chloroform-Methanol-Water buffer. Solubilized lipids were diluted in 1:2:1 parts of Chloroform-Methanol-HCl 50mM buffer and spotted into a nitrocellulose membrane at the desired final concentrations. Membranes were dried at RT for 1 hour and then stored at 4ºC ready to use. Membranes were blocked for 1 hour at RT with blocking buffer (2%BSA PBS1x) and incubated with purified protein, either TRPV1, TRPV2, MPD1, MPD2 or GFP at 9.5 µg/ml in blocking buffer for 1 hour at RT. After incubation membranes were washed 3 times in TTBS 1x and further analyzed by western blot against GFP tag.

Tryptophan quenching experiments

For the liposomes generation we depart from a chloroform solution of each phospholipid. The required volume is deposited on a ball rotavapor to obtain a final concentration of 1.5 mM lipid in the final suspension. The solution was rotary evaporated to a dry film of phospholipid attached to the balloon wall, which was resuspended in 2mL/ ball of 50mM Tris-HCl (pH 7.4), 150 mM NaCl, 10% glycerol and EDTA-free protease inhibitors. Vortexing alternating with agitation in a rotary evaporator is performed in order to hydratate the phospholipids and form a suspension containing basically large multilamellar liposome. Tryptophan endogenous fluorescence, excitation at 280nM emission at 332nM, was measured using a fluorimeter (SLM Aminco 8100). Proteins in 50mM Tris-HCl (pH 7.4), 150mM NaCl, 10% glycerol were incubated in a quartz cuvete and lipids reconstituted in the protein buffer were added at increasing concentrations.

TRPV2 activity assay

Inside out (ISO) vesicles, empty or containing rat TRPV2, were generated as described in Martins et al. (manuscript in preparation). The lipids were added at increasing concentrations and Fura8 fluorescence monitored upon lipid addition in a fluorimeter (SLM Aminco 8100). To monitor Fura8 ratio fluorescence was measured at 340 and 380 nm.

SUPPLEMENTAL INFORMATION

Supplemental information includes one figure and one table related to TRPV2 interactome GEO analysis.

ACKNOWLEDGMENTS

TRPV2 ARD plasmid was kindly provided by Dr. Rachelle Gaudet. pBT3-N bait empty vector was kindly provided by Dr. Igor Stargljar (Toronto University). pcDNA3 containing the cDNA for Snapin25 and SynaptotagminIX carrying a myc-his tag were kindly provided by Dr. Ferrer-Montiel (Miguel Hernandez University). This work was supported by the grants from Spanish Government (MICINN-SAF2010-21385). Donate Macian P. was supported by Generalitat de Catalunya, FI-DGR program. (FI-2013FIB00251). Peralválvarez Marín A. is the recipient of a Universidad Autonoma de Barcelona-Banco Santander fellowship.

REFERENCES

1. Montell C. The TRP superfamily of cation channels. Sci STKE. 2005;2005(272):re3.
2. Talavera K, Nilius B, Voets T. Neuronal TRP channels: thermometers, pathfinders and life-savers. Trends in Neurosciences. 2008. p. 287–95.
3. Liu C, Montell C. Forcing open TRP channels: Mechanical gating as a unifying activation mechanism. Biochem Biophys Res Commun. 2015;460(1):22–5.
4. Kaneko Y, Szallasi A. Transient receptor potential (TRP) channels: A clinical perspective. British Journal of Pharmacology. 2014. p. 2474–507.
5. Clapham DE. TRP channels as cellular sensors. Nature. 2003;426(6966):517–24.
6. Zubcevic L, Herzik MA, Chung BC, Liu Z, Lander

GC, Lee S-Y. Cryo-electron microscopy structure of the TRPV2 ion channel. Nat Struct Mol Biol [Internet]. 2016;23(November 2015):1–9. Available from: http://www.nature.com/doifinder/10.1038/nsmb.3159
7. Huynh KW, Cohen MR, Jiang J, Samanta A, Lodowski DT, Zhou ZH, et al. Structure of the full-length TRPV2 channel by cryo-EM. Nat Commun [Internet]. 2016;7:11130. Available from: http://www.nature.com/doifinder/10.1038/ncomms11130
8. Holakovska B, Grycova L, Bily J, Teisinger J. Characterization of calmodulin binding domains in TRPV2 and TRPV5 C-tails. Amino Acids [Internet]. 2011;40:741–8. Available from: http://www.ncbi.nlm.nih.gov/pubmed/20686800
9. Mercado J, Gordon-Shaag A, Zagotta WN, Gordon SE. Ca2+-dependent desensitization of TRPV2 channels is mediated by hydrolysis of phosphatidylinositol 4,5-bisphosphate. J Neurosci. 2010;30:13338–47.
10. Kanzaki M, Zhang YQ, Mashima H, Li L, Shibata H, Kojima I. Translocation of a calcium-permeable cation channel induced by insulin-like growth factor-I. Nat Cell Biol. 1999;1(3):165–70.
11. Stokes AJ, Shimoda LMN, Koblan-Huberson M, Adra CN, Turner H. A TRPV2-PKA signaling module for transduction of physical stimuli in mast cells. J Exp Med. 2004;200:137–47.
12. Perálvarez-Marín A, Doñate-Macian P, Gaudet R. What do we know about the transient receptor potential vanilloid 2 (TRPV2) ion channel? FEBS J [Internet]. 2013;280:5471–87. Available from: http://www.pubmedcentral.nih.gov/articlerender.fcgi?artid=3783526&tool=pmcentrez&rendertype=abstract
13. Lewinter RD, Skinner K, Julius D, Basbaum AI. Immunoreactive TRPV-2 (VRL-1), a capsaicin receptor homolog, in the spinal cord of the rat. J Comp Neurol [Internet]. 2004;470(4):400–8. Available from: http://www.ncbi.nlm.nih.gov/pubmed/14961565
14. Nedungadi TP, Dutta M, Bathina CS, Caterina MJ, Cunningham JT. Expression and distribution of TRPV2 in rat brain. Exp Neurol [Internet]. 2012;237(1):223–37. Available from: http://www.pubmedcentral.nih.gov/articlerender.fcgi?artid=3418486&tool=pmcentrez&rendertype=abstract
15. Shibasaki K, Murayama N, Ono K, Ishizaki Y, Tominaga M. TRPV2 enhances axon outgrowth through its activation by membrane stretch in developing sensory and motor neurons. J Neurosci. 2010;30:4601–12.
16. Lorin C, Vögeli I, Niggli E. Dystrophic cardiomyopathy: role of TRPV2 channels in stretch-induced cell damage. Cardiovasc Res [Internet]. 2015;106(1):153–62. Available from: http://www.ncbi.nlm.nih.gov/pubmed/25616416
17. Monet M, Lehen'kyi V, Gackiere F, Firlej V, Vandenberghe M, Roudbaraki M, et al. Role of cationic channel TRPV2 in promoting prostate cancer migration and progression to androgen resistance. Cancer Res. 2010;70:1225–35.
18. Zhang X, Li L, McNaughton P a. Proinflammatory Mediators Modulate the Heat-Activated Ion Channel TRPV1 via the Scaffolding Protein AKAP79/150. Neuron. 2008;59(3):450–61.
19. Barnhill JC, Stokes AJ, Koblan-Huberson M, Shimoda LMN, Muraguchi A, Adra CN, et al. RGA protein associates with a TRPV ion channel during biosynthesis and trafficking. J Cell Biochem. 2004;91:808–20.
20. Stokes AJ, Wakano C, Del Carmen K a., Koblan-Huberson M, Turner H. Formation of a physiological complex between TRPV2 and RGA protein promotes cell surface expression of TRPV2. J Cell Biochem. 2005;94:669–83.
21. Monet M, Gkika D, Lehen'kyi V, Pourtier A, Abeele F Vanden, Bidaux G, et al. Lysophospholipids stimulate prostate cancer cell migration via TRPV2 channel activation. Biochim Biophys Acta - Mol Cell Res [Internet]. 2009;1793:528–39. Available from: http://dx.doi.org/10.1016/j.bbamcr.2009.01.003
22. Snider J, Kittanakom S, Damjanovic D, Curak J, Wong V, Stagljar I. Detecting interactions with membrane proteins using a membrane two-hybrid assay in yeast. Nat Protoc [Internet]. 2010;5:1281–93. Available from: http://dx.doi.org/10.1038/nprot.2010.83
23. Doñate-Macián P, Perálvarez-Marín A. Dissecting domain-specific evolutionary pressure profiles of transient receptor potential vanilloid subfamily members 1 to 4. PLoS One [Internet]. 2014;9:e110715. Available from: http://www.pubmedcentral.nih.gov/articlerender.fcgi?artid=4204936&tool=pmcentrez&rendertype=abstract
24. Morenilla-Palao C, Planells-Cases R, García-Sanz N, Ferrer-Montiel A. Regulated exocytosis contributes to protein kinase C potentiation of vanilloid receptor activity. J Biol Chem. 2004;279:25665–72.
25. Kittanakom S, Chuk M, Wong V, Snyder J, Edmonds D, Lydakis A, et al. Analysis of membrane protein complexes using the split-ubiquitin membrane yeast two-hybrid (MYTH) system. Methods Mol Biol [Internet]. 2009;548:247–71. Available from: http://www.springerlink.com/index/10.1007/978-1-59745-540-4\nhttp://www.ncbi.nlm.nih.gov/pubmed/19521829
26. Garcia-Elias A, Berna-Erro A, Rubio-Moscardo F, Pardo-Pastor C, Mrkonjić S, Sepúlveda RV, et al. Interaction between the Linker, Pre-S1, and TRP Domains Determines Folding, Assembly, and Trafficking of TRPV Channels. Structure [Internet]. 2015;1–10. Available from: http://linkinghub.elsevier.com/retrieve/pii/S096921261500221X
27. Schwarz K, Natarajan S, Kassas N, Vitale N, Schmitz F. The synaptic ribbon is a site of phosphatidic acid generation in ribbon synapses. J Neurosci [Internet]. 2011;31(44):15996–6011. Available from: http://www.ncbi.nlm.nih.gov/pubmed/22049442
28. Yao J, Liu B, Qin F. Modular thermal sensors in temperature-gated transient receptor potential (TRP) channels. Proc Natl Acad Sci U S A. 2011;108(27):11109–14.
29. Vergarajauregui S, Martina J a, Puertollano R. LAPTMs regulate lysosomal function and interact with mucolipin 1: new clues for understanding mucolipidosis type IV. J Cell Sci [Internet]. 2011;124(Pt 3):459–68. Available from: http://www.pubmedcentral.nih.gov/articlerender.fcgi?artid=3022000&tool=pmcentrez&rendertype=abstract
30. Hille B. Ion Channel Excitable Membranes. Sunderland Massachusetts USA. 2001. p. 1–37.
31. Ufret-Vincenty C a, Klein RM, Hua L, Angueyra J, Gordon SE. Localization of the PIP2 Xensor of TRPV1 Ion Channels. J Biol Chem [Internet]. 2011;286(11):9688–98. Available from: http://www.pubmedcentral.nih.gov/articlerender.fcgi?artid=3058964&tool=pmcentrez&rendertype=abstract
32. Garcia-Elias A, Mrkonjic S, Pardo-Pastor C, Inada

H, Hellmich UA, Rubio-Moscardó F, et al. Phosphatidylinositol-4,5-biphosphate-dependent rearrangement of TRPV4 cytosolic tails enables channel activation by physiological stimuli. Proc Natl Acad Sci U S A [Internet]. 2013;110(23):9553–8. Available from: http://www.pnas.org/content/110/23/9553.long

33. Jahn O, Tenzer S, Werner HB. Myelin proteomics: Molecular anatomy of an insulating sheath. Molecular Neurobiology. 2009. p. 55–72.

34. Gil OD, Zanazzi G, Struyk a F, Salzer JL. Neurotrimin mediates bifunctional effects on neurite outgrowth via homophilic and heterophilic interactions. J Neurosci. 1998;18(22):9312–25.

35. Cohen MR, Johnson WM, Pilat JM, Kiselar J, Defrancesco-lisowitz A, Zigmond RE. 2 via Extracellular Signal-Regulated Kinase Signaling To Enhance Neurite Outgrowth in Developing Neurons. 2015;35(24):4238–52.

36. Nieto-Posadas A, Picazo-juárez G, Llorente I, Jara-oseguera A, Morales-Lázaro S, Escalante-Alcalde D, et al. Lysophosphatidic acid directly activates TRPV1 through a C-terminal binding site. Nat Chem Biol [Internet]. 2012;8(1):78–85. Available from: http://www.nature.com/doifinder/10.1038/nchembio.712\nhttp://www.ncbi.nlm.nih.gov/pubmed/22101604

37. Kahn DW, Morell P. Phosphatidic acid and phosphoinositide turnover in myelin and its stimulation by acetylcholine. J Neurochem. 602;50(5):1542–50.

38. Yamamoto S, Gotoh M, Kawamura Y, Yamashina K, Yagishita S, Awaji T, et al. Cyclic phosphatidic acid treatment suppress cuprizone-induced demyelination and motor dysfunction in mice. Eur J Pharmacol [Internet]. 2014;741:17–24. Available from: http://linkinghub.elsevier.com/retrieve/pii/S0014999914005779

39. Nadra K, de Preux Charles A-S, Médard J, Hendriks WT, Han G, Grès S, et al. Phosphatidic acid mediates demyelination in Lpin1 mutant mice. Genes Dev [Internet]. 2008;22(12):1647–61. Available from: http://www.pubmedcentral.nih.gov/articlerender.fcgi?artid=2428062&tool=pmcentrez&rendertype=abstract

40. Shannon P, Markiel A, Ozier O, Baliga NS, Wang JT, Ramage D, et al. Cytoscape: A software Environment for integrated models of biomolecular interaction networks. Genome Res. 2003;13(11):2498–504.

41. Montojo J, Zuberi K, Rodriguez H, Kazi F, Wright G, Donaldson SL, et al. GeneMANIA cytoscape plugin: Fast gene function predictions on the desktop. Bioinformatics. 2010;26(22):2927–8.

42. Maere S, Heymans K, Kuiper M. BiNGO: A Cytoscape plugin to assess overrepresentation of Gene Ontology categories in Biological Networks. Bioinformatics. 2005;21(16):3448–9.

43. Jahnel R, Bender O, Münter LM, Dreger M, Gillen C, Hucho F. Dual expression of mouse and rat VRL-1 in the dorsal root ganglion derived cell line F-11 and biochemical analysis of VRL-1 after heterologous expression. Eur J Biochem. 2003;270:4264–71.

Suplementary information

A

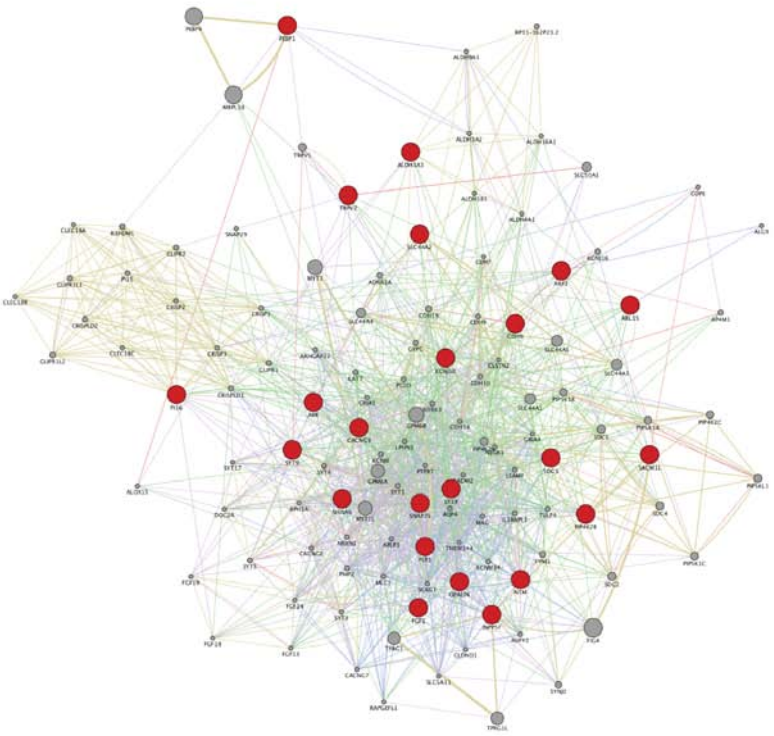

B

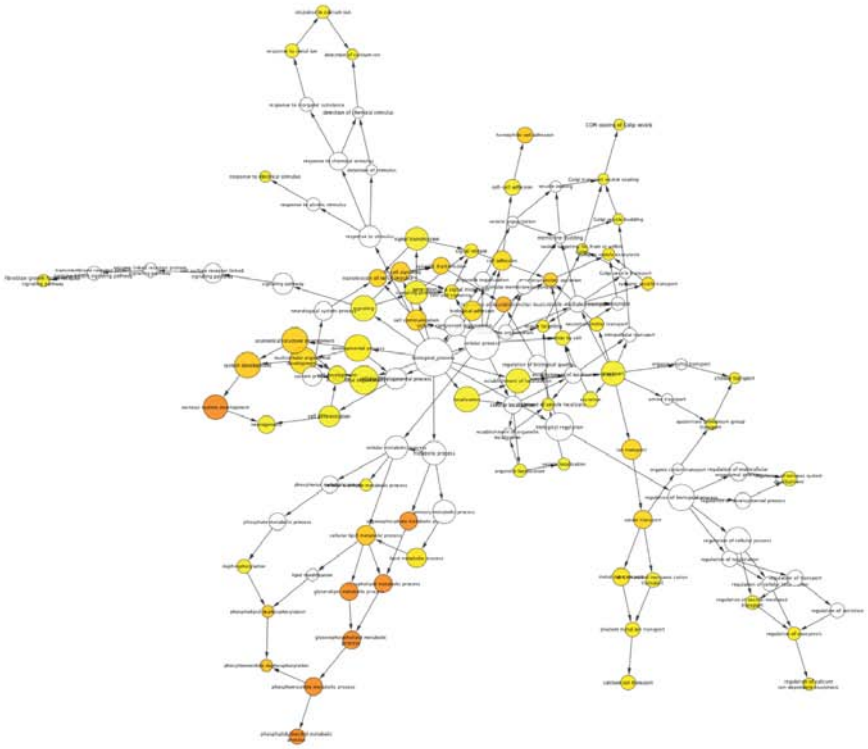

SUPLEMENTARY INFORMATION. TRPV2 Gene Enrichment Analysis (GEO). A) TRPV2 interaction partners gene enrichment by Genemania App algorithm (Cytoscape). Interactome showing the 100 closest related genes to TRPV2 interactors based on colocalization, co-expression, physical interactions and domain conservation. B) Bingo App (Cytoscape) analysis of the 100 closest genes TRPV2 network. Colour represents the p-value association between the Go-term and TRPV2 network. The red colour indicates the most statistically significant associations with TRPV2 network, followed by yellow colour. White Go-terms are the least significant associated Go-terms.

Go term ID	Process	Association	p val	pval correct	% genes	% genes GoID	Genes
30384	phosphoinositide metabolic process	12	6,42E-10	5,84E-07	12/91 13.1%	78/14303 0.5%	FIG4 ALG9 INPP5F SACM1L PIP5KL1 PIP4K2A PIP5K1A PIP4K2B PIP5K1B PIP4K2C PIP5K1C SYNJ2
46488	phosphatidylinositol metabolic process	7	1,00E-07	4,21E-05	7/91 7.6%	18/14303 0.1%	PIP5KL1 PIP4K2A PIP5K1A PIP4K2B PIP5K1B PIP4K2C PIP5K1C
6650	glycerophospholipid metabolic process	12	1,39E-07	4,21E-05	12/91 13.1%	121/14303 0.8%	FIG4 ALG9 INPP5F SACM1L PIP5KL1 PIP4K2A PIP5K1A PIP4K2B PIP5K1B PIP4K2C PIP5K1C SYNJ2
7399	nervous system development	29	5,24E-07	1,19E-04	29/91 31.8%	1155/14303 8.0%	SNAP25 DOC2A MYT1L NTM SDC2 NRXN1 PEBP1 AQP4 FGF1 RAPGEFL1 RPH3A PIP5K1C GPM6B NTRK3 APLP1 LSAMP SYNJ2 MYT1 ALDH3A2 FIG4 ALDH1A3 MAG FGF14 SYNJ1 FGF19 IL1RAPL1 PLP1 FGF13 SCRG1
46486	glycerolipid metabolic process	12	5,72E-06	1,04E-03	12/91 13.1%	166/14303 1.1%	FIG4 ALG9 INPP5F SACM1L PIP5KL1 PIP4K2A PIP5K1A PIP4K2B PIP5K1B PIP4K2C PIP5K1C SYNJ2
6644	phospholipid metabolic process	12	4,06E-05	6,16E-03	12/91 13.1%	197/14303 1.3%	FIG4 ALG9 INPP5F SACM1L PIP5KL1 PIP4K2A PIP5K1A PIP4K2B PIP5K1B PIP4K2C PIP5K1C SYNJ2
19637	organophosphate metabolic process	12	7,51E-05	9,76E-03	12/91 13.1%	208/14303 1.4%	FIG4 ALG9 INPP5F SACM1L PIP5KL1 PIP4K2A PIP5K1A PIP4K2B PIP5K1B PIP4K2C PIP5K1C SYNJ2
1505	regulation of neurotransmitter levels	7	2,36E-03	2,69E-01	7/91 7.6%	68/14303 0.4%	SYT4 SNAP25 PCLO SYT1 DOC2A PEBP1 ALDH9A1
46856	phosphoinositide dephosphorylation	3	9,92E-03	1,00E+00	3/91 3.2%	4/14303 0.0%	INPP5F SACM1L SYNJ2
44255	cellular lipid metabolic process	15	1,81E-02	1,65E+00	15/91 16.4%	550/14303 3.8%	ALG9 SACM1L ALOX15 SYNJ2 FIG4 ALDH1A3 INPP5F PIP5KL1 PLP1 PIP4K2A PIP5K1A PIP4K2B PIP5K1B PIP4K2C PIP5K1C
48731	system development	34	2,35E-02	1,95E+00	34/91 37.3%	2422/14303 16.9%	SNAP25 DOC2A MYT1L NTM SDC2 NRXN1 ALOX15 PEBP1 AQP4 FGF1 RAPGEFL1 RPH3A PIP5K1C CACNG2 GPM6B NTRK3 APLP1 LSAMP SYNJ2 MYT1 ALDH3A2 FIG4 ALDH1A3 MAG FGF14 SYNJ1 FGF19 FGF18 IL1RAPL1 PLP1 SDC1 FGF13 SCRG1 ALDH9A1
7156	homophilic cell adhesion	8	2,65E-02	2,01E+00	8/91 8.7%	138/14303 0.9%	CDH6 PTPRT CLSTN2 CDH10 CDH9 CDH18 CDH7 CDH19
7269	neurotransmitter secretion	5	3,46E-02	2,42E+00	5/91 5.4%	37/14303 0.2%	SYT4 SNAP25 PCLO SYT1 DOC2A
7267	cell cell signaling	15	3,94E-02	2,56E+00	15/91 16.4%	586/14303 4.0%	SYT5 SYT4 SNAP25 SYT1 DOC2A PEBP1 FGF1 ADRA1A FGF14 PCLO FGF18 PLP1 KCNMB4 FGF13 ALDH9A1
46839	phospholipid dephosphorylation	3	4,91E-02	2,98E+00	3/91 3.2%	6/14303 0.0%	INPP5F SACM1L SYNJ2
48856	anatomical structure development	35	6,75E-02	3,84E+00	35/91 38.4%	2656/14303 18.5%	SNAP25 SDC4 DOC2A MYT1L NTM SDC2 NRXN1 ALOX15 PEBP1 AQP4 FGF1 RAPGEFL1 RPH3A PIP5K1C CACNG2 GPM6B NTRK3 APLP1 LSAMP SYNJ2 MYT1 ALDH3A2 FIG4 ALDH1A3 MAG FGF14 SYNJ1 FGF19 FGF18 IL1RAPL1 PLP1 SDC1 FGF13 SCRG1 ALDH9A1
19226	transmition of nerve impulse	11	1,07E-01	5,71E+00	11/91 12.0%	342/14303 2.3%	SYT5 SYT4 SNAP25 PCLO SYT1 DOC2A PLP1 PEBP1 KCNMB4 CACNG2 ALDH9A1
7154	cell comunication	17	1,20E-01	6,05E+00	17/91 18.6%	811/14303 5.6%	SYT5 SYT4 SNAP25 SYT1 DOC2A PEBP1 FGF1 ADRA1A ARHGAP32 FGF14 PCLO FGF18 PLP1 KCNMB4 FGF13 CACNG2 ALDH9A1
7268	synaptic transmission	10	1,43E-01	6,85E+00	10/91 10.9%	288/14303 2.0%	SYT5 SYT4 SNAP25 PCLO SYT1 DOC2A PLP1 PEBP1 KCNMB4 ALDH9A1
6811	ion transport	16	1,84E-01	8,37E+00	16/91 17.5%	751/14303 5.2%	KCNJ6 KCNJ10 SLC44A1 SLC44A2 TRPV2 SLC5A11 MLC1 KCNJ16 TRPV1 ADRA1A CACNG7 KCNMB4 CACNG2 CACNG3 GRIA3 GRIA4
6812	cation transport	13	2,07E-01	8,97E+00	13/91 14.2%	513/14303 3.5%	KCNJ6 KCNJ10 SLC44A1 SLC44A2 TRPV2 SLC5A11 KCNJ16 TRPV1 ADRA1A CACNG7 KCNMB4 CACNG2 CACNG3
7275	multicellular organismal development	36	3,22E-01	1,33E+01	36/91 39.5%	2972/14303 20.7%	SNAP25 SDC4 DOC2A MYT1L NTM SDC2 NRXN1 ALOX15 PEBP1 AQP4 FGF1 ADRA1A RAPGEFL1 RPH3A PIP5K1C CACNG2 GPM6B NTRK3 APLP1 LSAMP SYNJ2 MYT1 ALDH3A2 FIG4 ALDH1A3 MAG FGF14 SYNJ1 FGF19 FGF18 IL1RAPL1 PLP1 SDC1 FGF13 SCRG1 ALDH9A1
7155	cell adhesion	15	3,83E-01	1,48E+01	15/91 16.4%	710/14303 4.9%	PTPRT CLSTN2 NEGR1 NTM NRXN1 APLP1 SDC3 LSAMP CDH9 CDH7 CDH6 MAG CDH10 CDH18 CDH19
22610	biological adhesion	15	3,89E-01	1,48E+01	15/91 16.4%	711/14303 4.9%	PTPRT CLSTN2 NEGR1 NTM NRXN1 APLP1 SDC3 LSAMP CDH9 CDH7 CDH6 MAG CDH10 CDH18 CDH19
48489	synaptic vesicle transport	4	4,81E-01	1,75E+01	4/91 4.3%	32/14303 0.2%	SNAP25 PCLO SYNJ1 DOC2A
6629	lipid metabolic process	16	6,54E-01	2,29E+01	16/91 17.5%	834/14303 5.8%	ALG9 SACM1L ALOX15 SYNJ2 ALDH3A2 FIG4 ALDH1A3 INPP5F PIP5KL1 PLP1 PIP4K2A PIP5K1A PIP4K2B PIP5K1B PIP4K2C PIP5K1C
30001	metal ion transport	11	7,50E-01	2,53E+01	11/91 12.0%	423/14303 2.9%	CACNG7 KCNJ6 KCNJ10 TRPV2 SLC5A11 KCNMB4 KCNJ16 TRPV1 CACNG2 ADRA1A CACNG3
17158	regulation of calcium ion dependent exocytosis	3	1,07E+00	3,37E+01	3/91 3.2%	15/14303 0.1%	SYT1 DOC2A SYT9
16079	synaptic vesicle exocytosis	3	1,07E+00	3,37E+01	3/91 3.2%	15/14303 0.1%	SNAP25 PCLO DOC2A
15871	choline transport	2	1,20E+00	3,63E+01	2/91 2.1%	3/14303 0.0%	SLC44A1 SLC44A2
17157	regulation of exocytosis	4	1,71E+00	4,91E+01	4/91 4.3%	44/14303 0.3%	SYT1 DOC2A IL1RAPL1 SYT9
23061	signal release	5	1,83E+00	4,91E+01	5/91 5.4%	83/14303 0.5%	SYT4 SNAP25 PCLO SYT1 DOC2A
6836	neurotransmitter transportgeneration of signal cell cell signaling	5	1,83E+00	4,91E+01	5/91 5.4%	83/14303 0.5%	SYT4 SNAP25 PCLO SYT1 DOC2A
3001	generation of a signal cell to cell signaling	5	1,83E+00	4,91E+01	5/91 5.4%	83/14303 0.5%	SYT4 SNAP25 PCLO SYT1 DOC2A
6816	calcium ion transport	6	2,02E+00	5,12E+01	6/91 6.5%	133/14303 0.9%	CACNG7 TRPV2 TRPV1 CACNG2 ADRA1A CACNG3
32502	developmental process	36	2,03E+00	5,12E+01	36/91 39.5%	3234/14303 22.6%	SNAP25 SDC4 DOC2A MYT1L NTM SDC2 NRXN1 ALOX15 PEBP1 AQP4 FGF1 ADRA1A RAPGEFL1 RPH3A PIP5K1C CACNG2 GPM6B NTRK3 APLP1 LSAMP SYNJ2 MYT1 ALDH3A2 FIG4 ALDH1A3 MAG FGF14 SYNJ1 FGF19 FGF18 IL1RAPL1 PLP1 SDC1 FGF13 SCRG1 ALDH9A1
70838	divalent metal ion transport	6	2,66E+00	6,54E+01	6/91 6.5%	140/14303 0.9%	CACNG7 TRPV2 TRPV1 CACNG2 ADRA1A CACNG3
6903	vesicle targeting	3	3,52E+00	8,42E+01	3/91 3.2%	22/14303 0.1%	ARF1 SNAP29 COPE
51592	response to calcium ion	4	5,00E+00	1,17E+02	4/91 4.3%	58/14303 0.4%	SYT1 PEBP1 KCNMB4 SDC1
16337	cell cell adhesion	8	5,14E+00	1,17E+02	8/91 8.7%	290/14303 2.0%	CDH6 PTPRT CLSTN2 CDH10 CDH9 CDH18 CDH7 CDH19
32501	multicellular organismal process	43	6,00E+00	1,33E+02	43/91 47.2%	4375/14303 30.5%	SNAP25 SDC4 DOC2A MYT1L NTM SDC2 NRXN1 ALOX15 PEBP1 AQP4 FGF1 ADRA1A RAPGEFL1 RPH3A PCLO KCNMB4 PIP5K1C CACNG2 GPM6B SYT5 SYT4 SYT1 NTRK3 APLP1 TRPV2 LSAMP SYNJ2 TRPV1 MYT1 ALDH3A2 FIG4 ALDH1A3 MAG FGF14 SYNJ1 FGF19 FGF18 IL1RAPL1 PLP1 SDC1 FGF13 SCRG1 ALDH9A1
48468	cell development	12	6,44E+00	1,40E+02	12/91 13.1%	632/14303 4.4%	FIG4 SNAP25 NTM SDC2 FGF19 NRXN1 FGF18 PLP1 PEBP1 SDC1 PIP5K1C CACNG2
15674	di tri valent inorganic cation transport	6	8,95E+00	1,89E+02	6/91 6.5%	176/14303 1.2%	CACNG7 TRPV2 TRPV1 CACNG2 ADRA1A CACNG3
6810	transport	29	9,70E+00	1,99E+02	29/91 31.8%	2577/14303 18.0%	SNAP25 ARF1 DOC2A SLC44A1 SLC44A2 SLC5A11 MLC1 AQP4 ADRA1A RPH3A AP4M1 CACNG7 PCLO KCNMB4 CACNG2 SNAP29 CACNG3 GRIA3 GRIA4 SYT4 KCNJ6 KCNJ10 SYT1 APLP1 TRPV2 KCNJ16 TRPV1 SYNJ1 COPE
6081	cellular aldehyde metabolic process	3	9,84E+00	1,99E+02	3/91 3.2%	31/14303 0.2%	ALDH3A2 ALDH1A3 ALDH9A1
60627	regulation of vesicle mediated transport	5	1,04E+01	2,05E+02	5/91 5.4%	121/14303 0.8%	SYT1 SYNJ1 DOC2A IL1RAPL1 SYT9
51179	localization	32	1,10E+01	2,13E+02	32/91 35.1%	2984/14303 20.8%	SNAP25 ARF1 DOC2A SLC44A1 SLC44A2 SLC5A11 MLC1 AQP4 ADRA1A RPH3A AP4M1 CACNG7 PCLO PIP5K1A KCNMB4 CACNG2 SNAP29 CACNG3 GRIA3 GRIA4 SYT4 KCNJ6 KCNJ10 SYT1 APLP1 TRPV2 KCNJ16 SYNJ2 TRPV1 SYNJ1 FGF19 COPE
8543	fibroblast growth factor receptor signaling pathway	3	1,18E+01	2,14E+02	3/91 3.2%	33/14303 0.2%	FGF19 FGF18 FGF1
51650	establishment of vesicle location	3	1,18E+01	2,14E+02	3/91 3.2%	33/14303 0.2%	ARF1 SNAP29 COPE
23052	signaling	33	1,19E+01	2,14E+02	33/91 36.2%	3130/14303 21.8%	PTPRT SNAP25 ARF1 DOC2A PEBP1 FGF1 ADRA1A RAPGEFL1 ABR PCLO INPP5F PIP5K1A KCNMB4 PIP4K2B CACNG2 GRIA3 GRIA4 SYT5 SYT4 SYT1 NTRK3 APLP1 TRPV1 ARHGAP32 FGF14 FGF19 FGF18 IL1RAPL1 PLP1 SDC1 FGF13 LPHN3 ALDH9A1

51234	establishment of localization	29	1,20E+01	2,14E+02	29/91 31.8%	2611/14303 18.2%	SNAP25 ARF1 DOC2A SLC44A1 SLC44A2 SLC5A11 MLC1 AQP4 ADRA1A RPH3A AP4M1 CACNG7 PCLO KCNMB4 CACNG2 SNAP29 CACNG3 GRIA3 GRIA4 SYT4 KCNJ6 KCNJ10 SYT1 APLP1 TRPV2 KCNJ16 TRPV1 SYNJ1 COPE
5513	detection of calcium ion	2	1,40E+01	2,45E+02	2/91 2.1%	9/14303 0.0%	SYT1 KCNMB4
23046	signaling process	25	1,62E+01	2,73E+02	25/91 27.4%	2156/14303 15.0%	PTPRT SNAP25 ARF1 DOC2A PEBP1 FGF1 ADRA1A RAPGEFL1 ABR PCLO INPP5F PIP5K1A KCNMB4 CACNG2 SYT5 SYT4 SYT1 APLP1 ARHGAP32 FGF14 FGF18 IL1RAPL1 PLP1 FGF13 ALDH9A1
23060	signal transmission	25	1,62E+01	2,73E+02	25/91 27.4%	2156/14303 15.0%	PTPRT SNAP25 ARF1 DOC2A PEBP1 FGF1 ADRA1A RAPGEFL1 ABR PCLO INPP5F PIP5K1A KCNMB4 CACNG2 SYT5 SYT4 SYT1 APLP1 ARHGAP32 FGF14 FGF18 IL1RAPL1 PLP1 FGF13 ALDH9A1
48200	golgi transport vesicle coating	2	1,74E+01	2,83E+02	2/91 2.1%	10/14303 0.0%	ARF1 COPE
48205	coating of vesicle golgi	2	1,74E+01	2,83E+02	2/91 2.1%	10/14303 0.0%	ARF1 COPE
51648	vesicle localization	3	1,79E+01	2,86E+02	3/91 3.2%	38/14303 0.2%	ARF1 SNAP29 COPE
32940	secretion by cell	6	2,00E+01	3,14E+02	6/91 6.5%	206/14303 1.4%	SYT4 SNAP25 PCLO SYT1 DOC2A SNAP29
48194	golgi vesicle budding	2	2,12E+01	3,22E+02	2/91 2.1%	11/14303 0.0%	ARF1 COPE
15697	quaternary ammonium group transport	2	2,12E+01	3,22E+02	2/91 2.1%	11/14303 0.0%	SLC44A1 SLC44A2
16311	dephosphorylation	5	2,31E+01	3,42E+02	5/91 5.4%	145/14303 1.0%	PTPRT INPP5F SYNJ1 SACM1L SYNJ2
22008	neurogenesis	11	2,33E+01	3,42E+02	11/91 12.0%	637/14303 4.4%	FIG4 SNAP25 MAG SYNJ1 NTM SDC2 NRXN1 NTRK3 IL1RAPL1 PLP1 PIP5K1C
48199	vesicle targeting to from golgi	2	2,54E+01	3,66E+02	2/91 2.1%	12/14303 0.0%	ARF1 COPE
46903	secretion	7	2,73E+01	3,88E+02	7/91 7.6%	295/14303 2.0%	SYT4 SNAP25 PCLO SYT1 DOC2A AQP4 SNAP29
10038	response to metal ion	5	2,92E+01	4,08E+02	5/91 5.4%	153/14303 1.0%	SYT1 PEBP1 KCNMB4 SDC1 GRIA3
51960	regulation of nervous system development	6	3,25E+01	4,43E+02	6/91 6.5%	227/14303 1.5%	FIG4 SNAP25 MAG SYNJ1 NTRK3 IL1RAPL1
51640	organelle localization	4	3,26E+01	4,43E+02	4/91 4.3%	96/14303 0.6%	ARF1 SYNJ2 SNAP29 COPE
51602	response to electrical stimulus	2	3,47E+01	4,64E+02	2/91 2.1%	14/14303 0.0%	KCNJ6 PEBP1
30154	cell differenciation	20	3,61E+01	4,76E+02	20/91 21.9%	1668/14303 11.6%	SNAP25 MYT1L NTM SDC2 NRXN1 NTRK3 PEBP1 FGF1 MYT1 FIG4 MAG SYNJ1 FGF19 FGF18 IL1RAPL1 PLP1 SDC1 PIP5K1C CACNG2 GPM6B

lipid metabolism
nervous system and cell development
ion transport
vesicle transport
neurotransmitter and synaptic regulation
cell adhesion
other
signaling cascades

List of GO-terms associated with TRPV2 enriched network. Go-term ID, p-values, p-values corrected, gene number and percentage of genes from the network and genes from the network included within each Go-term are annotated. The box with colour shows the cellular process manual annotation, acording to the legend.

Chapter V

Transient Receptor Potential Vanilloid 4 (TRPV4) controls cellular transcription-translation and viral translation through the interaction and modulation of Dead box helicase DDX3X.

Specific objectives

- Identify potential interactors for TRPV4 to broaden the knowledge on the regulation of this channel.
- Determine the main roles carried out by TRPV4 interactome.
- Identify functional implications of newly described TRPV4 interactions.

CHAPTER V

Manuscript

CHAPTER V /TRPV4 interaction DDX3X OPEN

Transient Receptor Potential Vanilloid 4 (TRPV4) controls cellular transcription-translation and viral translation through the interaction and modulation of Dead box helicase DDX3X.

Pablo Doñate-Macian[1], Jenny Jungfleisch[2], Carlos Pardo-Pastor[3], Fanny Rubio-Moscardo[3], Alejandro Berna-Erro[3], Juana Díez[2], Alex Perálvarez-Marín[1] , Miguel Valverde[3].

TRPV4 is a non-selective ion channel member of the Transient Receptor Potential (TRP) family that is widely expressed in human epithelial tissues. TRPV4 plays an important role in integration of extracellular insults such as high temperatures, mechanical or osmotic stretch within the epithelium, although the molecular mechanisms by which TRPV4 exerts its function and regulates its activity are mostly unknown.

To identify novel TRPV4 interaction partners we have performed a membrane yeast two hybrid (MYTH) screening and identified 44 new potential interactors for TRPV4. Further characterization of TRPV4 interactome shows high association with cellular processes related to signalling, immune system responses, calcium metabolism or apoptosis. Among the putative protein-protein interactions (PPI) derived TRPV4 functions, immune system and viral infection processes are the most statistically significant associations.

We further characterize and functionally validate TRPV4 interaction with DDX3X, a RNA helicase involved in regulation of viral infection at different levels. This study establishes the first approach to define potential regulatory pathways for TRPV4 in immune system response to viral infection.

1 Unitat de Biofisica, Departament de Bioquímica I Biologia molecular. Universitat Autonoma de Barcelona (UAB) Bellaterra, Barcelona, 08193, Spain.

2 Department of Experimental and Health Sciences, Universitat Pompeu Fabra, 08003 Barcelona, Spain

3 Laboratory of Molecular Physiology and Channelopathies, Dept. of Experimental and Health Sciences, Universitat Pompeu Fabra, C/ Dr. Aiguader 88, Barcelona, 08003, Spain.

Local and global calcium transients produced by TRP channels tightly regulate gene transcription, resulting in modulation of diverse cellular events such as cellular motility and proliferation, muscle contraction or sensory transduction [1]. Despite the huge efforts in identifying downstream effectors of TRP channels, the signalling pathways that couple channel function to transcription and lately cell regulation, are still poorly understood. So far, the best characterized regulatory processes for TRPs, as for most ion channels, consists in the linkage to calcium related proteins such as calmodulin and phosphorylation-dependent regulation[2]. TRPV4 is a non-selective ion channel from the Transient Receptor Potential (TRP) family, which is ubiquitously expressed within the human body and mainly found in epithelial tissues [3], the first barrier in contact with the external environment. TRPV4 channel evoke calcium currents in response to extracellular insults such as high temperatures (38°C) [4], hypotonic shock [5] or mechanical stretch [6].

TRPV4 N- and C-terminus bind calmodulin potentiating channel activity [7, 8]. Indeed, several proteins have shown to promote a sensitized state of TRPV4. Myosin binds to the C-terminal calmodulin binding pocket and sensitizes the channel [2]. SRC kinases directly phosphorylate TRPV4 at the N-terminus and affect channel activation [9], while inositol triphosphate receptor (IP3R) enhances TRPV4 activity by settling a connection between the TRPV4-mediated extracellular calcium influx and the intracellular calcium stores [10]. Lipid metabolism also regulates TRPV4 activity, specially phosphatidylinositol 4,5-biphosphate (PIP2), whose binding sensitizes the channel in a process that is modulated by Pacsin3 [11]. Although upstream regulation of TRPV4 activity has been quite characterized, few studies identified TRPV4 partners that might mediate in lately TRPV4-mediated cellular functions. Among its described roles, TRPV4 controls cell adhesion and motility by controlling adherent junctions and focal adhesions through its interaction with proteins from these complexes, such as E-cadherin and integrins, respectively [12, 13, 14]. Furthermore, TRPV4 associates with several scaffolding proteins such as AKAP5 [15] and the cytoskeleton [16], linking extracellular stimuli to calcium metabolism and cellular structural organization and integrity.

Here we report a membrane yeast two hybrid (MYTH) that determined a set of new potential TRPV4 protein-protein interactions (PPI) and unravel new physiological implications for TRPV4 beyond what has been previously described. TRPV4 PPI-based network predicted potential functional implications of TRPV4 in immune system regulation and viral infection. Interaction of TRPV4 with DDX3X, a multifunctional DEAD Box family RNA helicase involved in diverse steps of viral infection and immune response [17], was further evaluated. DDX3X is an ATP dependent RNA helicase used for the cell to control several processes in the mRNA metabolism. TRPV4 functionally relates with DDX3X, regulating the helicase expression levels and cellular location. These finding broaden our understanding of the diverse functional regulation of TRPV4 and TRPV subfamily of channels in cell physiology.

Results

TRPV4 potential interaction partners. In order to determine new potential interaction partners and novel TRPV4 potential roles a yeast two hybrid assay specific for membrane proteins MYTH [18] was performed (Fig. 1a). MYTH is a split ubiquitin yeast based method that allows the expression of full length membrane proteins in their natural environment, embedded in the membrane, and tagged with a bait tag composed of the C-terminus of Ubiquitin (CUB) and a transcription factor (TF) (Fig. 1a and b). Prey proteins contain the N-terminus of Ubiquitin engineered to avoid spontaneous Ubiquitin refolding (NUBG). Thus, only when bait and prey interact the Ubiquitin will refold and the degradation ubiquitin complex (DUB) will release the TF that will go to the nucleus and start the expression of reporter genes (Fig. 1a).

Two baits were generated for TRPV4, carrying the bait tag on the N-terminus or C-terminus of the channel. The expression of the two baits was confirmed by Western blot against bait tag (Fig. 1b). Upon co-transformation of a human brain cDNA library with more than 10^7 clones as preys, TRPV4 baits determined a total of 44 potential interactors (Fig. 1c). The intensity of the colony blue colour, due to ß-galactosidase reporter, can be taken as a measure of the interaction strength. The more intense the blue stain the more constitutive, strong, the interaction is, whereas the lighter the stain the more transient, weak. Among interactors we found several already described TRPV4 partners such as calmodulin (CALM3), related calmodulin enzymes (CamKII) and a member of cadherin family (CDH6) [12, 19, 7].

TRPV4 interactome associates with immune response. To deepen in the potential TRPV4 physiological regulation, a molecular systems interactomics approach was employed. TRPV4 interactors determined by MYTH assay were used as template to build a putative TRPV4 PPI-based interactome. Gene enrichment based on protein co-localization, gene co-expression, genetic interactions and domain conservation was used to construct the network (Fig. 2a). Statistically significant (corrected p-values below than 0.05) GO-terms associated with the enriched TRPV4 interactome were manually clustered into cellular processes attending to their functional implications (Fig. 2a). The number of statistically significant GO-terms within each cellular process were quantified, being the most common GO-terms those related to cellular signalling processes, apoptosis, immune system response, metabolism, calcium regulation and cellular structure formation (Fig. 2a and supplementary).

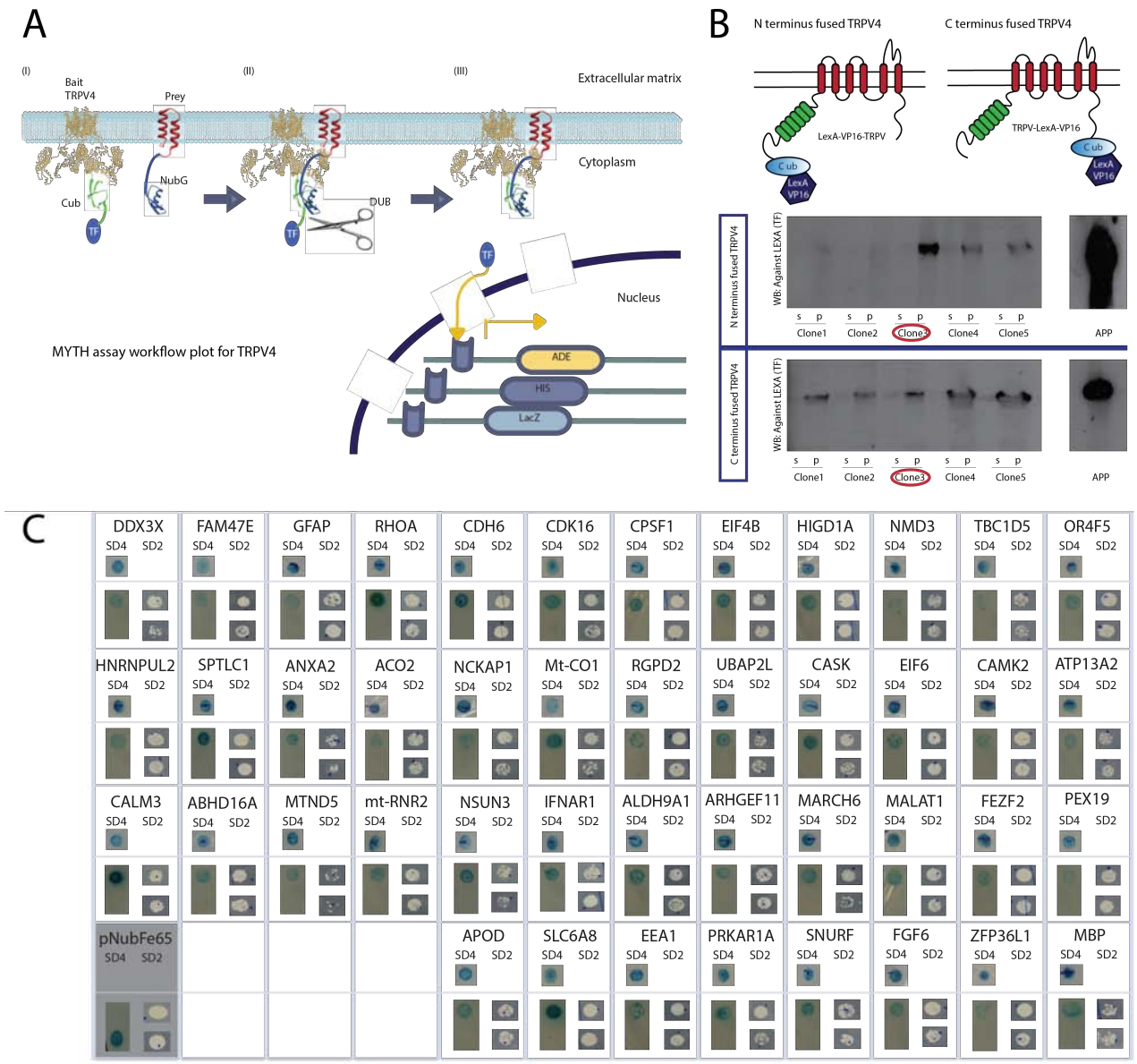

Figure 1. TRPV4 Membrane Yeast Two Hybrid Screen (MYTH). a) Workflow for MYTH assay. I. TRPV4 tagged with the bait C-terminus of ubiquitin (CUB) and VP16-LexA transcription factor (TF) was transformed in the Yeast reporter strain. II. cDNA library transformation of preys tagged with N-terminus of ubiquitin (NUBG). Upon interaction of bait and prey, ubiquitin is refolded and the degradation ubiquitin complex (DUB) releases the TF. III. TF goes to the nucleus and starts the expression of several reporter genes integrated in the strain that codify for auxotrophic markers Histidine, Adenine and ß-galactosidase enzyme. **b**) TRPV4 N-terminus and C-terminus bait expression confirmed by Western Blot (WB). APP fused to bait tag was used as positive control for the WB. **c**) Positive interaction partners determined by our MYTH screen. SD2 (non selective media), SD4 (selective media). First row within each interactor box corresponds to the image of the colony when firstly isolated from selective media (SD4). Second row corresponds to the re-transformation of the TRPV4 bait strain with each specific bait to confirm the interaction. Third row contains the transformation of the control strain pNUBFe65 carrying a non related bait as control for the specificity of the interaction.

Having a look into the genes associated to the most significant cellular processes we found that signalling cascades are mainly related to growth factors such as FGF6, cAMP-dependent protein kinases such as PRKAR1A or aldehyde dehydrogenases like ALD9A1 (Fig. 2b and supplementary). Apoptosis was represented by members of RHO GTP-ase signalling complex such as RHOA and ARHGEF1, whereas the calcium regulation associated to TRPV4 is related to calmodulin (CALM3) and calmodulin kinase CamKII (Fig. 2b and supplementary). Immune system responses are associated to viral infection related genes such as IFNAR1, the receptor for type I Interferons, that activates the JAK-STAT signalling pathway [20] or DDX3X, an ATP-dependent RNA helicase from Dead helicase family involved in mRNA metabolism, innate immunity and viral infection (Fig. 2b) [17]. Although

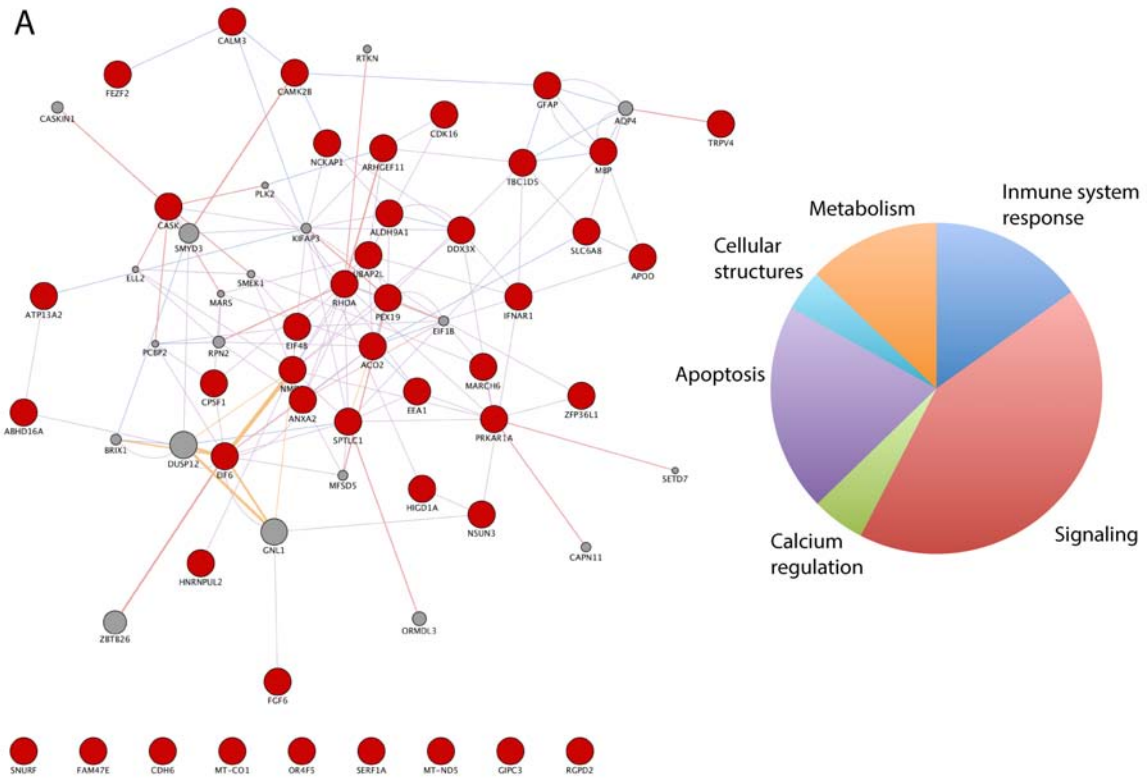

B

Process		Genes	pValue (highest association)
Inmune system response		DDX3, IFNAR1, RHOA	2.4 10-3
Signaling		TRPV4, FGF6, ARHGEF11, PRKA1A, ALD9A1, CamK2B	9.3 10-3
Calcium regulatory process		TRPV4, CALM3, CamK2B	2.2 10-2
Apoptosis		RHOA, ARHGEF11	4.2 10-2
Cellular structures		RHOA, ANXA2	4.2 10-2
Metabolic process		CDK16, MT-CO1, CASK, CamK2B	4.3 10-2

Figure 2. Systems biology approach for TRPV4 MYTH interactor screen. a) TRPV4 gene enriched interaction network by Genemania algorithm (see methods for further detail) based on protein co-localization, gene co-expression, genetic interactions and domain conservation. Red dots represent the potential interactors identified by MYTH screen. The pie chart represents statistically significant GO-terms clustered by their function (cellular process). The width of each pie potion corresponds to the number of GO-terms included within each cellular process. **b**) Table showing the MYTH TRPV4 partners included within each cluster of GO-terms. The p-value assigned to each cellular process corresponds to the most significant GO-term association to TRPV4 interactome within that cluster.

less abundant in number of GO-terms, the highest p-values for GO-term associations with TRPV4 network correspond to immune system processes and viral infection (p-value= 2.4 10^{-3}) (Fig. 2b and supplementary), leading us to further explore potential implications of TRPV4 in the immune system by characterizing some of these potential interactions, which have not been described previously elsewhere, to the best of our knowledge, opening new physiological roles for TRPV4.

TRPV4 interacts with ATP-dependent Dead Box Helicase 3 (DDX3X). Among the TRPV4 interactions related to immune system regulation we found DDX3X. In the cytosolic cellular context, DDX3X is involved in the formation of pre-initiation translation complex by its interaction with EIF4F and the translation of 5´structured mRNAs [21]. In the nucleus, DDX3X binds to the promoters of genes such as E-cadherin or IFNB1 and regulates their transcription [22, 23]. Thus, DDX3X plays important roles mediating cell adhesion and innate immune responses. Viruses have developed systems to highjack DDX3X for their own profit, making this protein essential for the translation of some viral proteins [24]. In the epithelium TRPV4 and DDX3X have some functional overlapping as both are capable to control at different levels mechanisms such as focal adhesions. TRPV4 interacts with E-cadherin and β-catenin and the channel expression and function play a role in focal adhesions formation [12, 25], whereas DDX3X controls cell adhesion by modulating E-cadherin and β-catenin expression levels [22, 26]. To confirm the veracity of TRPV4-DDX3X interaction, co-immunoprecipitation assay in HEK293 mammalian cell

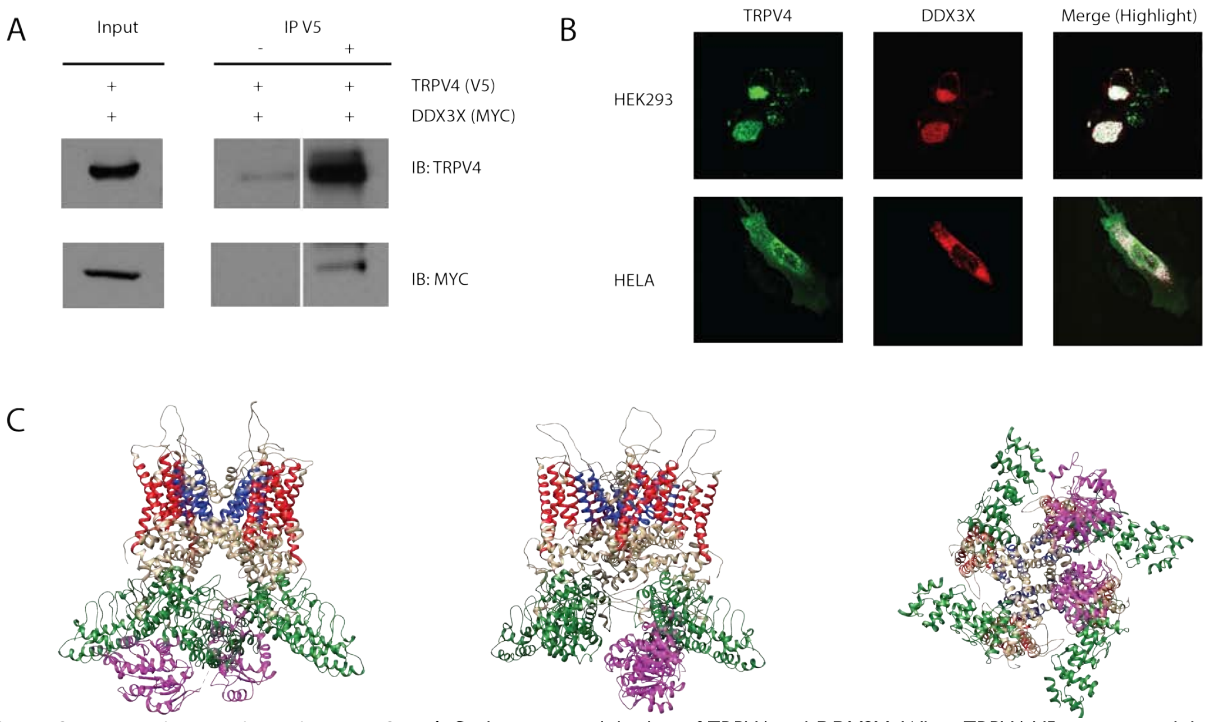

Figure 3. TRPV4 interaction with DDX3X. a) Co-Immunoprecipitation of TRPV4 and DDX3X. When TRPV4-V5tag was precipitated DDX3X-Myc tag was present in the eluted fraction, whereas no DDX3X was found in the control elution, lacking the antibody to precipitate TRPV4. **b**) Immunofluorescence of transfected HEK293 and HeLa mammalian cells. TRPV4-V5 tagged (green channel) and DDX3X-Myc tagged (red channel) were overexpressed in HEK293 and HeLa cell lines. Merge channel shows the co-localization between TRPV4 and DDX3X channels (White spots). **c**) TRPV4 DDX3X docking showing potential binding site for DDX3X within Ankyrin repeats domain (ARD) of TRPV4. TRPV4 is coloured in beige with several domains highlighted to ease the visualization. ARD domain (green), transmembrane segments 1-4, TM1-4 (red) and TM5-6 (dark blue). DDX3X is coloured in purple.

line overexpressing TRPV4 and DDX3X was carried out. When TRPV4 tagged with the V5 viral epitope was precipitated with an antibody against V5 tag (IP V5), TRPV4 was detected in the elution accompanied by DDX3X (Fig. 3a), whereas TRPV4 was hardly seen and DDX3X was not present in the control elution, when V5 antibody was absent (Fig. 3a). This indicates that TRPV4 forms complexes with DDX3X in a mammalian system, which was further addressed by immunofluorescence. When transiently transfected, TRPV4 was mainly located in internal membranous pools, producing an ER-like staining, and at the plasma membrane of either HEK293 or HeLa cells (Fig. 3b). DDX3X was mainly present in the cytosol (Fig. 3b). TRPV4 and DDX3X co-localized, shown as white pixels in the merge channel (Fig. 3b). Despite co-localization, either the Pearson coefficient (R= 0.4) or the distribution patterns were quite dissimilar between TRPV4 and DDX3, arguing for a potential transient nature of TRPV4-DDX3X interaction. Finally, interaction surface was mapped by computational means. Using docking software DOCK/PIERR the 10 potential binding places with higher score were mapped to the N-terminal ARD domain of TRPV4 (Fig. 3c), which locates within the cytosol. Here we show the docking position with higher free energy score (Fig. 3c). Further experimental validation is needed to undercover the binding site between TRPV4 and DDX3X.

TRPV4 controls DDX3X expression levels. Data mining from Genome Expression Omnibus (GEO) revealed that TRPV4 depletion by short hairpin (sh) RNA interference in an adipocyte cell line might produce a decrease in DDX3X mRNA levels [27]. We tried to corroborate if DDX3X protein expression is altered upon TRPV4 depletion. Human bronchial epithelial (HBE) cell line, a cell type that endogenously expresses TRPV4 and DDX3X, was infected either with a sh-control or a sh-TRPV4 RNA to generate stable HBE cell lines control or lacking TRPV4 channel, respectively. Depletion of TRPV4 was tested by calcium imaging measurements (Fig. 4a). When treated with GSK1016790A, a specific TRPV4 agonist, HBE original cell line presents a prominent calcium increase, measured by the Fura2 ratio 340/380, with around 90% of the cells responding (Fig 4a). sh-control HBE line is still able to produce intracellular TRPV4 mediated calcium increases, although amplitude and number of responding cells were decreased (Fig. 4a). Sh-TRPV4 HBE cell line presents an almost total depletion of GSK1016790A mediated calcium increase, pointing to a proper abrogation of TRPV4 activity (Fig. 4a), which was further evaluated by WB (Fig. 4b). Sh-TRPV4 HBE cells present a decrease in TRPV4 protein expression levels, and according to the previous reports, DDX3X expression was extremely reduced in sh-TRPV4 (p-value 0.0227)(Fig. 4b). Furthermore, DDX3X

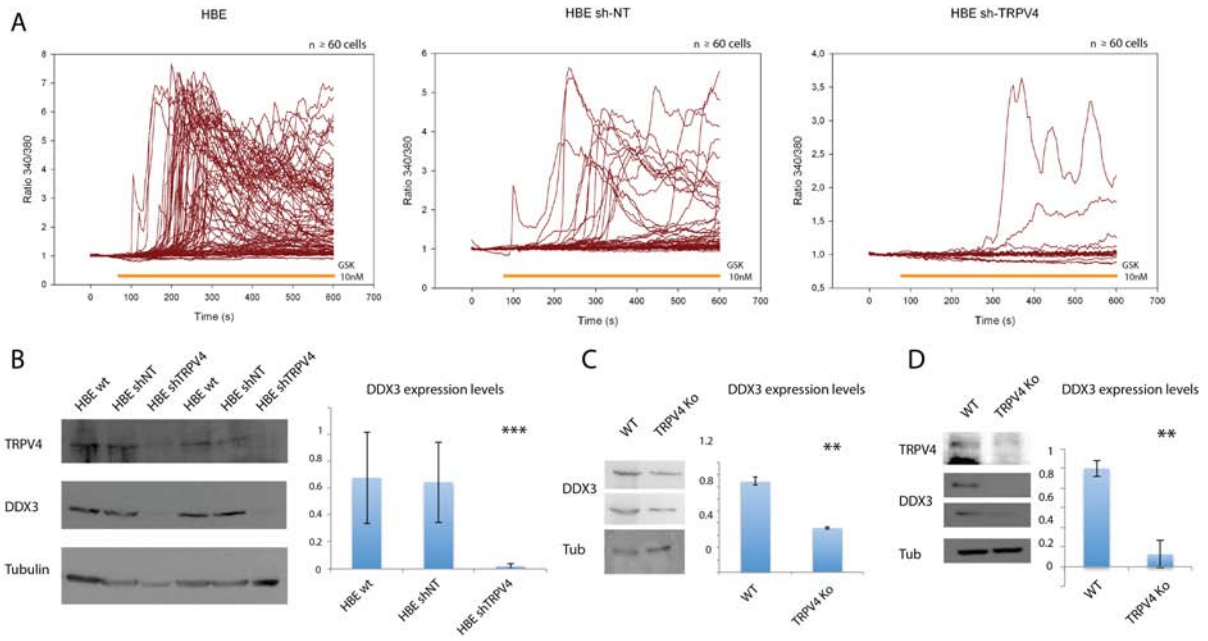

Figure 4. TRPV4 depletion leads to a decrease in DDX3X expression levels. a) Calcium imaging measurements of HBE cell lines. From left to right, HBE original strain, sh-control and sh-TRPV4. Intracellular calcium levels are represented by the Fura2 ratio 340/380 (Y axis). GSK1016790A was added at the minute 1 (X axis). Each red line represents a single cell measurement. **b**, **c** and **d**) Western blot against TRPV4 and DDX3X of HBE generated cell lines, **b**, WT and TRPV4 KO mice lung protein extracts, **c**, and MEF cell lines from WT and TRPV4 KO mice, **d**. Tubulin was included as loading control. Bar graphs represent DDX3X expression levels normalized by tubulin of 3 independent samples (n=3).

expression is reduced in TRPV4 knock out mice lung tissue (p-value 0.003, Fig. 4c) and TRPV4-KO mouse embryonic fibroblasts (MEF) (p-value less than 0.0001, Fig. 4d). The consistency of DDX3X depletion in different epithelial cells and tissues from different organisms argue for a widely extended mechanism that requires TRPV4 to maintain DDX3X protein levels.

TRPV4 activation promotes DDX3X translocation to the nucleus. DDX3X is a RNA helicase that locates mainly within the cytoplasm, although it shuttles between the nucleus and the cytoplasm carrying out diverse functions in both cellular compartments. In our attempt to determine potential functional implications of TRPV4-DDX3X interaction we wondered whether DDX3X cytosol-nuclear balance may change upon TRPV4 activation or not. Transiently transfected HeLa cells treated with the TRPV4 specific agonist GSK1016790A were visualized by immunofluorescence. Upon GSK1016790A treatment, non-transfected TRPV4 cells show no significant changes in DDX3X location, whereas TRPV4 transfected cells show a clear accumulation of DDX3X within the nucleus (Fig. 5a). This translocation of DDX3X from cytosol to the nucleus is inhibited by a TRPV4 specific antagonist, HC067047, pointing to the channel specific functioning as the trigger of DDX3X mobilization (Fig. 5a). To test the channel specificity of this interaction we used HeLa cells transiently transfected with TRPV1, a very close TRPV4-related ion channel from the same TRP subfamily. Activation of these cells by capsaicin, a specific agonist of TRPV1, leads to a similar translocation of DDX3X to the nucleus (Fig. 5b), arguing for a potential conservation of this mechanism among TRPV channels.

Additionally, GSK1016790A treatment produced a re-arrangement of TRPV4, which adopts a vesicular distribution with a markedly perinuclear staining (Fig. 5a). This rearrangement could be due to channel internalization, something that might explain previous reports that showed a calcium independent desensitization and decrease in TRPV4 plasma membrane levels after GSK1016790A activation [28]. Same effect and channel re-location was observed for TRPV1 after Capsaicin treatment (Fig. 5b).

DDX3X translocation to the nucleus is calcium dependent. TRPV4 activation by GSK1016790A leads to an intracellular calcium increase. It is already known that many transcription factors such as NFAT can be translocated to the nucleus upon changes in the calcium levels [29]. To assess whether DDX3X translocation is driven by similar mechanisms or not, the same experiment was performed incubating the cells in a calcium free medium. In this medium addition of GSK1016790A does not evoke calcium currents and the translocation of DDX3X was not observed, indicating that the process is calcium-mediated (Fig. 6a).

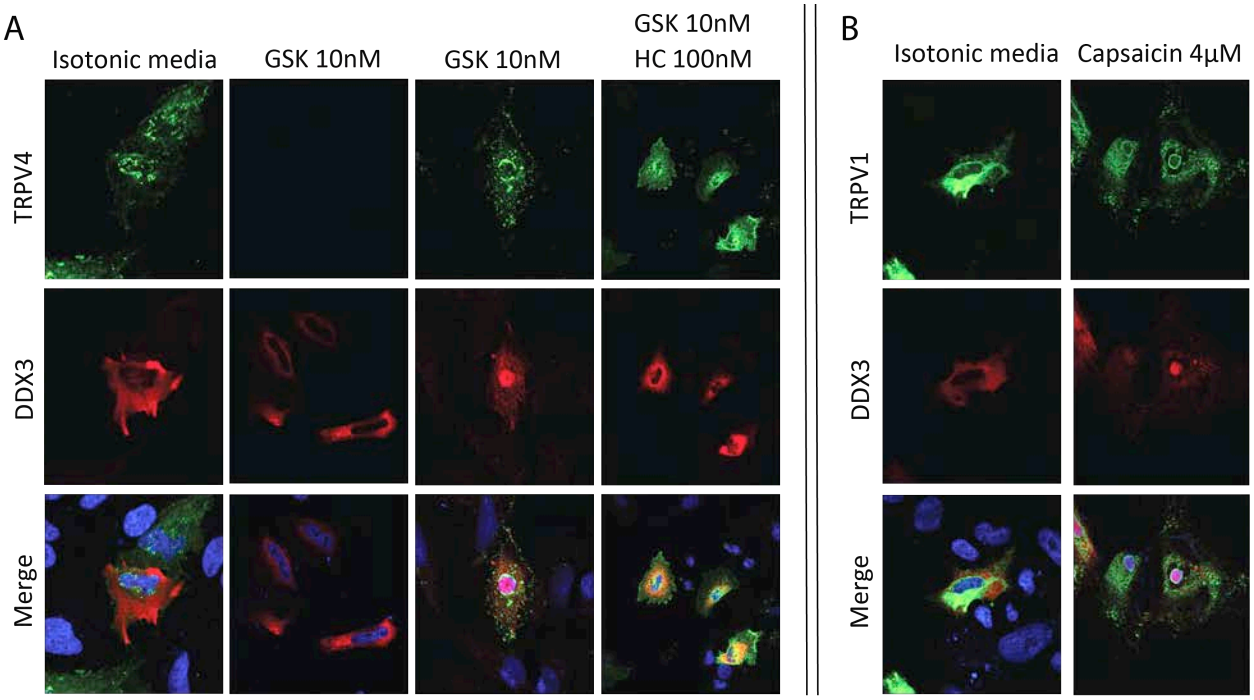

Figure 5. DDX3X translocates to the nucleus upon activation of TRPV channels. **a**) Transiently transfected HeLa cells expressing TRPV4 (green) and DDX3X (red). **b**) Transiently transfected HeLa cells expressing TRPV1 (green) and DDX3X (red). Merged channels include nuclear staining (Blue) to ease the visualization of DDX3X location.

Interestingly, DDX3X adopts a more membranous stain pattern, that may reflect a potential recruitment of the protein to the membrane (Fig. 6a). Contrary, Ionomycin treatment, that generates pores in the cell membranes and produces an unspecific entry of calcium to the cell, did not alter DDX3X localization (Fig. 6a). Similarly, Thapsigargin treatment, that increases cytosolic calcium levels by inhibiting the SERCA pump and therefore the calcium entry to the ER, lately producing an ER calcium depletion, did not alter DDX3X cytosolic location (Fig 6a). All together, these results indicate that DDX3X translocation process is dependent on the specific calcium entry through TRPV4 from the extracellular medium and might be not only related to unspecific calcium increases.

As the process seems to require TRPV4-coupled calcium entry, we asked if calcium related modulators already described to interact with TRPV4, such as calmodulin, mediate in the TRPV4 evoked DDX3X translocation. The cells were incubated with broad-spectrum calmodulin inhibitors, W7 and Calmidazolium (Fig. 6b). The presence of these compounds does not affect DDX3X cytosolic location, although translocation to the nucleus upon GSK1016790A addition was abrogated, either when W7 and Calmidazolium were used separatedly or in combination (Fig. 6b). Interestingly, other inhibitors of kinases downstream of ion channels such as KT5720 inhibitor of PKA, PP2 inhibitor of SRCs or AACoCF3 Inhibitor of PLA2 did not prevent DDX3X translocation (Supplementary information).

TRPV4 binds calmodulin on its N- and C-termini [78]. To investigate if calmodulin binding to the channel is important for the TRPV4-calmodulin dependent DDX3X translocation we tested a mutant lacking the C-terminal calmodulin binding site, Δ-Cam TRPV4, which is functional and responds to GSK1016790A. Δ-Cam TRPV4 was able to translocate DDX3X in a similar way than the wild type TRPV4 channel (Fig. 6c), indicating that the calmodulin binding site on the C-terminus is dispensable for the TRPV4-dependent DDX3 translocation. Further investigation on the N-terminus calmodulin binding will help to clarify if calmodulin-TRPV4 interaction is required for the TRPV4-DDX3X interaction.

The mobilization of proteins between cellular compartments is often mediated by phosphorylation processes. As DDX3X translocation is conducted by calmodulin, CamKII, a calcium/calmodulin dependent kinase that has been proposed as a downstream effector of TRPV channel activation, was inhibited by the specific blocker KN-93 and TRPV4 mediated translocation of DDX3X evaluated (Fig. 6c). KN-93 does not affect the cytosolic location of DDX3X but it does block the translocation of DDX3X to the nucleus upon TRPV4 activation (Fig 6c), determining the need of CamKII activity and potential phosphorylation of DDX3X as crucial step for TRPV4 control over DDX3X location.

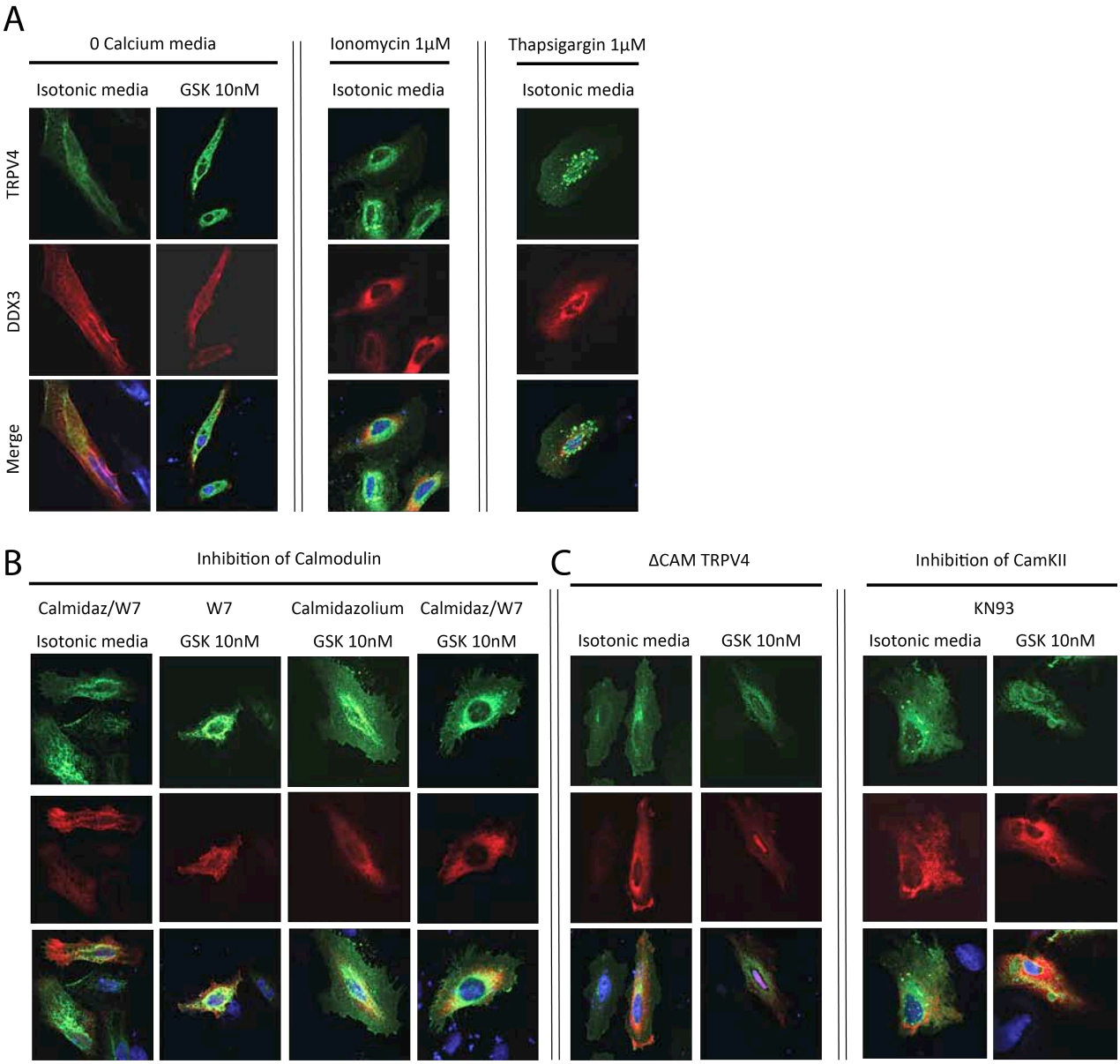

Figure 6. TRPV mediated DDX3X translocation is calcium/Calmodulin/CamKII dependent. **a**, **b** and **c**) Transiently transfected HeLa cells expressing TRPV4 (green) and DDX3X (red). Merged channels include nuclear staining (Blue) to ease the visualization of DDX3X location. **a**) Calcium dependency of DDX3X translocation. **b**) Calmodulin dependency of DDX3X translocation. **c**) Calmodulin binding and CamKII dependency of DDX3X translocation.

DDX3X is recruited to TRPV4 complex upon channel activation. The nuclear translocation mediated by TRPV4 activity might require of DDX3X location in close proximity to the TRPV4, calmodulin, CamKII complex. In vivo imaging of transiently transfected HeLa cells upon GSK1016790A treatment revealed a significant rapid increase of TRPV4-DDX3X co-localization (Pearson coefficient increase of 0.2, Fig. 7). This increase in co-localization was maintained for around 2-4 minutes and followed by a strong decay as DDX3X was gradually accumulated in the nucleus (Fig. 7). Initial increase and subsequent decay in TRPV4-DDX3X co-localization were statistically significant when compared to the basal co-locatization levels (p-values 0.0097 and 0.0008 respectively for 3 independent experiments, Fig. 7).

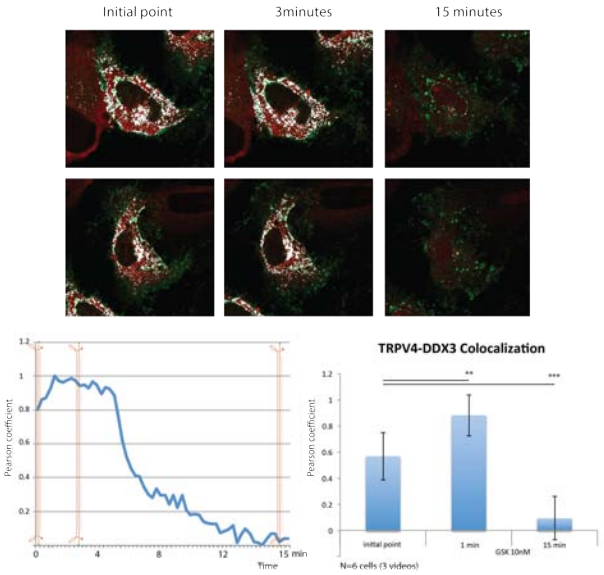

Figure 7. TRPV4 and DDX3X increase their co-localization upon channel activation, followed by DDX3X nuclear translocation. Above, images of two cells at different time points: 0 minutes, 3 minutes and 15 minutes after GSK1016790A treatment. Bottom left, time line plot of co-localization. Pearson coefficient (Y axis) was plotted along time after GSK1016790A treatment, showing an early increase in Pearson coefficient followed by a strong decay. Bottom right, mean and standard deviation of Pearson coefficients for TRPV4-DDX3X co-localization at three time points: 0, 3 and 15 minutes after GSK1016790A addition (n=3).

TRPV4 control over transcription and translation. In the cytosol, DDX3X participates in the translation of structured 5´UTR (untranslated region) mRNAs [21], while within the nucleus, DDX3X binds to several promoters such as the E-cadherin and IFNB1 promoters and enhances IFNB1 transcription while inhibit the E-cadherin expression [23, 22], affecting processes of transcription and translation. As TRPV4 presence affects DDX3X expression levels and TRPV4 activity is able to control DDX3X location, we wondered if TRPV4 might mediate in transcription and translation through the control of DDX3X. In order to asses if TRPV4 presence or activity affects transcription and translation, we constructed several luciferase reporters containing an SV40 promoter, that will allow the visualization of general transcriptional changes, followed by highly structured 5´UTRs of genes of our interest: C-MYC, SOX9, E-cadherin, TGFB1 and BACE.

First, a cell viability assay (MTT) was performed to check whether the different treatments used during the transcription-translation experiments lead to mortality, affecting the reporter readouts. HEK293 transiently transfected with empty vector (pcDNA3) or TRPV4 and subjected to isotonic medium, GSK1016790A, HC067047, calcium-free medium or BAPTA treatments present similar viability (Fig. 8a), allowing the comparison between conditions.

Overexpression of DDX3X in HEK293 cells produced a significant decrease in the expression of E-cadherin and TGFB1 constructs (p-values 0.0181 and 0.0022 respectively), whereas no significant changes were observed for SOX9, C-MYC and BACE (Fig. 8b). This observation implies a major effect of DDX3X overexpression in the translation of 5´UTR from E-cadherin and TGFB1 genes. DDX3X transfection produces no general effects in transcription as some reporters used present no significant differences. Overexpression of TRPV4 lead to a dramatic and significant decrease of transcriptional-translational levels for all the reporters used (p-values below 0.0001; Fig. 8b), pointing to a general role of TRPV4 in gene regulation both at transcription and translation levels. TRPV4 activation upon hypotonic cell swelling leads to a significant increase in transcription translation levels of C-MYC, E-cadherin, TGFB1 and SOX9 (p-values 0.0289, 0.0005, 0.0495 and 0.0003, respectively; Fig. 8c). No changes were observed in cells transfected with BACE (Fig. 8c) or with empty vector. Moreover, the activation of TRPV4 by the specific agonist, GSK1016790A in TRPV4 transiently transfected cells produced a significant decrease of all reporters (p-values 0.01, 0.2041 and 0.0034, respectively; Fig. 8d), indicating that activation of TRPV4 has a general effect on transcription and translation, i.e. in genic regulation. Cells were treated with HC067047 which was able to revert the decrease in transcription and translation provoked by TRPV4 activation with GSK1016790A (Fig. 8d).

To understand the mechanism of TRPV4 in transcription and translation we used the E-cadherin reporter construct to compare between different TRPV4 mutants. TRPV4 121AAWAA, a mutant that responds to the agonist GSK1016790A but is insensitive to hypotonicity, was able to rescue the phenotype observed after hypotonic shock (Fig. 8e). The B isoform of the channel codifies for a TRPV4 isoform, which is not able to tetramerize or be trafficked to the plasma membrane. This mutant shows the same levels of transcription and translation of E-cadherin as compared to the empty vector transfection (Fig. 8e). Δ-Cam presented the same transcription-translation levels than TRPV4 wild type (Fig. 8e). The analysis here presented points to the need of functional TRPV4 in the plasma membrane to regulate transcription and translation.

As the observed effects are dependent on channel function we wondered whether they were calcium sensitive. Ionomycin treatment produce a significant decrease in transcription-translation levels, although the decrease was 8 fold smaller than the observed upon TRPV4 transfection (p-values 0.0304 and less than 0.0001 respectively; Fig. 8f).

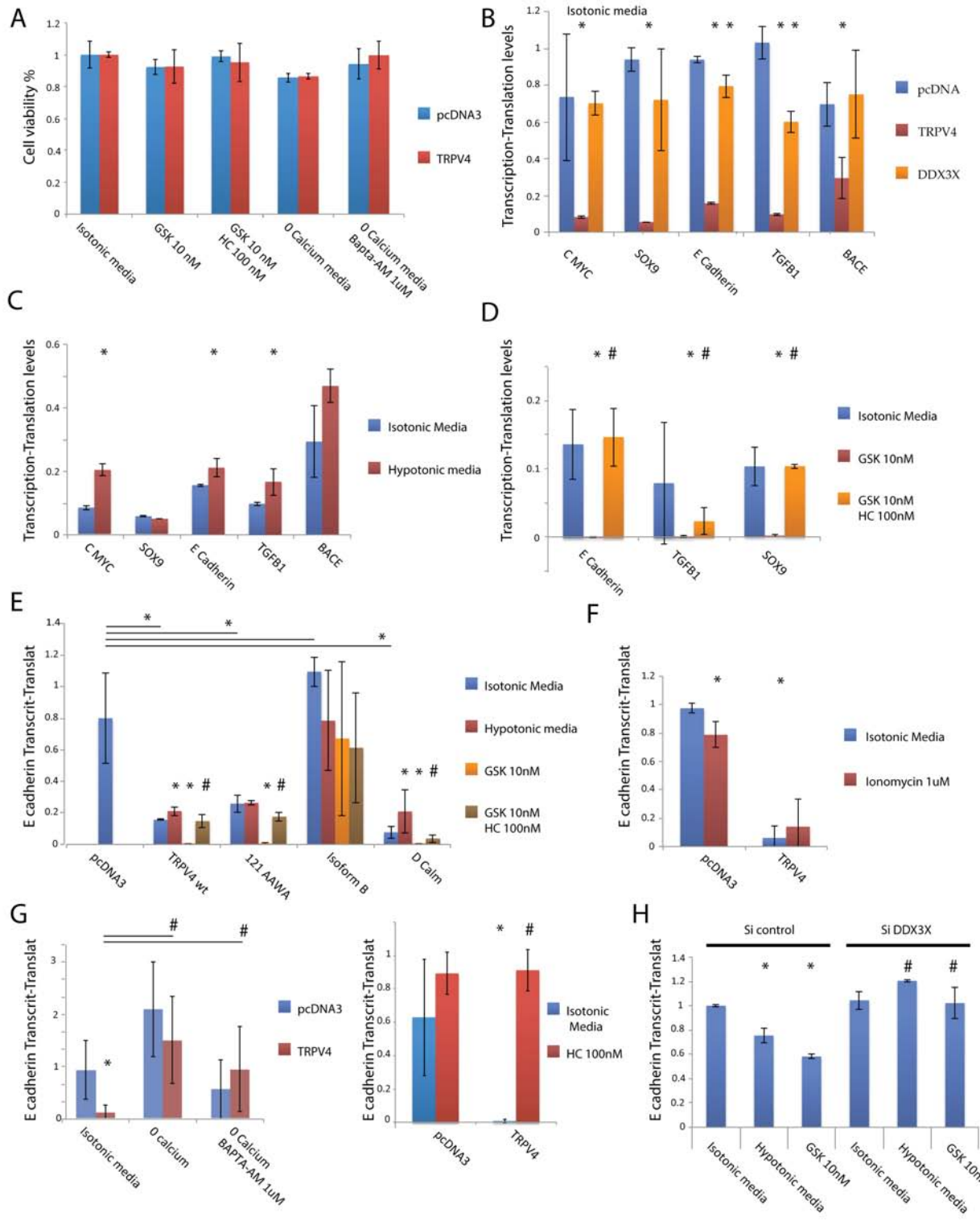

Figure 8. TRPV4 control of Transcription-Translation. **a**) MTT viability assay of HEK293 cells subject to several treatments: GSK1016790A, HC067047, Calcium starvation and BAPTA-AM (n=3). **b**) Transcription-translation monitoring using luciferase reporters for SV40 promoter and 5´UTR of CMYC, SOX9, E-cadherin, TGFB1 and BACE genes. Transiently transfected HEK293 cells over-expressing pcDNA3 (empty vector), TRPV4 or DDX3X were tested (n=3). **c**) Transcription-translation changes upon hypotonic cell swelling in HEK293 transiently transfected with TRPV4 (n=3). **d**) Transcription-translation changes upon GSK1016790A treatment in HEK293 transiently transfected with TRPV4 (n=3). **e**) E-cadherin transcription-translation levels produced by the transfection and activation of TRPV4 mutants (n=3). **f**) E-cadherin transcription-translation levels upon Ionomycin treatment (n=3). **g**) E-cadherin

Transcription-translation levels in HEK293 cells transiently transfected with empty vector or TRPV4 and subject to calcium depletion and channel basal activity inhibition (n=3). **h**) E-cadherin Transcription-translation levels in HBE cells treated with hypotonic media or GSK1016790A. Cells were transiently transfected with Si-control or Si-DDX3X RNA interference (n=3).

Furthermore, when grown in a calcium-free medium or upon BAPTA addition to avoid intracellular calcium rises, there were no significant differences in transcription or translation upon TRPV4 transfection (Fig. 8g). The use of the TRPV4 specific antagonist, HC067047, prevents the decrease observed in transcription or translation (Fig. 8g). These results argue for a specific calcium entry through TRPV4 as main responsible of the observed changes in transcription or translation.

HBE cell line was transiently transfected with the E-cadherin reporter and a short interference RNA, either mock or against DDX3X. HBE cells were treated with hypotonic media or GSK1016790A in order to promote TRPV4 activation. TRPV4 activity produced a significant decrease in E-cadherin transcription and translation (p-values 0.0021 and below 0.0001, respectively). This effect was reverted upon DDX3X depletion by siRNA (Fig. 8h).

TRPV4 regulates viral translation. DDX3X not only regulates transcription or translation of cellular structured 5´UTR, but it plays an important role in viral infection, as some virus highjack DDX3X to promote the translation of their own RNAs, which is a relatively conserved mechanism. Ded1, the yeast DDX3X ortholog, is crucial for translation of the viral polymerase-like protein 2a, encoded by Brome mosaic virus (BMV) RNA2 [24]. Accordingly, TRPV4 MYTH interactome showed a high association with viral infection and immune system processes, which opens the possibility that the function of TRPV4 over DDX3X can also be related with viral protein translation. Taking advantage of the model system *Saccharomyces cerevisiae* we compared the wild type strain with the ΔYVC1 strain, where YVC1, the TRP channel homolog in yeast[30], was deleted. These two strains were transformed with the viral RNA 2a to monitor the protein 2 expression levels. Deletion of YVC1 gene produced a significant decrease in the viral 2a protein levels (below 50% of translation, p-value 0.0039), indicating that viral protein translation was affected (Fig. 9a). To corroborate that TRPV4 is responsible for this effect, ΔYVC1 strain was transfected with the human TRPV4 expression baits from the initial yeast two hybrid screen. Both plasmids, revert to some extent the decay in viral protein translation (Fig. 9b). In the case of TRPV4 N-terminal tagged (pBT3-N TRPV4) the recovery of viral translational levels was almost complete, whereas C-terminal tagged TRPV4 was 30% less efficient to revert the effect of YVC1 depletion in viral translation (Fig. 9b).

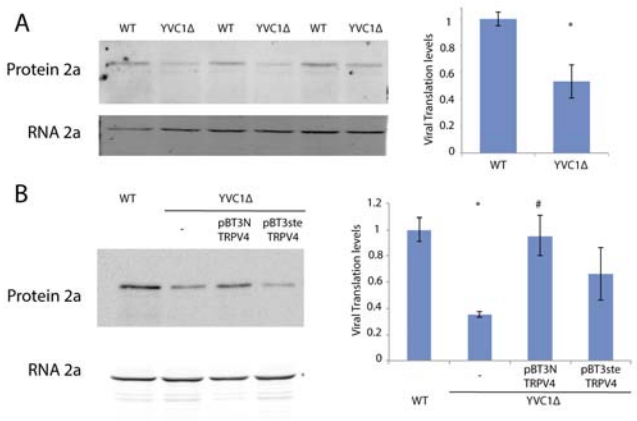

Figure 9. TRPV4 control over viral RNA translation. **a**) Western blot and qPCR against viral protein 2a from wild type and ΔYVC1 yeast strains. **b**) Western blot and qPCR against viral protein 2a from wild type and ΔYVC1 yeast strain transformed with TRPV4 MYTH bait constructs. Viral translation levels were quantified as the ratio between protein and RNA levels for 3 independent samples (n=3), plotted as a bar plot **a** and **b**.

Discussion

Despite the huge efforts carried out to elucidate the mechanisms underlying TRPV4 regulation over cell physiology, there is still a lot to know about the potential effectors located downstream of this channel. Here we report a yeast two hybrid screen that identified 44 potential interactors for TRPV4 (Fig. 1). Among the identified partners we found proteins that already have been associated with TRPV4 such as calmodulin (CALM3)[7] or E-cadherin (CDH6)[12], which are good indicators of the accuracy of our approach. Gene enrichment analysis of TRPV4 interactome obtained by MYTH highlighted the association of this set of proteins with cellular processes such as signalling and calcium regulation, typical actions for an ion channel, and immune system regulation or apoptosis (Fig. 2). The lowest p-values indicating the highest levels of association were related to immune system responses and viral infection regulation (Fig. 2 and supplementary). Indeed, TRP channels have shown to play diverse roles in immune system. For instance, TRPV4 activation by hypotonic stress triggers developmental immunity in skin keratinocytes through TGFB1/NFKB signalling pathway [31]. In airway epithelia, TRPV4 regulates immune response at several levels. In the lungs, TRPV4 promotes macrophage activation [32] and stimulates smooth muscle cell proliferation [33]. Furthermore, TRPV4 mediates pulmonary inflammation upon chemical insult [34], affecting through its activity the epithelial barrier function and membrane permeability of the respiratory epithelia [35], which potentially increases susceptibility to opportunistic infections .

Concerning to response to virus, no specific role for TRPV4 has been proposed to date, although TRPV4 inhibition regulates T cell activation by suppressing tumour necrosis factor, interleukin-2, interferon-γ release and effector cytokines production [36], which may have an impact in immune system performance upon viral insult. It has been shown that replication of many viruses is related to intracellular calcium concentration and TRPs modulate ion concentrations. Studies in neuroblastoma cells with close homolog TRPV1 and distant related TRP member TRPA1 revealed an upregulation in TRPs expression levels upon Rhinovirus infection [37], suggesting potential implications of TRPs in viral infection and pathogenesis.

Among the TRPV4 MYTH partner genes related to viral infection, we determined the interaction with DDX3X, a cytoplasmatic RNA helicase from the Dead box family of helicases (Fig. 3). This is the first time a member of the Dead box helicase family is described to directly interact with an ion channel. TRPV4-DDX3X interaction implies the direct link of extracellular insults sensed by the channel such as osmolality or temperature to regulation of transcription-translation mediated by the helicase. Although DDX members have not been related to TRPV channels previously, this family of helicases carries out roles related to TRPV members. Plant DDX homologs are crucial for plant surveillance upon high salinity and cold insult [38, 39]. Furthermore, DDX3X mutation produced thermal sensitivity in hamster BHK21 cells, arresting cell cycle at 39,5°C in the G1 to S transition phase [40]. Altogether, these evidences highlight the potential functional coupling of these two protein families.

Specifically, TRPV4-DDX3X interaction entails several functional implications. We showed that DDX3X and TRPV4 levels are linked in epithelial tissues from human and mice (Fig. 4). Silencing or knocking down TRPV4 leads to a decay in DDX3X expression levels. This mechanism might partially explain the role of TRPV4 in regulation of adherent junctions [12] and trailing adhesion [13], as DDX3X negatively modulates cell adhesion and motility by increasing Snail levels and by regulating RAC-1 signalling pathway [41, 26]. These evidences point to DDX3X as potential effector of TRPV4, with potential pathophysiological implications, since DDX3X levels correlate with cancer malignancy [22].

TRPV4 channel activation leads to nuclear translocation of DDX3X (Fig. 5), arguing for a coupling of TRPV4 and DDX3X in the same signalling pathway. Translocation is mediated in the case of Ded1, DDX3X yeast homolog, by the importins CRM1 and MEX67 that keep the equilibrium between nuclear and cytosolic DDX3X [42]. TRPV4-mediated nuclear translocation of DDX3X is dependent on the extracellular calcium entry coupled to the channel and calmodulin/CamKII activity (Fig. 6). Furthermore, it might imply the recruitment of DDX3X to TRPV4/Calmodulin/CamKII complex (Fig. 7), an issue that should be further addressed by Förster Resonance Energy Transfer (FRET) and Total Internal Reflection Fluorescence (TRIF). DDX3X binds to calmodulin in a phosphorylation dependent manner [43], so it is expected that DDX3X would specifically bind to TRPV4/Calmodulin/CamKII complex upon TRPV4-mediated calcium entry and the appropriate calcium-dependent modifications happening on the complex. As the effect that we observed occurs in the plasma membrane, far from the nucleus, we speculate that channel activation leads to posttranslational modifications of DDX3X, potentially phosphorylations by CamKII, that result in an increase of DDX3X translocation to the nucleus.

Our study also reports that TRPV4 expression can modulate the transcription and translation of a heterogeneous group of genes (Fig. 8), arguing for a potential TRPV4-mediated general regulation of transcription-translation. The fact that TRPV4 overexpression in HEK293 leads to a stronger change in transcription-translation of these reporters than DDX3X might imply that TRPV4 control over transcription-translation is not a single pass path, but rather an arborescence path, so the observed effects might be mediated by several transcriptional and translational factors downstream of TRPV4, with DDX3X being just one of them. Indeed, factors such as NFKB have been already located downstream of TRPV4 activity [44]. In HBE, with endogenous TRPV4 and DDX3X levels, the effect of TRPV4 activation is reverted upon DDX3X silencing, indicating that although this helicase might not be the only player downstream of TRPV4, it carries most part of the channel effect over transcription-translation in this cell line and, by inference, potentially in the epithelial airways.

Finally, among the implications of DDX3X in transcription and translation related to viral infection, its yeast homolog Ded1 mediates in viral translation of RNA 2a protein, being a crucial gene for this process [24]. Depletion of the yeast TRPV4 homolog YVC1 (ΔYVC1) results in a decrease in translation of RNA 2a, that was recovered upon TRPV4 transformation into the ΔYVC1 yeast strain (Fig. 9). Decrease in Ded1 levels results in a similar effect. Thus, a plausible explanation is that depletion of TRPV4 homolog YVC1 might potentially decrease Ded1 levels, similar to what we observed in mice and human cells and epithelial tissues.

In conclusion, our study indicates that TRPV4 plays a role in immune system response to viral infection, which in part is mediated by its interaction with DDX3X. At least in our cell biology experiments TRPV4 controls DDX3X levels in human and mice epithelial tissues and its activity regulates DDX3X translocation to the nucleus in a TRPV4/calcium/Calmodulin/CamKII dependent manner. Furthermore, TRPV4 has an effect over general transcription and translation through DDX3X and other potential factors coupled to the channel activity. This control on transcription-translation is mostly mediated by DDX3X in epithelial tissues and might have potential relevance in the translation of viral RNAs and other infectious agents.

Methods

Membrane Yeast Two Hybrid Assay (MYTH). MYTH assay was previously described by Snider and colleagues (27). MYTH reporter strain NMY51, containing reporter genes HIS3, ADE2, and lacZ downstream of lexA operators, was purchased from Dualsystems Biotech (P01401-P01429). Western blot against LexA tag was used to confirm the correct expression of the generated baits. NMY51 yeast cells expressing GFP tagged baits were fixed and visualized using a Leica TCS SP5 confocal microscope. The MYTH assay was performed essentially following the provider instructions (P01401-P01429). Transformation efficiency of the human brain cDNA library into NMY51 carrying the bait constructs was higher than $2x10^6$. Transformants were plated into SD selective agar plates. pBT3-N TRPV4 was plated SD-His Ade 7,5mM 3AT plates and pBT3-STE TRPV4 SD-His Ade 10mM 3AT plates for C-TRPV4, After incubation at 30 °C for 3–5 days, transformants were transfered into selective plates whit same stringency but containing 5-bromo-4-chloro-3-indolyl-β,d-galactopyranoside (X-Gal). Prey plasmids were then recovered by miniprep kit, transformed into Dh5α E. coli competent cells, purified from E. coli, and sequenced. Isolated prey plasmids carrying a putative interaction partner were then re-transformed into NMY51 strain containing the original bait to confirm the interaction.

Gene enrichment and network analysis. Genes determined by the MYTH assay for TRPV4 (44 hits) were used to construct a network in Cytoscape with Genemania App. The network was constructed using as template the Genemania Human genome and adding the 100 closest related genes based on colocalization, co-expression, physical interactions and domain conservation. Bingo Cytoscape app was used to find Go-Term categories statistically enriched within the TRPV4 network. P-values of Go-terms were calculated with the hypergeometric test and corrected with the Benjamini&Hochberg FDR algorithm. Statistically significant Go-Terms were manually clustered by their function as cellular processes. Each cellular process includes a series of functionally related Go-Terms from Bingo analysis. TRPV4 partners associated to each cellular process were quantified and represented as a pie chart.

DNA plasmids and clonings. pBT3-STE vector (P03233), control bait protein pTSU-APP, control prey pPR3-N (P01401-P01429) and cDNA library from human brain (P12227,) were purchased from Dualsystems. Human TRPV4 full length was cloned into pPR3-N and pBT3-STE within SfiI sites.
pcDNA3 TRPV4 vector and TRPV4 V5 tagged vector within the first extracellular loop were previously generated in Valverde Lab. DDX3X myc/flag tag was kindly provided by Dr. Hiroshi Yoshizawa from Niigata University.
Luciferase reporters were constructed using the pGL4 plasmid from Promega (E665A). Sv40 promoter was cloned within SfiI site. 5´UTR from BACE, C-Myc, E-cadherin, TGFB1 and Sox9 were cloned within KpnI, HindIII sites.

Cell cultures and transfection. MEF, HEK293 and HeLa cells were cultured in Dulbecco's modified Eagle's medium (DMEM, D6046 Sigma) supplemented with 10% FBS, 100 units/mL penicillin and 100 µg/mL streptomycin. HBE were cultured in HBE media. Transfection was performed using polyethyleneimine (PEI, Polysciences, 23966). HEK293 cells overexpressing the transfected constructs were lysed 48 hours after transfection and membrane proteins solubilized for 30 min at 4°C in lysis buffer (50mM Tris-HCL pH 7.4, 150mM NaCl, 5mM EDTA, 0.5% NP40, 1mM DTT, 10mM 13-GP, 0.1mM Na_3VO_4, 1ug/ul pepstatin, 2ug/ul aprotinin, 0.1mM PMSF, 1mM benzamidine and EDTA-free protease inhibition cocktail, ROCHE 11873580001). Cell extracts were centrifuged at 14000g at 4°C for 10 min to remove aggregates.

Western blot. Lysates and immunoprecipitates were loaded into SDS-page gels and run at 100mV for 90 min. Gels were transferred to nitrocellulose membranes into an iBlot cast (IB1001, Invitrogen). Membranes were blocked in blocking buffer (5% non-fat-dry milk TTBS 1x) ON at 4°C. Primary antibodies were incubated in blocking buffer for 1 hour RT. Primary antibodies were diluted as follows: anti LexA tag (sc-107150, SantaCruz) 1:1000, anti V5 tag (R9612-25, Sigma) 1:1000, anti Myc tag (M4439, Sigma) 1:1000, anti DDX3X (37160, Abcam) 1:1000, anti TRPV4 (self generated) 1:1000, Secondary antibodies were incubated for 1 hour at RT. Anti mouse (NXA931, GE healthcare) and anti rabbit (NA934, GE healthcare) were used at 1:2000 dilution in blocking buffer. Membranes were developed with West Pico chemoluminiscent substrate (34080, Thermo Fisher).

Co-Immunoprecipitations. Soluble fractions from cell lysis were used as input for co-immunoprecipitations. Cell extracts at 1 µg/ µl (500 µg total protein) were incubated ON at 4°C with anti V5 antibody (R9612-25, Sigma). Immuno-complexes were then incubated with 50uL of sepharose beads (17-0618-01, GE) for 2 hours at 4°C. After incubation complexes were washed with PBS1x buffer 3 times. Immunoprecipitated complexes were denatured with SDS-PAGE sample buffer (90°C for 5 min), separated by SDS-PAGE and analyzed by western blotting.

Immunostain and imaging. HeLa transiently transfected cells on coverslips were fixed in 4%PFA for 10 minutes 24 hours post-transfection. Cell were then permeabilized in 0.1% Triton PBS1x for 10 minutes and blocked in 2% BSA 1%FBS for 1 hour. Antibodies were used in a 1:1000 dilution against TRPV4 and Myc. Secondary antibodies A555 Mouse (A21424, Lifetechnologies) and A647 Rabbit (A21245, Lifetechnologies) were used in a 1:2000 dilution. All antibodies were diluted in blocking buffer and incubated for 1 hour. Nuclear staining was performed with Dapi (62248, ThermoFisher), dilution 1:1000 for 10 minutes. All coverlids were mounted with Mowiol.

Docking. TRPV4 3D model was constructed based on TRPV1 Cryo-EM solved structure (3J5P, PDB). DDX3 structure (2I4I, PDB) was previously solved. Molecular docking studies were performed with DOCK/PIERR docking algorithm based on residue contact potential PIE and atomic potential PISA. Dock/Pierr server (http://clsb.ices.utexas.edu/web/dock.html) from the Computational Life Sciences and Biology.

Luciferase assay. Cells were seeded in a 96 well plate at a density of 10.000/well. For luciferase assays, 200 ng of a given reporter construct, 20 ng of renilla (E2940, Promega) and/or 300 ng of pcDNA3 empty/TRPV4/DDX3X per 3 wells were used for transfection. We did triplicates of 3 wells. After transfection, cells were maintained in 100 µl of growth media 24 hours and then treated as desired. Treatments were performed overnight.

After treatment, cells were lysed in 50 µl of Optimem plus 50 µl of 1X passive lysis buffer (PLB buffer from Promega) at room temperature for 15 minutes. For dual luciferase assay, lysates were subjected after first readout to analysis of firefly renilla luciferase (50 µl of stop and glow buffer and 1 µl renilla substrate). Luminescence was read. Each sample was red for 7 times for the reporter and 7 times for the Renilla. Values here represented are ratio Reporter/Renilla, to standardize the data by the number of transfected cells in each well.

References

1. Bootman, M. D. *et al.* Calcium signalling: an overview. *Semin. Cell Dev. Biol.* **12,** 3–10 (2001).
2. Masuyama, R. *et al.* Calcium/calmodulin-signaling supports TRPV4 activation in osteoclasts and regulates bone mass. *J. Bone Miner. Res.* **27,** 1708–1721 (2012).
3. McAlexander, M. A., Luttmann, M. a, Hunsberger, G. E. & Undem, B. J. Transient receptor potential vanilloid 4 activation constricts the human bronchus via the release of cysteinyl leukotrienes. *J. Pharmacol. Exp. Ther.* **349,** 118–25 (2014).
4. Güler, A. D. *et al.* Heat-evoked activation of the ion channel, TRPV4. *J. Neurosci.* **22,** 6408–6414 (2002).
5. Liedtke, W. *et al.* Vanilloid receptor-related osmotically activated channel (VR-OAC), a candidate vertebrate osmoreceptor. *Cell* **103,** 525–35 (2000).
6. Suzuki, M., Mizuno, A., Kodaira, K. & Imai, M. Impaired pressure sensation in mice lacking TRPV4. *J. Biol. Chem.* **278,** 22664–22668 (2003).
7. Phelps, C. B., Wang, R. R., Choo, S. S. & Gaudet, R. Differential regulation of TRPV1, TRPV3, and TRPV4 sensitivity through a conserved binding site on the ankyrin repeat domain. *J. Biol. Chem.* **285,** 731–40 (2010).
8. Strotmann, R., Schultz, G. & Plant, T. D. Ca2+-dependent potentiation of the nonselective cation channel TRPV4 is mediated by a carboxy terminal calmodulin binding site. *J Biol Chem* **30,** 30 (2003).
9. Xu, H. *et al.* Regulation of a transient receptor potential (TRP) channel by tyrosine phosphorylation: Src family kinase-dependent tyrosine phosphorylation of TRPV4 on TYR-253 mediates its response to hypotonic stress. *J. Biol. Chem.* **278,** 11520–11527 (2003).
10. Garcia-Elias, A., Lorenzo, I. M., Vicente, R. & Valverde, M. A. IP3 receptor binds to and sensitizes TRPV4 channel to osmotic stimuli via a calmodulin-binding site. *J. Biol. Chem.* **283,** 31284–31288 (2008).
11. Cuajungco, M. P. *et al.* PACSINs bind to the TRPV4 cation channel: PACSIN 3 modulates the subcellular localization of TRPV4. *J. Biol. Chem.* **281,** 18753–18762 (2006).
12. Sokabe, T., Fukumi-Tominaga, T., Yonemura, S., Mizuno, A. & Tominaga, M. The TRPV4 channel contributes to intercellular junction formation in keratinocytes. *J. Biol. Chem.* **285,** 18749–18758 (2010).
13. Mrkonji??, S. *et al.* TRPV4 participates in the establishment of trailing adhesions and directional persistence of migrating cells. *Pflugers Arch. Eur. J. Physiol.* **467,** 2107–2119 (2015).
14. Alessandri-Haber, N., Dina, O. a, Joseph, E. K., Reichling, D. B. & Levine, J. D. Interaction of transient receptor potential vanilloid 4, integrin, and SRC tyrosine kinase in mechanical hyperalgesia. *J. Neurosci.* **28,** 1046–1057 (2008).
15. Sonkusare, S. K. *et al.* AKAP150-dependent cooperative TRPV4 channel gating is central to endothelium-dependent vasodilation and is disrupted in hypertension. *Sci. Signal.* **7,** ra66 (2014).
16. Becker, D., Bereiter-Hahn, J. & Jendrach, M. Functional interaction of the cation channel transient receptor potential vanilloid 4 (TRPV4) and actin in volume regulation. *Eur. J. Cell Biol.* **88,** 141–152 (2009).
17. Valiente-Echeverr??a, F., Hermoso, M. A. & Soto-Rifo, R. RNA helicase DDX3: At the crossroad of viral replication and antiviral immunity. *Reviews in Medical Virology* **25,** 286–299 (2015).
18. Snider, J. *et al.* Detecting interactions with membrane proteins using a membrane two-hybrid assay in yeast. *Nat. Protoc.* **5,** 1281–1293 (2010).
19. Goswami, C., Kuhn, J., Heppenstall, P. A. & Hucho, T. Importance of non-selective cation channel TRPV4 interaction with cytoskeleton and their reciprocal regulations in cultured cells. *PLoS One* **5,** (2010).
20. Marijanovic, Z., Ragimbeau, J., van der Heyden, J., Uzé, G. & Pellegrini, S. Comparable potency of IFNalpha2 and IFNbeta on immediate JAK/STAT activation but differential down-regulation of IFNAR2. *Biochem. J.* **407,** 141–151 (2007).
21. Soto-Rifo, R. *et al.* DEAD-box protein DDX3 associates with eIF4F to promote translation of selected mRNAs. *EMBO J.* **31,** 3745–56 (2012).
22. Botlagunta, M. *et al.* Oncogenic role of DDX3 in breast cancer biogenesis. *Oncogene* **27,** 3912–3922 (2008).
23. Schröder, M., Baran, M. & Bowie, A. G. Viral targeting of DEAD box protein 3 reveals its role in TBK1/IKKepsilon-mediated IRF activation. *EMBO J.* **27,** 2147–2157 (2008).
24. Noueiry, a O., Chen, J. & Ahlquist, P. A mutant allele of essential, general translation initiation factor DED1 selectively inhibits translation of a viral mRNA. *Proc. Natl. Acad. Sci. U. S. A.* **97,** 12985–12990 (2000).
25. Kida, N. *et al.* Importance of transient receptor potential vanilloid 4 (TRPV4) in epidermal barrier function in human skin keratinocytes. *Pflugers Arch.* **463,** 715–25 (2012).
26. Chen, H.-H., Yu, H.-I., Cho, W.-C. & Tarn, W.-Y. DDX3 modulates cell adhesion and motility and cancer cell metastasis via Rac1-mediated signaling pathway. *Oncogene* 1–11 (2014). doi:10.1038/onc.2014.190
27. Ye, L. *et al.* TRPV4 is a regulator of adipose oxidative metabolism, inflammation, and energy homeostasis. *Cell* **151,** 96–110 (2012).
28. Jin, M. *et al.* Determinants of TRPV4 activity following selective activation by small molecule agonist GSK1016790A. *PLoS One* **6,** (2011).
29. Scott, E. S., Malcomber, S. & O'Hare, P. Nuclear translocation and activation of the transcription factor NFAT is blocked by herpes simplex virus infection. *J Virol* **75,** 9955–9965 (2001).
30. Palmer, C. P. *et al.* A TRP homolog in Saccharomyces cerevisiae forms an intracellular Ca(2+)-permeable channel in the yeast vacuolar membrane. *Proc. Natl. Acad. Sci. U. S. A.* **98,** 7801–7805 (2001).
31. Galindo-Villegas, J. *et al.* TRPV4-Mediated Detection of Hyposmotic Stress by Skin Keratinocytes Activates Developmental Immunity. *J. Immunol.* **196,** 738–749 (2016).
32. Hamanaka, K. *et al.* TRPV4 channels augment macrophage activation and ventilator-induced lung injury. *Am. J. Physiol. Lung Cell. Mol. Physiol.* **299,** L353–62 (2010).
33. Zhao, L., Sullivan, M. N., Chase, M., Gonzales, A. L. & Earley, S. Calcineurin/nuclear factor of activated T cells-coupled vanilliod transient receptor potential channel 4 Ca2+ sparklets stimulate airway smooth muscle cell proliferation. *Am. J. Respir. Cell Mol. Biol.* **50,** 1064–1075 (2014).
34. Balakrishna, S. *et al.* TRPV4 inhibition counteracts edema and inflammation and improves pulmonary function and oxygen saturation in chemically induced acute lung injury.

Am. J. Physiol. Lung Cell. Mol. Physiol. **307,** L158–L172 (2014).
35. Sidhaye, V. K., Schweitzer, K. S., Caterina, M. J., Shimoda, L. & King, L. S. Shear stress regulates aquaporin-5 and airway epithelial barrier function. *Proc. Natl. Acad. Sci. U. S. A.* **105,** 3345–50 (2008).
36. Majhi, R. K. *et al.* Functional expression of TRPV channels in T cells and their implications in immune regulation. *FEBS J.* **282,** 2661–2681 (2015).
37. Abdullah, H., Heaney, L. G., Cosby, S. L. & McGarvey, L. P. a. Rhinovirus upregulates transient receptor potential channels in a human neuronal cell line: implications for respiratory virus-induced cough reflex sensitivity. *Thorax* **69,** 46–54 (2013).
38. Tuteja, N. *et al.* Pea p68, a DEAD-box helicase, provides salinity stress tolerance in transgenic tobacco by reducing oxidative stress and improving photosynthesis machinery. *PLoS One* **9,** (2014).
39. Guan, Q. *et al.* A DEAD Box RNA Helicase Is Critical for Pre-mRNA Splicing, Cold-Responsive Gene Regulation, and Cold Tolerance in Arabidopsis. *Plant Cell* **25,** 1–16 (2013).
40. Fukumura, J., Noguchi, E., Sekiguchi, T. & Nishimoto, T. A temperature-sensitive mutant of the mammalian RNA helicase, DEAD-BOX X isoform, DBX, defective in the transition from G1 to S phase. *J. Biochem.* **134,** 71–82 (2003).
41. Sun, M., Song, L., Zhou, T., Gillespie, G. Y. & Jope, R. S. The role of DDX3 in regulating Snail. *Biochim. Biophys. Acta - Mol. Cell Res.* **1813,** 438–447 (2011).
42. Senissar, M. *et al.* The DEAD-box helicase Ded1 from yeast is an mRNP cap-associated protein that shuttles between the cytoplasm and nucleus. *Nucleic Acids Res.* 1–18 (2014). doi:10.1093/nar/gku584
43. Jang, D. J., Guo, M. & Wang, D. Proteomic and biochemical studies of calcium- and phosphorylation-dependent calmodulin complexes in mammalian cells. *J. Proteome Res.* **6,** 3718–3728 (2007).
44. Wang, J., Wang, X. W., Zhang, Y., Yin, C. P. & Yue, S. W. Ca2+ influx mediates the TRPV4-NO pathway in neuropathic hyperalgesia following chronic compression of the dorsal root ganglion. *Neurosci. Lett.* **588,** 159–165 (2015).

Supplementary information

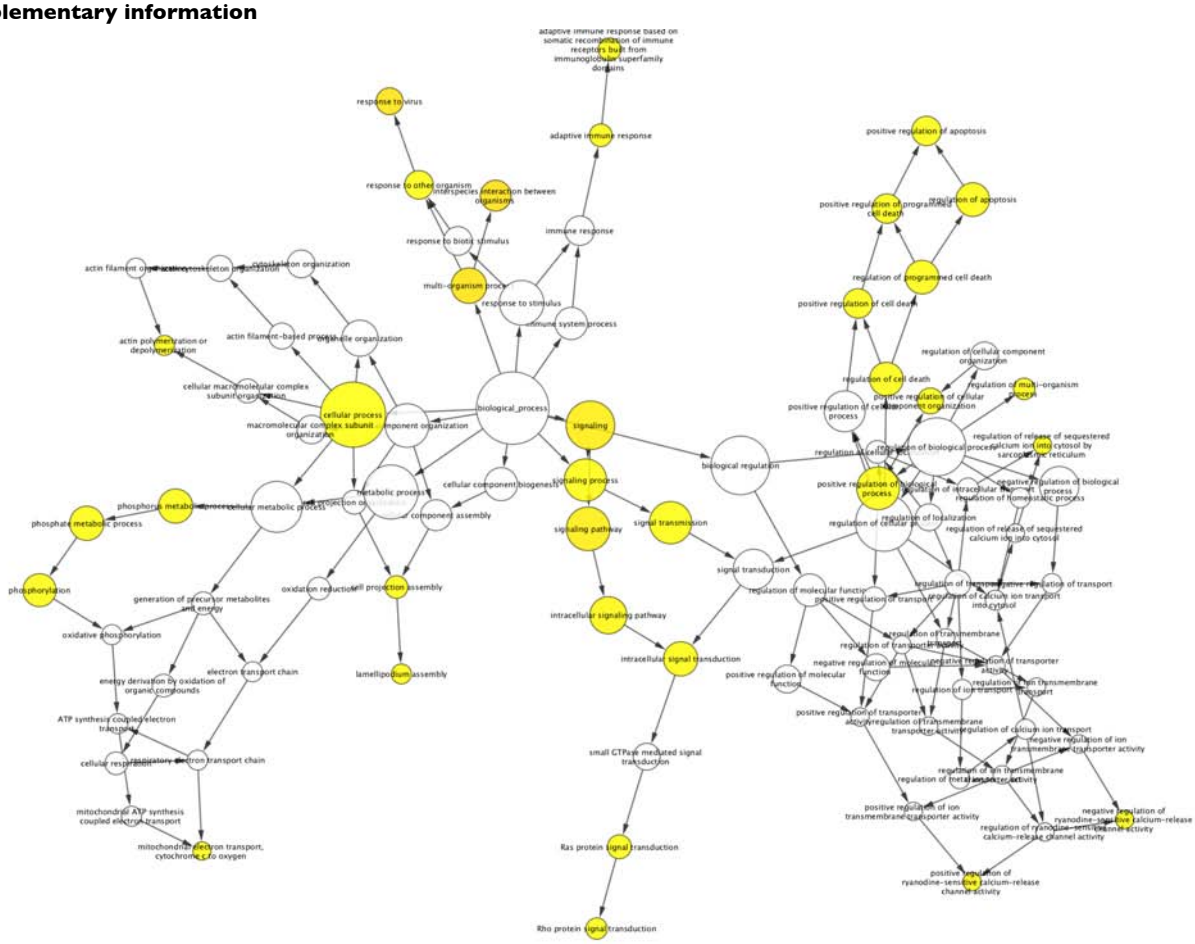

TRPV4 Gene Enrichment Analysis (GEO). Bingo App algorythm (Cytoscape) analysis of the 100 closest genes TRPV4 network. Color represents p-value association between the Go-term and TRPV4 network. The red color indicates the most statistically significant associations with TRPV4 network, followed by yellow color. White Go-terms are the least significant associated Go-terms.

Go-ID	Go-terms	pValue	pValue corr	association	% genes	Genes
44419	interspecies interaction between organism	1,48E-02	2,38E+01	14	14/129 10.8%	YWHAE BNIP3L FH DDX3X F11R CENPA RHOA SRPK1 XPO1 IRF3 PACS1 MBP IKBKG TRIM22
9615	response to virus	5,44E-02	3,61E+01	9	9/129 6.9%	IFNAR2 BNIP3L IRF3 IFNB1 PCBP2 IFNA2 IFNA8 TRIM22 IFNAR1
51704	multi-organism process	6,74E-02	3,61E+01	21	21/129 16.2%	IFNAR2 YWHAE BNIP3L FH DDX3X IFNB1 IFNA2 F11R IFNA8 CENPA RHOA SRPK1 P2RX7 XPO1 IRF3 PACS1 PCBP2 MBP IKBKG TRIM22 IFNAR1
23052	signaling	2,31E-01	9,29E+01	49	49/129 37.9%	YWHAE RTKN IFNA2 FGF6 AKAP10 FNTA CLP1 ARHGDIA NUP62 RAC1 IKBKG KIFAP3 JAK1 IFNAR2 ARHGEF11 IL15RA DUSP3 IL18 TYK2 GNL1 RHOA IRF3 PRKAR1A SNURF IFNAR1 ALDH9A1 CAMK2B ROCK2 PEX11B STK3 CDC42 CASKIN1 MBP WASF2 ARFGEF2 CDKN2A IFNB1 WNT7B SRPK1 NFKB2 P2RX7 TRPV4 ID1 ABI1 PDE3A CALM3 CALM1 RAB5A FGFR2
23033	signaling pathway	3,06E-01	9,86E+01	37	37/129 28.6%	YWHAE RTKN ROCK2 IFNA2 STK3 CDC42 FGF6 FNTA CLP1 ARHGDIA NUP62 RAC1 IKBKG WASF2 JAK1 IFNAR2 ARHGEF11 ARFGEF2 DUSP3 CDKN2A IFNB1 WNT7B TYK2 RHOA SRPK1 P2RX7 IRF3 PRKAR1A TRPV4 ID1 ABI1 SNURF CALM3 CALM1 RAB5A FGFR2 IFNAR1
60316	positive regulation of ryanodine-sensitive calcium release channel	8,08E-01	2,17E+02	2	2/129 1.5%	CALM3 CALM1
23034	intracellular signaling pathway	9,53E-01	2,19E+02	24	24/129 18.6%	IFNAR2 YWHAE ARHGEF11 ARFGEF2 RTKN DUSP3 ROCK2 CDKN2A TYK2 RHOA STK3 SRPK1 CDC42 P2RX7 IRF3 PRKAR1A ARHGDIA SNURF RAC1 IKBKG RAB5A WASF2 IFNAR1 JAK1
35556	negative regulation of ryanodyne sensitive calcium release channel	1,68E+00	3,38E+02	19	19/129 14.7%	IFNAR2 ARHGEF11 RTKN DUSP3 CDKN2A TYK2 RHOA STK3 SRPK1 CDC42 P2RX7 IRF3 ARHGDIA RAC1 IKBKG RAB5A WASF2 IFNAR1 JAK1
60315	lamellipodium assembly	2,41E+00	4,21E+02	2	2/129 1.5%	CALM3 CALM1
30032	response to other organism	3,02E+00	4,21E+02	3	3/129 2.3%	CYFIP1 RAC1 WASF2
51707	adaptative inmune response based on somatic recombination of inmune receptors	3,78E+00	4,21E+02	11	11/129 8.5%	IFNAR2 P2RX7 BNIP3L IRF3 IFNB1 PCBP2 IFNA2 MBP IFNA8 TRIM22 IFNAR1
2460	adaptative inmune response	4,19E+00	4,21E+02	5	5/129 3.8%	IL18 LIG4 MBP GNL1 NFKB2
2250	positive regulation of biological process	4,47E+00	4,21E+02	5	5/129 3.8%	IL18 LIG4 MBP GNL1 NFKB2
48518	positive regulation of biological process	4,48E+00	4,21E+02	35	35/129 27.1%	YWHAE FH CDKN1B RPN2 ROCK2 IFNA2 STK3 ACAT1 CDC42 FGF6 FNTA ARHGDIA NUP62 MBP RAC1 IKBKG KIFAP3 ARHGEF11 BNIP3L DUSP3 ANXA2 CDKN2A IFNB1 PLK2 WNT7B IL18 LIG4 CASK RHOA P2RX7 SNURF CALM3 CALM1 FGFR2 IFNAR1
10880	regulation of release of sequestered calcium ion into cytosol by sarcoplasmic reticulum	4,79E+00	4,21E+02	2	2/129 1.5%	CALM3 CALM1
7266	Rho protein signal transduction	4,95E+00	4,21E+02	4	4/129 3.1%	ARHGEF11 RTKN ARHGDIA RHOA
7265	Ras protein signal transduction	5,26E+00	4,21E+02	6	6/129 4.6%	ARHGEF11 RTKN CDKN2A ARHGDIA WASF2 RHOA
23046	signaling process	6,06E+00	4,21E+02	34	34/129 26.3%	CAMK2B RTKN PEX11B STK3 CDC42 FGF6 AKAP10 FNTA ARHGDIA CASKIN1 MBP RAC1 IKBKG KIFAP3 WASF2 JAK1 IFNAR2 ARHGEF11 IL15RA DUSP3 CDKN2A TYK2 GNL1 RHOA SRPK1 NFKB2 P2RX7 IRF3 PRKAR1A TRPV4 PDE3A RAB5A IFNAR1 ALDH9A1
23060	signal transmission	6,06E+00	4,21E+02	34	34/129 26.3%	CAMK2B RTKN PEX11B STK3 CDC42 FGF6 AKAP10 FNTA ARHGDIA CASKIN1 MBP RAC1 IKBKG KIFAP3 WASF2 JAK1 IFNAR2 ARHGEF11 IL15RA DUSP3 CDKN2A TYK2 GNL1 RHOA SRPK1 NFKB2 P2RX7 IRF3 PRKAR1A TRPV4 PDE3A RAB5A IFNAR1 ALDH9A1
42981	regulation of apoptosis	6,32E+00	4,21E+02	18	18/129 13.9%	YWHAE ARHGEF11 BNIP3L CDKN1B CDKN2A IFNB1 IFNA2 IL18 LIG4 RHOA STK3 P2RX7 FNTA ARHGDIA NUP62 PDE3A RAC1 IKBKG
43065	positive regulation of apoptosis	6,54E+00	4,21E+02	12	12/129 9.3%	YWHAE ARHGEF11 P2RX7 BNIP3L CDKN1B CDKN2A IFNB1 IFNA2 IL18 RAC1 IKBKG STK3
16310	phosphorylation	6,87E+00	4,21E+02	17	17/129 13.1%	CAMK2B CAMK2D MT-ND5 ROCK2 PLK2 CASK TYK2 STK3 SRPK1 CDK9 P2RX7 ABI1 MT-CO2 MT-CO3 FGFR2 CDK16 JAK1
43068	positive regulation of programmed cell death	6,94E+00	4,21E+02	12	12/129 9.3%	YWHAE ARHGEF11 P2RX7 BNIP3L CDKN1B CDKN2A IFNB1 IFNA2 IL18 RAC1 IKBKG STK3
43067	regulation of programed cell death	7,05E+00	4,21E+02	18	18/129 13.9%	YWHAE ARHGEF11 BNIP3L CDKN1B CDKN2A IFNB1 IFNA2 IL18 LIG4 RHOA STK3 P2RX7 FNTA ARHGDIA NUP62 PDE3A RAC1 IKBKG
8154	actin polymerization or depolymerization	7,31E+00	4,21E+02	3	3/129 2.3%	ABI1 RAC1 WASF1
10942	positive regulation of cell death	7,51E+00	4,21E+02	12	12/129 9.3%	YWHAE ARHGEF11 P2RX7 BNIP3L CDKN1B CDKN2A IFNB1 IFNA2 IL18 RAC1 IKBKG STK3
43900	regulation of multi-organism process	7,70E+00	4,21E+02	4	4/129 3.1%	P2RX7 IFNB1 PCBP2 MBP
30031	cell projection assembly	7,74E+00	4,21E+02	5	5/129 3.8%	P2RX7 CYFIP1 PCM1 RAC1 WASF2
10941	regulation of cell death	7,75E+00	4,21E+02	18	18/129 13.9%	YWHAE ARHGEF11 BNIP3L CDKN1B CDKN2A IFNB1 IFNA2 IL18 LIG4 RHOA STK3 P2RX7 FNTA ARHGDIA NUP62 PDE3A RAC1 IKBKG
6123	mitochondrial electron transport, cytocrome c to oxigen	7,94E+00	4,21E+02	2	2/129 1.5%	MT-CO2 MT-CO3
6793	phosphorus metabolic process	8,38E+00	4,21E+02	19	19/129 14.7%	CAMK2B CAMK2D MT-ND5 DUSP3 ROCK2 PLK2 CASK TYK2 STK3 SRPK1 CDK9 P2RX7 DUSP12 ABI1 MT-CO2 MT-CO3 FGFR2 CDK16 JAK1
6796	phosphate metabolic process	8,38E+00	4,21E+02	19	19/129 14.7%	CAMK2B CAMK2D MT-ND5 DUSP3 ROCK2 PLK2 CASK TYK2 STK3 SRPK1 CDK9 P2RX7 DUSP12 ABI1 MT-CO2 MT-CO3 FGFR2 CDK16 JAK1
51130	positive regulation of cellular compoment organization	9,09E+00	4,43E+02	8	8/129 6.2%	CDC42 P2RX7 ANXA2 ROCK2 ARHGDIA MBP RAC1 RHOA
9987	cellular process	1,04E+01	4,93E+02	101	101/129 78.2%	NCKAP1 CYFIP1 RTKN MT-ND5 AQP4 F11R CDH6 FGF6 FNTA CLP1 ARHGDIA OIP5 FAM65B KIFAP3 EIF1AX LIG4 CASK PRKAR1A MT-CO2 MT-CO3 IFNAR1 RPN2 PEX11B ZFP36L1 STK3 ACAT1 PCBP2 DNAJC21 MBP BRIX1 LTA4H SMYD3 MPST CPSF1 PLK2 ELL2 SRPK1 NFKB2 CDK9 EIF2S3 EIF6 TRPV4 ID1 PDE3A UBA1 ACO2 OSBPL1A RAB5A FGFR2 CDK16 YWHAE CDKN1B IFNA2 SETD7 CDC73 EEA1 DUSP12 PCM1 SPTLC1 XPO1 SPTLC2 NUP62 RAC1 IKBKG FEZF2 JAK1 ARHGEF11 DUSP3 ANXA2 IL18 TYK2 GNL1 RHOA IRF3 PACS1 SNURF ALDH9A1 CAMK2B FH CAMK2D ROCK2 VPS4B RGPD2 CENPA CDC42 ORMDL3 GCNT3 WASF1 WASF2 EIF4B ARFGEF1 ARFGEF2 PEX19 CDKN2A IFNB1 TPK1 WNT7B P2RX7 MARS ABI1 ATP13A2

inmune system response
signaling
calcium signaling
apoptosis
cellular structures
metabolism

List of GO-terms associated with TRPV4 enriched network. Go-term ID, p-values, p-values corrected, gene number and percentage of genes from the network and genes from the network included within each Go-term are annotated. The box with color shows the cellular process manual annotation, according to the legend.

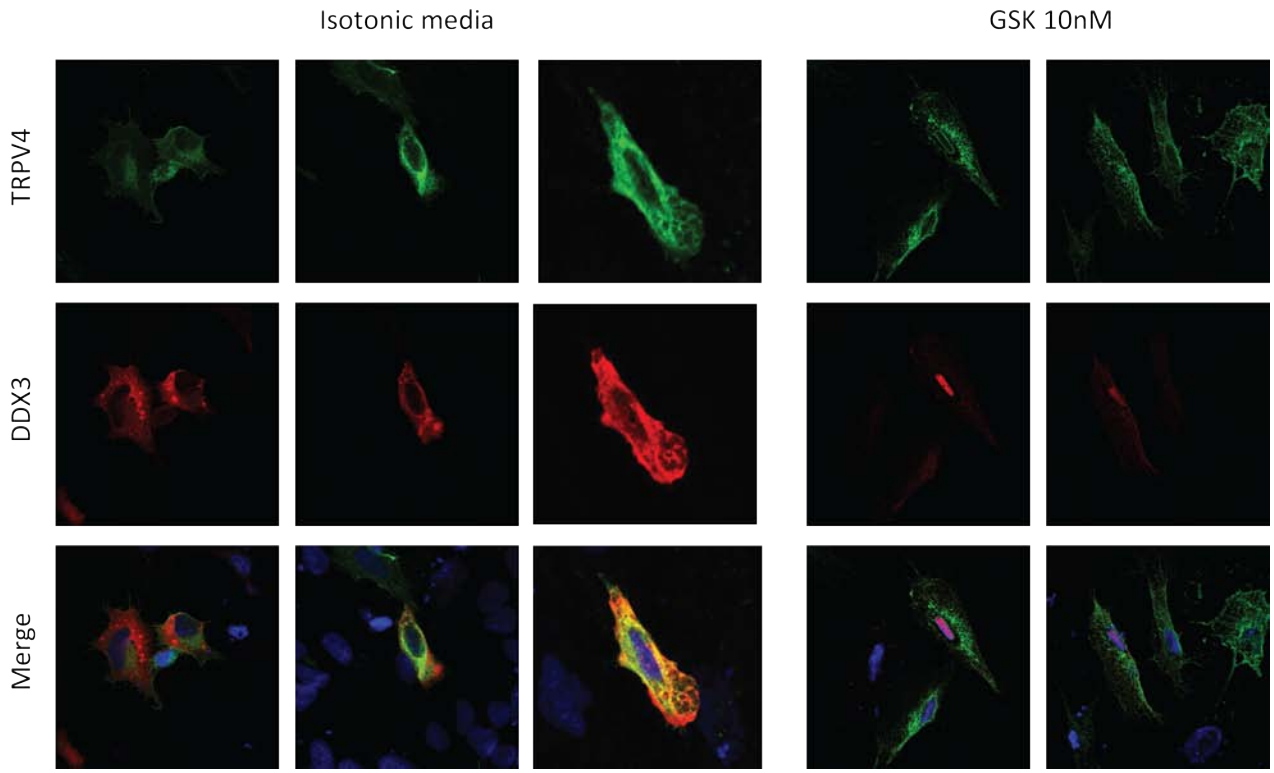

DDX3X translocation is not dependent on PKA, PLA2 or SRCs. Transiently transfected HeLa cells expressing TRPV4 (green) and DDX3X (red). Cells were treated with a cocktail of inhibitors KT5720, ACCoCF3 and PP2 that impair PKA, PLA2 and SRC enzymes. The treatment did not alter DDX3X or TRPV4 location. Treatment with GSK produced an rearrangement of TRPV4 and the translocation of DDX3X to the nucleus in a similar way to what was previously described without inhibition of these enzymes.

General Discussion

Discussion

1. Conservation among sequence and structural functional implications in TRPV subfamily

Our data in Chapter II determined the evolutionary pressure exerted over the TRPV1-4 channels and their structural domains. Our data agrees with the already proposed evolution pattern for TRPVs attending to phylogenetic clustering and chromosomal location (Fig. 11) [73, 236]. TRPV4 forms a very homogenous cluster with higher purifying selection followed by TRPV1, TRPV3 and finally TRPV2 (Fig. 1 in Chapter II), which argues for an earlier divergence from TRPV4 and TRPV1-3 ancestors, followed by several gene duplications that lead to the generation of TRPV1, TRPV2 and TRPV3. In fact, TRPV2 might be still under positive selection indicating some functional overlapping with its close relatives, which could lead to functional/pharmacological compensation effects as has been observed in mild-phenotype TRPV2 knock-out mouse [237]. Pharmacologically, TRPV2 has no specific endogenous or exogenous ligand, whereas it is modulated by broad spectrum TRPV drugs, such as 2-APB or ruthenium red, which also target other TRPVs (Annex table 1) [167].

The purifying evolutionary pressure trend on specific domains, such as ARD, MPD, TMD and TRP domain (TRP box linker and TRP box) indicates that TRPV1-4 channels share a common minimal functional scaffold unit, comprising from the ARD to the TRP domain (Fig. 2 in Chapter II). Interestingly, TRPV1 and TRPV2 structures have been recently solved by Cryo-EM and the comparison of both structures corroborates the high structural similarity between these channels (Fig. 2) [42, 44, 45]. Although there is no available structure for TRPV3 and TRPV4, the domain distribution and folding is expected to be similar to TRPV1 and TRPV2 according with our domain conservation analysis.

Our study focuses the attention on the high conservation and thus potential functional/structural relevance of domains such as MPD, loop 4 between S4 and S5 and the TRP linker (post-S6 segment and TRP domain). These regions are conserved not only for each channel but among all TRPV1-4, linking these domains to the intrinsic channel functioning rather than to a channel specific regulation. For instance, MPD domain of TRPV1 and TRPV4 (pre-S1) has been related to channel folding, as its interaction with the TRP box C-terminal domain is essential for proper channel assembly [238]. MPD has been also related to thermal sensation [239], which might imply that thermal sensing diversity among TRPV1-4 is determined by the small changes within the MPD. Sequence analysis revealed the potential of MPD to work as a syntaxin binding domain by its LKRSF motif (Fig. 5 in Chapter II). It has

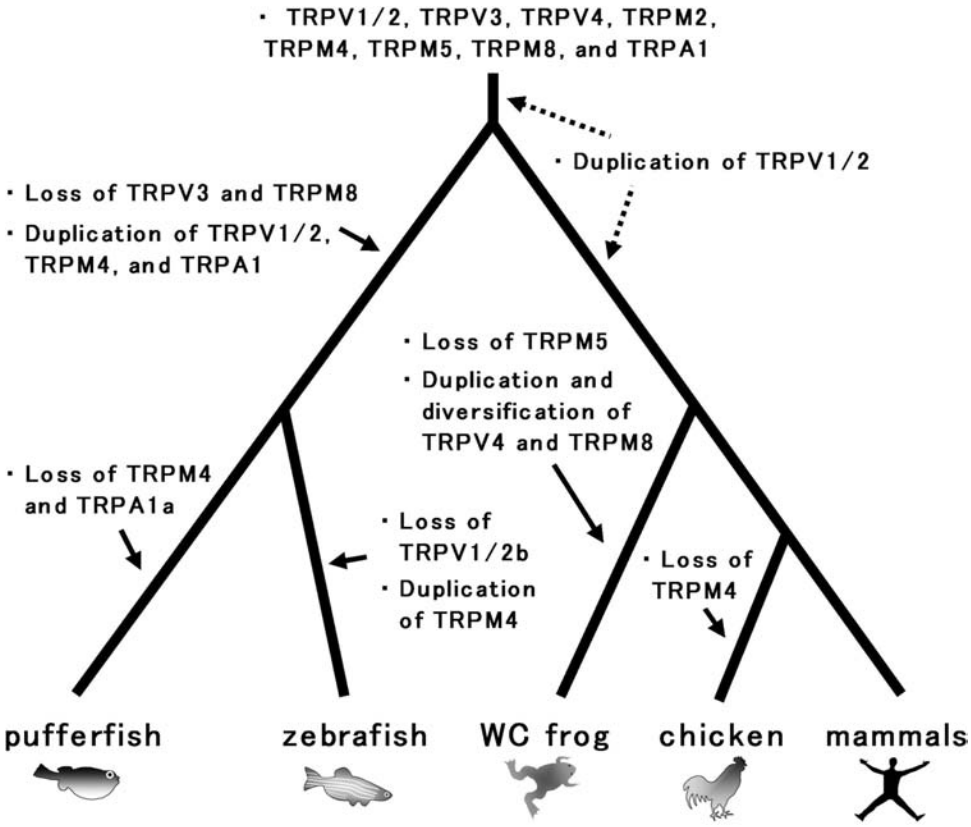

Figure 11. Inferred evolutionary history of the vertebrate thermo-TRP homologs. The inferred evolutionary events, gene duplication and gene loss are indicated on the respective branches. Pufferfish (Tetraodontidae) and zebrafish (*Danio rerio*) as representatives of teleost fishes, western clawed frog (WC frog, *Xenopus tropicalis*) as representative of amphibian, chicken (*Gallus gallus*) as representative of birds and mammals. Figure from Saito et al 2006 [73].

been already described the interaction of TRPV1 N-terminus with Synaptotagmin IX and Snapin25, although the exact location of the TRPV1 binding pocket has not been determined [205]. The presence of the LKRSF consensus motif within MPD domain points to this region as the putative binding pocket for the SNARE complex, which might be conserved among TRPV1-4 attending to the high conservation of the region and the LKRSF motif. Furthermore, MPD sequence reveals the potential to bind lipids by the distribution and nature of its amino acids, although no previous study has determined the specific binding of lipids to this domain. To the best of our knowledge our work is the first describing the dual role of MPD domain as a SNARE and lipid binding region within TRPVs (Chapter IV), pointing this region as one of the key areas, not just for protein folding [238], but for channel trafficking itself.

Likewise, the highly conserved Loop 4 of TRPV4 contains cholesterol-recognizing motifs that bind to this lipidic molecule and regulate channel trafficking and cellular distribution [240]. Interestingly, TRPV4 has coevolved with MVK and GLTP, enzymes involved in sterol biosynthesis [240], which might indicate the tightly regulation that lipids and lipid metabolism exert over TRPVs. Additionally, naturally occurring variants in the highly conserved loop 4 of TRPV3 and TRPV4 results in a channel gain of function that is associated to pathophysiological conditions such as Olmsted syndrome or metabotropic dysplasia and spondyloepiphyseal dysplasia Maroteaux, respectively (Fig. 10) [221, 229, 230]. The fact that mutations in this region produce changes in channel functioning demonstrates its high implication in TRPV structure and function regulation.

Distal N-terminus, extracellular loops and distal C-terminus are the main source of variability along TRPV1-4 sequences (Fig. 2 in Chapter II). These regions are highly variable among channels and very specific for each channel. Our domain conservation mapping points to a very heterogeneous potential functional/structural implication of these domains among TRPVs. These areas might contribute to the differential regulation of each TRPV, as extracellular sensing domains (e.g. drug binding), and intracellular signalling domains (e.g. phosphorylation).

Our conservation mapping allows the inference of already described domains in one TRPV member to the other members of the subfamily (Fig. 5 in Chapter II). PIP2 binding and AKAP79 binding domains for all TRPVs 1–4 are highly conserved and might be a common regulatory mechanism for all these channels. In fact, AKAP5 binding has been already described for all TRPV1-4 and its function further assessed for TRPV1 and TRPV4 [191]. In the case of PIP2, its binding to TRPV1 [241], TRPV2 [197], and TRPV3 [242] has been mapped to the highly conserved proximal C-terminal domain, the region contiguous to the TRP box motif. TRPV4 seem to bind PIP2 in a different manner, within the distal N-terminal domain [243]. Although not described to the date, our sequence analysis suggests that C-terminal PIP2 binding domain might be conserved in TRPV4 (Fig. 5 in ChapterII).

2. N-terminal role in trafficking of TRPVs

We have reported in Chapter III that the deletion of the distal N-terminus of TRPV2, the first 74 aminoacids, is enough to deplete the channel trafficking to the plasma membrane when observed by *in vivo* confocal imaging or cell surface biotinylation assays (Fig. 2 in Chapter III). TRPV5 distal N-terminus has been described to carry out similar functions. Deletions of distal N-terminus of TRPV5, the first 34 amino acids and the first 75 amino acids, were retained in the endoplasmic reticulum in contrast to the

wild-type TRPV5 when observed by immunohistochemistry [52]. This report matches to our observations by in vivo confocal imaging of TRPV2 deletion of first 74 amino acids (Fig2a in Chapter III). De Groot and colleagues showed that a limited amount of N-terminal TRPV5 mutants escaped the endoplasmic reticulum and reached the plasma membrane, as shown by cell surface biotinylation, in agreement with our results showing a highly decreased but still present fraction of TRPV2 in the plasma membrane (Fig. 2b and c in Chapter III). Distal N-terminus deletions of TRPV5 did not reach the Golgi apparatus and present a lack of complex glycosylation [52] whereas TRPV2 still presents the two bands on the WB characteristic of glycosylated and not glycosylated forms (Fig. 1b and 2b in ChapterIII). The fact that TRPV2 N-terminal deletions reached the glycosylation step whereas TRPV5 deletions did not might indicate that although the role of the distal N-terminus might be similar, it controls trafficking at different checkpoints for each channel. Altogether this data suggest an important role of distal N-terminus in TRPV2 trafficking and potentially in the trafficking of other members of TRPV subfamily, as in the case of TRPV5, despite low sequence domain conservation. Furthermore, the N-terminal TRPV5 deletion up to residue 34 and 75 abolished channel function [52], which has not been determined in the case of TRPV2 due to the difficulties to approach TRPV2 channel function, attending to the limited access to a TRPV2 functional assay.

Generally, TRP channels have very diverse mechanisms that regulate trafficking and, subsequently, channel performance and function. Among TRPV members, interaction of TRPV4 and TRPV1 with OS-9 in the ER mediated by the channel N-terminal region prevents channel trafficking to the plasma membrane [244]. PACSIN3 binds to the TRPV4 distal N-terminal PRD domain, within the same regions as PIP2, and enhance the relative amount of TRPV4 in the plasma membrane [245]. PIP2 binding to the PRD domain of TRPV4 sensitizes the channel to the cell swelling and heat [243]. In the case of TRPV1 it has been described that phosphorylation at S116 by PRKD enhances its activity in DRG neurons.

In conclusion, N-terminal domain seems to play an important role in trafficking of TRPVs, which lately will have an impact on TRPV function and performance. In the case of TRPV2 depletion of the distal N-terminus, the region prior to the ARD, is enough to promote channel accumulation in internal stores, reducing TRPV2 levels in the plasma membrane and potentially channel function.

3. Topological determinants of TRPV2 folding

Our experimental data from Chapter III determined that TRPV2 follows a transmembrane topology of 6 transmembrane segments, as was previously inferred from homology with potassium channels [31, 32] and lately with TRPV1 [42] and TRPV2 [45, 44] Cryo-EM structures. Our data constitutes the first accurate mapping of the transmembrane helices for TRPV2, that when superposed to the already available Cryo-EM structure of TRPV1 allows to have a very complete approach to the conformation of the transmembrane domain of TRPV2. Furthermore, the comparison between these two channel transmembrane segments allows the evaluation of the topological folding conservation among TRPV members. The TRPV2 membrane-embedded domain sequence prediction matches the TM helix disposition of the TM1-TM6 of TRPV1 (Fig. 4b in Chapter III). Recently, TRPV2 structure has been solved by two different groups using rabbit and rat TRPV2 [44, 45], with 3.8A and 4.4A respectively. When superposed to the solved Cryo-EM structure for rat TRPV2, our mapping shows a high correlation with the TM helices of the model (Fig. 12a). This fact is an indicator of the accuracy of our approach, justifying the use of this technique to the fine mapping of transmembrane segments of those TRP channels with no structure available to the date, including other IMPs. The fitting of the two structures available to the date determined the high conservation of the domain helices, although the general arrangement in space of those is quite divergent (Fig. 12b). Mainly, the relative positions of some loops and the distances between helices are divergent, whereas general structure topology and folding is conserved (Fig. 12b). The differences between the two models might be due to species specific arrangements of some regions or differences in the protocol to obtain the sample. In any case both structures display a general shared arrangement with highly homologous transmembrane spatial distribution. Comparision of TRPV2 structure to TRPV1 also highlights the conservation of the spatial distribution between these two channels and potentially other members of TRPV subfamily (Fig. 12b).

Our experiments carried out to map *in vitro* TRPV2 topology were performed with a construct lacking the most part of the N-terminal domain of the channel, the first 336 amino acids, which account for the distal N-terminus and the complete ARD (Fig. 3 in Chapter III). Despite the N-terminal truncation, TRPV2 was properly folded within the lipid bilayer. The same TRPV2 mutant, ΔARD-TRPV2, was not able to traffic to the plasma membrane, determined by confocal imaging and biotinylation assay (Fig. 2 in Chapter III). This fact indicates that N-terminal region might be needed for other channel processes rather than insertion in the ER membranes, such as channel tetramerization, glycosylation or interaction with chaperone proteins to allow membrane translocation. Although it has not been described for

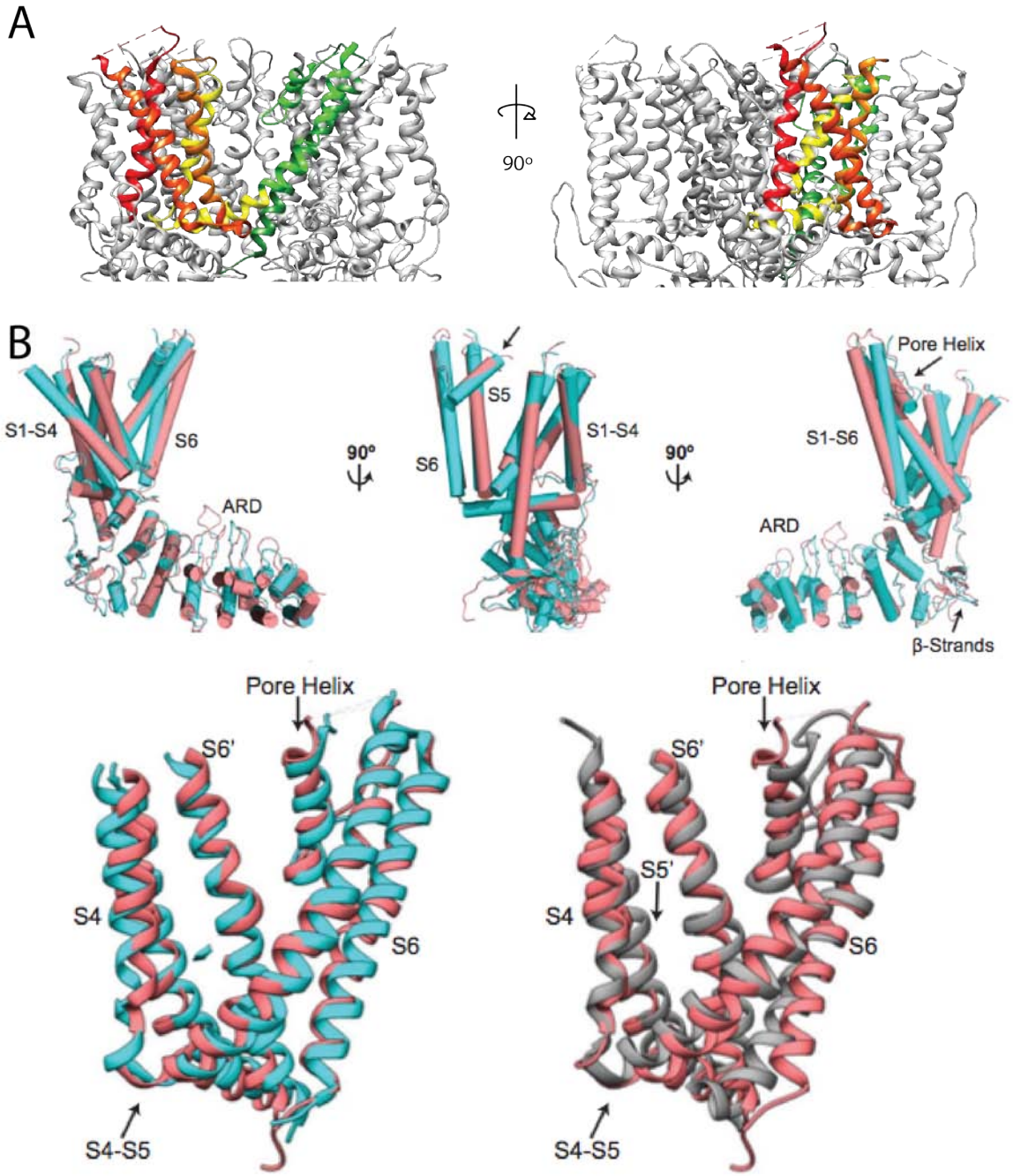

Figure 12. TRPV2 channel transmembrane domain arrangement. A) Drawing of the mapping determined by the glycosylation screen on rat TRPV2 Cryo-EM structure. Coloured in red TM1 (till the end of primer 1 used in our glycosylation assay), in dark orange TM2, in orange TM3, in yellow TM4, in green TM5 and in dark green TM6. B) Superposition of TRPV2 Cryo-EM available structures from rat (magenta), rabbit (cyan) and TRPV1 from rat (grey), showing the spatial arrangement of the different domains along the monomers and the transmembrane regions. Figure adapted from Huynh et al [45].

TRPV2, the ARD indeed plays a key role in channel oligomerization. The analysis of several natural splice variants of TRPV4 determined that the ARD domain is necessary for oligomerization, and lack of ARD leads to a strong accumulation of TRPV4 in the ER [246]. Nonetheless, not only N-terminus seems to play an important role in plasma membrane, TRPV4 C-terminus is also involved in trafficking and TRPV4 mutants with a length of 828 to 844 amino acids (Full length 871aa) are retained in the ER [247]. Channel trafficking is a complex matter that clusters processes such as membrane insertion, glycosylation, Golgi maturation, vesicle trafficking and protein chaperone interaction [248]. The balance between all these processes will result in a correct protein distribution in the plasma membrane, but further experimental characterization is required to know which processes are altered besides membrane insertion in our truncated forms.

Our topology mapping also determined that TRPV2 TM5 and TM6 work as an independent module for protein insertion in the membrane (Fig. 4 in Chapter III). This might indicate the functioning of the pore forming region independently of the other segments of the transmembrane domain, although the proper channel functioning requires of the coupling of the 6TMs in order to translate the stimuli sensing into cationic currents evoked by the channel pore. Despite correct helix insertion within the lipid bilayer, tetramerization of the TM5-6 isolated regions in order to form the pore region has not been assessed and according with previous reports on TRP truncated forms would not be expected. TRPV mutants lacking ARD or carrying point mutations in N- or C-terminal domains seem to produce channels that are unable to tetramerize, which emphasizes the need of the TRPV cytosolic domains to promote the correct oligomerization of the subunits [246, 238]. In this context, isolatedly expressed TM5-6 segments from TRPV2 might be insufficient to establish a stable interaction between subunits, however further experimental validation is required to address if TM5-6 region might act as a minimal TRP pore unit.

4. TRPVs and lipid metabolism

Transient receptor potential channels are tightly related to lipids. Lipidic secondary messengers in metabolic signalling cascades regulate TRPVs at least at two different levels: direct interaction with the channel or modulation of PKC activity (Fig. 13).

Direct interaction: The binding of several lipidic compounds functions as trigger of TRPV channel gating. TRPV1 is activated by anandamide or hydroxioctadecadienoic acid (HODE) [156, 157]. Farnesyl pyrophosphate (FPP), an intermediate metabolite in the mevalonate pathway, has been identified as

endogenous ligand for TRPV3 [173] and TRPV4 is activated by direct binding of 5,6-EET, a metabolite result of arachidonic acid processing by P450 cytochrome. PIP2 binds to TRPVs and promotes a sensitized state of the channels, promoting its activation by other stimuli (Fig. 13a). For instance, TRPV4 directly binds PIP2 in the N-terminal domain [243], whereas TRPV2 binds this phospholipid in the C-terminal region [197] and TRPV1 has PIP2 binding sites in N- and C-terminal domains [199]. Recently, TRPV1 structure has been solved using advantage of lipid nanodiscs technology, showing specific phospholipid interactions that enhance the binding of agonists such as RTX toxin to TRPV1 [249]. The analysis on TRPV1 embedded in lipid nanodisc allowed the determination of phospholipids that form stable interactions with Arg534 in TRPV1, located in the extracellular loop between the S3 and S4 helices (Fig. 13b) [249]. The lipid binding is modified upon toxin binding to TRPV1 and the arrangement of these 3 elements probably determines the overall affinity and kinetics of toxin binding. Furthermore the same study reported the existence of a resident phosphatidylinositol lipid in the capsaicin pocket, whose branched acyl chains extend upwards between S4 of one subunit and S5 and S6 of an adjacent subunit. The lipid is bound by electrostatic interactions of the phospholipid polar head with Arg409 in the cytoplasmic N-terminal segment preceding S1, MPD domain, or Lys571 and Arg575 within the S4–S5 linker (Fig.13b) [249].

Modulation by lipid metabolism: The activation of GPCR signaling cascades mediates in TRPVs function by either direct interaction with the ion channels or by the production of intracellular second messengers. When phospholipases are activated via GPCR, hydrolysis of inositol phospholipids by phospholipase C (PLC) produces an increase in DAG amounts contained in the membranes, that in turn activates PKC (Fig. 13) [250]. The early production of DAG is transient and reverts back to basal levels within few seconds or minutes, overlapping temporarily with the formation of inositol 1, 4, 5-triphosphate (IP3) and the rise of the intracellular calcium concentration (Fig. 13a). Lately, the cellular responses mediate the formation of DAG with a slow onset and a more sustained rise. Late DAG increase is derived from the hydrolysis of major components of the phospholipid bilayer such as phosphatidylcholine (PC) by phospholipase D (PLD) to yield phosphatidic acid, which is subsequently dephosphorylated to form DAG (Fig.13a). The activity of PLC and PLD is encompassed with a signal-dependent release of arachidonic acid through phospholipase A2 (PLA2) catalytic activity (Fig. 13a). The fatty acid (FFA), and lysophosphatidylcholine (LPC), the products of PC hydrolysis, are enhancers of PKC activity (Fig. 13a) [251].

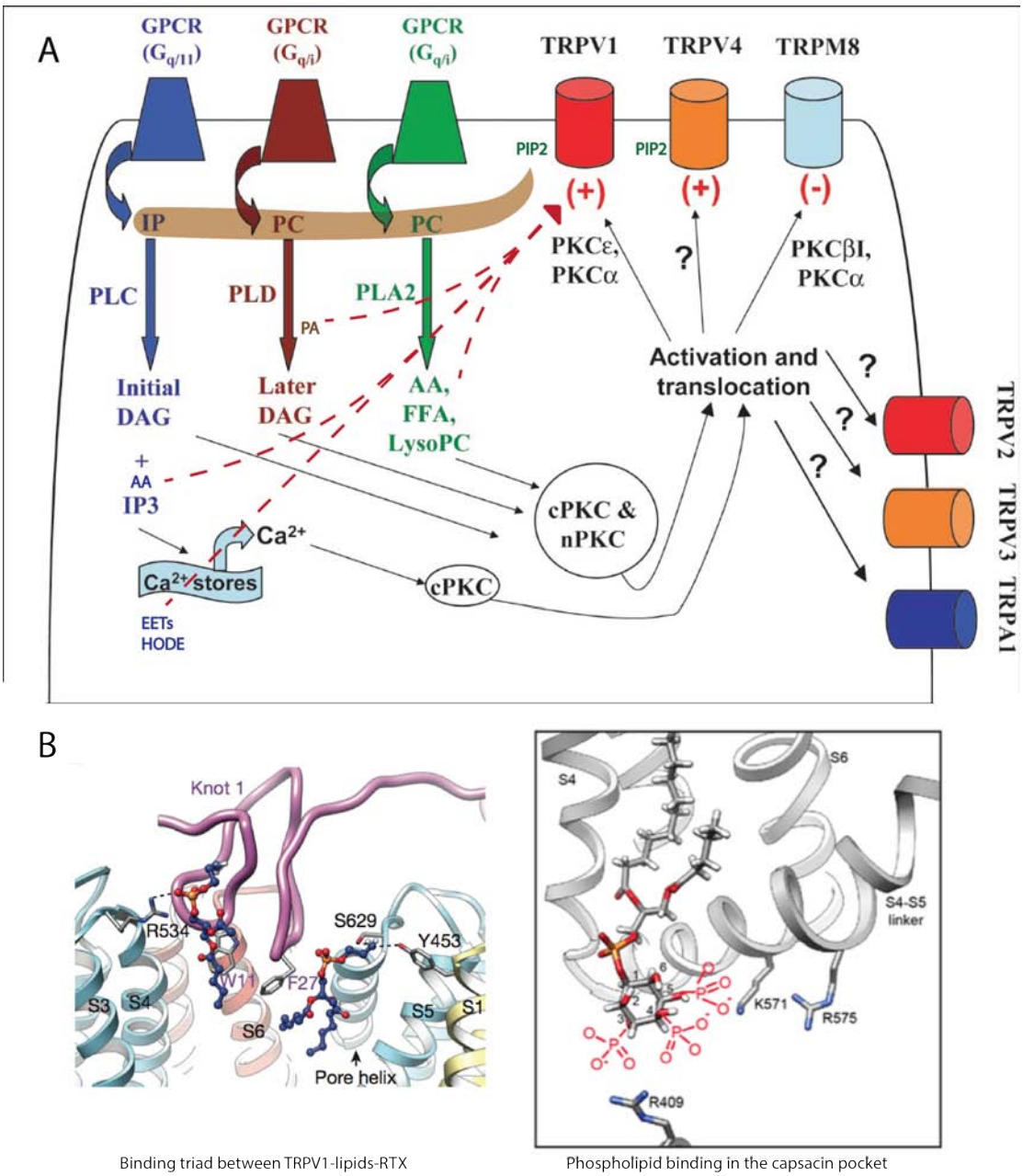

Binding triad between TRPV1-lipids-RTX

Phospholipid binding in the capsacin pocket

Figure 13. TRP channels are linked to the cellular lipid metabolism. A) TRPVs activity and plasma membrane trafficking is affected by the activity of lipid metabolic enzymes, which shape the lipid composition of the cellular compartments and modulate the channel functioning depending on the cellular lipid concentrations. Lipidic compounds modulate TRP channel functioning at two levels, by directly binding the channels, promoting an open or sensitized state of the channel and by modulating the activity of lipid-dependent kinases, such as PKC, which in turn will modulate channel by phosphorylation. GPCRs upstream of lipid metabolism are targets for TRPV channel indirectly modulation. Diacyglycerol (DAG), Phospholipase C (PLC), Inositol 1,4,5-triphosphate (IP3), intracellular calcium (Ca^{2+}), Phosphatidic acid (PA), Phosphatidylcholine (PC), Phospholipase D (PLD), Arachidonic acid (AA), Phospholipase A2 (PLA2), cis-unsaturated fatty acid (FFA), Phosphatidylinositol 4,5-bisphosphate (PIP2), lysophosphatidylcholine (lysoPC) and Inositol phospholipids (IP). Figure adapted from Mandadi et al 2011 [252]. B) Binding pockets of TRPV1 determined by Cryo-EM structure in lipid nanodiscs, showing the binding of lipids in the

loop between S3 and S4 (left) and within the capsaicin pocket (right). RTX toxin is coloured in purple and lipids mediating TRPV1 RTX interaction in blue with polar heads in red (left). Lipid charges were coloured in red and the amino acids of TRPV1 that potentially interact with them in blue (right) Figure adapted from Gao et al 2016 [249].

TRPVs might be directly phosphorylated by PKC. TRPV1 is phosphorylated at the S502, T704 and S800 residues and PKC mediated phosphorylation of these sites sensitizes the channel to activation in DGR neurons by agonist as capsaicin [194]. PKC epsilon is the predominant isoform that targets S502 and S800 sites on TRPV1 for functional regulation. There are no reports concerning TRPV2 and TRPV3 regulation by PKC, although indirectly, TRPV2 increased activity has been partially linked to PLD/PKC functioning in human skeletal cells of Duchenne muscular dystrophy [253]. Additionally, TRPV4 has been characterized to have putative PKC phosphorylation sites, including residues S162, S189 and T175 and S824 [254, 255]. Modulation of TRPV4 function by PKC promotes a sensitized state of the channel and might mediate in hyperalgesia [255].

Our sequence conservation analysis in Chapter II reveals the potential general regulation of TRPV1-4 by PIP2 binding on the C-terminal tail. The binding of PIP2 within this region links directly lipid metabolism to channel folding and function. In general, PIP2 binding promotes a channel sensitized state. Furthermore, MPD domain was postulated as a putative binding site for lipidic compounds attending to the nature of its amino acid sequence, widening the regions of the channel that might mediate in the lipid-TRPV relationship.

Our data in Chapter IV determines that TRPV1 and TRPV2 co-localize with PA (Fig 5c in Chapter IV), one of the intermediate metabolites in the PLD signalling cascade. Analysis of TRPV1 and TRPV2 MPD domain further confirmed *in vitro* the potential direct binding of PA to this highly conserved channel domain (Fig 5a and b in Chapter IV). The recently discovered potential role of Arg409 residue, within the MPD of TRPV1, in the phospholipid binding to the channel [249] might confirm the capability of lipid binding of the MPD domain that we have determined in Chapter IV, although point mutation analysis may confirm this interaction. It is possible that mutating these residues alter channel folding and/or structure, hindering the approach to this matter. Attending to the high conservation of MPD domain and that we observed a similar lipid binding pattern for MPD domains of TRPV1 and TRPV2, the mechanisms underlying this interaction might be conserved in other TRPVs. Furthermore, TRPV2 activity seems to be regulated by PA levels using a vesicle based calcium assay (Fig 6 in Chapter IV). Our results widen the knowledge of the regulation of TRPVs by the lipidic environment and GPCR-coupled signalling

cascades (Fig. 13). We have linked another metabolite in the PLD pathway, PA, to TRPV regulation potentially through a direct interaction, although further validation analysis has to be done in order to establish the dependency of TRPV2-PA binding to the channel activation. At this point, we can not discard that PA modulation of TRPV activity is carried out through the PLD-coupled signalling cascades described above (Fig. 13).

5. TRPV interactomics, new horizons for channel regulation.

Ion channels, as any other protein, are subject of tight intracellular regulation exerted by other cellular protein partners. Regulation of ion channels is even more complex as they are also modulated by extracellular stimuli and their activity produces changes in intracellular environment and several signalling cascades. Knowing the proteins that surround and regulate TRPVs is compulsory in order to understand the location-dependent regulation of these channels within the cellular gear machinery. Such a knowledge will allow a proper channel targeting in order to treat channel related pathologies. A lot of studies have been carried out in order to identify new TRP partners. Despite this huge effort, most of the PPIs identification has been based in sequence similarity. Most part of TRPs still remain orphan in terms of PPIs (Table 4) and the big divergence between the number of already identified PPIs for the most studied channels and those yet to be addressed highlights the huge lack of information about some TRP channel modulation (Table 4).

Our data in Chapters IV and V have expanded the already described regulation of TRPVs within TRPV1-4 subgroup, and generally for all TRPs. Our yeast two hybrid screen specific for membrane proteins (MYTH) has shed some light on TRPV modulation and especially on TRPV2 and TRPV4. These channels were chosen because the number of known interaction partners is low when compared to other TRPs such as TRPV1 or TRPC3, giving a wide margin for new PPI identification (Table 4). We have identified 2 new potential partners for TRPV1 and 20 for TRPV2 (Fig. 2 in Chapter IV), and 44 for TRPV4 (Fig.1 in Chapter V).

In the case of TRPV1 the number of interactors obtained was surprisingly small, just two, despite the huge amount of TRPV1 already described interactions (Table 4). This fact points to a very low efficiency of TRPV1 in our system due to low expression levels or not proper folding. TRPV2 produced 20 new partners, which is a good amount when compared to the 9 already described interactors (Table 4). The new putative TRPV2 partners are highly interconnected between them (Fig. 3 in Chapter IV),

TRPC		TRPV		TRPM		TRPML		TRPP		TRPA	
channel	PPI number	channel	PPI number	channel	PPI number	channel	PPI number	channel	PPI number	channel	PPI number
TRPC1	56	TRPV1	94	TRPM1	3	TRPML1	33	TRPP1	116	TRPA1	8
TRPC2	13	TRPV2	9	TRPM2	6	TRPML2	3	TRPP2	8		
TRPC3	115	TRPV3	4	TRPM3	4	TRPML3	8	TRPP3	1		
TRPC4	38	TRPV4	38	TRPM4	7						
TRPC5	59	TRPV5	17	TRPM5	0						
TRPC6	46	TRPV6	20	TRPM6	6						
TRPC7	12			TRPM7	13						
				TRPM8	5						
Total	339	Total	182	Total	44	Total	44	Total	125	Total	8

Table 4. TRP channel protein protein interaction (PPI) statistics. 706 already determined TRP partners contained in the TRIP database (www.TRPchannel .org). Classification based on the statistics of the webpage, showing the number of interactors for each TRP channel, clustered by subfamilies. The data contained was obtained from 431 curated publications.

although there is no newly defined interactor in common with the already known for TRPV2. This lack in cohesion between our experiments and the previous reports might be due to the limited knowledge in TRPV2 regulation, with very few described partners and potentially lots of them yet to be discovered (Table 4). Statistically, if 50% of TRPV2's identified interactors in our experiment were false positives, we would have duplicated the number of known physically interacting proteins for TRPV2. Conversely, biological processes determined by our MYTH screen for TRPV2 are related to lipid metabolism, neuronal system development or ion transport and signalling cascades (Fig. 3 in Chapter IV), functions that are to some extent already associated to TRPV2 physiological and molecular mechanisms. By instance, TRPV2 is involved in axon outgrowth and its activity is regulated by PIP2 [94, 197]. In this sense, the potential veracity of our newly described interactors is cross-validated and indicates that MYTH partners might be mediators in those TRPV2 coupled cellular processes. Nevertheless, further functional studies are needed to determine to which extent newly identified partners are truly coupled to TRPV2.

In the case of TRPV4, some proteins that were already described as TRPV partners were identified by our screen. Calm3, that is bound to TRPV4 N- and C-terminus [198, 200], is an example of already described TRPV interactors (Fig. 1 in Chapter V and Fig. 14). Furthermore, TRPV4 putative interactors form a cluster surrounding calmodulin, with 8 interactors that are known already to interact with Calm3 (Fig. 14). The presence of already connected proteins strengthens the validity of the MYTH assay, as it might indicate the determination of proteins located within the same complexes or signalling networks. Furthermore, TRPV4 interactome is associated with cellular processes that range from signalling and ion transport to immune system response and apoptosis (Fig. 2 in chapter V), processes as in the case of TRPV2 already related to TRPV4 function.

Among the determined interactors there is one common between TRPV2 and TRPV4: CDH6, a type II cadherin that may play a role in kidney development as well as endometrium and placenta formation, and related to cancer development (Fig. 2 in ChapterIV and Fig. 1 in Chapter V) [256]. The presence of common proteins might indicate the involvement of both TRPVs in common processes, although the possibility of being just spurious partners can not be discarded. Concerning CDH6, there is no report of TRPV2 playing an important role in adherent junction or interacting with constituent proteins of these cellular structures, whereas TRPV4 has been located in adherent junction and involved in the intercellular junction formation [130]. Although different isoform, the existence of an already known link between TRPVs and CDHs points to the potential truly nature of TRPV2-TRPV4-CDH6 interactions, which might be interesting to further validate.

From a broad perspective, the MYTH approach newly identified TRPV2 and TRPV4 partners that are easily interconnected within the already known TRPV1-4 network (Table 5), (Fig. 15a and b). The networks represent in black nodes the already known interactors for TRPV1-4 channels and the edges represent known links between proteins attending to the already described information on physical interactions, co-localization, interaction bioinformatics prediction, co-expression, pathway identity, shared domain containing and genetic interactions. The networks displayed here intend to show general attributes of the TRPV1-4 interactome. We highlighted in colour (blue and yellow for TRPV2 and TRPV4, respectively) our newly identified potential partners by MYTH in order to visualize their integration within the TRPV1-4 network (Fig. 15b). Furthermore, the addition of our partners to the already described ones increases TRPV1-4 network interconnectivity (Table. 5), pointing to a further enrichment in already described TRPVs related complexes or signalling cascades. Although interconnectivity was enhanced, the nature of the interactions established within the network suffered very small changes in

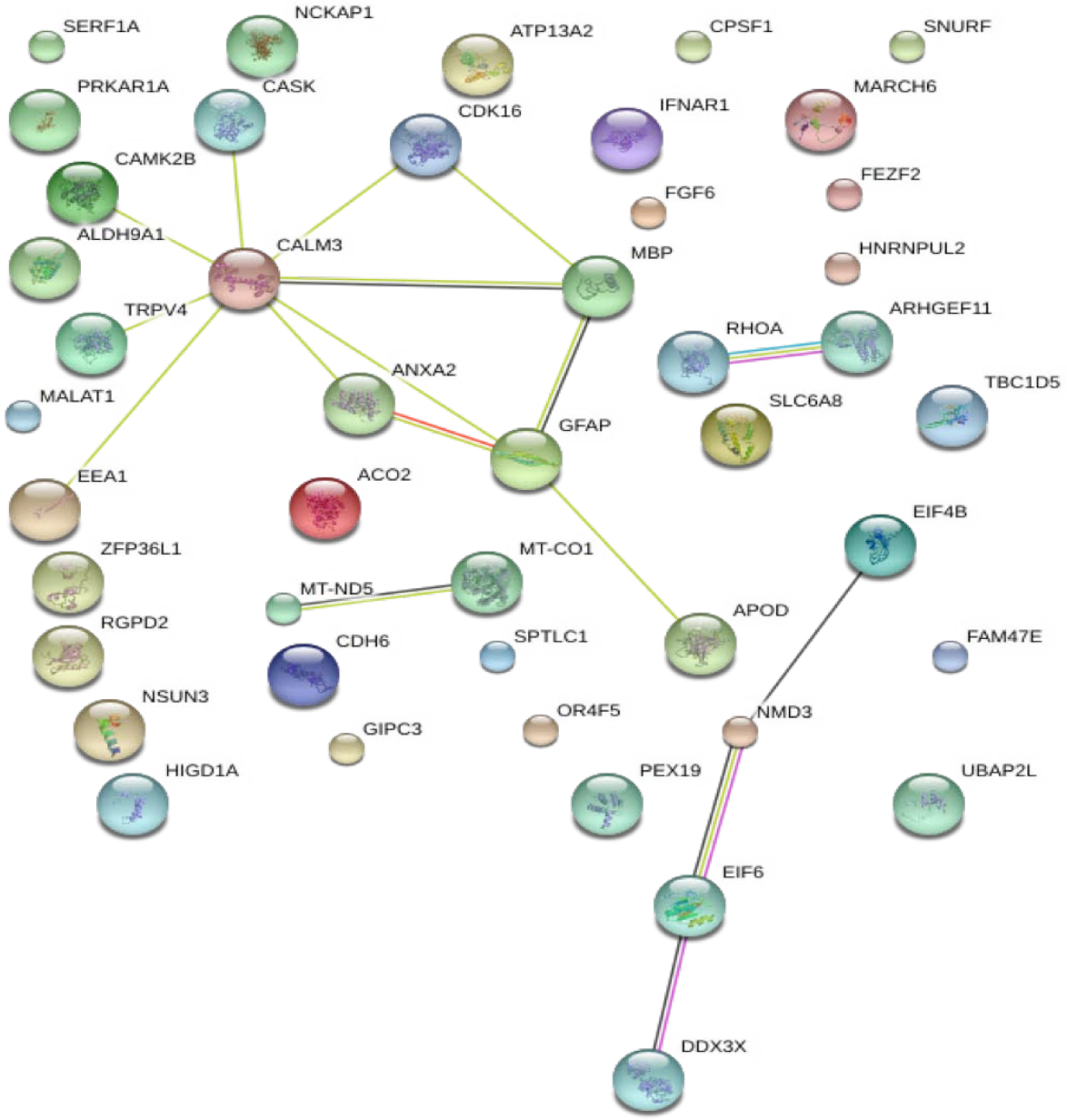

Figure 14. TRPV4 MYTH interactome from STRING PPI database. The lines represent already described physical interactions between the linked proteins. There are two main protein clusters of PPI. First cluster gathers around Calm3 and calmodulin signalling, including TRPV4. Second cluster includes proteins related to translation initiation that are involved in DNA and RNA metabolism, DDX3X, EIF6, NMD3 and EIF4B.

their ratios (Table 5), indicating that addition of our interactors enhance the interconnection between TRPV1-4 partners independently of the nature of the linkage. Minor changes were observed in the ratios of physical interactions, co-expression and co-localization (Table 5). Physical interaction ratio was decreased upon addition of our newly described partners (Table 5). This effect is an artifact, as we did not define the new interactors as physical interactions, given the fact that most part of them still require a proper validation that confirms the veracity of our assay. Co-expression and co-localization rations were increased upon addition of MYTH interactors (Table 5), pointing to a shared spatial distribution between the previously established TRPV partners and the newly described ones. Altogether, the established new interactors in this thesis enhance the interconnectivity and understanding of the already known TRPV1-4 regulation.

	TRPVs interactome	TRPVs plus MYTH interactome
Edges	5742	9399
Nodes	217	289
Interconnetivity (ratio Edges/nodes)	26,46	32,52
Physical interaction	51.86%	49.08%
Co-expression	28.57%	30.67%
Predicted	9.63%	9.84%
Co-localization	3.62%	5.01%
Genetic interactions	1.95%	2.53%
Pathway	2.86%	1.91%
Shared protein domain	1.50%	0.95%

Table 5. TRPV1-4 interaction network features. Comparison between TRPV1-4 pre-established interaction network and TRPV1-4 network including MYTH newly described interactors for TRPV2 and TRPV4. Edges and nodes were quantified, the ratio between edges and nodes was taken as estimation of network interconnectivity. Percentage of interactions within the network based on physical interactions, co-localization, bioinformatics prediction, co-expression, genetic interactions, pathway and shared domains were quantified and annotated.

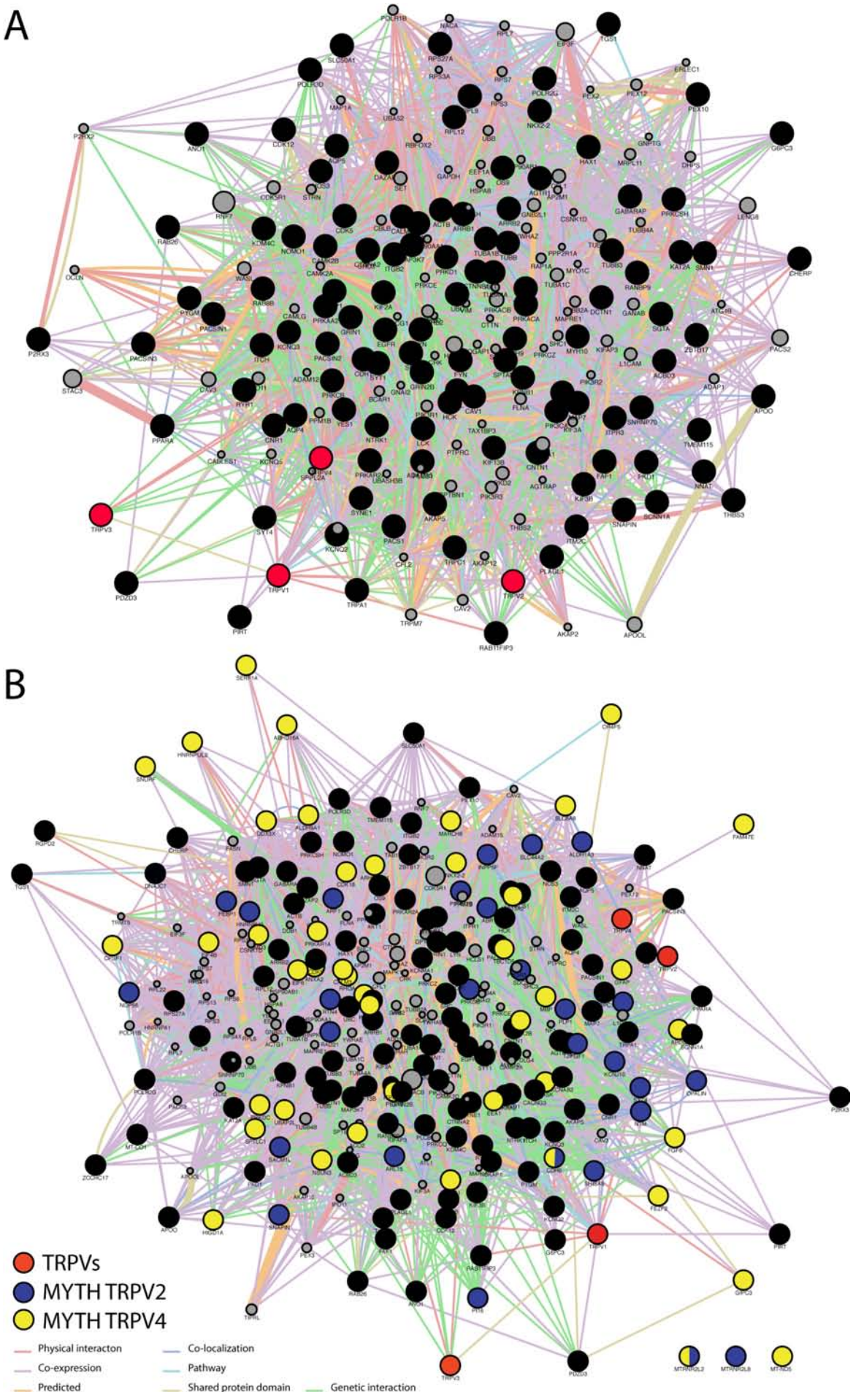
A
B
TRPVs
MYTH TRPV2
MYTH TRPV4
Physical interacton
Co-expression
Predicted
Co-localization
Pathway
Shared protein domain
Genetic interaction

Figure 15. TRPV1-4 interactome overview obtained from Genemania APP, cytoscape. A) Already known TRPV1-4 interaction partners linked attending to the already described physical interactions, co-localization, interaction bioinformatics prediction, co-expression, pathway identity, shared domain containing and genetic interaction. TRPVs were coloured in red to highlight their position. Black dots are the already known TRPV1-4 partners. B) TRPV2 and TRPV4 proteins determined by our MYTH assays and Co-IPs were added to the interactome, coloured in blue and yellow respectively.

6. Putative model of DDX3X regulation by TRPV4 channel

Our results in Chapter V show a tight relationship between TRPV4 and DDX3X expression levels (Fig. 4 in Chapter V). Depletion of TRPV4 in epithelial cells leads to a strong decay in DDX3X, which has been previously reported by expression microarray profiling in an adipocyte cell line [257]. The observation of a decay even in DDX3X mRNA levels (transcription) might imply that regulation of DDX3X expression is not directly linked to TRPV4 but rather mediated by transcription factors located downstream of channel function (Fig. 16).

Presence and basal activity of TRPV4 generates a calcium leakage within the cell that is coupled to the calcium dependent kinases and phosphatases specifically associated to the channel, such as CamKII or PKC (Fig. 16a). We postulate to an enhancement of DDX3X transcription driven by this basal activation. The calcium leakage will enhance the activity of those calcium dependent kinases/phosphatases in vicinity of TRPV4, which will produce post-translational modifications, most probably phosphorylations, in transcription factors in charge of DDX3X transcription, such as p53 (Fig. 16a) [258]. The modification of those transcription factors will promote their activity and end with an enhancement of DDX3X expression (Fig. 16a). In the absence of TRPV4, there is no basal calcium leakage and the kinases/phosphatases associated to the channel are not coupled to the calcium signalling. In this context transcription factors downstream of those kinases are not modified and the transcription of DDX3X is not promoted (Fig. 16b).

Among transcription factors, DDX3X promoter requires the binding of the tumor suppressor p53 to promote the helicase transcription [259]. p53 is regulated by calcium metabolism and might work as link between TRPV4 and DDX3X (Fig. 16a). CamKII overexpression leads to an increase in p53 mRNA and protein levels in vascular smooth muscle [260] and CamKII activity promotes the phosphorylation of residues within the N-terminal transactivation domain of p53, such as Serine 20 (Fig. 16a). Phosphorylation at S20 of p53 enhances the activity of the transcription factor and the transcription of

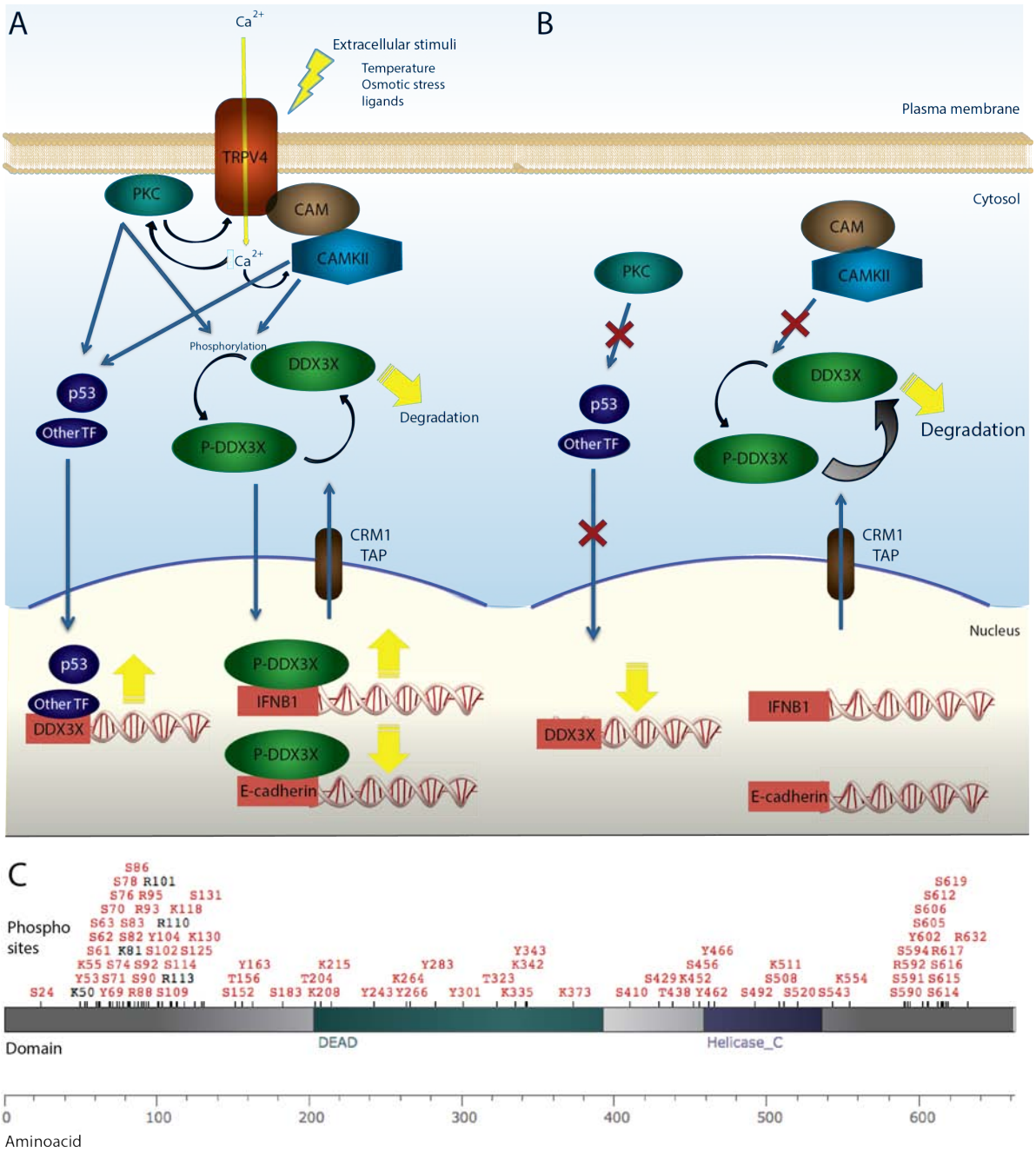

Figure 16. Putative model of DDX3X regulation by TRPV4. A) TRPV4 activity promotes the entry of calcium within the cell. Upon calcium entry, calcium dependent enzymes coupled to TRPV4 and located in its vicinity promote posttranslational modification, mainly phosphorylation, of downstream effectors. p53 and other transcription factors (TF) will translocate to the nucleus and promote DDX3X transcription. DDX3X is modified and those modifications lead to a stabilization of the protein levels and the translocation to the nucleus, where it leads to changes in transcription of genes such as IFNB1 or E-cadherin. B) Depletion of TRPV4 delocalizes kinases and phosphatases coupled to the channel and the calcium metabolism. This uncouples p53 promotion of DDX3X transcription and might lead to an imbalance of DDX3X equilibrium, promoting protein degradation. C) Phosphorylation site map of DDX3X, showing the high number of phosphorylated residues in DDX3X sequence. Image obtained from www.phosphosite.org.

p53 target genes (Fig. 16a) [261], in a similar way to what we propose as model of DDX3X downregulation.

Although the decay of DDX3X protein levels upon TRPV4 silencing might be due to transcription regulation it can not be discarded that the direct protein interaction of TRPV4 with DDX3X might be also required for the helicase stabilization. DDX3X is a complex protein that suffers a multitude of posttranslational modifications, among them DDX3X contains a large number of phosphorylation sites (Fig. 16c). Our main hypothesis is that upon TRPV4 mediated calcium entry DDX3X is recruited to the TRPV4/Cam/CamKII complex and phosphorylated by the kinases coupled to the channel (Fig 16a). DDX3X phosphorylated form will be released from the complex and the posttranslational modifications suffered might promote DDX3X activity. Indeed, phosphorylation of DDX3X at residue Thr204 by CyclinB/cdc2 regulates DDX3X function [262] and phosphorylation at residues S181, S183, S240, S269, S429, T438, S442, S456, S520, T542 and S543 by TBK1 is crucial for DDX3X induction of IFN transcription (Fig. 16a) [263]. From a dynamic perspective the cell will keep a balance in DDX3X phosphorylation levels depending on the basal activity of TRPV4 and the Cam/CamKII complex. This balance will control DDX3X expression, location and function to maintain a tuned functioning of the helicase according to the extracellular stimuli sensed by TRPV4 (Fig. 16a). Upon TRPV4 silencing the complex will not be formed so calcium will not be coupled to the corresponding Cam/CamKII enzymes and DDX3X will not be phosphorylated. This might translate in an uncoupled DDX3X function, which might lead to degradation of the protein (Fig. 16b).

Our results locate TRPV4 in the context of the innate immunity response within the epithelium. By the regulation of intracellular calcium levels, DDX3X helicase protein levels and DDX3X cellular location, TRPV4 might modulate the intracellular signalling cascades coupled to Toll-Like Receptors (TLRs) and other Pattern Recognition Receptors (PRRs) at several key points. Furthermore, this function might be conserved for other TRPVs, as TRPV1 activation by capsaicin produced a similar DDX3X nuclear translocation.

7. Role of TRPVs in innate immune system

Among the explored potential roles where TRPVs, and specifically TRPV4, are involved, we have paid special attention in Chapter V to immune system responses to external insults related to PRRs, which is mainly driven by TLRs. The coupling of innate immune response associated to TLR requires the participation of calcium signalling as second messenger. Among the ion channels present in the

epithelial tissues, TRPs have been postulated as the responsible for this calcium influx. In trigeminal neurons LPS sensitizes TRPV1 to capsaicin in a TLR4 dependent manner. LPS potentiation on TRPV1 channel activity is inhibited by selective TLR4 antagonist (Fig. 17a) [264]. Similarly, TRPV2 mediates in the intracellular calcium signalling induced by LPS, TNFα and IL-6 in RAW264 macrophage cell line [265] (Fig. 17a). TLR4 activation induce the activation of PLD and PKC, which is able to trigger TRPs activity, and thereby TRPV4 activation through the metabolization of lipids [266, 267]. PLD is activated by LPS/TLR4/Myd88 pathway and regulates TNFα expression and production through S6K1/JNK/c-Jun in RAW264 macrophage cell line [267]. TLR regulation of GPCRs and consequently TRPs might partially explain the observed intracellular LPS mediated calcium currents (Fig. 17b). Our results in Chapter V broaden the potential molecular mechanisms mediated by TRPV4 in innate immune response, with implications in response to bacterial infections, which has been previously described for TRPVs; and to the response to virus.

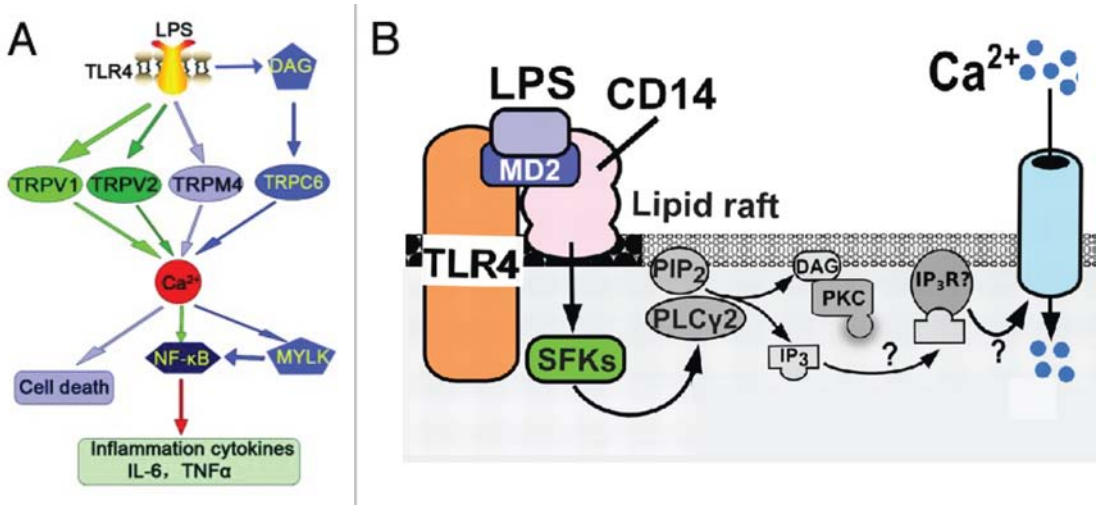

Figure 17. TLR activation modulates TRP channels through the modulation of GPCR activity and lipid metabolism. A. LPS mediated activation of TLR4 has been associated with TRPV1, TRPV2, TRPM4 and TRPC6 function. TRP activation leads to an increase in intracellular calcium that regulates downstream factor such as NFKB. Lately the signalling cascades coupled to these factors end with cell death or the generation of an inflammatory response. Figure adapted from Han et al 2014 [268]. B. LPS induced activation of TLR4 promotes the activation of PLC and PLD enzymes. PLD2 activity cleaves Phosphatidylinositol 4,5-bisphosphate (PIP2) and produces Diacylglycerol (DAG) and Inositol 3-phosphate (IP3) which modulate the activity of calcium channels such as TRPs. Figure adapted from Fric et al 2012 [269].

Using computational and experimental tools we can build new hypothesis and provide specific knowledge for TRP channels. In this thesis, we have revised the current knowledge to define a working starting point for the TRPV1-4 subgroup. We have computationally dissected the primary sequence to build working hypothesis. We have experimentally characterized topological domains, and we have enter in the TRPV interactomics field towards defining new research paths for this interesting subset of somatosensors.

Conclusions

Conclusions

The contribution of this thesis to broaden the whole picture of TRP channel regulation and physiology can be summarized in the following conclusions:

Chapter I

- TRPV2 available bibliography was revised to establish a starting point for our research.

Chapter II

- This work provides a first structural insight into the multidomain organization and conservation of TRPV1-4 channels.

- Evolutionary pressure rate have been established for TRPV1-4 proteins. TRPV1, TRPV3, and TRPV4 channels have a higher evolutionary pressure, purifying selection, than TRPV2, which is more divergent among current species. The highest purifying selection has been exerted on TRPV4, the most conserved member of this group either in mammals or vertebrates.

- Our evolutionary divergence approach argues for a first diversion between TRPV4 and TRPV1-TRPV3. Finally TRPV2 would have appeared more recently due to TRPV1 gene duplication and ongoing positive selection in order to adapt new physiological roles for TRPV2 channel.

- TRPV1-4 channels were divided into functional domains and the divergence/conservation mapped within the domains. We found that TRPV1-4 members share a very similar pattern of conservation along their sequence. Regions such as the distal N-terminus, some extracellular loops, such as the loop 5, and the distal C-terminus of TRPV1-4 channels are highly divergent, probably under positive selection. These domains are very specific for each one of the channels and might be involved in specific channel functions rather than general structural or functional issues such as gating or folding. TRPV1-4 channels share a common minimal functional scaffold unit, comprising the ARD to the TRP domain, with a high purifying evolutionary pressure trend on specific domains, such as ARD, MPD, TMD and TRP domain (TRP box linker and TRP box).

- This study establishes a methodology to dissect multidomain membrane proteins from primary sequence and evolutionary perspective towards predicting potential functional and structural sequence hallmarks.

Chapter III

- TRPV2 is mainly expressed in intracellular membrane compartments, mainly ER, when transiently transfected in HEK293 cells. We further investigate the role of the N-terminus of TRPV2 in channel assembly and trafficking by generating two truncations lacking the distal N-terminal domain and the entire ARD domain respectively. TRPV2 N-terminal domain, the region previous to ARD domain is involved in membrane targeting of TRPV2. Truncation of distal N-terminal domain results in a stronger intracellular accumulation of TRPV2.

- TRPV2 insertion in the plasma membrane is cotranslational and it happens even when the entire ARD has been deleted.

- Using an in vitro glycosylation system we were able to map the transmembrane helices with high accuracy. The topology of TRPV2 is similar to the already established structure of TRPV1, which accounts for the potential high conservation of transmembrane folding of TRPV subfamily.

- TRPV2 transmembrane domain is formed by two independent modules: the TM1-4 and the TM5-6. Both transmembrane modules can be inserted into the membrane independently.

Chapter IV

- Several know TRPV1 interactions have been translated to TRPV2, TRPV1´s closest homolog. SNARE complex proteins, Snapin25 and Synaptotagmin IX (SYT9) are capable to interact with both, TRPV1 and TRPV2. Furthermore, we have mapped the interaction to a high conserved domain in the N-terminus of TRPV channels, the membrane proximal domain, MPD. This region is located between the ARD and the first transmembrane segment.

- TRPV1 and TRPV2 protein partners have been expanded by means of a yeast two hybrid specific for membrane proteins (MYTH). We found 2 new putative interactors for TRPV1 and 20 for TRPV2.

- Interaction between TRPV2 and Opalin, PLP1, ARL15, ABR, NTM and CACNG3 were further validated. TRPV2 interaction with Opalin, ABR, NTM and CACNG3 were mapped to the ARD domain of TRPV2. These might be promising candidates to characterize further physiological implications.

- TRPV2 MYTH interactome has been used to identify potential physiological implications of TRPV2 using a systems biology approach. Among the most representative potential roles we found the regulation by lipid metabolism and neural system development.

- TRPV1 and TRPV2 were screened for lipid binding and we determined the direct binding of phosphatidic acid (PA) to the MPD domain of both channels. TRPV1 and TRPV2 co-localized with PA membrane microdomains and PA addition to TRPV2 containing vesicles activate the channel gating, producing an increase in calcium within the vesicles.

Chapter V

- TRPV4 interactome was expanded by means of a yeast two hybrid specific for membrane proteins (MYTH). Here we reported 44 new potential TRPV4 partners.

- TRPV4 MYTH derived interactome has been used to identify potential physiological implications of TRPV4. Among the most representative potential roles we found high association with diverse group of processes, ranging from cell signalling to immune system regulation or apoptosis. Immune response processes were the most significant association with TRPV4 interactome.

- Among TRPV4 potential interactors related to immune system, we further validated its interaction with DDX3X, an RNA helicase from the Dead box helicase family, which is involved in innate immune response to viral infection at diverse levels.

- TRPV4 expression regulates DDX3X protein levels in mice epithelial fibroblast (MEF) cell line, mice lung tissue extract and human bronquial epithelial (HBE) cell line.

- TRPV4 activity promotes DDX3X translocation to the nucleus. This process is mediated by the calcium entry from the extracellular media through the channel. Furthermore it requires of calmodulin and CamKII activity and might imply a recruitment of DDX3X to the TRPV4/Calmodulin/CamKII complex in order to promote the translocation of the helicase.

- TRPV4 activity regulates transcription and translation of diverse reporters. Transient transfection of TRPV4 evokes changes in general transcription-translation mainly due to the basal activity of the channel, which is know to increase the basal cytosolic calcium levels. Channel activation and calcium entry further modulate the transcription-translation of diverse reporters. Although regulation is calcium dependent, unspecific calcium entry mediated by Ionomycin produced small changes compared to transient transfection or activation. This points

to a need of coupling calcium entry to channel surroundings and potentially to the channel PPI complex.

- The effects of TRPV4 activity in transcription-translation are just partially explained by DDX3X function, pointing to the existence of more transcriptional and translational factors downstream of TRPV4 in HEK293 cells. In HBE the observed effect in transcription-translation is mainly mediated by DDX3X, as depletion of the helicase impaired the decrease observed upon channel activation.

- DDX3X yeast homolog Ded1 is in charge of viral RNA 2a translation. Depletion of TRPV4 yeast homolog YVC1 leads to a decay in viral 2a protein translation, similar to what it is observed upon Ded1 impairment. This decay was recovered upon TRPV4 transformation in the YVC1 yeast strain. Together our results indicate that TRPV4 is able to control cell transcription and translation and plays an important role in the modulation of DDX3X-mediated viral translation.

Bibliography

[1] B. Martinac and A. Kloda, “Evolutionary origins of mechanosensitive ion channels,” in *Progress in Biophysics and Molecular Biology*, 2003, vol. 82, no. 1–3, pp. 11–24.

[2] M. D. Carattino, “Structural mechanisms underlying the function of epithelial sodium channel/acid-sensing ion channel.,” *Curr. Opin. Nephrol. Hypertens.*, vol. 20, no. 5, pp. 555–60, 2011.

[3] B. Hille, “Ion Channel Excitable Membranes,” *Sunderland Massachusetts USA*. pp. 1–37, 2001.

[4] M. Whitaker, “Calcium at fertilization and in early development.,” *Physiol. Rev.*, vol. 86, no. 1, pp. 25–88, 2006.

[5] R. Ranganathan, “Evolutionary origins of ion channels,” *Proc.Natl.Acad.Sci.U.S.A.*, vol. 91, no. 9, pp. 3484–3486, 1994.

[6] I. S. Gabashvili, B. H. a. Sokolowski, C. C. Morton, and A. B. S. Giersch, “Ion channel gene expression in the inner ear.,” *J. Assoc. Res. Otolaryngol.*, vol. 8, no. 3, pp. 305–28, 2007.

[7] M. Almén, K. J. Nordström, R. Fredriksson, and H. B. Schiöth, “Mapping the human membrane proteome: a majority of the human membrane proteins can be classified according to function and evolutionary origin,” *BMC Biol.*, vol. 7, no. 1, p. 50, 2009.

[8] M. M. C. Kuo, W. J. Haynes, S. H. Loukin, C. Kung, and Y. Saimi, “Prokaryotic K+ channels: From crystal structures to diversity,” *FEMS Microbiology Reviews*, vol. 29, no. 5. pp. 961–985, 2005.

[9] S. D. Buckingham, J. F. Kidd, R. J. Law, C. J. Franks, and D. B. Sattelle, “Structure and function of two-pore-domain K+ channels: Contributions from genetic model organisms,” *Trends in Pharmacological Sciences*, vol. 26, no. 7. pp. 361–367, 2005.

[10] J. T. Littleton and B. Ganetzky, “Ion Channels and Synaptic Organization : Analysis of the Drosophila Genome Ion channels are the physical substrates that underlie,” *Neuron*, vol. 26, no. 0896–6273 SB - M, pp. 35–43, 2000.

[11] U. B. Kaupp and R. Seifert, “Cyclic nucleotide-gated ion channels.,” *Physiol. Rev.*, vol. 82, no. 3, pp. 769–824, 2002.

[12] D. Burke, J. Howells, and S. E. Tomlinson, “Hcn channels: Function and clinical implications,” *Neurology*, vol. 81, no. 5. pp. 513–514, 2013.

[13] B. Coste, J. Mathur, M. Schmidt, T. J. Earley, S. Ranade, M. J. Petrus, A. E. Dubin, and A. Patapoutian, “Piezo1 and Piezo2 are essential components of distinct mechanically activated cation channels,” *Science*, vol. 330, no. 6000, pp. 55–60, 2010.

[14] T. J. Jentsch, V. Stein, F. Weinreich, and A. A. Zdebik, “Molecular structure and physiological function of chloride channels,” *Physiol. Rev.*, vol. 82, no. 2, pp. 503–568, 2002.

[15] J. Zheng, “Molecular mechanism of TRP channels,” *Compr. Physiol.*, vol. 3, no. 1, pp. 221–242, 2013.

[16] F. H. Yu and W. a Catterall, “Overview of the voltage-gated sodium channel family.,” *Genome Biol.*, vol. 4, no. 3, p. 207, 2003.

[17] G. Webster and C. I. Berul, “An update on channelopathies: From mechanisms to management,” *Circulation*, vol. 127, no. 1, pp. 126–140, 2013.

[18] B. Nilius and G. Owsianik, “Transient receptor potential channelopathies.,” *Pflugers Arch.*, vol. 460, no. 2, pp. 437–50, 2010.

[19] T. Bose, a Cieślar-Pobuda, and E. Wiechec, “Role of ion channels in regulating Ca^{2+} homeostasis during the interplay between immune and cancer cells.,” *Cell Death Dis.*, vol. 6, p. e1648, 2015.

[20] D. J. Cosens and a Manning, “Abnormal electroretinogram from a Drosophila mutant.,” *Nature*, vol. 224, no. 5216, pp. 285–287, 1969.

[21] B. Minke, “The history of the Drosophila TRP channel: the birth of a new channel superfamily.,” *J. Neurogenet.*, vol. 24, no. 4, pp. 216–233, 2010.

[22] D. E. Clapham, “TRP channels as cellular sensors.,” *Nature*, vol. 426, no. 6966, pp. 517–524, 2003.

[23] D. E. Clapham, C. Montell, G. Schultz, and D. Julius, “International Union of Pharmacology . XLIII . Compendium of Voltage-Gated Ion Channels : Transient Receptor Potential Channels,” *Pharmacol. Rev.*, vol. 55, no. 4, pp. 591–596, 2003.

[24] L. Arias-Darraz, D. Cabezas, C. K. Colenso, M. Alegría-Arcos, F. Bravo-Moraga, I. Varas-Concha, D. E. Almonacid, R. Madrid, and S. Brauchi, “A Transient Receptor Potential Ion Channel in Chlamydomonas Shares Key Features with Sensory Transduction-Associated TRP Channels in Mammals.,” *Plant Cell*, vol. 27, no. 1, pp. 177–88, 2015.

[25] G. L. Wheeler and C. Brownlee, “Ca2+ signalling in plants and green algae - changing channels,” *Trends in Plant Science*, vol. 13, no. 9. pp. 506–514, 2008.

[26] Y. Chang, G. Schlenstedt, V. Flockerzi, and A. Beck, “Properties of the intracellular transient receptor potential (TRP) channel in yeast, Yvc1,” *FEBS Letters*, vol. 584, no. 10. pp. 2028–2032, 2010.

[27] V. Denis and M. S. Cyert, “Internal Ca2+ release in yeast is triggered by hypertonic shock and mediated by a TRP channel homologue,” *J. Cell Biol.*, vol. 156, no. 1, pp. 29–34, 2002.

[28] C. P. Palmer, X. L. Zhou, J. Lin, S. H. Loukin, C. Kung, and Y. Saimi, “A TRP homolog in Saccharomyces cerevisiae forms an intracellular Ca(2+)-permeable channel in the yeast vacuolar membrane.,” *Proc. Natl. Acad. Sci. U. S. A.*, vol. 98, no. 14, pp. 7801–7805, 2001.

[29] X. Cai, “Unicellular Ca2+ signaling ‘toolkit’ at the origin of metazoa,” *Mol. Biol. Evol.*, vol. 25, no. 7, pp. 1357–1361, 2008.

[30] B. Nilius and G. Owsianik, “The transient receptor potential family of ion channels,” *Genome Biol.*, vol. 12, no. 3, p. 218, 2011.

[31] G. Owsianik, D. D’Hoedt, T. Voets, and B. Nilius, “Structure-function relationship of the TRP channel superfamily,” *Reviews of Physiology, Biochemistry and Pharmacology*, vol. 156. pp. 61–90, 2006.

[32] R. Gaudet, “TRP channels entering the structural era.,” *J. Physiol.*, vol. 586, no. Pt 15, pp. 3565–75, 2008.

[33] C. J. McCleverty, E. Koesema, A. Patapoutian, S. A. Lesley, and A. Kreusch, “Crystal structure of the human TRPV2 channel ankyrin repeat domain.,” *Protein Sci.*, vol. 15, no. 9, pp. 2201–6, 2006.

[34] P. V. Lishko, E. Procko, X. Jin, C. B. Phelps, and R. Gaudet, “The Ankyrin Repeats of TRPV1 Bind Multiple Ligands and Modulate Channel Sensitivity,” *Neuron*, vol. 54, no. 6, pp. 905–918, 2007.

[35] C. B. Phelps, R. J. Huang, P. V. Lishko, R. R. Wang, and R. Gaudet, “Structural analyses of the ankyrin repeat domain of TRPV6 and related TRPV ion channels,” *Biochemistry*, vol. 47, no. 8, pp. 2476–2484, 2008.

[36] Y. Fujiwara and D. L. Minor, “X-ray Crystal Structure of a TRPM Assembly Domain Reveals an Antiparallel Four-stranded Coiled-coil,” *J. Mol. Biol.*, vol. 383, no. 4, pp. 854–870, 2008.

[37] H. Yamaguchi, M. Matsushita, A. C. Nairn, and J. Kuriyan, “Crystal structure of the atypical protein kinase domain of a TRP channel with phosphotransferase activity,” *Mol. Cell*, vol. 7, no. 5, pp. 1047–1057, 2001.

[38] Y. Yu, M. H. Ulbrich, M.-H. Li, Z. Buraei, X.-Z. Chen, A. C. M. Ong, L. Tong, E. Y. Isacoff, and J. Yang, “Structural and molecular basis of the assembly of the TRPP2/PKD1 complex.,” *Proc. Natl. Acad. Sci. U. S. A.*, vol. 106, no. 28, pp. 11558–11563, 2009.

[39] K. Mio, T. Ogura, S. Kiyonaka, Y. Hiroaki, Y. Tanimura, Y. Fujiyoshi, Y. Mori, and C. Sato, “The TRPC3 Channel Has a Large Internal Chamber Surrounded by Signal Sensing Antennas,” *J. Mol. Biol.*, vol. 367, no. 2, pp. 373–383, 2007.

[40] V. Y. Moiseenkova-Bell, L. a Stanciu, I. I. Serysheva, B. J. Tobe, and T. G. Wensel, “Structure of TRPV1 channel revealed by electron cryomicroscopy.,” *Proc. Natl. Acad. Sci. U. S. A.*, vol. 105, no. 21, pp. 7451–7455, 2008.

[41] H. Shigematsu, T. Sokabe, R. Danev, M. Tominaga, and K. Nagayama, “A 3.5-nm structure of rat TRPV4 cation channel revealed by zernike phase-contrast cryoelectron microscopy,” *J. Biol. Chem.*, vol. 285, no. 15, pp. 11210–11218, 2010.

[42] M. Liao, E. Cao, D. Julius, and Y. Cheng, “Structure of the TRPV1 ion channel determined by electron cryo-microscopy.,” *Nature*, vol. 504, no. 7478, pp. 107–12, 2013.

[43] C. E. Paulsen, J. Armache, Y. Gao, Y. Cheng, and D. Julius, “Structure of the TRPA1 ion channel suggests regulatory mechanisms,” *Nature*, vol. 520, no. 7548, pp. 511–517, 2015.

[44] L. Zubcevic, M. A. Herzik, B. C. Chung, Z. Liu, G. C. Lander, and S.-Y. Lee, “Cryo-electron microscopy structure of the TRPV2 ion channel,” *Nat. Struct. Mol. Biol.*, vol. 23, no. November 2015, pp. 1–9, 2016.

[45] K. W. Huynh, M. R. Cohen, J. Jiang, A. Samanta, D. T. Lodowski, Z. H. Zhou, and V. Y. Moiseenkova-Bell, “Structure of the full-length TRPV2 channel by cryo-EM,” *Nat. Commun.*, vol. 7, p. 11130, 2016.

[46] T. Hofmann, M. Schaefer, G. Schultz, and T. Gudermann, “Subunit composition of mammalian transient receptor potential channels in living cells,” *Proc. Natl. Acad. Sci. U. S. A.*, vol. 99, no. 11, pp. 7461–6, 2002.

[47] R. Gaudet, “A primer on ankyrin repeat function in TRP channels and beyond.,” *Mol. Biosyst.*, vol. 4, no. 5, pp. 372–9, 2008.

[48] S.-Y. Lau, E. Procko, and R. Gaudet, “Distinct properties of Ca2+-calmodulin binding to N- and C-terminal regulatory regions of the TRPV1 channel,” *J. Gen. Physiol.*, vol. 140, no. 5, pp. 541–555, 2012.

[49] D. B. van Rossum, R. L. Patterson, S. Sharma, R. K. Barrow, M. Kornberg, D. L. Gill, and S. H. Snyder, “Phospholipase Cgamma1 controls surface expression of TRPC3 through an intermolecular PH domain.,” *Nature*, vol. 434, no. 7029, pp. 99–104, 2005.

[50] A. Fleig and R. Penner, “The TRPM ion channel subfamily: Molecular, biophysical and functional features,” *Trends in Pharmacological Sciences*, vol. 25, no. 12. pp. 633–639, 2004.

[51] B. Holakovska, L. Grycova, M. Jirku, M. Sulc, L. Bumba, and J. Teisinger, “Calmodulin and S100A1 protein interact with N terminus of TRPM3 channel,” *J. Biol. Chem.*, vol. 287, no. 20, pp. 16645–16655, 2012.

[52] T. De Groot, E. A. E. Van Der Hagen, S. Verkaart, V. A. M. Te Boekhorst, R. J. M. Bindels, and J. G. J. Hoenderop, “Role of the transient receptor potential vanilloid 5 (TRPV5) protein N terminus in channel activity, tetramerization, and trafficking,” *J. Biol. Chem.*, vol. 286, no. 37, pp. 32132–32139, 2011.

[53] L. Gregorio-Teruel, P. Valente, J. M. González-Ros, G. Fernández-Ballester, and A. Ferrer-Montiel,

"Mutation of I696 and W697 in the TRP box of vanilloid receptor subtype I modulates allosteric channel activation.," *J. Gen. Physiol.*, vol. 143, no. 3, pp. 361–75, 2014.

[54] C. a Ufret-Vincenty, R. M. Klein, L. Hua, J. Angueyra, and S. E. Gordon, "Localization of the PIP2 Xensor of TRPV1 Ion Channels," *J. Biol. Chem.*, vol. 286, no. 11, pp. 9688–98, 2011.

[55] Y. Karashima, J. Prenen, V. Meseguer, G. Owsianik, T. Voets, and B. Nilius, "Modulation of the transient receptor potential channel TRPA1 by phosphatidylinositol 4,5-biphosphate manipulators," *Pflugers Arch. Eur. J. Physiol.*, vol. 457, no. 1, pp. 77–89, 2008.

[56] S. Yamaguchi, A. Tanimoto, K. I. Otsuguro, H. Hibino, and S. Ito, "Negatively charged amino acids near and in transient receptor potential (TRP) domain of TRPM4 channel are one determinant of its Ca2+ sensitivity," *J. Biol. Chem.*, vol. 289, no. 51, pp. 35265–35282, 2014.

[57] E. Friedlova, L. Grycova, B. Holakovska, J. Silhan, H. Janouskova, M. Sulc, V. Obsilova, T. Obsil, and J. Teisinger, "The interactions of the C-terminal region of the TRPC6 channel with calmodulin," *Neurochem. Int.*, vol. 56, no. 2, pp. 363–366, 2010.

[58] B. Holakovska, L. Grycova, J. Bily, and J. Teisinger, "Characterization of calmodulin binding domains in TRPV2 and TRPV5 C-tails.," *Amino Acids*, vol. 40, pp. 741–8, 2011.

[59] D. Baez-Nieto, J. P. Castillo, C. Dragicevic, O. Alvarez, and R. Latorre, "Thermo-TRP channels: Biophysics of polymodal receptors," in *Advances in Experimental Medicine and Biology*, 2011, vol. 704, pp. 469–490.

[60] D. E. Clapham, "Calcium Signaling," *Cell*, vol. 131, no. 6. pp. 1047–1058, 2007.

[61] E. Cao, M. Liao, Y. Cheng, and D. Julius, "TRPV1 structures in distinct conformations reveal activation mechanisms.," *Nature*, vol. 504, no. 7478, pp. 113–8, 2013.

[62] C. Koike, T. Obara, Y. Uriu, T. Numata, R. Sanuki, K. Miyata, T. Koyasu, S. Ueno, K. Funabiki, A. Tani, H. Ueda, M. Kondo, Y. Mori, M. Tachibana, and T. Furukawa, "TRPM1 is a component of the retinal ON bipolar cell transduction channel in the mGluR6 cascade.," *Proc. Natl. Acad. Sci. U. S. A.*, vol. 107, no. 1, pp. 332–7, 2010.

[63] R. L. Patterson, D. B. van Rossum, D. L. Ford, K. J. Hurt, S. S. Bae, P. G. Suh, T. Kurosaki, S. H. Snyder, and D. L. Gill, "Phospholipase C-gamma is required for agonist-induced Ca2+ entry.," *Cell*, vol. 111, pp. 529–541, 2002.

[64] K. Itsuki, Y. Imai, H. Hase, Y. Okamura, R. Inoue, and M. X. Mori, "PLC-mediated PI(4,5)P2 hydrolysis regulates activation and inactivation of TRPC6/7 channels," *J Gen Physiol*, vol. 143, no. 2, pp. 183–201, 2014.

[65] K. Kuwahara, Y. Wang, J. McAnally, J. A. Richardson, R. Bassel-Duby, J. A. Hill, and E. N. Olson, "TRPC6 fulfills a calcineurin signaling circuit during pathologic cardiac remodeling," *J. Clin. Invest.*, vol. 116, no. 12, pp. 3114–3126, 2006.

[66] C. Lorin, I. Vögeli, and E. Niggli, "Dystrophic cardiomyopathy: role of TRPV2 channels in stretch-induced cell damage.," *Cardiovasc. Res.*, vol. 106, no. 1, pp. 153–62, 2015.

[67] K. Sałat and B. Filipek, "Antinociceptive activity of transient receptor potential channel TRPV1, TRPA1, and TRPM8 antagonists in neurogenic and neuropathic pain models in mice.," *J. Zhejiang Univ. Sci. B*, vol. 16, no. 3, pp. 167–78, 2015.

[68] Y. Kaneko and A. Szallasi, "Transient receptor potential (TRP) channels: A clinical perspective," *British Journal of Pharmacology*, vol. 171, no. 10. pp. 2474–2507, 2014.

[69] M. J. Caterina, M. a Schumacher, M. Tominaga, T. a Rosen, J. D. Levine, and D. Julius, "The capsaicin receptor: a heat-activated ion channel in the pain pathway.," *Nature*, vol. 389, no. 6653, pp. 816–824, 1997.

[70] C. Montell, "The TRP superfamily of cation channels.," *Sci. STKE*, vol. 2005, no. 272, p. re3, 2005.

[71] Z. Gong, "Two Interdependent TRPV Channel Subunits, Inactive and Nanchung, Mediate Hearing in Drosophila," *J. Neurosci.*, vol. 24, no. 41, pp. 9059–9066, 2004.

[72] S. Saito, N. Fukuta, R. Shingai, and M. Tominaga, "Evolution of vertebrate transient receptor potential vanilloid 3 channels: Opposite temperature sensitivity between mammals and western clawed frogs," *PLoS Genet.*, vol. 7, no. 4, 2011.

[73] S. Saito and R. Shingai, "Evolution of thermoTRP ion channel homologs in vertebrates.," *Physiol. Genomics*, vol. 27, no. 3, pp. 219–230, 2006.

[74] R. Jahnel, O. Bender, L. M. Münter, M. Dreger, C. Gillen, and F. Hucho, "Dual expression of mouse and rat VRL-1 in the dorsal root ganglion derived cell line F-11 and biochemical analysis of VRL-1 after heterologous expression," *Eur. J. Biochem.*, vol. 270, pp. 4264–4271, 2003.

[75] E. Mezey, Z. E. Toth, D. N. Cortright, M. K. Arzubi, J. E. Krause, R. Elde, A. Guo, P. M. Blumberg, and A. Szallasi, "Distribution of mRNA for vanilloid receptor subtype 1 (VR1), and VR1-like immunoreactivity, in the central nervous system of the rat and human," *Proc. Natl. Acad. Sci. U. S. A.*, vol. 97, no. 7, pp. 3655–3660, 2000.

[76] J. C. Roberts, J. B. Davis, and C. D. Benham, "[3H]Resiniferatoxin autoradiography in the CNS of wild-type and TRPV1 null mice defines TRPV1 (VR-1) protein distribution," *Brain Res.*, vol. 995, no. 2, pp. 176–183, 2004.

[77] T. Mannari, S. Morita, E. Furube, M. Tominaga, and S. Miyata, "Astrocytic TRPV1 ion channels detect blood-borne signals in the sensory circumventricular organs of adult mouse brains," *Glia*, vol. 61, no. 6, pp. 957–971, 2013.

[78] S. Doly, J. Fischer, and M. Conrath, "The vanilloid receptor-1 (TRPV1) is expressed in some rat dorsal horn NK1 cells," *Brain Res.*, vol. 1004, no. 1–2, pp. 203–207, 2004.

[79] M. R. Zahner, D.-P. Li, S.-R. Chen, and H.-L. Pan, "Cardiac vanilloid receptor 1-expressing afferent nerves and their role in the cardiogenic sympathetic reflex in rats.," *J. Physiol.*, vol. 551, no. Pt 2, pp. 515–23, 2003.

[80] A. H. Morice and P. Geppetti, "Cough. 5: The type 1 vanilloid receptor: a sensory receptor for cough," *Thorax*, vol. 59, no. 3, pp. 257–258, 2004.

[81] A. Avelino, C. Cruz, I. Nagy, and F. Cruz, "Vanilloid receptor 1 expression in the rat urinary tract," *Neuroscience*, vol. 109, no. 4, pp. 787–798, 2002.

[82] M. D. Southall, T. Li, L. S. Gharibova, Y. Pei, G. D. Nicol, and J. B. Travers, "Activation of epidermal vanilloid receptor-1 induces release of proinflammatory mediators in human keratinocytes.," *J. Pharmacol. Exp. Ther.*, vol. 304, no. 1, pp. 217–222, 2003.

[83] D. J. Cavanaugh, A. T. Chesler, A. C. Jackson, Y. M. Sigal, H. Yamanaka, R. Grant, D. O'Donnell, R. A. Nicoll, N. M. Shah, D. Julius, and A. I. Basbaum, "Trpv1 reporter mice reveal highly restricted brain distribution and functional expression in arteriolar smooth muscle cells.," *J. Neurosci.*, vol. 31, no. 13, pp. 5067–77, 2011.

[84] D. Yang, Z. Luo, S. Ma, W. T. Wong, L. Ma, J. Zhong, H. He, Z. Zhao, T. Cao, Z. Yan, D. Liu, W. J. Arendshorst, Y. Huang, M. Tepel, and Z. Zhu, "Activation of TRPV1 by dietary capsaicin improves endothelium-dependent vasorelaxation and prevents hypertension," *Cell Metab.*, vol. 12, no. 2, pp. 130–141, 2010.

[85] N. Agopyan, J. Head, S. Yu, and S. A. Simon, "TRPV1 receptors mediate particulate matter-induced apoptosis.," *Am. J. Physiol. Lung Cell. Mol. Physiol.*, vol. 286, no. 3, pp. L563–72, 2004.

[86] J. Peng and Y. J. Li, "The vanilloid receptor TRPV1: Role in cardiovascular and gastrointestinal protection," *European Journal of Pharmacology*, vol. 627, no. 1–3. pp. 1–7, 2010.

[87] F. Cruz, "Mechanisms involved in new therapies for overactive bladder," *Urology*, vol. 63, no. 3 Suppl 1, pp. 65–73, 2004.

[88] Y. Akiba, S. Kato, K. Katsube, M. Nakamura, K. Takeuchi, H. Ishii, and T. Hibi, "Transient receptor potential vanilloid subfamily 1 expressed in pancreatic islet beta cells modulates insulin secretion in rats.," *Biochem. Biophys. Res. Commun.*, vol. 321, no. 1, pp. 219–25, 2004.

[89] A. Liapi and J. N. Wood, "Extensive co-localization and heteromultimer formation of the vanilloid receptor-like protein TRPV2 and the capsaicin receptor TRPV1 in the adult rat cerebral cortex," *Eur. J. Neurosci.*, vol. 22, no. 4, pp. 825–834, 2005.

[90] A. Wainwright, A. R. Rutter, G. R. Seabrook, K. Reilly, and K. R. Oliver, "Discrete expression of TRPV2 within the hypothalamo-neurohypophysial system: Implications for regulatory activity within the hypothalamic-pituitary-adrenal axis," *J. Comp. Neurol.*, vol. 474, no. 1, pp. 24–42, 2004.

[91] K. Muraki, Y. Iwata, Y. Katanosaka, T. Ito, S. Ohya, M. Shigekawa, and Y. Imaizumi, "TRPV2 Is a Component of Osmotically Sensitive Cation Channels in Murine Aortic Myocytes," *Circ. Res.*, vol. 93, no. 9, pp. 829–838, 2003.

[92] J. D. Cahoy, B. Emery, A. Kaushal, L. C. Foo, J. L. Zamanian, K. S. Christopherson, Y. Xing, J. L. Lubischer, P. a Krieg, S. a Krupenko, W. J. Thompson, and B. a Barres, "A transcriptome database for astrocytes, neurons, and oligodendrocytes: a new resource for understanding brain development and function.," *J. Neurosci.*, vol. 28, no. 1, pp. 264–78, 2008.

[93] T. P. Nedungadi, M. Dutta, C. S. Bathina, M. J. Caterina, and J. T. Cunningham, "Expression and distribution of TRPV2 in rat brain.," *Exp. Neurol.*, vol. 237, no. 1, pp. 223–37, 2012.

[94] K. Shibasaki, N. Murayama, K. Ono, Y. Ishizaki, and M. Tominaga, "TRPV2 enhances axon outgrowth through its activation by membrane stretch in developing sensory and motor neurons," *J Neurosci*, vol. 30, pp. 4601–4612, 2010.

[95] H. J. Choi, D. Sun, and T. C. Jakobs, "Astrocytes in the optic nerve head express putative mechanosensitive channels.," *Mol. Vis.*, vol. 21, no. January, pp. 749–66, 2015.

[96] K. Shibasaki, Y. Ishizaki, and S. Mandadi, "Astrocytes express functional TRPV2 ion channels," *Biochem. Biophys. Res. Commun.*, vol. 441, pp. 327–332, 2013.

[97] J. Ahluwalia, H. Rang, and I. Nagy, "The putative role of vanilloid receptor-like protein-1 in mediating high threshold noxious heat-sensitivity in rat cultured primary sensory neurons," *Eur. J. Neurosci.*, vol. 16, no. 8, pp. 1483–1489, 2002.

[98] H. Ichikawa and T. Sugimoto, "Vanilloid receptor 1-like receptor-immunoreactive primary sensory neurons in the rat trigeminal nervous system," *Neuroscience*, vol. 101, no. 3, pp. 719–725, 2000.

[99] J. L. Gibbs, J. L. Melnyk, and a I. Basbaum, "Differential TRPV1 and TRPV2 channel expression in dental

pulp.," *J. Dent. Res.*, vol. 90, no. 6, pp. 765–770, 2011.

[100] H. Mihara, A. Boudaka, K. Shibasaki, A. Yamanaka, T. Sugiyama, and M. Tominaga, "Involvement of TRPV2 activation in intestinal movement through nitric oxide production in mice.," *J. Neurosci.*, vol. 30, no. 49, pp. 16536–16544, 2010.

[101] P. Gailly, "TRP channels in normal and dystrophic skeletal muscle," *Curr. Opin. Pharmacol.*, vol. 12, no. 3, pp. 326–334, 2012.

[102] J. Rubinstein, V. M. Lasko, S. E. Koch, V. P. Singh, V. Carreira, N. Robbins, A. R. Patel, M. Jiang, P. Bidwell, E. G. Kranias, W. K. Jones, and J. N. Lorenz, "Novel role of transient receptor potential vanilloid 2 in the regulation of cardiac performance.," *Am. J. Physiol. Heart Circ. Physiol.*, vol. 306, no. 4, pp. H574–84, 2014.

[103] Y. Katanosaka, K. Iwasaki, Y. Ujihara, S. Takatsu, K. Nishitsuji, M. Kanagawa, A. Sudo, T. Toda, K. Katanosaka, S. Mohri, and K. Naruse, "TRPV2 is critical for the maintenance of cardiac structure and function in mice.," *Nat. Commun.*, vol. 5, no. May, p. 3932, 2014.

[104] K. S. Park, Y. Kim, Y.-H. Lee, Y. E. Earm, and W.-K. Ho, "Mechanosensitive cation channels in arterial smooth muscle cells are activated by diacylglycerol and inhibited by phospholipase C inhibitor.," *Circ. Res.*, vol. 93, no. 6, pp. 557–64, 2003.

[105] I. Fantozzi, S. Zhang, O. Platoshyn, C. V Remillard, R. T. Cowling, and J. X.-J. Yuan, "Hypoxia increases AP-1 binding activity by enhancing capacitative Ca2+ entry in human pulmonary artery endothelial cells.," *Am. J. Physiol. Lung Cell. Mol. Physiol.*, vol. 285, no. 6, pp. L1233–L1245, 2003.

[106] G. Peng, W. Lu, X. Li, Y. Chen, N. Zhong, P. Ran, and J. Wang, "Expression of store-operated Ca2+ entry and transient receptor potential canonical and vanilloid-related proteins in rat distal pulmonary venous smooth muscle," *Am J Physiol Lung Cell Mol Physiol*, vol. 299, no. 5, pp. L621–30, 2010.

[107] E. Hisanaga, M. Nagasawa, K. Ueki, R. N. Kulkarni, M. Mori, and I. Kojima, "Regulation of calcium-permeable TRPV2 channel by insulin in pancreatic beta-cells.," *Diabetes*, vol. 58, pp. 174–84, 2009.

[108] T. M. Link, U. Park, B. M. Vonakis, D. M. Raben, M. J. Soloski, and M. J. Caterina, "TRPV2 has a pivotal role in macrophage particle binding and phagocytosis.," *Nat. Immunol.*, vol. 11, no. 3, pp. 232–9, 2010.

[109] D. Zhang, A. Spielmann, L. Wang, G. Ding, F. Huang, Q. Gu, and W. Schwarz, "Mast-cell degranulation induced by physical stimuli involves the activation of transient-receptor-potential channel TRPV2," *Physiol. Res.*, vol. 61, no. 1, pp. 113–124, 2012.

[110] C. I. Saunders, D. A. Kunde, A. Crawford, and D. P. Geraghty, "Expression of transient receptor potential vanilloid 1 (TRPV1) and 2 (TRPV2) in human peripheral blood," *Mol. Immunol.*, vol. 44, no. 6, pp. 1429–1435, 2007.

[111] E. Guatteo, K. K. H. Chung, T. K. Bowala, G. Bernardi, N. B. Mercuri, and J. Lipski, "Temperature sensitivity of dopaminergic neurons of the substantia nigra pars compacta: involvement of transient receptor potential channels.," *J. Neurophysiol.*, vol. 94, no. 5, pp. 3069–3080, 2005.

[112] J. Lipski, T. I. H. Park, D. Li, S. C. W. Lee, A. J. Trevarton, K. K. H. Chung, P. S. Freestone, and J. Z. Bai, "Involvement of TRP-like channels in the acute ischemic response of hippocampal CA1 neurons in brain slices," *Brain Res.*, vol. 1077, no. 1, pp. 187–199, 2006.

[113] I. P. Voronova, A. A. Tuzhikova, and T. V Kozyreva, "[Thermosensitive TRP channels gene expression in hypothalamus of normal rats and rats adapted to cold].," *Ross. Fiziol. zhurnal Im. I.M. Sechenova / Ross. Akad. Nauk*, vol. 98, no. 9, pp. 1101–1110, 2012.

[114] M. D. Angelica and Y. Fong, “NIH Public Access,” *October*, vol. 141, no. 4, pp. 520–529, 2008.

[115] G. D. Smith, M. J. Gunthorpe, R. E. Kelsell, P. D. Hayes, P. Reilly, P. Facer, J. E. Wright, J. C. Jerman, J.-P. Walhin, L. Ooi, J. Egerton, K. J. Charles, D. Smart, a D. Randall, P. Anand, and J. B. Davis, “TRPV3 is a temperature-sensitive vanilloid receptor-like protein.,” *Nature*, vol. 418, no. 6894, pp. 186–190, 2002.

[116] T. Kitahara, H. S. Li, and C. D. Balaban, “Changes in transient receptor potential cation channel superfamily V (TRPV) mRNA expression in the mouse inner ear ganglia after kanamycin challenge,” *Hear. Res.*, vol. 201, no. 1–2, pp. 132–144, 2005.

[117] P. Facer, M. A. Casula, G. D. Smith, C. D. Benham, I. P. Chessell, C. Bountra, M. Sinisi, R. Birch, and P. Anand, “Differential expression of the capsaicin receptor TRPV1 and related novel receptors TRPV3, TRPV4 and TRPM8 in normal human tissues and changes in traumatic and diabetic neuropathy,” *BMC Neurol.*, vol. 7, no. 1, p. 11, 2007.

[118] C. Radtke, N. Sinis, M. Sauter, S. Jahn, U. Kraushaar, E. Guenther, H. P. Rodemann, and H.-O. Rennekampff, “TRPV channel expression in human skin and possible role in thermally induced cell death.,” *J. Burn Care Res.*, vol. 32, no. 1, pp. 150–9, 2011.

[119] T. Miyamoto, M. J. Petrus, A. E. Dubin, and A. Patapoutian, “TRPV3 regulates nitric oxide synthase-independent nitric oxide synthesis in the skin.,” *Nat. Commun.*, vol. 2, p. 369, 2011.

[120] X. Cheng, J. Jin, L. Hu, D. Shen, X. ping Dong, M. A. Samie, J. Knoff, B. Eisinger, M. L. Liu, S. M. Huang, M. J. Caterina, P. Dempsey, L. E. Michael, A. A. Dlugosz, N. C. Andrews, D. E. Clapham, and H. Xu, “TRP channel regulates EGFR signaling in hair morphogenesis and skin barrier formation,” *Cell*, vol. 141, no. 2, pp. 331–343, 2010.

[121] I. Borbíró, E. Lisztes, B. I. Tóth, G. Czifra, A. Oláh, A. G. Szöllosi, N. Szentandrássy, P. P. Nánási, Z. Péter, R. Paus, L. Kovács, and T. Bíró, “Activation of transient receptor potential vanilloid-3 inhibits human hair growth.,” *J. Invest. Dermatol.*, vol. 131, pp. 1605–1614, 2011.

[122] R. Xiao, J. Tian, J. Tang, and M. X. Zhu, “The TRPV3 mutation associated with the hairless phenotype in rodents is constitutively active,” *Cell Calcium*, vol. 43, no. 4, pp. 334–343, 2008.

[123] T. Ueda, T. Yamada, S. Ugawa, Y. Ishida, and S. Shimada, “TRPV3, a thermosensitive channel is expressed in mouse distal colon epithelium,” *Biochem. Biophys. Res. Commun.*, vol. 383, no. 1, pp. 130–134, 2009.

[124] L. de Petrocellis, P. Orlando, A. S. Moriello, G. Aviello, C. Stott, A. A. Izzo, and V. di Marzo, “Cannabinoid actions at TRPV channels: Effects on TRPV3 and TRPV4 and their potential relevance to gastrointestinal inflammation,” *Acta Physiologica*, vol. 204, no. 2. pp. 255–266, 2012.

[125] W. Everaerts, B. Nilius, and G. Owsianik, “The vanilloid transient receptor potential channel TRPV4: From structure to disease,” *Progress in Biophysics and Molecular Biology*, vol. 103, no. 1. pp. 2–17, 2010.

[126] C. W. Bourque, S. Ciura, E. Trudel, T. J. E. Stachniak, and R. Sharif-Naeini, “Neurophysiological characterization of mammalian osmosensitive neurones.,” *Exp. Physiol.*, vol. 92, no. 3, pp. 499–505, 2007.

[127] K. Shibasaki, M. Suzuki, A. Mizuno, and M. Tominaga, “Effects of body temperature on neural activity in the hippocampus: regulation of resting membrane potentials by transient receptor potential vanilloid 4,” *J. Neurosci.*, vol. 27, no. 1529–2401 (Electronic), pp. 1566–1575, 2007.

[128] K. Shibasaki, K. Ikenaka, F. Tamalu, M. Tominaga, and Y. Ishizaki, “A novel subtype of astrocytes expressing TRPV4 (Transient Receptor Potential Vanilloid 4) Regulates neuronal excitability via release of gliotransmitters,” *J. Biol. Chem.*, vol. 289, no. 21, pp. 14470–14480, 2014.

[129] S. Mergler, M. Valtink, K. Taetz, M. Sahlmüller, G. Fels, P. S. Reinach, K. Engelmann, and U. Pleyer, "Characterization of transient receptor potential vanilloid channel 4 (TRPV4) in human corneal endothelial cells," *Exp. Eye Res.*, vol. 93, no. 5, pp. 710–719, 2011.

[130] T. Sokabe, T. Fukumi-Tominaga, S. Yonemura, A. Mizuno, and M. Tominaga, "The TRPV4 channel contributes to intercellular junction formation in keratinocytes," *J. Biol. Chem.*, vol. 285, no. 24, pp. 18749–18758, 2010.

[131] I. M. Lorenzo, W. Liedtke, M. J. Sanderson, and M. a Valverde, "TRPV4 channel participates in receptor-operated calcium entry and ciliary beat frequency regulation in mouse airway epithelial cells.," *Proc. Natl. Acad. Sci. U. S. A.*, vol. 105, no. 34, pp. 12611–12616, 2008.

[132] J. M. Fern??ndez-Fern??ndez, Y. N. Andrade, M. Arniges, J. Fernandes, C. Plata, F. Rubio-Moscardo, E. V??zquez, and M. A. Valverde, "Functional coupling of TRPV4 cationic channel and large conductance, calcium-dependent potassium channel in human bronchial epithelial cell lines," *Pflugers Arch. Eur. J. Physiol.*, vol. 457, no. 1, pp. 149–159, 2008.

[133] M. A. McAlexander, M. a Luttmann, G. E. Hunsberger, and B. J. Undem, "Transient receptor potential vanilloid 4 activation constricts the human bronchus via the release of cysteinyl leukotrienes.," *J. Pharmacol. Exp. Ther.*, vol. 349, no. 1, pp. 118–25, 2014.

[134] J. Li, P. Kanju, M. Patterson, W. L. Chew, S. H. Cho, I. Gilmour, T. Oliver, R. Yasuda, A. Ghio, S. A. Simon, and W. Liedtke, "TRPV4-mediated calcium influx into human bronchial epithelia upon exposure to diesel exhaust particles," *Environ. Health Perspect.*, vol. 119, no. 6, pp. 784–793, 2011.

[135] G. Zhu, A. Gulsvik, P. Bakke, S. Ghatta, W. Anderson, D. A. Lomas, E. K. Silverman, and S. G. Pillai, "Association of TRPV4 gene polymorphisms with chronic obstructive pulmonary disease," *Hum. Mol. Genet.*, vol. 18, no. 11, pp. 2053–2062, 2009.

[136] N. Cenac, C. Altier, J.-P. Motta, E. d'Aldebert, S. Galeano, G. W. Zamponi, and N. Vergnolle, "Potentiation of TRPV4 signalling by histamine and serotonin: an important mechanism for visceral hypersensitivity.," *Gut*, vol. 59, no. 4, pp. 481–488, 2010.

[137] E. D'Aldebert, N. Cenac, P. Rousset, L. Martin, C. Rolland, K. Chapman, J. Selves, L. Alric, J. Vinel, and N. Vergnolle, "Transient receptor potential vanilloid 4 activated inflammatory signals by intestinal epithelial cells and colitis in mice," *Gastroenterology*, vol. 140, no. 1, pp. 275–285, 2011.

[138] W. Everaerts, X. Zhen, D. Ghosh, J. Vriens, T. Gevaert, J. P. Gilbert, N. J. Hayward, C. R. McNamara, F. Xue, M. M. Moran, T. Strassmaier, E. Uykal, G. Owsianik, R. Vennekens, D. De Ridder, B. Nilius, C. M. Fanger, and T. Voets, "Inhibition of the cation channel TRPV4 improves bladder function in mice and rats with cyclophosphamide-induced cystitis," *Journal of Urology*, vol. 186, no. 2. p. 753, 2011.

[139] M. Skrzypski, M. Kakkassery, S. Mergler, C. Grötzinger, N. Khajavi, M. Sassek, D. Szczepankiewicz, B. Wiedenmann, K. W. Nowak, and M. Z. Strowski, "Activation of TRPV4 channel in pancreatic INS-1E beta cells enhances glucose-stimulated insulin secretion via calcium-dependent mechanisms," *FEBS Lett.*, vol. 587, no. 19, pp. 3281–3287, 2013.

[140] C. Jung, C. Fandos, I. M. Lorenzo, C. Plata, J. Fernandes, G. G. Gen??, E. V??zquez, and M. A. Valverde, "The progesterone receptor regulates the expression of TRPV4 channel," *Pflugers Arch. Eur. J. Physiol.*, vol. 459, no. 1, pp. 105–113, 2009.

[141] Y. N. Andrade, J. Fernandes, E. V??zquez, J. M. Fern??ndez-Fern??ndez, M. Arniges, T. M. S??nchez, M. Villal??n, and M. A. Valverde, "TRPV4 channel is involved in the coupling of fluid viscosity changes to epithelial ciliary activity," *J. Cell Biol.*, vol. 168, no. 6, pp. 869–874, 2005.

[142] S. a Gradilone, A. I. Masyuk, P. L. Splinter, J. M. Banales, B. Q. Huang, P. S. Tietz, T. V Masyuk, and N. F. Larusso, "Cholangiocyte cilia express TRPV4 and detect changes in luminal tonicity inducing bicarbonate secretion.," *Proc. Natl. Acad. Sci. U. S. A.*, vol. 104, no. 48, pp. 19138–43, 2007.

[143] S. Earley, T. J. Heppner, M. T. Nelson, and J. E. Brayden, "TRPV4 forms a novel Ca2+ signaling complex with ryanodine receptors and BKCa channels," *Circ. Res.*, vol. 97, no. 12, pp. 1270–1279, 2005.

[144] J. Krüger, C. Kunert-Keil, F. Bisping, and H. Brinkmeier, "Transient receptor potential cation channels in normal and dystrophic mdx muscle," *Neuromuscul. Disord.*, vol. 18, no. 6, pp. 501–513, 2008.

[145] K. Hamanaka, M.-Y. Jian, M. I. Townsley, J. a King, W. Liedtke, D. S. Weber, F. G. Eyal, M. M. Clapp, and J. C. Parker, "TRPV4 channels augment macrophage activation and ventilator-induced lung injury.," *Am. J. Physiol. Lung Cell. Mol. Physiol.*, vol. 299, no. 3, pp. L353–62, 2010.

[146] R. K. Majhi, S. S. Sahoo, M. Yadav, B. M. Pratheek, S. Chattopadhyay, and C. Goswami, "Functional expression of TRPV channels in T cells and their implications in immune regulation," *FEBS J.*, vol. 282, no. 14, pp. 2661–2681, 2015.

[147] S. Muramatsu, M. Wakabayashi, T. Ohno, K. Amano, R. Ooishi, T. Sugahara, S. Shiojiri, K. Tashiro, Y. Suzuki, R. Nishimura, S. Kuhara, S. Sugano, T. Yoneda, and A. Matsuda, "Functional gene screening system identified TRPV4 as a regulator of chondrogenic differentiation," *J. Biol. Chem.*, vol. 282, no. 44, pp. 32158–32167, 2007.

[148] L. I. Nakkrasae, N. Thongon, J. Thongbunchoo, N. Krishnamra, and N. Charoenphandhu, "Transepithelial calcium transport in prolactin-exposed intestine-like Caco-2 monolayer after combinatorial knockdown of TRPV5, TRPV6 and Ca v1.3," *J. Physiol. Sci.*, vol. 60, no. 1, pp. 9–17, 2010.

[149] J. G. J. Hoenderop, J. P. T. M. Van Leeuwen, B. C. J. Van Der Eerden, F. F. J. Kersten, A. W. C. M. Van Der Kemp, A. M. M??rillat, J. H. Waarsing, B. C. Rossier, V. Vallon, E. Hummler, and R. J. M. Bindels, "Renal Ca2+ wasting, hyperabsorption, and reduced bone thickness in mice lacking TRPV5," *J. Clin. Invest.*, vol. 112, no. 12, pp. 1906–1914, 2003.

[150] A. G. N. B. Vriens J., J. Vriens, G. Appendino, and B. Nilius, "Pharmacology of Vanilloid Transient Receptor Potential Cation Channels," *Mol. Pharmacol.*, vol. 75, no. 6, pp. 1262–1279, 2009.

[151] A. Ferrer-Montiel, A. Fernández-Carvajal, R. Planells-Cases, G. Fernández-Ballester, J. M. González-Ros, A. Messeguer, and R. González-Muñiz, "Advances in modulating thermosensory TRP channels.," *Expert Opin. Ther. Pat.*, vol. 22, no. 9, pp. 999–1017, 2012.

[152] S. E. Jordt, M. Tominaga, and D. Julius, "Acid potentiation of the capsaicin receptor determined by a key extracellular site.," *Proc. Natl. Acad. Sci. U. S. A.*, vol. 97, no. 14, pp. 8134–8139, 2000.

[153] M. Trevisani, D. Smart, M. J. Gunthorpe, M. Tognetto, M. Barbieri, B. Campi, S. Amadesi, J. Gray, J. C. Jerman, S. J. Brough, D. Owen, G. D. Smith, a D. Randall, S. Harrison, a Bianchi, J. B. Davis, and P. Geppetti, "Ethanol elicits and potentiates nociceptor responses via the vanilloid receptor-1.," *Nat. Neurosci.*, vol. 5, no. 6, pp. 546–551, 2002.

[154] L. Liu, W. Zhu, Z.-S. Zhang, T. Yang, a Grant, G. Oxford, and S. a Simon, "Nicotine inhibits voltage-dependent sodium channels and sensitizes vanilloid receptors.," *J. Neurophysiol.*, vol. 91, no. 4, pp. 1482–1491, 2004.

[155] N. Zhang, S. Inan, A. Cowan, R. Sun, J. M. Wang, T. J. Rogers, M. Caterina, and J. J. Oppenheim, "A proinflammatory chemokine, CCL3, sensitizes the heat- and capsaicin-gated ion channel TRPV1," *Proc. Natl. Acad. Sci. U. S. A.*, vol. 102, no. 12, pp. 4536–4541, 2005.

[156] D. Smart, M. J. Gunthorpe, J. C. Jerman, S. Nasir, J. Gray, A. I. Muir, J. K. Chambers, A. D. Randall, and J. B. Davis, "The endogenous lipid anandamide is a full agonist at the human vanilloid receptor (hVR1).," *Br. J. Pharmacol.*, vol. 129, no. 2, pp. 227–30, 2000.

[157] A. M. Patwardhan, A. N. Akopian, N. B. Ruparel, A. Diogenes, S. T. Weintraub, C. Uhlson, R. C. Murphy, and K. M. Hargreaves, "Heat generates oxidized linoleic acid metabolites that activate TRPV1 and produce pain in rodents," *J. Clin. Invest.*, vol. 120, no. 5, pp. 1617–1626, 2010.

[158] V. Lukacs, B. Thyagarajan, P. Varnai, A. Balla, T. Balla, and T. Rohacs, "Dual regulation of TRPV1 by phosphoinositides," *J Neurosci*, vol. 27, no. 26, pp. 7070–7080, 2007.

[159] S. W. Hwang, H. Cho, J. Kwak, S. Y. Lee, C. J. Kang, J. Jung, S. Cho, K. H. Min, Y. G. Suh, D. Kim, and U. Oh, "Direct activation of capsaicin receptors by products of lipoxygenases: endogenous capsaicin-like substances.," *Proc. Natl. Acad. Sci. U. S. A.*, vol. 97, no. 11, pp. 6155–6160, 2000.

[160] L. Urban and A. Dray, "Capsazepine, a novel capsaicin antagonist, selectively antagonises the effects of capsaicin in the mouse spinal cord in vitro," *Neurosci. Lett.*, vol. 134, no. 1, pp. 9–11, 1991.

[161] A. Bhattacharya, B. P. Scott, N. Nasser, H. Ao, M. P. Maher, A. E. Dubin, D. M. Swanson, N. P. Shankley, A. D. Wickenden, and S. R. Chaplan, "Pharmacology and antitussive efficacy of 4-(3-trifluoromethyl-pyridin-2-yl)-piperazine-1-carboxylic acid (5-trifluoromethyl-pyridin-2-yl)-amide (JNJ17203212), a transient receptor potential vanilloid 1 antagonist in guinea pigs.," *J. Pharmacol. Exp. Ther.*, vol. 323, no. 2, pp. 665–674, 2007.

[162] M. P. Maher, A. Bhattacharya, H. Ao, N. Swanson, N. T. Wu, J. Freedman, M. Kansagara, B. Scott, D. H. Li, W. A. Eckert, Y. Liu, K. Sepassi, M. Rizzolio, A. Fitzgerald, J. Liu, B. J. Branstetter, J. C. Rech, A. D. Lebsack, J. G. Breitenbucher, A. D. Wickenden, and S. R. Chaplan, "Characterization of 2-(2,6-dichloro-benzyl)-thiazolo[5,4-d]pyrimidin-7-yl]- (4-trifluoromethyl-phenyl)-amine (JNJ-39729209) as a novel TRPV1 antagonist," *Eur. J. Pharmacol.*, vol. 663, no. 1–3, pp. 40–50, 2011.

[163] S. Khalid, R. Murdoch, A. Newlands, K. Smart, A. Kelsall, K. Holt, R. Dockry, A. Woodcock, and J. a. Smith, "Transient receptor potential vanilloid 1 (TRPV1) antagonism in patients with refractory chronic cough: A double-blind randomized controlled trial.," *J Allergy Clin Immunol*, vol. 134, no. 1, pp. 56–62.e4, 2014.

[164] M. A. Wortley, M. A. Birrell, S. A. Maher, P. Round, J. Ford, and M. G. Belvisi, "Profiling Of XEN-D0501, A Novel TRPV1 Antagonist, In Pre-Clinical Models Of Cough," in *American journal of respiratory and critical care medicine*, 2014, pp. A4979–A4979.

[165] M. J. Caterina, T. a Rosen, M. Tominaga, a J. Brake, and D. Julius, "A capsaicin-receptor homologue with a high threshold for noxious heat.," *Nature*, vol. 398, no. 6726, pp. 436–441, 1999.

[166] L. De Petrocellis, A. Ligresti, A. S. Moriello, M. Allar??, T. Bisogno, S. Petrosino, C. G. Stott, and V. Di Marzo, "Effects of cannabinoids and cannabinoid-enriched Cannabis extracts on TRP channels and endocannabinoid metabolic enzymes," *Br. J. Pharmacol.*, vol. 163, no. 7, pp. 1479–1494, 2011.

[167] H. Z. Hu, Q. Gu, C. Wang, C. K. Colton, J. Tang, M. Kinoshita-Kawada, L. Y. Lee, J. D. Wood, and M. X. Zhu, "2-Aminoethoxydiphenyl borate is a common activator of TRPV1, TRPV2, and TRPV3," *J. Biol. Chem.*, vol. 279, no. 34, pp. 35741–35748, 2004.

[168] S. Bang, K. Y. Kim, S. Yoo, S. H. Lee, and S. W. Hwang, "Transient receptor potential V2 expressed in sensory neurons is activated by probenecid," *Neurosci. Lett.*, vol. 425, no. 2, pp. 120–125, 2007.

[169] V. Juvin, A. Penna, J. Chemin, Y.-L. Lin, and F.-A. Rassendren, "Pharmacological characterization and molecular determinants of the activation of transient receptor potential V2 channel orthologs by 2-aminoethoxydiphenyl borate.," *Mol. Pharmacol.*, vol. 72, no. 5, pp. 1258–68, 2007.

[170] A. M. Peier, "A Heat-Sensitive TRP Channel Expressed in Keratinocytes," *Science (80-.).*, vol. 296, no. 5575, pp. 2046–2049, 2002.

[171] M.-K. Chung, H. Lee, A. Mizuno, M. Suzuki, and M. J. Caterina, "2-Aminoethoxydiphenyl Borate Activates and Sensitizes the Heat-Gated Ion Channel TRPV3," *J. Neurosci.*, vol. 24, no. 22, pp. 5177–5182, 2004.

[172] a K. Vogt-Eisele, K. Weber, M. a Sherkheli, G. Vielhaber, J. Panten, G. Gisselmann, and H. Hatt, "Monoterpenoid agonists of TRPV3.," *Br. J. Pharmacol.*, vol. 151, no. 4, pp. 530–540, 2007.

[173] S. Bang, S. Yoo, T. J. Yang, H. Cho, and S. W. Hwang, "Farnesyl pyrophosphate is a novel pain-producing molecule via specific activation of TRPV3," *J. Biol. Chem.*, vol. 285, no. 25, pp. 19362–19371, 2010.

[174] M. K. Chung, A. D. G??ler, and M. J. Caterina, "Biphasic currents evoked by chemical or thermal activation of the heat-gated ion channel, TRPV3," *J. Biol. Chem.*, vol. 280, no. 16, pp. 15928–15941, 2005.

[175] A. Moussaieff, N. Rimmerman, T. Bregman, A. Straiker, C. C. Felder, S. Shoham, Y. Kashman, S. M. Huang, H. Lee, E. Shohami, K. Mackie, M. J. Caterina, J. M. Walker, E. Fride, and R. Mechoulam, "Incensole acetate, an incense component, elicits psychoactivity by activating TRPV3 channels in the brain.," *FASEB J.*, vol. 22, no. 8, pp. 3024–34, 2008.

[176] H. Z. Hu, R. Xiao, C. Wang, N. Gao, C. K. Colton, J. D. Wood, and M. X. Zhu, "Potentiation of TRPV3 channel function by unsaturated fatty acids," *J. Cell. Physiol.*, vol. 208, no. 1, pp. 201–212, 2006.

[177] S. M. Huang and M.-K. Chung, "Targeting TRPV3 for the Development of Novel Analgesics.," *Open Pain J.*, vol. 6, no. Spec Iss 1, pp. 119–126, 2013.

[178] S. Bang, S. Yoo, T. J. Yang, H. Cho, and S. Hwang, "17(R)-resolvin D1 specifically inhibits transient receptor potential ion channel vanilloid 3 leading to peripheral antinociception," *Br. J. Pharmacol.*, vol. 165, no. 3, pp. 683–692, 2012.

[179] W. Liedtke, Y. Choe, M. A. Martí-Renom, A. M. Bell, C. S. Denis, A. Sali, A. J. Hudspeth, J. M. Friedman, and S. Heller, "Vanilloid receptor-related osmotically activated channel (VR-OAC), a candidate vertebrate osmoreceptor.," *Cell*, vol. 103, no. 3, pp. 525–35, 2000.

[180] A. D. Güler, H. Lee, T. Iida, I. Shimizu, M. Tominaga, and M. Caterina, "Heat-evoked activation of the ion channel, TRPV4.," *J. Neurosci.*, vol. 22, no. 15, pp. 6408–6414, 2002.

[181] J. Vriens, G. Owsianik, B. Fisslthaler, M. Suzuki, A. Janssens, T. Voets, C. Morisseau, B. D. Hammock, I. Fleming, R. Busse, and B. Nilius, "Modulation of the Ca2+ permeable cation channel TRPV4 by cytochrome P450 epoxygenases in vascular endothelium," *Circ. Res.*, vol. 97, no. 9, pp. 908–915, 2005.

[182] J. Vriens, G. Owsianik, A. Janssens, T. Voets, and B. Nilius, "Determinants of 4 alpha-phorbol sensitivity in transmembrane domains 3 and 4 of the cation channel TRPV4," *J Biol Chem*, vol. 282, no. 17, pp. 12796–12803, 2007.

[183] K. S. Thorneloe, A. C. Sulpizio, Z. Lin, D. J. Figueroa, A. K. Clouse, G. P. McCafferty, T. P. Chendrimada, E. S. R. Lashinger, E. Gordon, L. Evans, B. A. Misajet, D. J. Demarini, J. H. Nation, L. N. Casillas, R. W. Marquis, B. J. Votta, S. A. Sheardown, X. Xu, D. P. Brooks, N. J. Laping, and T. D. Westfall, "GSK1016790A, a novel and potent transient receptor potential vanilloid 4 channel agonist induces urinary bladder contraction and hyperactivity: Part I.," *J. Pharmacol. Exp. Ther.*, vol. 326, no. 2, pp. 432–442, 2008.

[184] A. D. Grant, G. S. Cottrell, S. Amadesi, M. Trevisani, P. Nicoletti, S. Materazzi, C. Altier, N. Cenac, G. W. Zamponi, F. Bautista-Cruz, C. B. Lopez, E. K. Joseph, J. D. Levine, W. Liedtke, S. Vanner, N. Vergnolle, P. Geppetti, and N. W. Bunnett, "Protease-activated receptor 2 sensitizes the transient receptor potential vanilloid 4 ion channel to cause mechanical hyperalgesia in mice.," *J. Physiol.*, vol. 578, no. Pt 3, pp. 715–

733, 2007.

[185] J. Fernandes, I. M. Lorenzo, Y. N. Andrade, A. Garcia-Elias, S. A. Serra, J. M. Fern??ndez-Fern??ndez, and M. A. Valverde, "IP3 sensitizes TRPV4 channel to the mechano-and osmotransducing messenger 5???-6???-epoxyeicosatrienoic acid," *J. Cell Biol.*, vol. 181, no. 1, pp. 143–155, 2008.

[186] H. Watanabe, J. B. Davis, D. Smart, J. C. Jerman, G. D. Smith, P. Hayes, J. Vriens, W. Cairns, U. Wissenbach, J. Prenen, V. Flockerzi, G. Droogmans, C. D. Benham, and B. Nilius, "Activation of TRPV4 channels (hVRL-2/mTRP12) by phorbol derivatives," *J. Biol. Chem.*, vol. 277, no. 16, pp. 13569–13577, 2002.

[187] S. C. Stotz, J. Vriens, D. Martyn, J. Clardy, and D. E. Clapham, "Citral sensing by Transient [corrected] receptor potential channels in dorsal root ganglion neurons.," *PLoS One*, vol. 3, p. e2082, 2008.

[188] F. Vincent, A. Acevedo, M. T. Nguyen, M. Dourado, J. DeFalco, A. Gustafson, P. Spiro, D. E. Emerling, M. G. Kelly, and M. A. J. Duncton, "Identification and characterization of novel TRPV4 modulators," *Biochem. Biophys. Res. Commun.*, vol. 389, no. 3, pp. 490–494, 2009.

[189] K. S. Thorneloe, M. Cheung, W. Bao, H. Alsaid, S. Lenhard, M.-Y. Jian, M. Costell, K. Maniscalco-Hauk, J. A. Krawiec, A. Olzinski, E. Gordon, I. Lozinskaya, L. Elefante, P. Qin, D. S. Matasic, C. James, J. Tunstead, B. Donovan, L. Kallal, A. Waszkiewicz, K. Vaidya, E. A. Davenport, J. Larkin, M. Burgert, L. N. Casillas, R. W. Marquis, G. Ye, H. S. Eidam, K. B. Goodman, J. R. Toomey, T. J. Roethke, B. M. Jucker, C. G. Schnackenberg, M. I. Townsley, J. J. Lepore, and R. N. Willette, "An orally active TRPV4 channel blocker prevents and resolves pulmonary edema induced by heart failure.," *Sci. Transl. Med.*, vol. 4, no. 159, p. 159ra148, 2012.

[190] D. Dahan, T. Ducret, J.-F. Quignard, R. Marthan, J.-P. Savineau, and E. Esteve, "Implication of the ryanodine receptor in TRPV4-induced calcium response in pulmonary arterial smooth muscle cells from normoxic and chronically hypoxic rats," *AJP Lung Cell. Mol. Physiol.*, vol. 303, no. 9, pp. L824–L833, 2012.

[191] X. Zhang, L. Li, and P. a. McNaughton, "Proinflammatory Mediators Modulate the Heat-Activated Ion Channel TRPV1 via the Scaffolding Protein AKAP79/150," *Neuron*, vol. 59, no. 3, pp. 450–461, 2008.

[192] M. J. M. Fischer, J. Btesh, and P. a McNaughton, "Disrupting sensitization of transient receptor potential vanilloid subtype 1 inhibits inflammatory hyperalgesia.," *J. Neurosci.*, vol. 33, no. 17, pp. 7407–7414, 2013.

[193] J. Btesh, M. J. M. Fischer, K. Stott, and P. a McNaughton, "Mapping the binding site of TRPV1 on AKAP79: implications for inflammatory hyperalgesia.," *J. Neurosci.*, vol. 33, no. 21, pp. 9184–93, 2013.

[194] G. Bhave, H.-J. Hu, K. S. Glauner, W. Zhu, H. Wang, D. J. Brasier, G. S. Oxford, and R. W. Gereau, "Protein kinase C phosphorylation sensitizes but does not activate the capsaicin receptor transient receptor potential vanilloid 1 (TRPV1).," *Proc. Natl. Acad. Sci. U. S. A.*, vol. 100, no. 21, pp. 12480–12485, 2003.

[195] G. Bhave, W. Zhu, H. Wang, D. J. Brasier, G. S. Oxford, and R. W. Gereau IV, "cAMP-dependent protein kinase regulates desensitization of the capsaicin receptor (VR1) by direct phosphorylation," *Neuron*, vol. 35, no. 4, pp. 721–731, 2002.

[196] A. J. Stokes, L. M. N. Shimoda, M. Koblan-Huberson, C. N. Adra, and H. Turner, "A TRPV2-PKA signaling module for transduction of physical stimuli in mast cells.," *J. Exp. Med.*, vol. 200, pp. 137–147, 2004.

[197] J. Mercado, A. Gordon-Shaag, W. N. Zagotta, and S. E. Gordon, "Ca2+-dependent desensitization of TRPV2 channels is mediated by hydrolysis of phosphatidylinositol 4,5-bisphosphate.," *J. Neurosci.*, vol. 30, pp. 13338–13347, 2010.

[198] C. B. Phelps, R. R. Wang, S. S. Choo, and R. Gaudet, "Differential regulation of TRPV1, TRPV3, and TRPV4 sensitivity through a conserved binding site on the ankyrin repeat domain.," *J. Biol. Chem.*, vol. 285, pp. 731–40, 2010.

[199] L. Grycova, B. Holendova, L. Bumba, J. Bily, M. Jirku, Z. Lansky, and J. Teisinger, "Integrative Binding Sites within Intracellular Termini of TRPV1 Receptor," *PLoS One*, vol. 7, no. 10, 2012.

[200] R. Strotmann, G. Schultz, and T. D. Plant, "Ca2+-dependent potentiation of the nonselective cation channel TRPV4 is mediated by a carboxy terminal calmodulin binding site," *J Biol Chem*, vol. 30, p. 30, 2003.

[201] J. Lee, J. L. Saloman, G. Weiland, Q. S. Auh, M. K. Chung, and J. Y. Ro, "Functional interactions between NMDA receptors and TRPV1 in trigeminal sensory neurons mediate mechanical hyperalgesia in the rat masseter muscle," *Pain*, vol. 153, no. 7, pp. 1514–1524, 2012.

[202] H. H. Chuang, E. D. Prescott, H. Kong, S. Shields, S. E. Jordt, a I. Basbaum, M. V Chao, and D. Julius, "Bradykinin and nerve growth factor release the capsaicin receptor from PtdIns(4,5)P2-mediated inhibition.," *Nature*, vol. 411, no. 6840, pp. 957–962, 2001.

[203] A. Fernández-Carvajal, G. Fernández-Ballester, I. Devesa, J. M. González-Ros, and A. Ferrer-Montiel, "New strategies to develop novel pain therapies: Addressing thermoreceptors from different points of view," *Pharmaceuticals*, vol. 5, no. 1. pp. 16–48, 2011.

[204] B.-M. Xing, Y.-R. Yang, J.-X. Du, H.-J. Chen, C. Qi, Z.-H. Huang, Y. Zhang, and Y. Wang, "Cyclin-Dependent Kinase 5 Controls TRPV1 Membrane Trafficking and the Heat Sensitivity of Nociceptors through KIF13B," *J. Neurosci.*, vol. 32, no. 42, pp. 14709–14721, 2012.

[205] C. Morenilla-Palao, R. Planells-Cases, N. García-Sanz, and A. Ferrer-Montiel, "Regulated exocytosis contributes to protein kinase C potentiation of vanilloid receptor activity," *J. Biol. Chem.*, vol. 279, pp. 25665–25672, 2004.

[206] L. Sanz-Salvador, A. Andrés-Borderia, A. Ferrer-Montiel, and R. Planells-Cases, "Agonist- and Ca2+-dependent desensitization of TRPV1 channel targets the receptor to lysosomes for degradation," *J. Biol. Chem.*, vol. 287, no. 23, pp. 19462–19471, 2012.

[207] I. Devesa and A. Ferrer-montiel, "Trafficking of ThermoTRP Channels," *Membranes (Basel).*, pp. 525–564, 2014.

[208] M. Tominaga, M. J. Caterina, A. B. Malmberg, T. A. Rosen, H. Gilbert, K. Skinner, B. E. Raumann, A. I. Basbaum, and D. Julius, "The cloned capsaicin receptor integrates multiple pain-producing stimuli," *Neuron*, vol. 21, no. 3, pp. 531–543, 1998.

[209] M. J. Caterina, "Impaired Nociception and Pain Sensation in Mice Lacking the Capsaicin Receptor," *Science (80-.).*, vol. 288, no. 5464, pp. 306–313, 2000.

[210] J. B. Davis, J. Gray, M. J. Gunthorpe, J. P. Hatcher, P. T. Davey, P. Overend, M. H. Harries, J. Latcham, C. Clapham, K. Atkinson, S. A. Hughes, K. Rance, E. Grau, A. J. Harper, P. L. Pugh, D. C. Rogers, S. Bingham, A. Randall, and S. A. Sheardown, "Vanilloid receptor-1 is essential for inflammatory thermal hyperalgesia," *Nature*, vol. 405, no. 6783, pp. 183–187, 2000.

[211] J. Keeble, F. Russell, B. Curtis, A. Starr, E. Pinter, and S. D. Brain, "Involvement of transient receptor potential vanilloid 1 in the vascular and hyperalgesic components of joint inflammation," *Arthritis Rheum.*, vol. 52, no. 10, pp. 3248–3256, 2005.

[212] Y. Yiangou, P. Facer, N. H. C. Dyer, C. L. H. Chan, C. Knowles, N. S. Williams, and P. Anand, "Vanilloid receptor 1 immunoreactivity in inflamed human bowel," *Lancet*, vol. 357, no. 9265, pp. 1338–1339, 2001.

[213] D. A. Groneberg, A. Niimi, Q. T. Dinh, B. Cosio, M. Hew, A. Fischer, and K. F. Chung, "Increased expression of transient receptor potential vanilloid-1 in airway nerves of chronic cough," *Am. J. Respir. Crit. Care Med.*, vol. 170, no. 12, pp. 1276–1280, 2004.

[214] T. Nakajima, Y. Nishimura, T. Nishiuma, Y. Kotani, H. Nakata, and M. Yokoyama, “Cough Sensitivity in Pure Cough Variant Asthma Elicited Using Continuous Capsaicin Inhalation,” *Allergol Int*, vol. 55, pp. 149–155, 2006.

[215] Q. Wang, X. Bai, D. Xu, D. Xu, H. Li, J. Fang, H. Zhu, W. Fu, X. Cai, J. Wang, Z. Jin, Q. Wang, C. Xu, and J. Chang, “[TRPV1 UTR-3 polymorphism and susceptibility of childhood asthma of the Han Nationality in Beijing],” *Wei Sheng Yan Jiu*, vol. 38, no. 5, pp. 516–521, 2009.

[216] G. Cantero-Recasens, J. R. Gonzalez, C. Fandos, E. Duran-Tauleria, L. a M. Smit, F. Kauffmann, J. M. Antó, and M. a Valverde, “Loss of function of transient receptor potential vanilloid 1 (TRPV1) genetic variant is associated with lower risk of active childhood asthma.,” *J. Biol. Chem.*, vol. 285, no. 36, pp. 27532–5, 2010.

[217] L. L. Zhang, D. Y. Liu, L. Q. Ma, Z. D. Luo, T. B. Cao, J. Zhong, Z. C. Yan, L. J. Wang, Z. G. Zhao, S. J. Zhu, M. Schrader, F. Thilo, Z. M. Zhu, and M. Tepel, “Activation of transient receptor potential vanilloid type-1 channel prevents adipogenesis and obesity,” *Circ. Res.*, vol. 100, no. 7, pp. 1063–1070, 2007.

[218] R. Razavi, Y. Chan, F. N. Afifiyan, X. J. Liu, X. Wan, J. Yantha, H. Tsui, L. Tang, S. Tsai, P. Santamaria, J. P. Driver, D. Serreze, M. W. Salter, and H. M. Dosch, “TRPV1+ Sensory Neurons Control ?? Cell Stress and Islet Inflammation in Autoimmune Diabetes,” *Cell*, vol. 127, no. 6, pp. 1123–1135, 2006.

[219] T. Laragione, K. F. Cheng, M. R. Tanner, M. He, C. Beeton, Y. Al-Abed, and P. S. Gulko, “The cation channel Trpv2 is a new suppressor of arthritis severity, joint damage, and synovial fibroblast invasion,” *Clin. Immunol.*, vol. 158, no. 2, pp. 183–192, 2015.

[220] Y. Iwata, Y. Katanosaka, Y. Arai, M. Shigekawa, and S. Wakabayashi, “Dominant-negative inhibition of Ca2+ influx via TRPV2 ameliorates muscular dystrophy in animal models,” *Hum. Mol. Genet.*, vol. 18, no. 5, pp. 824–834, 2009.

[221] Z. Lin, Q. Chen, M. Lee, X. Cao, J. Zhang, D. Ma, L. Chen, X. Hu, H. Wang, X. Wang, P. Zhang, X. Liu, L. Guan, Y. Tang, H. Yang, P. Tu, D. Bu, X. Zhu, K. Wang, R. Li, and Y. Yang, “Exome sequencing reveals mutations in TRPV3 as a cause of Olmsted syndrome,” *Am. J. Hum. Genet.*, vol. 90, no. 3, pp. 558–564, 2012.

[222] S. Duchatelet, S. Pruvost, S. de Veer, S. Fraitag, P. Nitschké, C. Bole-Feysot, C. Bodemer, and A. Hovnanian, “A new TRPV3 missense mutation in a patient with Olmsted syndrome and erythromelalgia.,” *JAMA dermatology*, vol. 150, no. 3, pp. 303–6, 2014.

[223] S. Duchatelet, L. Guibbal, S. De Veer, S. Fraitag, P. Nitschk??, M. Zarhrate, C. Bodemer, and A. Hovnanian, “Olmsted syndrome with erythromelalgia caused by recessive transient receptor potential vanilloid 3 mutations,” *British Journal of Dermatology*, vol. 171, no. 3. pp. 675–678, 2014.

[224] C. Ni, M. Yan, J. Zhang, R. Cheng, J. Liang, D. Deng, Z. Wang, M. Li, and Z. Yao, “A novel mutation in TRPV3 gene causes atypical familial Olmsted syndrome,” *Sci. Rep.*, vol. 6, p. 21815, 2016.

[225] M. Sulk, S. Seeliger, J. Aubert, V. D. Schwab, F. Cevikbas, M. Rivier, P. Nowak, J. J. Voegel, J. Buddenkotte, and M. Steinhoff, “Distribution and expression of non-neuronal transient receptor potential (TRPV) ion channels in rosacea,” *J Invest Dermatol*, vol. 132, no. 4, pp. 1253–1262, 2012.

[226] W. Tian, Y. Fu, A. Garcia-Elias, J. M. Fernández-Fernández, R. Vicente, P. L. Kramer, R. F. Klein, R. Hitzemann, E. S. Orwoll, B. Wilmot, S. McWeeney, M. a Valverde, and D. M. Cohen, “A loss-of-function nonsynonymous polymorphism in the osmoregulatory TRPV4 gene is associated with human hyponatremia.,” *Proc. Natl. Acad. Sci. U. S. A.*, vol. 106, no. 33, pp. 14034–14039, 2009.

[227] M. J. Rock, J. Prenen, V. A. Funari, T. L. Funari, B. Merriman, S. F. Nelson, R. S. Lachman, W. R. Wilcox, S. Reyno, R. Quadrelli, A. Vaglio, G. Owsianik, A. Janssens, T. Voets, S. Ikegawa, T. Nagai, D. L. Rimoin, B. Nilius, and D. H. Cohn, “Gain-of-function mutations in TRPV4 cause autosomal dominant brachyolmia.,”

Nat. Genet., vol. 40, no. 8, pp. 999–1003, 2008.

[228] S. Loukin, Z. Su, and C. Kung, "Increased basal activity is a key determinant in the severity of human skeletal dysplasia caused by TRPV4 mutations," *PLoS One*, vol. 6, no. 5, 2011.

[229] N. Camacho, D. Krakow, S. Johnykutty, P. J. Katzman, S. Pepkowitz, J. Vriens, B. Nilius, B. F. Boyce, and D. H. Cohn, "Dominant TRPV4 mutations in nonlethal and lethal metatropic dysplasia," *Am. J. Med. Genet. Part A*, vol. 152, no. 5, pp. 1169–1177, 2010.

[230] G. Nishimura, J. Dai, E. Lausch, S. Unger, A. Megarban??, H. Kitoh, O. H. Kim, T. J. Cho, F. Bedeschi, F. Benedicenti, R. Mendoza-Londono, M. Silengo, M. Schmidt-Rimpler, J. Spranger, B. Zabel, S. Ikegawa, and A. Superti-Furga, "Spondylo-epiphyseal dysplasia, Maroteaux type (pseudo-Morquio syndrome type 2), and parastremmatic dysplasia are caused by TRPV4 mutations," *Am. J. Med. Genet. Part A*, vol. 152, no. 6, pp. 1443–1449, 2010.

[231] D. Krakow, J. Vriens, N. Camacho, P. Luong, H. Deixler, T. L. Funari, C. A. Bacino, M. B. Irons, I. A. Holm, L. Sadler, E. B. Okenfuss, A. Janssens, T. Voets, D. L. Rimoin, R. S. Lachman, B. Nilius, and D. H. Cohn, "Mutations in the Gene Encoding the Calcium-Permeable Ion Channel TRPV4 Produce Spondylometaphyseal Dysplasia, Kozlowski Type and Metatropic Dysplasia," *Am. J. Hum. Genet.*, vol. 84, no. 3, pp. 307–315, 2009.

[232] H.-X. Deng, C. J. Klein, J. Yan, Y. Shi, Y. Wu, F. Fecto, H.-J. Yau, Y. Yang, H. Zhai, N. Siddique, E. T. Hedley-Whyte, R. Delong, M. Martina, P. J. Dyck, and T. Siddique, "Scapuloperoneal spinal muscular atrophy and CMT2C are allelic disorders caused by alterations in TRPV4.," *Nat. Genet.*, vol. 42, pp. 165–169, 2010.

[233] G. Landouré, A. a Zdebik, T. L. Martinez, B. G. Burnett, H. C. Stanescu, H. Inada, Y. Shi, A. a Taye, L. Kong, C. H. Munns, S. S. Choo, C. B. Phelps, R. Paudel, H. Houlden, C. L. Ludlow, M. J. Caterina, R. Gaudet, R. Kleta, K. H. Fischbeck, and C. J. Sumner, "Mutations in TRPV4 cause Charcot-Marie-Tooth disease type 2C.," *Nat. Genet.*, vol. 42, no. 2, pp. 170–174, 2010.

[234] P. Doñate-Macián and A. Perálvarez-Marín, "Dissecting domain-specific evolutionary pressure profiles of transient receptor potential vanilloid subfamily members 1 to 4.," *PLoS One*, vol. 9, p. e110715, 2014.

[235] P. Doñate-Macian, M. Bañó-Polo, J.-L. Vazquez-Ibar, I. Mingarro, and A. Perálvarez-Marín, "Molecular and topological membrane folding determinants of transient receptor potential vanilloid 2 channel," *Biochem. Biophys. Res. Commun.*, no. May, pp. 2–7, 2015.

[236] J. Abramowitz and L. Birnbaumer, "Know thy neighbor: A survey of diseases and complex syndromes that map to chromosomal regions encoding TRP channels," *Handb. Exp. Pharmacol.*, vol. 179, pp. 379–408, 2007.

[237] U. Park, N. Vastani, Y. Guan, S. N. Raja, M. Koltzenburg, and M. J. Caterina, "TRP vanilloid 2 knock-out mice are susceptible to perinatal lethality but display normal thermal and mechanical nociception.," *J. Neurosci.*, vol. 31, no. 32, pp. 11425–36, 2011.

[238] A. Garcia-Elias, A. Berna-Erro, F. Rubio-Moscardo, C. Pardo-Pastor, S. Mrkonjić, R. V. Sepúlveda, R. Vicente, F. González-Nilo, and M. A. Valverde, "Interaction between the Linker, Pre-S1, and TRP Domains Determines Folding, Assembly, and Trafficking of TRPV Channels," *Structure*, pp. 1–10, 2015.

[239] J. Yao, B. Liu, and F. Qin, "Modular thermal sensors in temperature-gated transient receptor potential (TRP) channels.," *Proc. Natl. Acad. Sci. U. S. A.*, vol. 108, no. 27, pp. 11109–11114, 2011.

[240] S. Kumari, A. Kumar, P. Sardar, M. Yadav, R. K. Majhi, A. Kumar, and C. Goswami, "Influence of membrane cholesterol in the molecular evolution and functional regulation of TRPV4," *Biochem. Biophys. Res. Commun.*, vol. 456, no. 1, pp. 312–319, 2015.

[241] E. D. Prescott and D. Julius, “A modular PIP2 binding site as a determinant of capsaicin receptor sensitivity.,” *Science*, vol. 300, no. 5623, pp. 1284–1288, 2003.

[242] J. F. Doerner, H. Hatt, and I. S. Ramsey, “Voltage- and temperature-dependent activation of TRPV3 channels is potentiated by receptor-mediated PI(4,5)P2 hydrolysis.,” *J. Gen. Physiol.*, vol. 137, no. 3, pp. 271–288, 2011.

[243] A. Garcia-Elias, S. Mrkonjic, C. Pardo-Pastor, H. Inada, U. A. Hellmich, F. Rubio-Moscardó, C. Plata, R. Gaudet, R. Vicente, and M. A. Valverde, “Phosphatidylinositol-4,5-biphosphate-dependent rearrangement of TRPV4 cytosolic tails enables channel activation by physiological stimuli.,” *Proc. Natl. Acad. Sci. U. S. A.*, vol. 110, no. 23, pp. 9553–8, 2013.

[244] Y. Wang, X. Fu, S. Gaiser, M. K??ttgen, A. Kramer-Zucker, G. Walz, and T. Wegierski, “OS-9 regulates the transit and polyubiquitination of TRPV4 in the endoplasmic reticulum,” *J. Biol. Chem.*, vol. 282, no. 50, pp. 36561–36570, 2007.

[245] M. P. Cuajungco, C. Grimm, K. Oshima, D. D'Hoedt, B. Nilius, A. R. Mensenkamp, R. J. M. Bindels, M. Plomann, and S. Heller, “PACSINs bind to the TRPV4 cation channel: PACSIN 3 modulates the subcellular localization of TRPV4,” *J. Biol. Chem.*, vol. 281, no. 27, pp. 18753–18762, 2006.

[246] M. Arniges, J. M. Fernández-Fernández, N. Albrecht, M. Schaefer, and M. A. Valverde, “Human TRPV4 channel splice variants revealed a key role of ankyrin domains in multimerization and trafficking,” *J. Biol. Chem.*, vol. 281, no. 3, pp. 1580–1586, 2006.

[247] D. Becker, M. Müller, K. Leuner, and M. Jendrach, “The C-terminal domain of TRPV4 is essential for plasma membrane localization.,” *Mol. Membr. Biol.*, vol. 25, no. 2, pp. 139–151, 2008.

[248] S. Cayouette and G. Boulay, “Intracellular trafficking of TRP channels,” *Cell Calcium*, vol. 42, no. 2, pp. 225–232, 2007.

[249] Y. Gao, E. Cao, D. Julius, and Y. Cheng, “TRPV1 structures in nanodiscs reveal mechanisms of ligand and lipid action,” *Nature*, pp. 1–17, 2016.

[250] Y. Nishizuka, “Intracellular signaling by hydrolysis of phospholipids and activation of protein kinase C.,” *Science (80-.).*, vol. 258, no. 5082, pp. 607–14, 1992.

[251] Y. Asaoka, S. ichi Nakamura, K. Yoshida, and Y. Nishizuka, “Protein kinase C, calcium and phospholipid degradation,” *Trends Biochem. Sci.*, vol. 17, no. 10, pp. 414–417, 1992.

[252] S. Mandadi, P. Armati, and B. Roufogalis, “Protein kinase C modulation of thermo-sensitive transient receptor potential channels: Implications for pain signaling,” *Journal of Natural Science, Biology and Medicine*, vol. 2, no. 1. p. 13, 2011.

[253] R. Harisseh, A. Chatelier, C. Magaud, N. Déliot, and B. Constantin, “Involvement of TRPV2 and SOCE in calcium influx disorder in DMD primary human myotubes with a specific contribution of α1-syntrophin and PLC/PKC in SOCE regulation.,” *Am. J. Physiol. Cell Physiol.*, vol. 304, no. 9, pp. C881–94, 2013.

[254] H. C. Fan, X. Zhang, and P. A. McNaughton, “Activation of the TRPV4 ion channel is enhanced by phosphorylation,” *J. Biol. Chem.*, vol. 284, no. 41, pp. 27884–27891, 2009.

[255] H. Peng, U. Lewandrowski, B. M??ller, A. Sickmann, G. Walz, and T. Wegierski, “Identification of a Protein Kinase C-dependent phosphorylation site involved in sensitization of TRPV4 channel,” *Biochem. Biophys. Res. Commun.*, vol. 391, no. 4, pp. 1721–1725, 2010.

[256] R. Paul, C. M. Ewing, J. C. Robinson, F. F. Marshall, K. R. Johnson, M. J. Wheelock, and W. B. Isaacs,

"Cadherin-6, a cell adhesion molecule specifically expressed in the proximal renal tubule and renal cell carcinoma," *Cancer Res.*, vol. 57, no. 13, pp. 2741–2748, 1997.

[257] L. Ye, S. Kleiner, J. Wu, R. Sah, R. K. Gupta, A. S. Banks, P. Cohen, M. J. Khandekar, P. Boström, R. J. Mepani, D. Laznik, T. M. Kamenecka, X. Song, W. Liedtke, V. K. Mootha, P. Puigserver, P. R. Griffin, D. E. Clapham, and B. M. Spiegelman, "TRPV4 is a regulator of adipose oxidative metabolism, inflammation, and energy homeostasis.," *Cell*, vol. 151, no. 1, pp. 96–110, 2012.

[258] D.-W. Wu, M.-C. Lee, J. Wang, C.-Y. Chen, Y.-W. Cheng, and H. Lee, "DDX3 loss by p53 inactivation promotes tumor malignancy via the MDM2/Slug/E-cadherin pathway and poor patient outcome in non-small-cell lung cancer.," *Oncogene*, vol. 33, no. 12, pp. 1515–26, 2014.

[259] D. W. Wu, W. S. Liu, J. Wang, C. Y. Chen, Y. W. Cheng, and H. Lee, "Reduced p21WAF1/CIP1 via alteration of p53-DDX3 pathway is associated with poor relapse-free survival in early-stage human papillomavirus-associated lung cancer," *Clin. Cancer Res.*, vol. 17, no. 7, pp. 1895–1905, 2011.

[260] H. a Singer, "Ca2+/calmodulin-dependent protein kinase II function in vascular remodelling.," *J. Physiol.*, vol. 590, pp. 1349–56, 2012.

[261] A. L. Craig, J. a Chrystal, J. a Fraser, N. Sphyris, Y. Lin, B. J. Harrison, M. T. Scott, I. Dornreiter, and T. R. Hupp, "The MDM2 ubiquitination signal in the DNA-binding domain of p53 forms a docking site for calcium calmodulin kinase superfamily members.," *Mol. Cell. Biol.*, vol. 27, no. 9, pp. 3542–3555, 2007.

[262] T. Sekiguchi, Y. Kurihara, and J. Fukumura, "Phosphorylation of threonine 204 of DEAD-box RNA helicase DDX3 by cyclin B/cdc2 in vitro," *Biochem. Biophys. Res. Commun.*, vol. 356, no. 3, pp. 668–673, 2007.

[263] D. Soulat, T. Bürckstümmer, S. Westermayer, A. Goncalves, A. Bauch, A. Stefanovic, O. Hantschel, K. L. Bennett, T. Decker, and G. Superti-Furga, "The DEAD-box helicase DDX3X is a critical component of the TANK-binding kinase 1-dependent innate immune response.," *EMBO J.*, vol. 27, no. 15, pp. 2135–2146, 2008.

[264] a Diogenes, C. C. R. Ferraz, a N. Akopian, M. a Henry, and K. M. Hargreaves, "LPS sensitizes TRPV1 via activation of TLR4 in trigeminal sensory neurons.," *J. Dent. Res.*, vol. 90, no. 6, pp. 759–64, 2011.

[265] K. Yamashiro, T. Sasano, K. Tojo, I. Namekata, J. Kurokawa, N. Sawada, T. Suganami, Y. Kamei, H. Tanaka, N. Tajima, K. Utsunomiya, Y. Ogawa, and T. Furukawa, "Role of transient receptor potential vanilloid 2 in LPS-induced cytokine production in macrophages," *Biochem Biophys Res Commun*, vol. 398, no. 2, pp. 284–289, 2010.

[266] H.-K. Lee, S. Yeo, J.-S. Kim, J.-G. Lee, Y.-S. Bae, C. Lee, and S.-H. Baek, "Protein kinase C-eta and phospholipase D2 pathway regulates foam cell formation via regulator of G protein signaling 2.," *Mol. Pharmacol.*, vol. 78, no. 3, pp. 478–85, 2010.

[267] C. H. Oh, S. Y. Park, and J. S. Han, "Phospholipase D1 is required for lipopolysaccharide-induced tumor necrosis factor-?? expression and production through S6K1/JNK/c-Jun pathway in Raw 264.7 cells," *Cytokine*, vol. 66, no. 1, pp. 69–77, 2014.

[268] H. Han and F. Yi, "New insights into TRP channels: Interaction with pattern recognition receptors," *Channels*, vol. 6950, no. January 2015, pp. 37–41, 2013.

[269] J. Fric, T. Zelante, A. Y. W. Wong, A. Mertes, H. B. Yu, and P. Ricciardi-Castagnoli, "NFAT control of innate immunity," *Blood*, vol. 120, no. 7. pp. 1380–1389, 2012.

[270] F. N. McNamara, A. Randall, and M. J. Gunthorpe, "Effects of piperine, the pungent component of black pepper, at the human vanilloid receptor (TRPV1).," *Br. J. Pharmacol.*, vol. 144, no. 6, pp. 781–790, 2005.

[271] A. T. Stein, C. A. Ufret-Vincenty, L. Hua, L. F. Santana, and S. E. Gordon, "Phosphoinositide 3-kinase binds to TRPV1 and mediates NGF-stimulated TRPV1 trafficking to the plasma membrane.," *J. Gen. Physiol.*, vol. 128, no. 5, pp. 509–22, 2006.

[272] C. Bavassano, L. Marvaldi, M. Langeslag, B. Sarg, H. Lindner, L. Klimaschewski, M. Kress, A. Ferrer-Montiel, and H. G. Knaus, "Identification of voltage-gated K+ channel beta 2 (Kvβ2) subunit as a novel interaction partner of the pain transducer Transient Receptor Potential Vanilloid 1 channel (TRPV1)," *Biochim. Biophys. Acta - Mol. Cell Res.*, vol. 1833, no. 12, pp. 3166–3175, 2013.

[273] H. Gao, Y. Wang, T. Wegierski, K. Skouloudaki, M. Pütz, X. Fu, C. Engel, C. Boehlke, H. Peng, E. W. Kuehn, E. Kim, A. Kramer-Zucker, and G. Walz, "PRKCSH/80K-H, the protein mutated in polycystic liver disease, protects polycystin-2/TRPP2 against HERP-mediated degradation," *Hum. Mol. Genet.*, vol. 19, no. 1, pp. 16–24, 2009.

[274] X. Cong, Y. Zhang, N.-Y. Yang, J. Li, C. Ding, Q.-W. Ding, Y.-C. Su, M. Mei, X.-H. Guo, L.-L. Wu, and G.-Y. Yu, "Occludin is required for TRPV1-modulated paracellular permeability in the submandibular gland.," *J. Cell Sci.*, vol. 126, no. Pt 5, pp. 1109–21, 2013.

[275] L.-C. Ching, Y. R. Kou, S.-K. Shyue, K.-H. Su, J. Wei, L.-C. Cheng, Y.-B. Yu, C.-C. Pan, and T.-S. Lee, "Molecular mechanisms of activation of endothelial nitric oxide synthase mediated by transient receptor potential vanilloid type 1.," *Cardiovasc. Res.*, vol. 91, no. 3, pp. 492–501, 2011.

[276] L. C. Ching, C. Y. Chen, K. H. Su, H. H. Hou, S. K. Shyue, Y. R. Kou, and T. S. Lee, "Implication of AMP-Activated Protein Kinase in Transient Receptor Potential Vanilloid Type 1-Mediated Activation of Endothelial Nitric Oxide Synthase," *Mol. Med.*, vol. 18, no. 5, pp. 805–815, 2012.

[277] Y. Wu, Y. Liu, P. Hou, Z. Yan, W. Kong, B. Liu, X. Li, J. Yao, Y. Zhang, F. Qin, and J. Ding, "TRPV1 Channels Are Functionally Coupled with BK(mSlo1) Channels in Rat Dorsal Root Ganglion (DRG) Neurons," *PLoS One*, vol. 8, no. 10, 2013.

[278] T. Rosenbaum, A. Gordon-Shaag, M. Munari, and S. E. Gordon, "Ca2+/calmodulin modulates TRPV1 activation by capsaicin.," *J. Gen. Physiol.*, vol. 123, no. 1, pp. 53–62, 2004.

[279] Y. Yang, H. Yang, Z. Wang, K. Varadaraj, S. S. Kumari, S. Mergler, Y. Okada, S. Saika, P. J. Kingsley, L. J. Marnett, and P. S. Reinach, "Cannabinoid receptor 1 suppresses transient receptor potential vanilloid 1-induced inflammatory responses to corneal injury," *Cell. Signal.*, vol. 25, no. 2, pp. 501–511, 2013.

[280] A. M. Bode, Y. Y. Cho, D. Zheng, F. Zhu, M. E. Ericson, W. Y. Ma, K. Yao, and Z. Dong, "Transient receptor potential type vanilloid 1 suppresses skin carcinogenesis," *Cancer Res.*, vol. 69, no. 3, pp. 905–913, 2009.

[281] T. K. Pareek, J. Keller, S. Kesavapany, N. Agarwal, R. Kuner, H. C. Pant, M. J. Iadarola, R. O. Brady, and A. B. Kulkarni, "Cyclin-dependent kinase 5 modulates nociceptive signaling through direct phosphorylation of transient receptor potential vanilloid 1.," *Proc. Natl. Acad. Sci. U. S. A.*, vol. 104, no. 2, pp. 660–665, 2007.

[282] E. Utreras, J. Keller, A. Terse, M. Prochazkova, M. J. Iadarola, and A. B. Kulkarni, "Transforming growth factor-β1 regulates Cdk5 activity in primary sensory neurons.," *J. Biol. Chem.*, vol. 287, no. 20, pp. 16917–29, 2012.

[283] S.-Y. Lee, "Identification of a protein that interacts with the vanilloid receptor.," *Biochem. Biophys. Res. Commun.*, vol. 331, no. 4, pp. 1445–1451, 2005.

[284] S. Kim, C. Kang, C. Y. Shin, S. W. Hwang, Y. D. Yang, W. S. Shim, M.-Y. Park, E. Kim, M. Kim, B.-M. Kim, H. Cho, Y. Shin, and U. Oh, "TRPV1 recapitulates native capsaicin receptor in sensory neurons in association with Fas-associated factor 1.," *J. Neurosci.*, vol. 26, no. 9, pp. 2403–12, 2006.

[285] S. Laínez, P. Valente, I. Ontoria-Oviedo, J. Estévez-Herrera, M. Camprubí-Robles, a Ferrer-Montiel, and R. Planells-Cases, "GABAA receptor associated protein (GABARAP) modulates TRPV1 expression and channel function and desensitization.," *FASEB J.*, vol. 24, no. 6, pp. 1958–1970, 2010.

[286] E. D. Por, S. M. Bierbower, K. A. Berg, R. Gomez, A. N. Akopian, W. C. Wetsel, and N. A. Jeske, "??-Arrestin-2 desensitizes the transient receptor potential vanilloid 1 (TRPV1) channel," *J. Biol. Chem.*, vol. 287, no. 44, pp. 37552–37563, 2012.

[287] E. D. Por, R. Gomez, A. N. Akopian, and N. a Jeske, "Phosphorylation regulates TRPV1 association with β-arrestin-2.," *Biochem. J.*, vol. 451, pp. 101–9, 2013.

[288] M. P. Rowan, S. M. Bierbower, M. A. Eskander, K. Szteyn, E. D. Por, R. Gomez, N. Veldhuis, N. W. Bunnett, and N. A. Jeske, "Activation of Mu Opioid Receptors Sensitizes Transient Receptor Potential Vanilloid Type 1 (TRPV1) via beta-Arrestin-2-Mediated Cross-Talk," *PLoS One*, vol. 9, no. 4, p. e93688, 2014.

[289] C. Goswami, T. B. Hucho, and F. Hucho, "Identification and characterisation of novel tubulin-binding motifs located within the C-terminus of TRPV1," *J. Neurochem.*, vol. 101, no. 1, pp. 250–262, 2007.

[290] C. Goswami, M. Dreger, R. Jahnel, O. Bogen, C. Gillen, and F. Hucho, "Identification and characterization of a Ca2+ -sensitive interaction of the vanilloid receptor TRPV1 with tubulin.," *J. Neurochem.*, vol. 91, no. 5, pp. 1092–1103, 2004.

[291] X. F. Zhang, P. Han, T. R. Neelands, S. McGaraughty, P. Honore, C. S. Surowy, and D. Zhang, "Coexpression and activation of TRPV1 suppress the activity of the KCNQ2/3 channel," *J Gen Physiol*, vol. 138, pp. 341–352, 2011.

[292] B. Storti, R. Bizzarri, F. Cardarellis, and F. Beltrams, "Intact microtubules preserve transient receptor potential vanilloid 1 (TRPV1) functionality through receptor binding," *J. Biol. Chem.*, vol. 287, no. 10, pp. 7803–7811, 2012.

[293] L. Li, F. Wang, X. Wei, Y. Liang, Y. Cui, F. Gao, J. Zhong, Y. Pu, Y. Zhao, Z. Yan, W. J. Arendshorst, B. Nilius, J. Chen, D. Liu, and Z. Zhu, "Transient receptor potential Vanilloid 1 activation by dietary capsaicin promotes urinary sodium excretion by inhibiting epithelial sodium channel α Subunit-Mediated sodium reabsorption," *Hypertension*, vol. 64, no. 2, pp. 397–404, 2014.

[294] D. Stanchev, M. Blosa, D. Milius, Z. Gerevich, P. Rubini, G. Schmalzing, K. Eschrich, M. Schaefer, K. Wirkner, and P. Illes, "Cross-inhibition between native and recombinant TRPV1 and P2X3 receptors," *Pain*, vol. 143, no. 1–2, pp. 26–36, 2009.

[295] J. H. M. Schuurs-Hoeijmakers, E. C. Oh, L. E. L. M. Vissers, M. E. M. Swinkels, C. Gilissen, M. A. Willemsen, M. Holvoet, M. Steehouwer, J. A. Veltman, B. B. A. De Vries, H. Van Bokhoven, A. P. M. De Brouwer, N. Katsanis, K. Devriendt, and H. G. Brunner, "Recurrent de novo mutations in PACS1 cause defective cranial-neural-crest migration and define a recognizable intellectual-disability syndrome," *Am. J. Hum. Genet.*, vol. 91, no. 6, pp. 1122–1127, 2012.

[296] A. Y. Kim, Z. Tang, Q. Liu, K. N. Patel, D. Maag, Y. Geng, and X. Dong, "Pirt, a Phosphoinositide-Binding Protein, Functions as a Regulatory Subunit of TRPV1," *Cell*, vol. 133, no. 3, pp. 475–485, 2008.

[297] N. A. Jeske, A. Diogenes, N. B. Ruparel, J. C. Fehrenbacher, M. Henry, A. N. Akopian, and K. M. Hargreaves, "A-kinase anchoring protein mediates TRPV1 thermal hyperalgesia through PKA phosphorylation of TRPV1," *Pain*, vol. 138, no. 3, pp. 604–616, 2008.

[298] L. Li, R. Hasan, and X. Zhang, "The basal thermal sensitivity of the TRPV1 ion channel is determined by PKCβII.," *J. Neurosci.*, vol. 34, no. 24, pp. 8246–58, 2014.

[299] M. Numazaki, T. Tominaga, H. Toyooka, and M. Tominaga, “Direct phosphorylation of capsaicin receptor VR1 by protein kinase Cε and identification of two target serine residues,” *J. Biol. Chem.*, vol. 277, no. 16, pp. 13375–13378, 2002.

[300] P. Ambrosino, M. V. Soldovieri, M. De Maria, C. Russo, and M. Taglialatela, “Functional and biochemical interaction between PPAR?? receptors and TRPV1 channels: Potential role in PPAR?? agonists-mediated analgesia,” *Pharmacol. Res.*, vol. 87, pp. 113–122, 2014.

[301] Y. Wang, N. Kedei, M. Wang, Q. J. Wang, A. R. Huppler, A. Toth, R. Tran, and P. M. Blumberg, “Interaction between protein kinase Cmu and the vanilloid receptor type 1.,” *J. Biol. Chem.*, vol. 279, no. 51, pp. 53674–53682, 2004.

[302] H. Zhu, Y. Yang, H. Zhang, Y. Han, Y. Li, Y. Zhang, D. Yin, Q. He, Z. Zhao, P. M. Blumberg, J. Han, and Y. Wang, “Interaction between protein kinase D1 and transient receptor potential V1 in primary sensory neurons is involved in heat hypersensitivity,” *Pain*, vol. 137, no. 3, pp. 574–588, 2008.

[303] J. S. Woo, D. H. Kim, P. D. Allen, and E. H. Lee, “TRPC3-interacting triadic proteins in skeletal muscle.,” *Biochem. J.*, vol. 411, no. 2, pp. 399–405, 2008.

[304] X. Zhang, J. Huang, and P. A. McNaughton, “NGF rapidly increases membrane expression of TRPV1 heat-gated ion channels.,” *EMBO J.*, vol. 24, no. 24, pp. 4211–4223, 2005.

[305] M. J. M. Fischer, D. Balasuriya, P. Jeggle, T. A. Goetze, P. A. McNaughton, P. W. Reeh, and J. M. Edwardson, “Direct evidence for functional TRPV1/TRPA1 heteromers,” *Pflugers Arch. Eur. J. Physiol.*, vol. 466, no. 12, pp. 2229–2241, 2014.

[306] N. Hellwig, N. Albrecht, C. Harteneck, G. Schultz, and M. Schaefer, “Homo- and heteromeric assembly of TRPV channel subunits.,” *J. Cell Sci.*, vol. 118, no. Pt 5, pp. 917–28, 2005.

[307] a R. Rutter, Q.-P. Ma, M. Leveridge, and T. P. Bonnert, “Heteromerization and colocalization of TrpV1 and TrpV2 in mammalian cell lines and rat dorsal root ganglia.,” *Neuroreport*, vol. 16, no. 16, pp. 1735–1739, 2005.

[308] M. Prager-Khoutorsky, A. Khoutorsky, and C. W. Bourque, “Unique Interweaved Microtubule Scaffold Mediates Osmosensory Transduction via Physical Interaction with TRPV1,” *Neuron*, vol. 83, no. 4, pp. 866–878, 2014.

[309] J. C. Barnhill, A. J. Stokes, M. Koblan-Huberson, L. M. N. Shimoda, A. Muraguchi, C. N. Adra, and H. Turner, “RGA protein associates with a TRPV ion channel during biosynthesis and trafficking,” *J. Cell. Biochem.*, vol. 91, pp. 808–820, 2004.

[310] Y. Kobayashi, Y. Katanosaka, Y. Iwata, M. Matsuoka, M. Shigekawa, and S. Wakabayashi, “Identification and characterization of GSRP-56, a novel Golgi-localized spectrin repeat-containing protein,” *Exp. Cell Res.*, vol. 312, no. 16, pp. 3152–3164, 2006.

[311] A. J. Stokes, C. Wakano, K. a. Del Carmen, M. Koblan-Huberson, and H. Turner, “Formation of a physiological complex between TRPV2 and RGA protein promotes cell surface expression of TRPV2,” *J. Cell. Biochem.*, vol. 94, pp. 669–683, 2005.

[312] W. Kim, E. J. Bennett, E. L. Huttlin, A. Guo, J. Li, A. Possemato, M. E. Sowa, R. Rad, J. Rush, M. J. Comb, J. W. Harper, and S. P. Gygi, “Systematic and quantitative assessment of the ubiquitin-modified proteome,” *Mol. Cell*, vol. 44, no. 2, pp. 325–340, 2011.

[313] S. a. Wagner, P. Beli, B. T. Weinert, M. L. Nielsen, J. Cox, M. Mann, and C. Choudhary, “A Proteome-wide, Quantitative Survey of In Vivo Ubiquitylation Sites Reveals Widespread Regulatory Roles,” *Mol. Cell.*

Proteomics, vol. 10, no. 10, pp. M111.013284–M111.013284, 2011.

[314] S. K. Sonkusare, T. Dalsgaard, A. D. Bonev, D. C. Hill-Eubanks, M. I. Kotlikoff, J. D. Scott, L. F. Santana, and M. T. Nelson, "AKAP150-dependent cooperative TRPV4 channel gating is central to endothelium-dependent vasodilation and is disrupted in hypertension.," *Sci. Signal.*, vol. 7, no. 333, p. ra66, 2014.

[315] V. Benfenati, M. Caprini, M. Dovizio, M. N. Mylonakou, S. Ferroni, O. P. Ottersen, and M. Amiry-Moghaddam, "An aquaporin-4/transient receptor potential vanilloid 4 (AQP4/TRPV4) complex is essential for cell-volume control in astrocytes.," *Proc. Natl. Acad. Sci. U. S. A.*, vol. 108, no. 6, pp. 2563–8, 2011.

[316] X. Liu, B. Bandyopadhyay, T. Nakamoto, B. Singh, W. Liedtke, J. E. Melvin, and I. Ambudkar, "A role for AQP5 in activation of TRPV4 by hypotonicity: Concerted involvement of AQP5 and TRPV4 in regulation of cell volume recovery," *J. Biol. Chem.*, vol. 281, no. 22, pp. 15485–15495, 2006.

[317] A. K. Shukla, J. Kim, S. Ahn, K. Xiao, S. K. Shenoy, W. Liedtke, and R. J. Lefkowitz, "Arresting a transient receptor potential (TRP) channel: ??-arrestin 1 mediates ubiquitination and functional down-regulation of TRPV4," *J. Biol. Chem.*, vol. 285, no. 39, pp. 30115–30125, 2010.

[318] P. Zhang, Y. Ma, Y. Wang, X. Ma, Y. Huang, R. A. Li, S. Wan, and X. Yao, "Nitric oxide and protein kinase G act on TRPC1 to inhibit 11,12-EET-induced vascular relaxation," *Cardiovasc. Res.*, vol. 104, no. 1, pp. 138–146, 2014.

[319] R. Masuyama, A. Mizuno, H. Komori, H. Kajiya, A. Uekawa, H. Kitaura, K. Okabe, K. Ohyama, and T. Komori, "Calcium/calmodulin-signaling supports TRPV4 activation in osteoclasts and regulates bone mass," *J. Bone Miner. Res.*, vol. 27, no. 8, pp. 1708–1721, 2012.

[320] E. J. Lee, S. H. Shin, S. Hyun, J. Chun, and S. S. Kang, "Mutation of a putative S-nitrosylation site of TRPV4 protein facilitates the channel activates.," *Animal Cells Syst. (Seoul).*, vol. 15, no. 2, pp. 95–106, 2011.

[321] X. Ma, J. Cao, J. Luo, B. Nilius, Y. Huang, I. S. Ambudkar, and X. Yao, "Depletion of intracellular ca2+ stores stimulates the translocation of vanilloid transient receptor potential 4-C1 heteromeric channels to the plasma membrane," *Arterioscler. Thromb. Vasc. Biol.*, vol. 30, no. 11, pp. 2249–2255, 2010.

[322] N. Kida, T. Sokabe, M. Kashio, K. Haruna, Y. Mizuno, Y. Suga, K. Nishikawa, A. Kanamaru, M. Hongo, A. Oba, and M. Tominaga, "Importance of transient receptor potential vanilloid 4 (TRPV4) in epidermal barrier function in human skin keratinocytes.," *Pflugers Arch.*, vol. 463, no. 5, pp. 715–25, 2012.

[323] H. Xu, H. Zhao, W. Tian, K. Yoshida, J. B. Roullet, and D. M. Cohen, "Regulation of a transient receptor potential (TRP) channel by tyrosine phosphorylation: Src family kinase-dependent tyrosine phosphorylation of TRPV4 on TYR-253 mediates its response to hypotonic stress," *J. Biol. Chem.*, vol. 278, no. 13, pp. 11520–11527, 2003.

[324] S. H. Shin, E. J. Lee, J. Chun, S. Hyun, and S. S. Kang, "Phosphorylation on TRPV4 Serine 824 Regulates Interaction with STIM1," *Open Biochem. J.*, vol. 9, pp. 24–33, 2015.

[325] D. Becker, J. Bereiter-Hahn, and M. Jendrach, "Functional interaction of the cation channel transient receptor potential vanilloid 4 (TRPV4) and actin in volume regulation," *Eur. J. Cell Biol.*, vol. 88, no. 3, pp. 141–152, 2009.

[326] K. Xiao, D. B. McClatchy, A. K. Shukla, Y. Zhao, M. Chen, S. K. Shenoy, J. R. Yates, and R. J. Lefkowitz, "Functional specialization of beta-arrestin interactions revealed by proteomic analysis.," *Proc. Natl. Acad. Sci. U. S. A.*, vol. 104, pp. 12011–12016, 2007.

[327] J. Huai, Y. Zhang, Q. M. Liu, H. Y. Ge, L. Arendt-Nielsen, H. Jiang, and S. W. Yue, "Interaction of transient receptor potential vanilloid 4 with annexin A2 and tubulin beta 5," *Neurosci. Lett.*, vol. 512, no. 1, pp. 22–

27, 2012.

[328] A. Garcia-Elias, I. M. Lorenzo, R. Vicente, and M. A. Valverde, “IP3 receptor binds to and sensitizes TRPV4 channel to osmotic stimuli via a calmodulin-binding site,” *J. Biol. Chem.*, vol. 283, no. 46, pp. 31284–31288, 2008.

[329] T. Wegierski, K. Hill, M. Schaefer, and G. Walz, “The HECT ubiquitin ligase AIP4 regulates the cell surface expression of select TRP channels.,” *EMBO J.*, vol. 25, no. 24, pp. 5659–5669, 2006.

[330] N. Alessandri-Haber, O. a Dina, E. K. Joseph, D. B. Reichling, and J. D. Levine, “Interaction of transient receptor potential vanilloid 4, integrin, and SRC tyrosine kinase in mechanical hyperalgesia.,” *J. Neurosci.*, vol. 28, no. 5, pp. 1046–1057, 2008.

[331] M. Suzuki, A. Hirao, and A. Mizuno, “Microtubule-associated [corrected] protein 7 increases the membrane expression of transient receptor potential vanilloid 4 (TRPV4).,” *J. Biol. Chem.*, vol. 278, no. 51, pp. 51448–51453, 2003.

[332] S. F. J. Van De Graaf, J. G. J. Hoenderop, A. W. C. M. Van Der Kemp, S. M. Gisler, and R. J. M. Bindels, “Interaction of the epithelial Ca2+ channels TRPV5 and TRPV6 with the intestine- and kidney-enriched PDZ protein NHERF4,” *Pflugers Arch. Eur. J. Physiol.*, vol. 452, no. 4, pp. 407–417, 2006.

[333] M. Köttgen, T. Benzing, T. Simmen, R. Tauber, B. Buchholz, S. Feliciangeli, T. B. Huber, B. Schermer, A. Kramer-Zucker, K. Höpker, K. C. Simmen, C. C. Tschucke, R. Sandford, E. Kim, G. Thomas, and G. Walz, “Trafficking of TRPP2 by PACS proteins represents a novel mechanism of ion channel regulation.,” *EMBO J.*, vol. 24, no. 4, pp. 705–16, 2005.

[334] D. D’Hoedt, G. Owsianik, J. Prenen, M. P. Cuajungco, C. Grimm, S. Heller, T. Voets, and B. Nilius, “Stimulus-specific modulation of the cation channel TRPV4 by PACSIN 3,” *J. Biol. Chem.*, vol. 283, no. 10, pp. 6272–6280, 2008.

[335] T. Wegierski, U. Lewandrowski, B. Müller, A. Sickmann, and G. Walz, “Tyrosine phosphorylation modulates the activity of TRPV4 in response to defined stimuli,” *J. Biol. Chem.*, vol. 284, no. 5, pp. 2923–2933, 2009.

[336] Y. Takayama, K. Shibasaki, Y. Suzuki, A. Yamanaka, and M. Tominaga, “Modulation of water efflux through functional interaction between TRPV4 and TMEM16A/anoctamin 1,” *FASEB J.*, vol. 28, no. 5, pp. 2238–2248, 2014.

[337] J. Du, X. Ma, B. Shen, Y. Huang, L. Birnbaumer, and X. Yao, “TRPV4, TRPC1, and TRPP2 assemble to form a flow-sensitive heteromeric channel,” *FASEB J.*, vol. 28, no. 11, pp. 4677–4685, 2014.

[338] X. Ma, S. Qiu, J. Luo, Y. Ma, C. Y. Ngai, B. Shen, C. O. Wong, Y. Huang, and X. Yao, “Functional role of vanilloid transient receptor potential 4-canonical transient receptor potential 1 complex in flow-induced ca2+ influx,” *Arterioscler. Thromb. Vasc. Biol.*, vol. 30, no. 4, pp. 851–858, 2010.

[339] X. Ma, B. Nilius, J. W. Y. Wong, Y. Huang, and X. Yao, “Electrophysiological properties of heteromeric TRPV4-C1 channels,” *Biochim. Biophys. Acta - Biomembr.*, vol. 1808, no. 12, pp. 2789–2797, 2011.

[340] M. K??ttgen, B. Buchholz, M. A. Garcia-Gonzalez, F. Kotsis, X. Fu, M. Doerken, C. Boehlke, D. Steffl, R. Tauber, T. Wegierski, R. Nitschke, M. Suzuki, A. Kramer-Zucker, G. G. Germino, T. Watnick, J. Prenen, B. Nilius, E. W. Kuehn, and G. Walz, “TRPP2 and TRPV4 form a polymodal sensory channel complex,” *J. Cell Biol.*, vol. 182, no. 3, pp. 437–447, 2008.

[341] A. P. Stewart, G. D. Smith, R. N. Sandford, and J. M. Edwardson, “Atomic force microscopy reveals the alternating subunit arrangement of the TRPP2-TRPV4 heterotetramer,” *Biophys. J.*, vol. 99, no. 3, pp. 790–797, 2010.

[342] J. Du, W. Y. Wong, L. Sun, Y. Huang, and X. Yao, “Protein kinase G inhibits flow-induced Ca2+ entry into collecting duct cells,” *J Am Soc Nephrol*, vol. 23, no. 7, pp. 1172–1180, 2012.

[343] S. H. Shin, E. J. Lee, S. Hyun, J. Chun, Y. Kim, and S. S. Kang, “Phosphorylation on the ser 824 residue of trpv4 prefers to bind with f-actin than with microtubules to expand the cell surface area,” *Cell. Signal.*, vol. 24, no. 3, pp. 641–651, 2012.

[344] J. A. Herrera-L??pez, M. A. Mej??a-Rivas, F. Vargas-Vorackova, and M. A. Valdovinos-D??az, “Capsaicin induction of esophageal symptoms in different phenotypes of gastroesophageal reflux disease,” *Rev. Gastroenterol. Mex.*, vol. 75, no. 4, pp. 396–404, 2010.

[345] R. A. Liddle, “The role of Transient Receptor Potential Vanilloid 1 (TRPV1) channels in pancreatitis,” *Biochimica et Biophysica Acta - Molecular Basis of Disease*, vol. 1772, no. 8. pp. 869–878, 2007.

[346] F.-J. Sun, W. Guo, D.-H. Zheng, C.-Q. Zhang, S. Li, S.-Y. Liu, Q. Yin, H. Yang, and H.-F. Shu, “Increased expression of TRPV1 in the cortex and hippocampus from patients with mesial temporal lobe epilepsy.,” *J. Mol. Neurosci.*, vol. 49, no. 1, pp. 182–93, 2013.

[347] L. Moezi, S. a Gaskari, H. Liu, S. K. Baik, a R. Dehpour, and S. S. Lee, “Anandamide mediates hyperdynamic circulation in cirrhotic rats via CB(1) and VR(1) receptors.,” *Br. J. Pharmacol.*, vol. 149, no. 7, pp. 898–908, 2006.

[348] K. Fujino, S. G. de la Fuente, Y. Takami, T. Takahashi, and C. R. Mantyh, “Attenuation of acid induced oesophagitis in VR-1 deficient mice.,” *Gut*, vol. 55, no. 1, pp. 34–40, 2006.

[349] M. Nabissi, M. B. Morelli, C. Amantini, V. Farfariello, L. Ricci-Vitiani, S. Caprodossi, A. Arcella, M. Santoni, F. Giangaspero, R. De Maria, and G. Santoni, “TRPV2 channel negatively controls glioma cell proliferation and resistance to Fas-induced apoptosis in ERK-dependent manner,” *Carcinogenesis*, vol. 31, no. 5, pp. 794–803, 2010.

[350] A. Oulidi, A. Bokhobza, D. Gkika, F. Vanden Abeele, V. Lehen’kyi, L. Ouafik, B. Mauroy, and N. Prevarskaya, “TRPV2 Mediates Adrenomedullin Stimulation of Prostate and Urothelial Cancer Cell Adhesion, Migration and Invasion,” *PLoS One*, vol. 8, no. 5, 2013.

Supplementary information

VI) Annex

	Stimuli	IC50	Ref.
TRPV1			
Agonist	Capsaicin	0.04-1 uM	[69]
	Anandamide	30 uM	[156]
	HODE	1 uM	[157]
	12S-HPETE	10 uM	[159]
	Piperine	38 uM	[270]
	Eugenol	1 mM	
	Resiniferatoxin	0.01-39 nM	[69]
	pH	5.5	[152]
	Temperature	≥43°C	[69]
Antagonist	Capsazepine	0.5 uM	[160]
	JNJ17203212	16 nM	[161]
	JNJ39729209	1 uM	[162]
	SB 705498	5 nM	[163]
	XEN-00501		[164]
TRPV3			
Agonist	2-APB	34 uM	[171]
	Camphor	100 uM	[170]
	Carvacol	100 uM	[172]
	Eugenol	100 uM	[172]
	Thymol	100 uM	[172]
	Temerature	≥34°C	[115]
	DPBA	100 uM	[174]
	6TBC	1 uM	[172]
	Incensole acetate	10 uM	[175]
Antagonist	HC-001403	1 uM	[177]
	GRC 15133	100 nM	[177]
	GRC 17173	100 nM	[177]
	17RD1	155 nM	[178]

	Stimuli	IC50	Ref.
TRPV2			
Agonist	2APB	129 uM	[167]
	9-tetrahydrocannabinol	14 uM	[166]
	cannabidiol	3.7 uM	[166]
	9-tetrahydrocannabivarin	10 uM	[166]
	Probenecid	10 uM	[168]
Antagonist	SKF96365	10 uM	[169]
	Amiloride	18 uM	[169]
	Tranilast		[100]
TRPV4			
Agonist	Hypotonicity		[179]
	Temperature	≥38°C	[180]
	4 α-PDD	1 uM	[182]
	5,6 EET	1 uM	[181]
	Arachidonic acid	10 uM	[181]
	BAA	1 uM	[182]
	GSK1016790A	10 nM	[183]
Antagonist	Citral	32 uM	[187]
	RN-1734	10 uM	[188]
	RN-9893	10 nM	[188]
	GSK2193874	40 nM	[189]
	HC 067047	48 nM	[190]

Annex table 1. TRPV4 pharmacology at a glance. Compendium of known agonist and antagonist of TRPV1-4 with their IC50 and bibliography annotated.

TRPV1 related proteins list come mainly from two high throughput screenings techniques: yeast two hybrid and Co-IP followed by mass spectrometry protein identification [271][272]. These studies identify numerous potential TRPV1 partners and determine the relationship of TRPV1 with PI3 kinase and voltage gated potassium channel beta 2 subunit respectively. Other studies used a pair-wise approach to characterize interactions and deepen in the regulatory effects of the complex. Annex table 2.

INTERACTOR	SCREEN	VALIDATION		Functional consecuence	Ref.
		in vitro	in vivo		
80K-H					[273]
Actin				F actin architecture is affected by TRPV1 activation by capsaicin in an ERK1/2 MLC2 dependent manner.	[272] [274]
AKAP5/AKAP150				AKAP are scaffolding proteins that target pro-inflamatory kinases to TRPV1. AKAP targeting enhances TRPV1 trafficking to the plasma membrane, sensitization of the channel and promotes hyperalgesia.	[191] [192] [193]
Akt				TRPV1 activation by ligands promotes phosphorylation of AKT and increases the formation of TRPV1-AKT/CamKII complex.	[275]
AMPKσ2				TRPV1 activation promotes phosphorylation of AMPK and eNOS in aortas of mice. TRPV1 trigger AMPK signaling, which leads to retarded development of atherosclerosis.	[276]
Apolipoprotein					[272]
Bkca				BK channels can be activated by calcium influx through TRPV1. The complex is present in DRG neurons where it plays a critical role in regulating the pain signal transduction pathway.	[277]
Calmodulin				Calmodulin binds to N- and C-terminal of TRPV1. N-terminal binding site mediates TRPV1 calcium dependent desensitization.	[48] [278] [199]
CaMKII				Inhibition CaMKII suppresses the ligand-induced increase in TRPV1 phosphorylation, formation of a TRPV1-eNOS complex, and eNOS activation.	[275]
Catenin-σ2					[271]
Catenin-Ƥ2					[271]
CB1				CB1 and TRPV1 colocalized in human and mouse corneal epithelium. Activation of CB1 reduced TRPV1 activity and TRPV1-induced inflammatory and scarring responses	[279]
Cbl				TRPV1 facilitates ubiquitination of EGFR by cbl, targeting EGFR to degradation.	[280]
CDK12					[272]
CDK5				Cdk5 positively regulates TRPV1 surface localization. Activation of Cdk5 promotes TRPV1 anterograde transport in vivo by direct phosphorylation of the channel.	[281] [282] [204]
CHERP					[271]
Contactin-1					[271]
DAP-150					[271]
DAZAP2					[271]
E-cadherin				TRPV1 co-localized and co-precipitated with E-cadherin and β-catenin, although TRPV1 activation does not lead to a re-distribution of E-cadherin or adherens junctions in submandibular epithelial cells.	[274]
Eferin/Rab11-FIP3				TRPV1 and Eferin highly colocalized in DRG cells, although this protein had no significant effect on TRPV1 channel activity in response to capsaicin.	[283]

Annex table 2 continued

INTERACTOR	SCREEN	VALIDATION		Functional consecuence	Ref.
		in vitro	in vivo		
EGFR				TRPV1 interaction with EGFR promotes EGFR ubiquitination and degradation, having a tumour suppressing effect in keratinocytes.	[280]
eNOS				Upon TRPV1 activation by ligands, eNOS is recruited to TRPV1 complex and phosphorylated, leading to an increased production of Nitric oxide.	[275] [276]
FAF1				FAF1 reduces the responses of TRPV1 to capsaicin, acid, and heat. Silencing FAF1 augments capsaicin sensitivity in native sensory neurons, pointing FAF1 as an integral component of TRPV1 complexes and constitutively modulator of TRPV1 activity.	[284]
GABARAP				GABARAP is a component of the TRPV1 signalling complex and contributes to increase the channel expression, to the trafficking to the plasma membrane, and to modulate TRPV1 channel gating and desensitization.	[285]
GCN5					[271]
Glucose 6 phosphatase					[272]
Glycogen phosphorylase					[272]
β -arrestin 2				β-arrestin 2 bind TRPV1 in a phosphorylation dependent manner, being crucial phosphorylation in Thr(370) of TRPV1. β-arrestin promotes TRPV1 desensitization by actively participating in a scaffolding mechanism to inhibit TRPV1 phosphorylation, thereby reducing TRPV1 sensitivity.	[286] [287] [288]
β -catenin				TRPV1 colocalized and co-precipitated with E-cadherin and β-catenin, although TRPV1 activation does not lead to changes in distribution or function of β-catenin in submandibular epithelial cells.	[274]
α-tubulin-3				TRPV1 binds to tubulin on its C-terminus.	[289]
α-tubulin-5 α-tubulin-1A				TRPV1 binds tubulin in the C-terminus in a calcium dependent manner and this interaction affects microtubule properties, such as microtubule sensitivity towards low temperatures and nocodazole. This fact points that the microtubule cytoskeleton may be a downstream of TRPV1 activation.	[290]
HAX-1					[271]
ITM2C					[271]
JMJD2C					[271]
KCNQ2/3				TRPV1 binds to KCNQ2 predominantly by the membrane spaning regions. TRPV1 activation inhibits KCNQ2 activity and this inhibition is dependent on calcium influx followed by PIP2 depletion and activation of protein phosphatase calcineurin.	[291]
KIF13B				KIF13B participates of Cdk5 mediated TRPV1 translocation. Cdk5 phosphorylates KIF13B at Thr-506 and this enhances TRPV1 translocation to the plasma membrane.	[204]
KIF2A					[271]
KIF3B					[271]
KPNα1					[271]
Kvβ2				TRPV1 trafficking and gating is enhanced in the presence of voltage-gated K potasium channel beta 2 subunit (Kvβ2)	[272]
Neuronatin					[271]
NKX2.2					[271]
NMDAR1 NMDAR2B				NMDAR1 interacts with TRPV1 in trigeminal ganglia, where NMDA triggers TRPV1 serine phosphorylation via PKC and CamKII. TRPV1 phosphorylation leads to channel sensitization and mechanical hyperalgesia.	[201]

Annex table 2 continued

INTERACTOR	SCREEN	VALIDATION		Functional consecuence	Ref.
		in vitro	in vivo		
NOMO1					[271]
α-tubulin-1B				TRPV1 bind to intact microtubules and the interaction maintain TRPV1 functionality. Upon microtubule disassembly TRPV1 agregates and loss function.	[292]
αENaC				TRPV1 activation by capsaicin reduced sodium reabsortion in the kidney by inhibiting αENaC expression and function.	[293]
αII-spectrin					[272]
OS-9				TRPV1 interacts with OS-9 potentially by a predicted binding domain on the N terminus of the channel. OS-9 functions in the ER as an auxiliary protein for TRPV4 maturation and a similar role has been proposed for TRPV1.	[244]
P2RX3				TRPV1 and P2RX3 interact with each other by a motif located at the C-terminal end of the P2RX3. TRPV presence and interaction promotes an inhibitory effect on P2RX3 activity.	[294]
PACS-1					[295]
PEX10 c					[271]
PI3K-p85Ⅱ					[271]
PI3K-p85α					[271]
PIRT				Noxious heat and capsaicin currents in PIRT deficient DRG neurons are significantly attenuated. Heterologous expression of PIRT enhances TRPV1 mediated currents. This potenciation of TRPV1 activity is determined by the binding of PIRT C-terminus to TRPV1 and the recruitment of several phosphoinositides, such as PIP2	[296]
PKA				PKA reduces TRPV1 desensitization by directly phosphorylating Ser 116 of TRPV1 N-terminus.	[195]
PKARIIα				PKARII binding site on AKAP5 is necessary for PKA enhancement of TRPV1 activity. Forms a complex with TRPV1, AKAP5 and PKA.	[297]
PKC				TRPV1 is directly phosphorylated by PKC at the S502, T704 and S800 residues. TRPV1 PKC mediated phosphorylation does not activate the channel but sensitized it to activation by TRPV1 agonist such as capsaicin.	[194]
PKC β				TRPV1 directly binds to PKC-β, leading to the activation and translocation of PKC-β. Activated PKC-β significantly increases the responsiveness of TRPV1 to heat by phosphorylating T704.	[298]
PKCþ				TRPV1 first intracellular loop and carboxyl terminus, S502 and S800, were phosphorylated by PKCepsilon. This phosphorylation is involved in the potentiation of the capsaicin-evoked currents by PMA and ATP.	[299]
PLAGL1					[271]
PLCα1				TRPV1 and PLC gamma are predicted to interact though pH domains in the N-terminus of the channel in a similar way to TRPC3. PLC regulates PIP2 levels by cleaving them, modulating channel activity through changes in lipid composition.	[49]
POLR2G					[271]
POLR3D					[271]
PPARα				PPARα activation by specific agonists in CHO cells induced the activation of TRPV1 with a higher degree of desensitization of the channel.	[300]
PRKD1/PKCT				PRKD1 phosphorylates TRPV1 N-terminus (S116) and enhances its activity in DRG neurons. The expression levels of PRKD1 influence TRPV1 channel activity in a positive way, developing and maintaining inflammatory heat hypersensitivity.	[301] [302]
RAB26					[271]
RAB8b					[272]
RANBP9					[271]

Annex table 2 continued

INTERACTOR	SCREEN	VALIDATION		Functional consecuence	Ref.
		in vitro	in vivo		
Ribosomal protein L9	■				[272]
RPL12	■				[271]
RyR1	■			TRPV1 forms part of the RyR1 complex in the triad junctions, where it may suffer similar functional crosstalk as TRPC3. TRPC3 and RyR1 interaction coordinates their calcium mediated influx and regulates muscle cell differentiation and contraction.	[303]
SGT	■				[271]
SMA3	■				[271]
SNAPIN	■	■	■	SNAPIN, a protein of vesicle SNARE complex, does not alter TRPV1 channel function but inhibit PKC mediated TRPV1 potentiation. PKC potentiation seems to be mediated by recruitment of TRPV1 to the plasma membrane through SNARE dependent exocytosis.	[205]
snRNP 70	■				[272]
Src	■		■	Src binds and phosphorylates TRPV1 at the Y200 residue, which results in an increase in the recruitment of TRPV1 channels to the plasma membrane.	[304]
Synaptotagmin 1 and 4	■	■	■	Synaptotagmin, proteins from SNARE complex, interacts with TRPV1 N-terminus and colocalizes with TRPV1 vesicles in DRG neurons. Synaptotagmins mediate TRPV1 recruitment to the plasma membrane upon PKC activation, leading to a potenciation of TRPV1 activity.	[205]
TAK1	■		■	TAK/JNK1 are downstream effectors of TRPV1 activity, leading to increases in pro-inflammatory and chemoattractant interleukin IL-6 and IL-8 release.	[279]
TGS1	■				[271]
Thrombospondin-3	■				[271]
TMEM115	■				[271]
TrkA	■		■	NGF, acting on the TrkA receptor, activates PI3 signalling pathway and promotes downstream effectors such as Src kinase binding and phosphorylation of TRPV1, potentiating channel activity. Furthermore, recruitment of PLC-gamma to TrkA is essential for NG-mediated potentiation of TRPV1 activity.	[202] [304]
TRPA1	■		■	TRPV1 can form heterotetramers with TRPA1 in a calcium dependent manner. TRPV1 heterotetramerization leads to a decrease in total current and lower shift in capsaicin voltage dependent gating. The presence of TRPA1 exerts an inhibitory effect on TRPV1 function.	[305]
TRPV2	■		■	TRPV1 and TRPV2 co-localize and interact in neurons from DRG and cerebral cortex. They constitute heterotetrameric channels that providing further functional diversity to TRPV subfamily.	[89] [306] [307]
TRPV3	■		■	TRPV3 is co-expressed in dorsal root ganglion neurons with TRPV1. When heterologously expressed, TRPV3 is able to associate with TRPV1 and may modulate its responses.	[115]
Tubulin			■	Microtubules physically interact with the C-terminus of TRPV1 at the cell membrane of osmosensory neurons and provide a pushing force that drives channels activation during shrinking.	[308]
UBP5	■				[271]
ZBTB17	■				[271]
ZO-1	■				[272]

Annex table 2. List of interactor partners for TRPV1 according to www.TRPchannels.org.

TRPV2 known interactors have been mainly determined by the validation of already described homologous interactions for TRPV1 [196], although some yeast two hybrids have yield new potential TRPV regulators [309][310]. All TRPV2 partners are listed in Annex table 3.

INTERACTOR	SCREEN	VALIDATION		Functional consecuence	Ref.
		in vitro	in vivo		
ACBD3				ACBD3 interacts with TRPV2 in mast cells and mediates the recruitment of the channel to PKA and PKARII complex.	[196]
AKAP5/AKAP150				AKAP are scaffolding proteins that are able to bind to several TRPVs, TRPV2 among them. In the case of TRPV2 interaction functional implications remain to be elucidated.	[191]
Calmodulin				Calmodulin is bound to the C-terminus of TRPV2 channel (654-683) but not in the N-terminus as in TRPV1 or TRPV4. The binding is dependent on basic aminoacids within this region, mainly R679 and K681.	[58] [197]
PKA				PKA mediates in vitro phosphorylation of TRPV2. In mast cells PKA phosphorylation of TRPV2 occurs in resting conditions, although it may be enhanced by cAMP mobilization.	[196]
PKARIIσ				PKARII potentially binds to ACBD3 and, together with AKAP5, recruits PKA to the proximity of TRPV2 channel.	[196]
RGA/RAG1AP1				RGA associates with TRPV2 within intracellular stores in rat mast cells upon glycosylation event. RGA plays a chaperone or targeting role for TRPV2 during the maturation of the channel, promoting TRPV2 recruitment to the plasma membrane.	[309] [311]
SYNE1				SYNE1 is a member of the spectrin family that play a role in the maintenance of Golgi structure and mediates protein trafficking, potentially involved in TRPV2 recruitment to the membrane.	[310]
TRPV1				TRPV1 and TRPV2 colocalize and interact in neurons from DRG and cerebral cortex, providing further functional diversity to TRPV subfamily.	[89] [306] [307]
UBC				Ubiquitin proteome-wide studies identified TRPV2 as potential partner.	[312] [313]

Annex table 3. List of interactor partners for TRPV2 according to www.TRPchannels.org.

TRPV3 is one of the least characterized TRPV in terms of protein interactions. Similarly to TRPV2, interaction with calmodulin and AKAP5 have been screened by inference and homology with TRPV1, which is also able to form TRPV1-TRPV3 heterotetramers [198][191][115]. All known TRPV3 interactors are listed in Annex table 4.

INTERACTOR	SCREEN	VALIDATION		Functional consecuence	Ref.
		in vitro	in vivo		
AKAP5/AKAP150				TRPV3, as other TRPV channels is able to bind the scaffolding proteins AKAP. The functional relevance of this interaction in the case of TRPV3 still remains unclear.	[191]
Calmodulin				TRPV3 binds calmodulin on its N-terminal ARD domain in a calcium dependent manner.	[197] [198]
EGFR				Activation of EGFR leads to increased TRPV3 channel activity, which stimulates TGF-alpha release and ultimately influences hair morphogenesis and skin barrier formation.	[120]
TRPV1				TRPV1 is able to form heterotetramers with TRPV3, increasing the functional variability of TRPV subfamily.	[115]

Annex table 4. List of interactor partners for TRPV3 according to www.TRPchannels.org.

TRPV4 partners have been determined by yeast two hybid assays, Co-IP coupled to mass spectrometry or inference by other close related proteins such as TRPV1. The functional relevance of TRPV4 interactions have been detailed analysed in most cases, figuring out very specific functional implications for those interactors. Annex table 5.

INTERACTOR	SCREEN	VALIDATION		Functional consecuence	Ref.
		in vitro	in vivo		
80K-H					[273]
AKAP5/AKAP150				Muscarinic receptor mediate activation of TRPV4 depending on protein kinase C (PKC) and the PKC-anchoring protein AKAP150, which bridges PKC to TRPV4 in myoendothelial projections of endothelial cells.	[314]
AQP-4				Astrocytes contain a TRPV4 AQP4 complex that acts as osmosensor and constitutes a key element in regulatory volume decrease (RVD) within the cell and the brain's volume homeostasis.	[315]
AQP-5				Exposure to hypotonocity promotes calcium entry through TRPV4 and regulation of cell volume (RVD) in the salivary gland. AQP-5 TRPV4 complex formation is enhanced upon hypotonic shock and is needed for calcium entry and RVD. Thus, TRPV4 and AQP5 concertedly control RVD in the salivary gland.	[316]
AT1aR				AT1aR (angiotensin receptor) and TRPV4 form a constitutive complex in the plasma membrane, and angiotensin stimulation leads to recruitment of beta-arrestin 1 to this complex, which in turn promotes TRPV4 ubiquitination and functional channel downregulation.	[317]
Bkca (Kca1.1)				TRPV4 associates with Kca1.1 and TRPC1 in smooth muscle cells and upon TRPV4 activation calcium influx promotes Kca1.1 activation. The complex couples NO and EET metabolism to potassium channel activity, controlling cell hyperpolarization and relaxation.	[318]
Calmodulin				TRPV4 activation reciprocally regulates Ca(2+)/calmodulin signaling, and promotes association of TRPV4 with myosin IIa in osteoclasts. TRPV4 binds calmodulin in its N-terminal ARD domain and C-terminal tail, with a potentiation effect on channel activity. Nitrosylation of TRPV4 cys853 residue in the N-terminus abrogates interaction with camodulin and inhibits channel activity.	[319] [320] [198] [200]
Caveolin-1				TRPV4 and TRPC1 colocalize with Caveolin 1 in internal vesicles of HUVEC cells. Upon internal calcium store depletion there is an increase in TRPV4 delivery to the plasma membrane mediated by Caveolin 1.	[321]
E-cadherin				TRPV4 is located where the cell-cell junctions are formed, and the channel deficiency caused abnormal cell-cell junction structures. TRPV4 activity was crucial for barrier formation and recovery.	[130] [322]
FYN				TRPV4 interacts with Src kinases such as FYN by their SH2 domain. Hypotonicity promotes Src family tyrosine kinase dependent tyrosine phosphorylation of TRPV4 at residue Tyr-253.	[323]
α-actin				TRPV4 interaction with F actin fibers is mediated by Ser824 and crucial for channel location and activity. F actin reorganization and TRPV4 activity are linked and cooperate to mediate in RVD during hypotonic shock.	[324] [325]
β-arrestin 1				β-arrestin 1 is recruited to AT1aR TRPV4 complex upon angiotensin stimulation and mediates TRPV4 ubiquitination and subsequently internalization and functional down-regulation. β-arrestin 1 acts as an adaptor of AIP4	[317]
β-arrestin 2					[326]
α-catenin				In keratinocytes TRPV4 is recruited to the adherent junction complex through β-catenin, promoting the increase of cytosolic calcium in the vicinity of adherent junctions, which in turns regulate complex formation and skin barrier formation and maturation.	[322] [130]

Annex table 5 continued

INTERACTOR	SCREEN	VALIDATION		Functional consecuence	Ref.
		in vitro	in vivo		
α1-tubulin-5				TRPV4 colocalizes and interacts with proteins of the cytoskeleton such as tubulin beta 5, although modulation of channel activity by this partnership remains to be addressed.	[327]
HCK				Member of Src kinase family that interacts with TRPV4 and potentially phosphorylates TRPV4 at residue Tyr-253.	[323]
IP3R3				IP3 receptor interacts with TRPV4 C-terminal domain, within the same region of calmodulin binding. Binding of IP3R sensitizes TRPV4 and connects extracellular calcium influx to intracellular calcium stores in order to initiate and maintain the oscillatory calcium signals triggered by hypotonicity.	[185] [328]
ITCH/AIP4				AIP4 ubiquitinates TRPV4 and this modification promotes the channel endocytosis, decreasing its amount at the plasma membrane and by instance the basal channel activity.	[329]
LCK				Member of Src kinase family that interacts with TRPV4 and potentially phosphorylates TRPV4 at residue Tyr-253.	[323]
LYN				Member of Src kinase family involved in mechanical transduction that interacts with TRPV4 and in vitro phosphorylates TRPV4 at residue Tyr-253.	[323] [330]
MAP7				MAP7 is a microtubule associated protein that interacts with TRPV4 C-terminal domain (798-809) and co localize with the channel in kidney and lung cells. The interaction increases the TRPV4 membrane expression.	[331]
MYH9 MYH10 Myosin-HIIA				Myosin is an essential player in contractility that associates with TRPV4 C-terminus in a calcium/calmodulin dependent manner and sensitized the channel to specific agonists. Deletion of calmodulin binding site, which is overlapped with Myosin binding site; reduces TRPV4 response to agonist in osteoclast.	[319]
NHERF4				PDZ containing protein that interacts with TRPV4 C terminus and acts as scaffolding protein exerting a potential regulation of channel assembly and localization at the plasma membrane.	[332]
α2-integrin				α2-integrin is implicated in mechanical transduction together with Src tyrosine kinases and exerts an important role for the development of mechanical hyperalgesia. TRPV4 direct interaction to α2-integrin is required in this process.	[330]
OS-9				OS9 interacts with the N-terminus of TRPV4 and impedes the release of TRPV4 from the ER, decreasing TRPV4 plasma membrane levels. OS-9 functions as an auxiliary protein for TRPV4 maturation, binding TRPV4 monomers and immature variants.	[244]
PACS-1				PACS-1, a sorting protein that recognizes acidic clusters, interacts with the N-terminal domain of TRPV4. This interaction may direct the localization of TRPV4 to distinct subcellular compartments.	[333]
Pacsin1				Pacsin1 is implicated in synaptic vesicular membrane trafficking and regulation of dynamin mediated endocytotic processes. Pacsin1 interacts with TRPV4 N-terminal proline rich domain, upstream of ARD.	[245]
Pacsin2				Pacsin2 as its close homolog Pacsin1 interacts with the N-terminal proline rich domain of TRPV4. Functional consequences of these two interactions remain elusive.	[245] [334]
Pacsin3				Pacsin3 binds to the N-terminal proline rich domain of TRPV4 This interaction enhances the relative amount of TRPV4 in the plasma membrane, inhibits the basal activity of TRPV4 and its activation by cell swelling and heat with no affection of agonist mediated activation. Mutations on the Pacsin binding pocket of TRPV4 revert the Pacsin3 mediated inhibition of the channel. Pacsin3 inhibitory effect is mediated by restriction access of TRPV4 to PIP2, which lead to a TRPV4 tails rearrangement that insensitize the channel to heat and hypotonicity.	[245] [334] [243]
RPS27A					[319]

Annex table 5 continued

INTERACTOR	SCREEN	VALIDATION		Functional consecuence	Ref.
		in vitro	in vivo		
Src				SRC directly phosphorylates TRPV4 at the N- and C-terminal Tyr 110 and Tyr 805 residues. N-terminal phosphorylation does not play a role in channel trafficking but sensitizes the channel and affects activation of TRPV4 by heat, mechanical stress and hypotonic cell swelling. C-terminal phosphorylation does not affect either channel trafficking or function.	[323] [335]
TMEM16A ANO1				TRPV4 and ANO1, a chloride channel, interact in choroid plexus epithelial cells. TRPV4 calcium evoked influx mediates ANO1 activation and ANO1 mediated chloride currents. This ANO1 activity is able to regulate water transport in the choroid plexus and mediate in cell volume decrease upon hypotonic shock.	[336]
TRPC1				Heteromeric TRPV4-C1-P2 complexes are formed in primary cultured rat mesenteric artery endothelial cells (MAECs). Functional characterization suggests that the 3 TRPs contribute to the ion permeation pore of the heteromeric channels. TRPV4 TRPC1 complex plays a key role in flow induced endothelial calcium influx by changing channel gating properties. TRPV4 TRPC1 channels were slightly more permeable to calcium and had a reduced sensitivity to calcium dependent inhibition. Furthermore, heterotetramers are easier to traffic to the plasma membrane than homotetrameric forms, increasing calcium influx in response to flow.	[337] [338] [321] [339]
TRPP1				TRPP1 and TRPV4 form heterotetramers with a 2:2 stoichiometry. Heterotetramers mediate the flow induced entry of calcium into collecting duct cells and form a mechanical and thermosensitive molecular sensor in the cilium of renal cysts, playing a role in ciliogenesis.	[337] [340] [341] [342]
Tubulin				Ser 824 residue of TRPV4 is phosphorylated by SGK1, which elicits the formation of the TRPV4 F-actin complex. This interaction links TRPV4 with the cytoskeleton.	[343]
UBC				Ubiquitination is one of the main processes regulating TRPV4 membrane expression levels. Ubiquitination of TRPV4 is mediated by AIP4 and impeded by Os-9 interaction.	[244] [329]
YES				Member of Src kinase family that interacts with TRPV4 and potentially phosphorylates TRPV4 at residue Tyr-253.	[323]

Annex table 5. List of interactor partners for TRPV4 according to www.TRPchannels.org.

Disease Name	Disgenet score	Ref.	Gene name	% of shared disease
Hyperalgesia	0.310	[210]	TNF	74
Inflammation	0.315	[211]	IL6	70
Pain	0.213	[69]	PTGS2	66
Obesity	0.213	[217]	IL1B	60
Heartburn	0.21	[344]	VEGFA	58
Pancreatitis	0.21	[345]	IL10	56
Neoplasm	0.21	-	TGFB1	55
Epilepsy, temporal lobe	0.21	[346]	TP53	54
Liver cirrhosis	0.21	[347]	IFNG	51
Esophageal diseases	0.21	[348]	IL1RN	50

Annex table 6. Disgenet (www.disgenet.org) summary of top 10 TRPV1 associated diseases (left side of the table) and top 10 related genes in pathological conditions (on the right), with the number of shared diseases as measure of gene pathological interconnectivity (on the right). Disgenet score is a correlation index, being a more significant protein-disease correlation with values closer to 1.

Disease Name	Disgenet score	Ref.	Gene name	% of shared disease
Neoplasm, malignant	0.001	[349]	IL6	21
Primary malignant neoplasm	0.001	[349]	TP53	21
Malignant neoplasm of bladder	0.001	[350]	VEGFA	21
Malignant neoplasm of prostate	0.001	[350]	MIR21	19
Prostate carcinoma	0.001	[350]	PTGS2	19
Muscular dystrophies	0.001	[220]	TNF	19
Glioma	0.001	[349]	CXCL8	19
Dystrophic cardiomyopathy	0.001	[66]	CDKN2A	18
Cardiomyopathies	0.001	[66]	CSF2	18
Carcinoma of bladder	0.001	[350]	HPGDS	18

Annex table 7. Disgenet (www.disgenet.org) summary of top 10 TRPV2 associated diseases (left side of the table) and top 10 related genes in pathological conditions (on the right), with the number of shared diseases as measure of gene pathological interconnectivity (on the right). Disgenet score is a correlation index, being a more significant protein-disease correlation with values closer to 1.

Disease Name	Disgenet score	Ref.	Gene name	% of shared disease
Olmsted syndrome	0.412	[221]	IL6	7
Dermatitis, atopic	0.1		VEGFA	6
Ganglion cysts	0.003		HLA-DRB1	5
Dermatitis	0.003		IL1B	5
Skin diseases	0.001		IL17D	5
Skin diseases, genetic	0.001		TNF	5
Migraine disorders	0.001		PTGS2	5
Migraine with aura	0.001		VIP	5
Pruritus	0.001		EDN1	5
Headache disorders, primary	0.001		GJB6	4

Annex table 8. Disgenet (www.disgenet.org) summary of top 10 TRPV3 associated diseases (left side of the table) and top 10 related genes in pathological conditions (on the right), with the number of shared diseases as measure of gene pathological interconnectivity (on the right). Disgenet score is a correlation index, being a more significant protein-disease correlation with values closer to 1.

Disease Name	Disgenet score	Ref.	Gene name	% of shared disease
Metatropic dwarfism	0.622	[229]	TNF	29
Spondylometaphyseal dysplasia Kozlowski type	0.621	[230]	IL6	24
Brachiolmia Type3	0.621	[227]	IL10	21
Parastremmatic dwarfism	0.421	[230]	VEGFA	20
Spinal muscular atrophy, scapuloperoneal	0.421	[232]	SOD1	19
Hereditary motor and sensory neuropathy	0.421	[232]	IL1B	19
Brachiolmia Type2	0.41	[230]	AGT	18

Digital arthropathy-brachydactyly	0.41	-		GSTT1	18
Pulmonary disease, chronic obstructive	0.213	[135]		APOE	18
Hyponatremia	0.212	[226]		BCL2	18

Annex table 9. Disgenet (www.disgenet.org) summary of top 10 TRPV4 associated diseases (left side of the table) and top 10 related genes in pathological conditions (on the right), with the number of shared diseases as measure of gene pathological interconnectivity (on the right). Disgenet score is a correlation index, being a more significant protein-disease correlation with values closer to 1.